

This item was submitted to [Loughborough's Research Repository](#) by the author.
Items in Figshare are protected by copyright, with all rights reserved, unless otherwise indicated.

Gas diffusion–flow injection interfaces for mass spectrometric and electrochemical detectors

PLEASE CITE THE PUBLISHED VERSION

PUBLISHER

© Onditi Ouma Anam

PUBLISHER STATEMENT

This work is made available according to the conditions of the Creative Commons Attribution-NonCommercial-NoDerivatives 2.5 Generic (CC BY-NC-ND 2.5) licence. Full details of this licence are available at:
<http://creativecommons.org/licenses/by-nc-nd/2.5/>

LICENCE

CC BY-NC-ND 2.5

REPOSITORY RECORD

Anam, Onditi O.. 2019. "Gas Diffusion–flow Injection Interfaces for Mass Spectrometric and Electrochemical Detectors". figshare. <https://hdl.handle.net/2134/28323>.

This item was submitted to Loughborough University as a PhD thesis by the author and is made available in the Institutional Repository (<https://dspace.lboro.ac.uk/>) under the following Creative Commons Licence conditions.



For the full text of this licence, please go to:
<http://creativecommons.org/licenses/by-nc-nd/2.5/>



Pilkington Library

Author/Filing Title ANAM, O.O.

Accession/Copy No.

040147115

Vol. No.

Class Mark

LOAN COPY

25 JUN 1999

0401471152



BADMINTON PRESS
18 THE HALFCROFT
SYSTON
LEICESTER, LE7 1L
ENGLAND
TEL : 0116 260 2917
FAX : 0116 260 6626

GAS DIFFUSION-FLOW INJECTION INTERFACES FOR MASS SPECTROMETRIC AND ELECTROCHEMICAL DETECTORS

by


Onditi Ouma Anam, B.Sc.(Hons), M.Sc., CChem, MRSC

A Doctoral Thesis
submitted in partial fulfilment of the requirements
for the award of
the degree of Doctor of Philosophy
of the
Loughborough University

November, 1996

Supervisor: Dr. Barry L. Sharp, B.Sc., Ph.D., DIC, CChem, FRSC

© by Onditi Ouma Anam 1996

| | |
|--|-----------|
|  Department of the Treasury Treasury | |
| Date | July 97 |
| Class | |
| Acc No. | 640147113 |

9/9103233

Dedicated
to my wife, Margaret Onditi;
our children, Faith, Anam Jr,
Rhodah and Lydia; and
parents, Mzee Anam Onditi and
Mama Otieno Anam.

ABSTRACT

Isotope tracer techniques are widely used in biological, agricultural, chemical and medical research. The use of stable isotopes is not complicated by health hazards, dangers of radiation or time limit for experiments as is the case for radioactive isotopes. However, the analytical methods available for the determination of stable isotopes are much less sensitive, considerably more complicated and time consuming than those for radioactive isotopes. Such methods usually require the use of a mass spectrometer and most employ the combustion technique (Dumas method) for sample presentation. Speciation can be achieved by an isotope ratio mass spectrometer coupled to a gas chromatograph (GC) and combustion interface. Such instruments are expensive and labour intensive. Additionally, the consumables and catalysts employed are costly.

In this work, a cheaper method for sample presentation was developed to replace the combustion system and to allow speciation without employing a GC/combustion interface. This was achieved by using the gas diffusion-flow injection technique. Gaseous analytes were generated by wet chemical methods and subsequently separated from the liquid donor stream in a gas diffusion-flow injection (GD-FI) system.

GD-FI-Isotope Ratio Mass Spectrometry (IRMS) was employed in this work for the determination of the $^{13}\text{C}/^{12}\text{C}$ ratio of inorganic carbon and the $^{15}\text{N}/^{14}\text{N}$ ratio of nitrogen containing compounds. In both cases, wet chemical methods were employed for the generation of CO_2 and N_2 respectively. In addition, a degassing system consisting of dual PTFE membranes was incorporated into the GD-FI system to remove the dissolved gases from the liquid streams, thus minimising the background.

The GD-FI interface was also coupled to a polarograph for the determination of Se(IV) by differential pulse cathodic stripping voltammetry. This involved the generation of H_2Se from Se(IV) , its separation and subsequent oxidation back to Se(IV) .

The versatility of the GD-FI technique was demonstrated by generating H_2S from sulphide and sulphite, SO_2 from sulphite, Br_2 from Br^- and Cl_2 from Cl^- and their determination by thermal conductivity detection and/or UV/VIS spectrophotometry.

ACKNOWLEDGEMENTS

I wish to express my sincere thanks to my supervisor, Dr. Barry Sharp, for the advice, encouragement and competent supervision of this research. I am also very grateful to Dr. Arnold Fogg for his encouragement and invaluable assistance especially in the aspects dealing with electroanalytical techniques.

Many thanks go to the Government of Kenya in conjunction with the World Bank for offering me the scholarship to undertake this research programme. I am also thankful to the Jomo Kenyatta University of Agriculture and Technology for nominating me to be a recipient of this scholarship.

My sincere thanks also go to all the technical staff in the Department of Chemistry including: Elaine Till, Bev Cooper, Simon Riggott, John Spray and Linda Sands for their help and co-operation throughout the entire period of my research programme.

I wish to express my gratitude to the Micromass for allowing me to work in their laboratory and for the support given. I am very grateful to Dr Tim Brockwell and Ron Daniels for the role they played in making my work with the isotope ratio mass spectrometer a success. I wish to thank all my research colleagues, especially Rahim H. M. Yussoff, Razili Ismail and Stephanie Barreau for their support. Many thanks to Azli Sulaiman for the invaluable assistance he offered me with computing, and to Dr. Silvana do Couto Jacob for her assistance in the initial stages of my project, thus enabling me to make a smooth start. I am equally grateful to Sister Julie Jensen for typing a part of this work.

I wish to thank my wife, Margaret; children, Faith, Anam Jr, Rhodah and Lydia; and my parents for their prayer, love, courage, support and understanding during the long period of my absence, without which it would have been impossible to accomplish this work.

TABLE OF CONTENTS

| | |
|---|----|
| ABSTRACT | iv |
| CHAPTER 1 INTRODUCTION | 1 |
| CHAPTER 2 FLOW INJECTION ANALYSIS | 5 |
| 2.1 INTRODUCTION | 5 |
| 2.2 PRINCIPLES OF FLOW INJECTION ANALYSIS | 7 |
| 2.2.1 Sample Dispersion | 7 |
| 2.2.2 FIA Manifold Design and Chemistry | 14 |
| 2.3 TECHNIQUES | 16 |
| 2.3.1 Multi-line Manifolds | 16 |
| 2.3.2 Merging Zone Principle | 17 |
| 2.3.3 Zone Sampling | 18 |
| 2.3.4 Sample Splitting | 18 |
| 2.3.5 Stopped Flow and Flow Injection Systems with Intermittent pumping. | 19 |
| CHAPTER 3 MEMBRANES AND MEMBRANE SEPARATIONS | 22 |
| 3.1 MEMBRANES | 22 |
| 3.1.1 Homogeneous (Non-porous) Membranes | 23 |
| 3.1.2 Asymmetric (Skin-type) Membranes | 23 |
| 3.1.3 Ion Exchange Membranes | 24 |
| 3.1.4 Microporous Membranes | 25 |
| 3.2 MEMBRANE SEPARATION PROCESSES | 26 |
| 3.3 DIFFUSION | 29 |
| 3.4 GAS DIFFUSION -FLOW INJECTION ANALYSIS (GD-FIA) | 31 |
| 3.4.1 Introduction | 31 |
| 3.4.2 The Transport Process | 32 |
| 3.4.3 Factors Affecting the Transmembrane Rate of Transport | 32 |

| | |
|--|-----------|
| 3.4.4 Membrane Separation Devices used for Gas Diffusion-Flow Injection Analysis | 35 |
| 3.4.3.1 <i>Sandwich Membrane Device</i> | 36 |
| 3.4.3.2 <i>Dual Membrane Sandwich Device</i> | 37 |
| 3.4.3.3 <i>Coaxial Device</i> | 37 |
| 3.4.3.4 <i>Stationary Configuration</i> | 38 |
| 3.4.3.5 <i>Devices with Open Interfaces</i> | 39 |
| 3.4.4 Flow Injection Manifolds Incorporating Separation Devices | 39 |
| CHAPTER 4 GAS/VAPOUR GENERATION | 42 |
| 4.1 HYDRIDE GENERATION | 42 |
| 4.2 GENERATION OF HYDROGEN SULPHIDE | 45 |
| 4.2.1 From Sulphide | 45 |
| 4.2.2 From Sulphate | 47 |
| 4.2.3 From Organic Sulphur Compounds | 48 |
| 4.3 GENERATION OF SULPHUR DIOXIDE | 48 |
| 4.3.1 From Sulphite | 48 |
| 4.3.2 From Sulphur | 50 |
| 4.4 GENERATION OF HALOGENS | 50 |
| 4.4.1 Generation of Bromine | 51 |
| 4.4.2 Generation of Chlorine | 51 |
| 4.5 GENERATION OF CARBON DIOXIDE | 52 |
| 4.5.1 From Organic Carbon | 52 |
| 4.6 GENERATION OF NITROGEN FROM NITROGEN CONTAINING COMPOUNDS | 54 |
| 4.6.1 Methods for Generating Nitrogen | 55 |
| 4.6.1.1 <i>Direct Combustion Method</i> | 55 |
| 4.6.1.2 <i>Kjeldahl-Rittenberg Method (Digestion-Distillation-Oxidation)</i> | 55 |

| | | |
|----------------------|---|---------------|
| CHAPTER 5 | STRIPPING VOLTAMMETRY | 64 |
| 5.1 | INTRODUCTION | 64 |
| 5.2 | PRINCIPLES OF VOLTAMMETRY | 65 |
| 5.3 | MASS TRANSPORT | 65 |
| | 5.3.1 Diffusion | 65 |
| | 5.3.2 Migration | 66 |
| | 5.3.3 Convection | 66 |
| 5.4 | ELECTRON TRANSFER | 67 |
| 5.5 | PRINCIPLES OF STRIPPING VOLTAMMETRY | 68 |
| 5.6 | INSTRUMENTATION | 70 |
| | 5.6.1 Reference Electrode | 70 |
| | 5.6.2 Auxiliary Electrode | 70 |
| | 5.6.3 Working Electrode | 71 |
| | 5.6.3.1 <i>Hanging Mercury Drop Electrode</i> | 71 |
| | 5.6.3.2 <i>Mercury Film Glassy Carbon Electrode</i> | 72 |
| | 5.6.3.3 <i>Chemically Modified Electrode</i> | 73 |
| 5.7 | SUPPORTING ELECTROLYTE | 74 |
| 5.8 | MODES OF STRIPPING VOLTAMMETRY | 74 |
| | 5.8.1 Differential Pulse Cathodic Stripping Voltammetry | 77 |
| | 5.8.2 Adsorptive Stripping Voltammetry | 78 |
| 5.9 | FLOW INJECTION-ELECTROCHEMICAL DETECTION | 79 |
| CHAPTER 6 | ISOTOPE RATIO MASS SPECTROMETRY | 82 |
| 6.1. | INTRODUCTION | 82 |
| 6.2. | PRINCIPLES AND INSTRUMENTATION | 82 |
| | 6.2.1 Ion Production by Electron Impact | 82 |
| | 6.2.2 Ion Separation | 84 |
| | 6.2.2.1 <i>Mass Analysis by Magnetic Sectors</i> | 84 |
| | 6.2.2.2 <i>Quadrupole Mass Analysers</i> | 86 |

| | | |
|------------------|--|-----|
| 6.2.2.3 | <i>Multi-collector Systems</i> | 88 |
| 6.2.3 | Detection of Ions | 88 |
| 6.2.3.1 | <i>The Faraday Cup</i> | 89 |
| 6.2.3.2 | <i>Electron Multiplier Detector</i> | 90 |
| 6.2.4 | Resolution | 91 |
| 6.2.5 | Vacuum System | 91 |
| 6.2.6 | Sample Inlet System | 92 |
| 6.3 | CALCULATIONS AND CORRECTIONS | 93 |
| 6.3.1 | Enrichment Delta | 93 |
| 6.3.2 | Isotopic abundance (Atom %) | 93 |
| 6.3.3 | Instrument corrections | 94 |
| 6.3.3.1 | <i>Carbon Dioxide Corrections (Craig)</i> | 94 |
| 6.3.3.2 | <i>Nitrogen Corrections</i> | 95 |
| CHAPTER 7 | DETERMINATION OF SULPHUR SPECIES | 97 |
| 7.1 | PRELIMINARY INVESTIGATIONS | 97 |
| 7.1.1 | Determination of Sample Injector Loop Volume | 97 |
| 7.1.2 | Calibration of Peristaltic Pumps | 99 |
| 7.2 | DETERMINATION OF SULPHIDE | 101 |
| 7.2.1 | Spectrophotometric Determination of Hydrogen Sulphide/ Sulphide by Methylene Blue Method | 101 |
| 7.2.2 | Generation of H ₂ S in a DPGD-FI System and its Determination by Thermal Conductivity Detector after PTFE Membrane Separation | 106 |
| 7.2.3 | Separation Efficiency of the PTFE Membrane for H ₂ S | 115 |
| 7.3 | DETERMINATION OF SULPHITE | 119 |
| 7.3.1 | Determination of Sulphite as Sulphur Dioxide by a Spectrophotometric Method | 119 |
| 7.3.2 | Separation Efficiency of the PTFE Membrane for SO ₂ | 122 |

| | |
|---|------------|
| 7.3.3 Spectrophotometric Determination of Sulphur Dioxide Generated from Sulphite | 126 |
| 7.3.4 Calibration for Sulphur Dioxide Generation using Off-line Determination of the Gas by UV/VIS Spectrophotometry | 131 |
| 7.3.5 Generation of Sulphur Dioxide from Sulphite in Gas Diffusion-Flow Injection System Interfaced to a Thermal Conductivity Detector | 132 |
| 7.3.6 Generation of Hydrogen Sulphide from Sulphite in the DPGD-FI System using Sodium Borohydride and its Determination by the Methylene Blue Method | 137 |
| 7.4 DETERMINATION OF SULPHATE | 139 |
| 7.4.1 Generation of H ₂ S from Sulphate in the DPGD-FI System and its Determination by UV/VIS Spectrophotometric Method | 139 |
| 7.4.2 Regeneration of Hydrogen Sulphide from Absorbed H ₂ S in Zinc Acetate Solution by Acidification | 140 |
| 7.5 DETERMINATION OF ORGANIC SULPHUR (L-CYSTEINE AND METHIONINE AMINO ACIDS) | 144 |
| 7.5.1 Introduction | 144 |
| 7.5.2 Determination of L-Cysteine as Hydrogen Sulphide by the Methylene Blue Spectrophotometric Method following the Generation and Separation of the Gas in the DPGD-FI System | 145 |
| 7.5.3 Generation of Hydrogen Sulphide from Methionine in the DPGD-FI System and its Determination by the Methylene Blue Method | 147 |
| 7.6 CONCLUSIONS | 147 |
| CHAPTER 8 DETERMINATION OF CARBON AS CARBON DIOXIDE | 151 |
| 8.1 INTRODUCTION | 151 |

| | | |
|------------------|--|-----|
| 8.2 | GENERATION OF CARBON DIOXIDE FROM ORGANIC CARBON IN THE DPGD-FI SYSTEM AND ITS DETERMINATION BY UV/VIS SPECTROPHOTOMETRIC METHOD (TOTAL ORGANIC CARBON (TOC) DETERMINATION) | 151 |
| 8.3 | UV/VIS SPECTROPHOTOMETRIC DETERMINATION OF TOTAL INORGANIC CARBON (TIC) AS CARBON DIOXIDE GENERATED AND SEPARATED IN THE DPGD-FI SYSTEM | 156 |
| 8.4 | DETERMINATION OF $^{13}\text{C}/^{12}\text{C}$ RATIO BY ISOTOPE RATIO MASS SPECTROMETRY | 161 |
| | 8.4.1 Apparatus for Generation of Carbon Dioxide | 162 |
| | 8.4.2 Reagents and Procedure | 162 |
| | 8.4.3 Method of Calculation | 163 |
| | 8.4.4 Results and Discussions | 165 |
| 8.5 | CONCLUSIONS | 169 |
| CHAPTER 9 | NITROGEN CONTAINING COMPOUNDS | 172 |
| 9.1 | INTRODUCTION | 172 |
| 9.2 | CONVERSION OF AMMONIUM-N COMPOUNDS TO NITROGEN | 172 |
| 9.3 | PRINCIPLES OF $^{15}\text{N}/^{14}\text{N}$ ISOTOPIC RATIO MEASUREMENT | 173 |
| 9.4 | THE GENERATION OF NITROGEN GAS AND ITS DETERMINATION BY THERMAL CONDUCTIVITY DETECTOR | 174 |
| 9.5 | THE DETERMINATION OF $^{15}\text{N}/^{14}\text{N}$ RATIO USING THE DPGD-FI SYSTEM INTERFACED TO AN ISOTOPE RATIO MASS SPECTROMETER | 178 |
| | 9.5.1 Precision of Measurement by Isotope Ratio Mass Spectrometer | 179 |
| | 9.5.2 Calibration Procedure | 180 |
| | 9.5.3 Isotopic Enrichment/Depletion | 185 |
| 9.6 | CONCLUSION | 187 |

| | | |
|-------------------|--|------------|
| CHAPTER 10 | DETERMINATION OF HALIDES | 190 |
| 10.1 | INTRODUCTION | 190 |
| 10.2 | GENERATION OF BROMINE IN THE FI SYSTEM AND ITS DETERMINATION BY SPECTROPHOTOMETRIC METHODS AFTER PTFE MEMBRANE SEPARATION | 190 |
| 10.2.1 | Phenolphthalein Method | 190 |
| 10.2.2 | Phenol Red Method | 194 |
| 10.2.3 | N,N-dimethyl- <i>p</i> -phenylenediamine Sulphate Method | 196 |
| 10.3 | SEPARATION EFFICIENCY OF PTFE (1 M LONG) FOR BROMINE GENERATED IN THE FIA SYSTEM | 198 |
| 10.4. | GENERATION OF CHLORINE IN THE DPGD-FI SYSTEM AND ITS DETERMINATION BY A SPECTROPHOTOMETRIC METHOD | 201 |
| 10.4.1 | Phenolphthalein Method | 201 |
| 10.4.2 | Phenol Red | 202 |
| 10.4.3 | N,N-dimethyl- <i>p</i> -phenylenediamine Sulphate Method | 202 |
| 10.5 | SEPARATION EFFICIENCY OF THE PTFE MEMBRANE (1 M LONG) FOR CHLORINE GENERATED IN FI SYSTEM | 205 |
| 10.6 | CONCLUSION | 206 |
| CHAPTER 11 | DETERMINATION OF SELENIUM BY DPGD- /STRIPPING VOLTAMMETRY | 209 |
| 11.1 | INTRODUCTION | 209 |
| 11.2 | DETERMINATION OF SELENIUM BY DIFFERENTIAL PULSE CATHODIC STRIPPING VOLTAMMETRY (DPCSV) ON A HANGING MERCURY DROP ELECTRODE | 213 |
| 11.2.1 | Introduction | 213 |
| 11.2.2 | Effect of varying Deposition Time | 214 |
| 11.2.3 | Influence of Concentration of HCl (Supporting Electrolyte) on Peak Current | 215 |
| 11.2.4 | Effect of using Copper in the Determination of Se (IV) by DPCSV | 216 |

| | |
|--|-----|
| 11.2.5 Effect of changing Deposition Potential on Peak Current | 217 |
| 11.2.6 Effect of changing Scan Rate on Peak Current | 218 |
| 11.2.7 Calibration-Case in which no Cu was not added (Static System) | 219 |
| 11.2.8 Calibration-Case in which Cu was added to enhance Sensitivity (Static System) | 220 |
| 11.2.9 Flow Injection-Selenium Hydride Generation and its Determination by DPCSV on a HMDE after PTFE Membrane Separation (Cu not added) | 222 |
| 11.3 DETERMINATION OF SELENIUM (IV) IN THE PRESENCE OF COPPER BY DIFFERENTIAL PULSE CATHODIC STRIPPING VOLTAMMETRY AT MERCURY FILM GLASSY CARBON ELECTRODE | 226 |
| 11.3.1 Effect of varying Deposition Potential on Peak Current | 227 |
| 11.3.2 Effect of varying Scan Rate on Peak Current | 228 |
| 11.3.3 Effect of varying Cu Concentration on Peak Current | 229 |
| 11.3.4 Calibration | 230 |
| 11.3.5 On-line Generation of Selenium Hydride in the DPGD-FI system followed by its Oxidation to Se(IV) by Ce(IV) and Subsequent Determination of Se(IV) by DPCSV at MFGCE (Wall Jet Electrode) | 232 |
| 11.4 DETERMINATION OF Se(IV) BY DIFFERENTIAL PULSE CATHODIC STRIPPING VOLTAMMETRY AT A Hg-Cu FILM ON A GLASSY CARBON ELECTRODE (STATIC SYSTEM) | 236 |
| 11.5 DIFFERENTIAL PULSE CATHODIC STRIPPING VOLTAMMETRIC DETERMINATION OF SELENIUM (IV) ON HANGING MERCURY DROP ELECTRODE MODIFIED WITH POLY-L-LYSINE | 236 |
| 11.5.1 Without Poly-l-lysine modifier | 237 |
| 11.5.2 With Poly-l-lysine and Copper | 238 |
| 11.6 PRELIMINARY EXPERIMENTS PERFORMED USING A CHEMICALLY MODIFIED MERCURY FILM ELECTRODE | 240 |

| | | |
|-------------------|--|------------|
| 11.7 | DETERMINATION OF SELENIUM (IV) BY DIFFERENTIAL PULSE CATHODIC STRIPPING VOLTAMMETRY AT MODIFIED MERCURY FILM ELECTRODE | 242 |
| 11.7.1 | Using Poly-l-lysine | 243 |
| 11.7.2 | Using Hexadecyltrimethyl ammonium bromide | 243 |
| 11.7.3 | Discussion | 248 |
| 11.8. | CONCLUSIONS | 249 |
| CHAPTER 12 | CONCLUSIONS AND RECOMMENDATIONS FOR FURTHER WORK | 252 |
| 12.1 | CONCLUSIONS | 254 |
| 12.2 | RECOMMENDATIONS FOR FURTHER WORK | 255 |

LIST OF ABBREVIATIONS

| | |
|--------|---|
| AAS | Atomic Absorption Spectroscopy |
| AES | Atomic Emission Spectroscopy |
| ASV | Anodic Stripping Voltammetry |
| DPCSV | Differential Pulse Cathodic Stripping Voltammetry |
| DPGD | Dual Phase Gas Diffusion |
| DPSV | Differential Pulse Stripping Voltammetry |
| EI | Electron Impact |
| FI | Flow Injection |
| FIA | Flow injection Analysis |
| GC | Gas Chromatography |
| GD | Gas Diffusion |
| GMPAS | Gas Phase Molecular Absorption Spectrometry |
| HG | Hydride Generation |
| HMDE | Hanging Mercury Drop Electrode |
| ICP | Inductively Coupled Plasma |
| IRMS | Isotope Ratio Mass Spectrometry |
| MECA | Molecular Emission Cavity Analysis |
| MIP | Microwave Plasma Emission |
| MFE | Mercury Film Electrode |
| MFGCE | Mercury Film Glassy Carbon Electrode |
| MS | Mass Spectrometry |
| PTFE | Polytetrafluoroethylene |
| RSD | Relative Standard Deviation |
| TCD | Thermal Conductivity Detector |
| TCM | Tetrachloromercurate (II) |
| TOC | Total Organic Carbon |
| UV/VIS | Ultraviolet/Visible |

**PAPERS IN PREPARATION FOR PUBLICATION AND MEETINGS
ATTENDED**

“Generation of SO_2 in the Dual Phase Gas Diffusion-Flow Injection System and Subsequent Determination by the Thermal Conductivity Detector”, B. L., Sharp and Onditi Ouma Anam.

“Determination of Hydrogen Sulphide Generated from Sulphide in the Dual Phase Gas Diffusion-Flow Injection System by the Thermal Conductivity Detector”, B. L. Sharp and Onditi Ouma Anam.

“Generation of Hydrogen Selenide from Se(IV) and its Separation in the Dual Phase Gas Diffusion-Flow Injection System and Subsequent Oxidation to Se(IV) by Ce(IV) prior to its Determination by the Differential Pulse Cathodic Stripping Voltammetry”, B. L. Sharp and Onditi Ouma Anam, Seminar held by the Royal Society of Chemistry, Analytical Division at Nottingham Trent University, 22-23 July 1996.

Chapter 1

CHAPTER ONE

INTRODUCTION

Isotope tracer methods have become a standard technique in biological, agricultural, chemical and medical research.¹ Such methods depend on the assumption that the isotopes of a given element are identical in their chemical behaviour.² As a basic requirement, the tracer should therefore behave in the same manner as the indigenous element. However, due to its different isotopic composition, identification of the tracer is possible at any stage of the process. The quantitative evaluation of results is based on the isotope dilution law that states that the ratio of tracer to indigenous isotope is constant for a system in equilibrium.¹ The tracer compound is often a radioactive isotope and the ratio of tracer to carrier in a sample can be determined by suitable detectors such as: Geiger Muller counters and liquid scintillation counters which have excellent sensitivity. The use of stable isotopes, in comparison to radioactive isotopes, as tracers is not complicated by health hazards, dangers of radiation to biological materials or time limit to the duration of experiments.³ The analytical methods available for the detection and determination of stable isotopes are much less sensitive, considerably more complicated and time consuming than the methods for radioactive isotopes. Generally, such methods require the use of a mass spectrometer which is an expensive instrument demanding continual care and skill for its successful operation.

The technique of ^{15}N labelling has become an accepted method for the investigation of the nitrogen cycle.⁴ Isotopic tracer studies of the nitrogen cycle have increased dramatically due to the availability of high precision isotope ratio mass spectrometers. Important agricultural applications of ^{15}N as a tracer have been in studying: the movement of nitrogen between soil and atmosphere through nitrogen fixation, NH_3 volatilisation and denitrification; the fate of fertiliser nitrogen applied to the soil, uptake and utilisation of this element by crops and metabolism in plants.⁵ In addition, it is important to obtain quantitative information on the nitrogen balance of the total biosphere

because of the possible consequence on the environment of the increasing use of nitrogen fertiliser. ^{15}N and ^{13}C have been used in pharmacology, as tracers for the identification of metabolites, and as internal standards for the estimation of drugs in biological fluids.⁴ In atmospheric pollution monitoring, the fate of man-made CO_2 can be studied by $^{13}\text{C}/^{12}\text{C}$ ratio determination. Such ratios, obtained from CO_2 , from the combustion of wood cellulose provides information on the global distribution of fossil fuel-derived from CO_2 . Also, the $^{13}\text{C}/^{12}\text{C}$ ratio has been used to detect adulteration of foods. This is possible because the ^{13}C content of the genuine component is different from that of the adulterant. ^2H tracer has been applied in clinical studies to determine total body water in situations where fluctuation of body hydration occurs.⁴ It has been suggested that ^{34}S may be useful in agricultural research on problems related to sulphur deficiency in the soil,⁴ and for environmental studies. ^{18}O can be used in studies of the mechanism of photosynthesis.⁴

Most of the mass spectrometers used for determining the total concentration of major elements (H, N, O, S) and isotope ratio determinations depend on the combustion technique (Dumas method^{1,5}) for sample presentation. These instruments are quite expensive and their operation is labour intensive as sample handling, including weighing, is performed manually. The consumables and catalysts employed are also costly. In addition, these instruments are suitable for the analysis of solids, but not for liquids. The requirements for the analytes used in such instruments are that they must be thermally stable, but easily volatilised. However, considerable loss of analyte occurs when volatile compounds are used. The other limitation to this method is that it cannot be used for speciation of non-volatile compounds. The speciation of volatile compounds, however, can be achieved by an isotope ratio mass spectrometer interfaced to a gas chromatograph. This involves the separation of various components of the sample by gas chromatography before individual components are introduced into the combustor/mass spectrometer for isotope mass ratio determination. Coupling of gas chromatography to mass spectrometry adds considerably to the cost of the system, causing an increase in the analysis cost for each sample.

To overcome these problems, it is important that a cheaper method of sample preparation is developed to replace the combustion system, thus reducing the overall cost of the instrument and the cost of each determination. In addition, this allows speciation to be performed by mass spectrometry without having to employ a GC/combustion interface. Wet methods for sample preparation, involving vapour generation, can be used to solve these problems. One of the most convenient ways of implementing this is by using flow injection technology. The vapour is generated on-line by chemical reaction of the sample and reagents and separated by a gas-liquid separator before its determination by mass spectrometry. The reason for using flow injection analysis is to take advantage of its benefits which include: simplicity in terms of hardware and operation, chemical versatility of the method, reproducibility of results and high sample throughput. Additionally, flow injection analysis allows chemical reactions to be performed on-line and the gaseous product to be monitored by the detector, without the reaction necessarily reaching a steady state.

REFERENCES

1. Fielder, R. and Proksch, G., *Anal. Chim. Acta*, 1975, **78**, 1.
2. Kolthoff, I. M. and Elving, P. J., *Treatise on Analytical Chemistry*, Interscience, New York, 1967, pp. 29-31.
3. Bremner, J. M., in *Methods of Soil: Part 2 Chemical and Microbiological Properties*, Ed. Black, C. A., American Society of Agronomy, Madison, 1969, pp. 1256-1286.
4. Elvidge, J. A. and Jones, J. R., *Isotope: Essential Chemistry and Applications*, Chemical Society, London, 1979.
5. Robinson, D. and Smith, K. A., in *Soil Analysis: Modern Instrumental Techniques*, 1991, Ed. Smith, K. A., Marcel Dekker, New York, 2nd Edn., pp. 465-503.

Chapter 2

CHAPTER TWO

FLOW INJECTION ANALYSIS

2.1 INTRODUCTION

Routine chemical analysis involves a number of operations such as: pipetting, diluting, mixing, filtering and transfer of solutions to analytical instruments which can be repetitive.¹ An analytical chemist performing such operations manually would take a long time to complete the analysis of a large number of samples of similar nature for the determination of a single species. Such problems are encountered in clinical chemistry, environmental studies and control, industrial processes and quality control.² Automation of the sample introduction steps and detection results in a decrease in analysis time and operating cost per determination.

Automated analysers are therefore commonly used in laboratories where large numbers of samples are received for analysis and the results are required within a short period. The advantages attributed to the use of automated analysers include: handling of large numbers of samples which can be processed with acceptable precision and accuracy, a meaningful statistical treatment of data, elimination of human participation in many routine manipulations and the more efficient use of reagents.²

Automated analysers can be classified into batch and continuous flow analysers, the classification being based on the design and method of operation.³ In batch analysers, each discrete sample is assigned a container, which may be a sample cup or a sample bag, within which it is held through all the steps of analysis. This approach has one major advantage of preventing cross-contamination between samples, hence samples preserve their identity and cannot be mismatched as each container carries an identification label. Batch analysers, however, suffer from one serious disadvantage, that of being mechanically very complex as they have many moving parts that may become worn out and hence require replacement.

In continuous flow analysers, the samples are analysed in a flowing stream of fluid. A pump (usually a peristaltic pump) is used to propel the carrier and reagent streams within the conduits of the analyser. The pump also takes care of aspiration of the sample.³ Operations such as dialysis, filtration, extraction, decantation, dilution, preconcentration, addition of reagents and mixing can be performed in the flowing stream before the analyte is measured by a flow-through detector. The first commercial continuous flow analyser was developed by Skeggs, and was based on air-segmentation.⁴ The advantages offered by air-segmented continuous analysers include: a reduction of reagent consumption, a high sample throughput and allowing different assays to be performed simultaneously since the pump head can be made to accommodate many flow streams. Air-segmentation is used to: limit sample dispersion, minimise carry-over and cross-contamination, facilitate mixing of samples with reagents by generating turbulent flows and to scrub the walls of the analytical conduits.⁵

There are, however, disadvantages in using air segmentation. For example, the presence of air causes a pulsation of the flow, because of its compressibility, which in turn leads to instability of the analytical signal.⁶ A debubbler has to be used to remove air from the stream before it enters the flow-through detector. Other problems associated with using air bubbles include: controlling the size of the air bubbles, variation of the pressure drop and flow velocities for different tubing materials and build up of static electricity which disturbs potentiometric sensors since air bubbles in plastic tubes act as electrical insulators. Air bubbles also lower the efficiency of dialysis, gas diffusion across membranes and solvent extraction. Additionally, the movement of the carrier stream cannot be exactly controlled, instantly stopped or restarted.⁷ The use of chromatographic columns is also incompatible with the presence of air bubbles.

To solve the problems caused by air segmentation, electronic gating of the detector (bubble gating in the flow cell) has been incorporated into the design of an air-segmented continuous analyser.^{8,9} However, this kind of system is very expensive. For air-segmented

continuous flow analysers, the portion of the peak that can be used for quantitation is the steady state plateau where chemical reactions have come to equilibrium.

Ruzicka and Hansen ³ and Stewart ¹⁰ independently introduced a new concept of continuous flow analysis, based on injecting the sample into a rapidly flowing carrier stream, which has no air-segmentation, this is known as Flow Injection Analysis (FIA).

2.2 PRINCIPLES OF FLOW INJECTION ANALYSIS

Flow injection analysis is that type of continuous flow analysis that uses an unsegmented continuous carrier stream into which highly reproducible volumes of sample are injected with subsequent detection of the analyte. The technique of flow injection analysis depends on reproducible timing and sample injection, and controllable sample dispersion.^{3,11} This feature obviates the requirement of reaching steady state which is in great contrast to the approach taken in air-segmented continuous flow analysers.

2.2.1 Sample Dispersion

When a sample is injected into the carrier stream, it forms a zone that is transported to a detector.⁷ A typical single-line flow injection analysis manifold is shown in Figure 2.1.

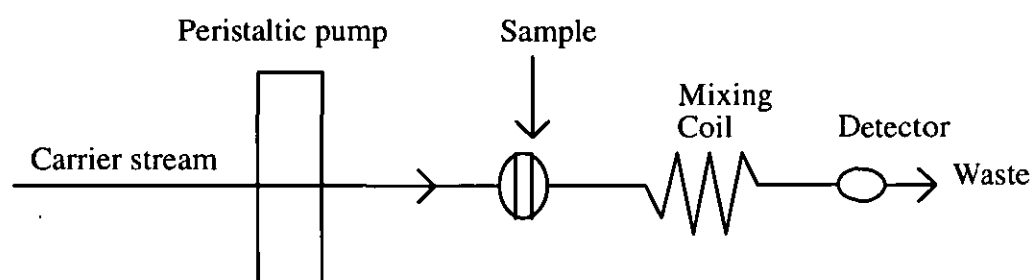


Figure 2.1 Single-line flow injection analysis manifold

As the sample moves downstream, under laminar flow conditions, dispersion occurs to form a concentration gradient as shown in Figure 2.2. The magnitude of dispersion in a practical

system depends on factors such as sample volume, tube length, tubing bore size, flow rates, and coil diameters.

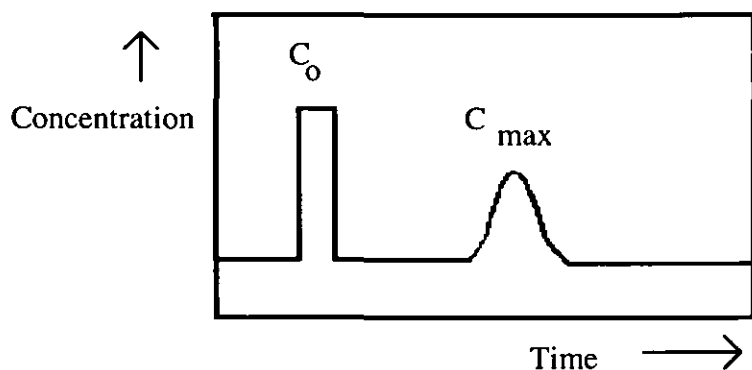


Figure 2.2 Concentration of the sample before and after passing through the FIA system.

Dispersion may be controlled by varying these factors, thus allowing optimisation of flow injection analysis for many applications.⁵ The dispersion D has been defined as the ratio of original analyte concentration C_o to the concentration of the analyte in that element of fluid corresponding to the maximum of the peak C_{max} .^{12,13} Thus

$$D = \frac{C_o}{C_{max}} \quad (2.1)$$

The dispersion coefficient (D) allows comparison of different manifolds and also provides a means of varying and monitoring the extent of sample dilution.¹¹

Ruzicka and Hansen^{12,13} classified dispersion as limited, medium and large depending on the value of the dispersion coefficient, D . Limited dispersion ($D = 1-3$) is preferred when FIA is used simply as a sample presentation technique and minimum or zero sample dilution is required. Medium dispersion ($D = 3-10$) can be used for procedures in which reagents are mixed to form coloured, electroactive, fluorescent, and other products that can be sensed by

a flow through detector. Large dispersion ($D > 10$) can be used to give a significant degree of mixing between the sample and carrier stream to form a well developed gradient, as is necessary when carrying out continuous flow titrations.⁵

The mechanisms contributing to the dispersion of the injected sample in the FIA manifold are convective and diffusional transport.¹⁴ These are shown in Figure 2.3.

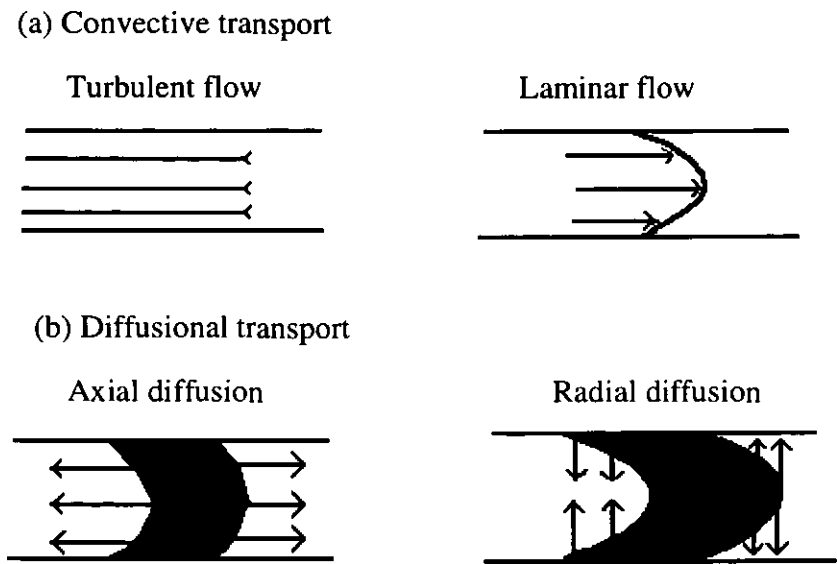


Figure 2.3 Types of transport in closed tubes: (a) convective transport (b) diffusional transport.

Convective transport, occurring under laminar flow conditions, yields a parabolic velocity profile with molecules at the tube walls having zero linear velocity while those at the centre travel at twice the mean velocity. Diffusional transport consists of axial and radial diffusion. Axial diffusion is due to the horizontal concentration gradient at the leading and trailing edges of the injected sample zone. This contributes minimally to the overall dispersion. Radial diffusion, on the other hand, results from the concentration differences perpendicular to the direction of the flow. This type of diffusional transport contributes significantly to the overall dispersion. This is due to its tendency to balance

concentrations such that the molecules located at the tube walls tend to move to the centre, whereas those at the centre travel outwards. The time dependant concentration profile of the sample injected into the FIA manifold and the various types of transport are time dependent as shown in Figure 2.4

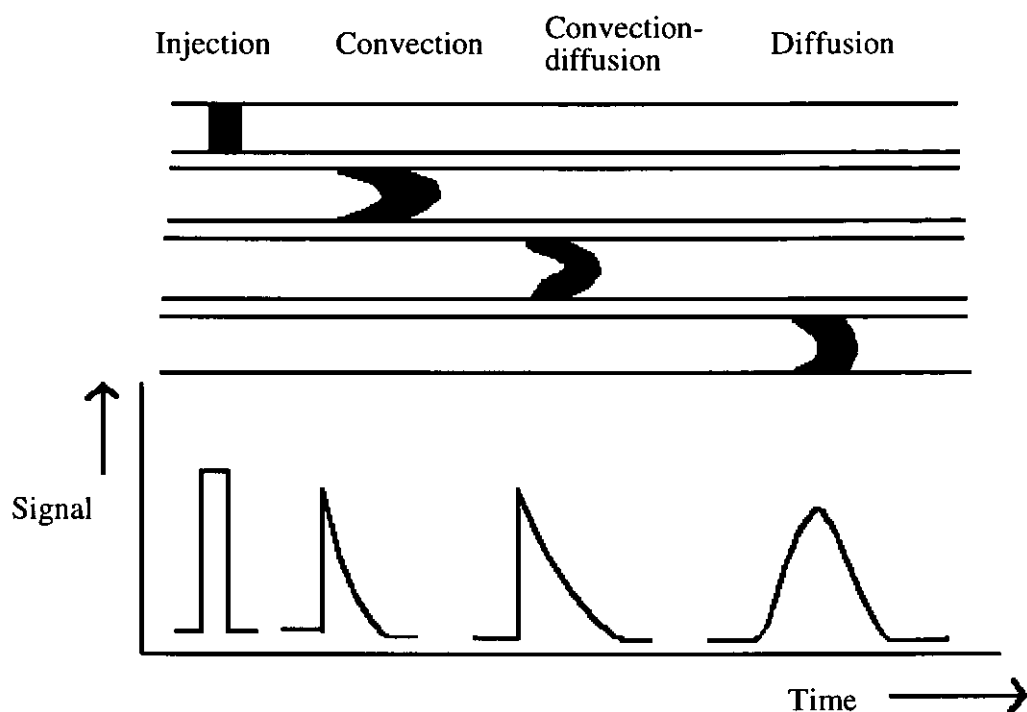


Figure 2.4 Sample dispersion and signal profile

During the early stages of sample introduction into the continuous carrier stream, the shape of the sample bolus is controlled by convection. However, diffusion predominates in the later stages.

Taylor^{15,16} and Aris¹⁷ derived a theory describing these two limiting situations. According to Taylor,^{15,16} when a sample is introduced into a liquid stream moving in laminar flow and disperses by convection alone, the shape of the sample plug becomes distorted in time in a paraboloid. In addition, he showed that the effect of molecular diffusion gives rise to dispersion with an apparent diffusion coefficient, k , given by:

$$k = \frac{a^2 u^2}{48D} \quad (2.2)$$

where D is the molecular diffusion coefficient, a is the radius of the tube and u is the velocity of the liquid stream. Aris found that the distribution tends to normality and that the effective distribution coefficient (K) is the sum of the molecular diffusion coefficient (D) and Taylor's apparent distribution coefficient (k). Thus

$$K = k + D \quad (2.3)$$

Therefore:

$$K = D + \frac{a^2 u^2}{48D} \quad (2.4)$$

Taylor's solutions only hold for low flow-rates and very long reactors which help to compensate for radial concentration changes and favour the diffusion phenomenon. These solutions do not apply to most FIA systems because the nature of the dispersion in these systems is an intermediate one in which both convection and diffusion play a significant part.¹⁸ Vanderslice *et al.* have demonstrated that FIA systems can be described in terms of laminar flow equations.¹⁸ These relate to diffusion-convection processes that operate in the laminar flow region where flow injection analysis experiments are generally carried out. The solutions of these equations give expressions for the initial appearance of a peak at the detector (travel time from injection valve to detector) and the total time of observation of the peak (baseline to baseline time duration which is a measure of dispersion). The Vanderslice expressions which relate the travel time (t_a) and baseline-to-baseline time (Δt_B) to the geometric and hydrodynamic characteristics of the FIA system are shown below.

$$t_a = \frac{109a^2 D^{0.025}}{f} \frac{L^{1.025}}{q^{1.025}} \quad (2.5)$$

$$\Delta t_B = \frac{35.4a^2f}{D^{0.36}} \frac{L^{0.64}}{q^{0.64}} \quad (2.6)$$

where q is the flow rate; L , the tube length; a , the radius of the tube; D , the diffusion coefficient; and f , an empirical factor varying with experimental conditions from 0.5-1.0.

The overall dispersion within the FIA system can be taken as the sum of dispersion arising from the injection, transport and detector as follows:

$$D = D_{\text{injection}} + D_{\text{transport}} + D_{\text{detector}} \quad (2.7)$$

where $D_{\text{injection}}$ is the dispersion due to the sample volume and to the geometric aspects of the system, $D_{\text{transport}}$ is the dispersion due to the reaction geometry and the flow-rate, and D_{detector} is the dispersion due to the flow cell. The $D_{\text{transport}}$ makes the most significant contribution to the overall dispersion. The dispersion in a FIA manifold caused by flow in the narrow tube increases with the square root of the mean residence time according to the following equation:⁷

$$D = \frac{2\pi^{3/2}R^2D_f^{1/2}T^{1/2}}{S_v} \quad (2.8)$$

where D_f is the axial dispersion coefficient, R is the tube radius, T is the residence time and S_v is the sample volume. An expression for the dispersion coefficient of an FIA system which relates it to the geometric characteristics of the reactor (length, radius), some hydrodynamic aspects (linear velocity and residence time), and the injected sample volume (S_v) has also been proposed.¹⁴

$$D = \frac{2\pi^{3/2}R^2(Lu\delta t_r)^{1/2}}{S_v} \quad (2.9)$$

where L is the length of the tube, u is the linear velocity, t_r is the mean residence time, S_v is the injected sample volume and δ is the longitudinal dispersion number which is related to the standard deviation of a non-Gaussian FIA curve according to the following:

$$\delta = \frac{1}{8}(8(\sigma^2 + 1)^{1/2} - 1) \quad (2.10)$$

where σ is the standard deviation of a non-Gaussian curve.

The dispersion of a sample can be manipulated by changing the flow rate, sample volume, tube length, and tube internal diameters. If the desired dilution has not been obtained after changing these parameters, a mixing chamber may be incorporated into the FIA system. The inclusion of a mixing chamber in a FIA system has the effect of creating a broad peak with a long tail. There will be reduction of sample throughput when the mixing chamber is included in the FIA as the introduction of the next sample can only be made after the entire tail of the preceding sample has left the detector. To solve the problems of peak broadening and peak tailing, zone sampling and sample splitting techniques are used.¹¹

Coiled tubes are a commonly used reactor geometry because this can conveniently accommodate any length of tubing in the experimental set-up. In addition, the secondary flow within the coiled tube promotes mixing in the radial direction, resulting in more symmetrical, higher and narrower peaks than those obtained in identical straight tubes.⁷ Knitted coils have also been applied in FIA.¹⁹ Knitting has been found to be most convenient for short reactors, being useful for promoting intense mixing. Long coils should be avoided because as the reaction coil length increases, troubles arise from increase in the hydrodynamic pressure and decrease in the analytical speed. The single string bead reactor²⁰ has also been used. This reactor was formed by using a pipette and a

funnel to pack dry glass beads with a mean diameter of 0.4 mm into a polyethylene tube of 0.6 mm diameter.

2.2.2 FIA manifold design and chemistry

The design of the FIA manifold is very important to the analytical chemist because it determines the extent of sample dispersion or dilution that takes place as the sample moves through the manifold. It is important that the injection valve and connectors should have effectively zero dead volume, and the flow cell volume should be as small as possible so that they do not significantly contribute to the overall dispersion in the system. By varying the configuration of the analytical manifold, undesirable sample dispersion can be avoided and controlled.

Changes in manifold design are usually made to cater for the specific needs of the method and detector being used.¹¹ The optimisation of manifold design for carrying out particular chemistry takes priority over the concern of minimising sample dispersion. For example, for a flow injection analysis system in which a chemical reaction between the sample and reagent occurs to form a product, a change in total flow rate results in a change in the signal obtained. Increasing the total flow rate has the effect of decreasing the reaction time. This means that for a chemical reaction which is not at equilibrium, as is sometimes the case in FIA methods, the time available for the reaction to proceed towards equilibrium is reduced, resulting in a lower signal.¹¹

The effect of changing the flow rate ratio (in multi-line manifolds-see next section) may result in a change in total flow rate, hence the reaction time would change with subsequent change in signal. Further, the resulting change in relative concentration of sample and reagent may change the rate of product formation. This is dependent on the reaction kinetics and that the chemical reaction has not attained equilibrium.¹¹

The effect of changing the coil length would change the observed signal for a reaction that has not reached equilibrium. Increase in coil length results in an increase in reaction time. Changes in internal diameter of the coil may also have a significant effect on the observed signal especially if the change is large.

Changes in sample volume would effect the observed signal, but most of this observed change would be due to physical dispersion characteristics and not any chemical kinetic effects.

Generally, improved sensitivity can be obtained by allowing a reaction to proceed closer to equilibrium. As has been shown, this increase in residence time can be achieved by a number of ways. However, the most effective means is that which increases the residence time without unduly increasing the dispersion. For example, stopped flow conditions completely remove convective dispersion (although diffusive dispersion still occurs) and allow long reaction times. Similarly, a heated reactor can enhance reaction rates without greatly affecting dispersion.¹¹ Also, coiled and other secondary flow reactors increase residence time whilst minimising dispersion.

When a chemical reaction is to take place in the flow injection manifold, the effects of stoichiometry and chemical kinetics are mapped onto the dispersion characteristics of the manifold. Provided that the reaction is fast and the reagents are in excess at all points in the manifold, then the observed profile is that due to the physical process alone. However, if the reaction is slow compared with the residence time and if the reaction stoichiometry is not satisfied, distortion of the signal peak will occur.

2.3 TECHNIQUES

2.3.1 Multi-line manifolds

A dual-line, single reagent FIA manifold is shown in Figure 2.5 in which a sample is injected into a carrier stream and subsequently merged with the reagent stream, at the point of confluence, before passing through the mixing coil to the detector.

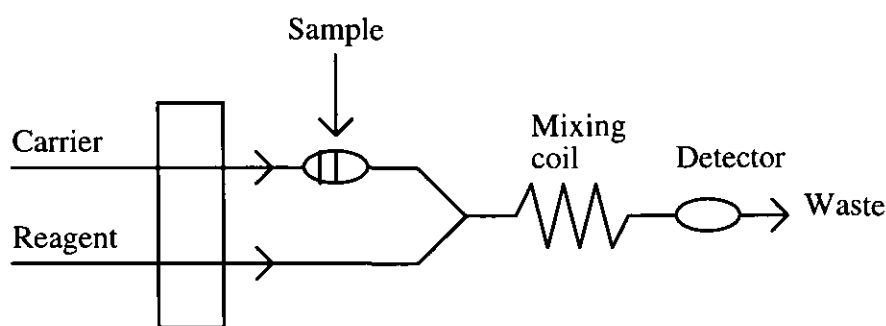


Figure 2.5 Dual-line FIA system

A peristaltic pump is used to propel the carrier and reagent streams. The flow characteristics and mixing are very reproducible at the point where union of sample and reagent occurs. With reproducible physical mixing, measurement of the signal can be done at any point on the rising part of the peak and not necessarily at the plateau where steady state conditions have been achieved.¹³ Addition of chemical reactions to a FIA system does not significantly change the physical characteristics such as, the reproducible physical mixing. However, since temperature and pressure affect the chemical kinetics, these parameters should be held constant in FIA systems. A FIA manifold with multi-channels, works on the same principle as the dual line system. In a multi-line system, the location of the merging points depends on function of the channel and are dictated by the sequence of the processes prior to detection.

2.3.2 Merging zone principle

Bergamin *et al.*²⁵ used the merging zone principle to solve the problems caused by the momentary disturbance of regular flow when the sample is forced into the carrier stream.

This can cause a change in the blank values when the reagent absorbs significantly at the wavelength used. The peaks due to very dilute sample will be distorted or negative peaks may appear. To solve these problems, while increasing sensitivity, the confluence configuration was used (see Figure 2.6). The determination of nitrite, sulphate and chloride were carried out using this technique. The normal configuration (where sample was directly introduced in the moving carrier stream) was compared with the confluence configuration for the determination of chloride by the UV/VIS spectrophotometric method. It was observed that better peak shape was obtained by employing the confluence configuration as compared to the straight configuration in which peak distortion occurred. This was due to the attenuation of the dilution effect by better conditions of mixing between the sample and the reagent at the confluence point. In the confluence configuration, the sample was injected into the water stream and not into the reagent stream. At the confluence point, the sample plug in the water stream and the reagent stream met, mixed partly, and were carried to a reaction coil to facilitate further mixing.

A double merging zone principle was also described to minimise the use of expensive reagents.²⁶ In this method, both sample and reagent were introduced into inert carrier streams, with synchronised merging and interaction. The merging zone system suffers from one main drawback, that of variable baseline signal.⁷

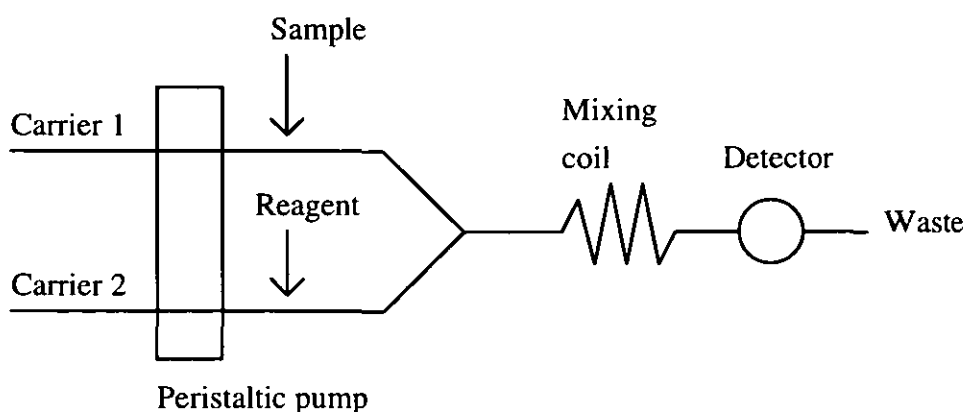


Figure 2.6 Confluence configuration arrangement.

2.3.3 Zone sampling

Zone sampling is based on injection of sample into an initial carrier stream where it is diluted and a considerable peak broadening takes place. The dispersed sample is directed to a second injection port which cuts a selected portion of the entire sample zone and injects it into the second carrier stream.¹¹ The timing between injection in carrier streams 1 and 2 can be used to vary the degree of dilution. Precise timing is essential in this process.

One advantage of the zone sampling technique is that a high degree of dispersion is more efficiently achieved by sampling a small portion of a dispersed zone, and injecting it into a second carrier stream, than the use of very small volumes, long coils or mixing chambers. The other advantages of this technique include the possibility of carrying out simultaneous determinations of species and the construction of calibration graphs with one standard by using suitable time interval values.²⁷

2.3.4 Sample splitting

Sample splitting can be achieved by injecting a sample into a continuous carrier stream, followed by diversion of a major portion of the sample zone to waste and its replacement by

a new carrier stream or reagent stream.¹¹ Since the flow rate is slow between diversion and merging points, the distance between these points should be kept short.

2.3.5 Stopped flow and flow injection systems with intermittent pumping

In order to increase the residence time of a sample in a FIA system, the velocity of the carrier stream should be decreased rather than increasing the length of the reaction coil, because the latter technique results in a greater increase in dispersion.¹³ When the carrier stream ceases to move (when flow rate is zero), convective dispersion also ceases, and the dispersion coefficient D becomes independent of time. By using intermittent pumping, the reaction time is increased during the stop interval when the carrier stream does not move. The sample zone can be reproducibly held within the flow cell by using electronic timing which is activated by a microswitch connected to the injection valve. The delay time and length of stop time can be chosen to suit a specific chemical reaction rate.¹²

Intermittent flow systems have been used in clinical chemistry for enzymatic glucose determination using glucose dehydrogenase coupled with spectrophotometric measurement of the co-enzyme NADH.²⁸ They have also been used for the determination of sulphur dioxide, using a formaldehyde catalyst, to form a coloured complex of *p*-rosaniline which is detected by spectrophotometry.

The stop flow technique may use any section of a dispersed sample zone for measurement. Dispersion along the peak zone can be exploited to optimise the sample/reagent ratio for a particular assay without the need to change any other feature of the manifold.¹³

REFERENCES

1. Smith, K. A. and Scott, K. A., in *Soil Analysis-Modern Instrumental Technique*, Ed. Smith, K. A., Marcel Dekker, New York, 2nd edn., 1991, pp 183-227.
2. Mottola, H. A., *Anal. Chem.*, 1981, **53**, 1312A.
3. Ruzicka, J. and Hansen, E. H., *Anal. Chim. Acta*, 1975, **78**, 145.
4. Stewart, K. K., *Talanta*, 1981, **28**, 789.
5. Ranger, C .B., *Anal. Chem.*, 1981, **53**, 20A.
6. Wamsley, T. A., Abernathy, M. H. and Fowler, R. T., *Clin. Chem.*, 1980, **26**, 530.
7. Ruzicka, J. and Hansen, E .H., *Flow Injection Analysis*, New York; John Wiley and Sons, 1988.
8. Patton, C. J., Rabb, M. and Crouch, S. R., *Anal. Chem.*, 1982, **54**, 1113.
9. Vogt, W., Braun, S. L., Wilhelm, S. and Schwab, H., *Anal. Chem.*, 1982, **54**, 596
10. Stewart, K. K., Beecher, G. R. and Hare, P. E., *Anal. Biochem.*, 1976, **70**, 167.
11. Karlberg, B. and Pacey, G. E., *Flow Injection Analysis-A Practical Guide*, Amsterdam, Elsevier, 1989.
12. Ruzicka, J. and Hansen, E. H., *Anal. Chim. Acta*, 1980, **114**, 19.
13. Ruzicka, J. and Hansen, E. H., *Anal. Chim. Acta*, 1978, **99**, 37.
14. Valcarcel, M., Laque de Castro, M. D., *Flow Injection Analysis: Principles and Applications*, Ellis Horwood, New York, 1987, p 56-99.
15. Taylor, G., *Proc. Roy. Soc. Lond.* 1953, **A219**, 186.
16. Taylor, G., *Proc. Roy.Soc. Lond.* 1954, **A223**, 446.
17. Aris, R., *Proc. Roy. Soc. Lond.* 1956, **A235**, 67.
18. Vanderslice, J. T., Stewart, K. K., Rosenfeld, A. G. and Higgs, D. J., *Talanta*, 1981, **28**, 11.
19. Ruzicka, J. and Hansen, E. H., *Anal. Chim. Acta.*, 1984, **161**, 1.
20. Reijn, J. M., Van Der Linden, W. E., and Poppe, H., *Anal. Chim. Acta*, 1981, **123**, 229.
21. Canham, J. S., and Pacey, G. E., *Anal Chim. Acta*, 1988, **214**, 385.
22. Miyazaki, A. and Reimer, R..A., *J. Anal. At. Spectrom.*, 1993, **8**, 449.

23. Stroh, A., and Vollkopf, U., *J. Anal. At. Spectrom.*, 1993, **8**, 35.
24. Wang, X., Viczian, M., Lasztity, A. and Barnes, M., *J. Anal. At. Spectrom.*, 1988, **3**, 821.
25. Bergamin, F. H., Reis, B. F. and Zagatto, E. A. G., *Anal. Chim. Acta*, 1978, **97**, 427.
26. Bergamin, F. H., Krug, F. J. and Zagatto, E. A. G., *Anal. Chim. Acta*, 1978, **101**, 17.
27. Reis, B. F., Jacintho, A. O., Mortatti, J., Krug, F. J., Zagatto, E. A. G., Bergamin, F. H. and Pessenda, L. C. R., *Anal. Chim. Acta*, 1981, **123**, 221
28. Ruzicka, J. and Hansen, E. H., *Anal. Chim. Acta*, 1979, **106**, 207.

Chapter 3

CHAPTER THREE

MEMBRANES AND MEMBRANE SEPARATIONS

3.1 MEMBRANES

A membrane can be defined as a semi-permeable barrier between two phases, which prevents intimate contact between phases and restricts the movement of molecules across it in a very specific manner.¹ This barrier can be solid, liquid or gas. The manner of restriction of molecular motion by membranes can take several forms which include size exclusion, differences in diffusion coefficient, electrical charge and differences in solubility.

Separation of substances by membranes has not been widely used in analytical chemistry because they are expensive and are generally sensitive to temperature, pH and chemical environment.^{1,2} Also, membranes may also suffer from fouling (any coating on the membrane surface which reduces the flux or separation performance). However, there are several advantages that can be achieved by using membrane separation of substances in analytical chemistry. These include: simplicity and compactness in the design of apparatus, ecological cleanliness, the continuous nature of the process and the possibility of automation.² These advantages have led to the rapid development and use of technological process such as the desalination of natural waters by reverse osmosis and electrodialysis, the membrane separation of mixtures and ultra filtration production of enzymes.

Membranes can be classified on the basis of material (natural/synthetic), structure (porous/non-porous), application and mechanism of action (adsorptive, diffusive, ion-exchange and non-selective). Since a synthetic membrane has been employed in this study, types of synthetic membranes will be discussed.

3.1.1 Homogeneous (non-porous) membranes

These membranes consist of a homogeneous film across which a mixture of chemical species is transported by molecular diffusion (permeation). The separation of components in a mixture is directly related to transport rates within the interface, which are determined by both diffusivities and concentration of each component in the film. Chemical species of similar size, and hence similar diffusivity, can be separated efficiently by homogeneous membranes when their concentrations are significantly different.³ The transport across the homogeneous membrane is based on both solubility and molecular diffusion.⁴ The overall process involves dissolution of the analyte in the membrane, diffusing transport in the condensed phase across the membrane and desorption (evaporation, diffusion) on the other side where it is absorbed by a suitable acceptor stream. The solubility and not volatility of the species determines the selectivity of the membrane separation. Silicone rubber (polydimethylsiloxane) is the most commonly used material for preparing homogeneous membranes due to its chemical and mechanical stability and high permeation rates for a variety of analytes.

3.1.2 Asymmetric (skin)-type membranes

These are membranes which have a graduated or laminated structure which influences the transport properties.⁵ The structure of asymmetric membranes consists of an extremely thin (0.1-1 μm) polymer layer (skin) supported on a 1 mm thick microporous substrate.¹ Fractionation takes place in the skin layer.⁶ The thin skin represents the actual discriminating element and may be porous or homogeneous material, or neutral material such as silicone rubber, or charged ion exchanger.¹ Examples of asymmetric membranes are coated cellophane, skinned ultra filtration membrane and graft co-polymer membranes.

3.1.3 Ion exchange membranes

Ion exchange membranes can be used not only for separation of different ionic species and enhancement of selectivity, but also for separation and effective collection of volatile analytes or gases such as ammonia, sulphur dioxide and others.¹ These membranes are submicroporous in structure with no microscopic pores, but carrying fixed ionised groups which may be positive (anion exchange such as alkyl ammonium groups) or negatively (cation exchange such as sulphonic or carboxylic groups) charged.

Membranes that consist of a mixture of positively and negatively charged microscopic segments are called *mosaic membranes*.¹ Separation by ion exchange membranes is achieved by the structure of membrane matrix and by exclusion of co-ions such as ions with the same charge as the fixed ions. For instance, in cation exchange membranes, the fixed ions are in electrical equilibrium with mobile cations in the polymer interstices. The mobile anions are completely excluded from the cation exchange membrane due to the electrical charge being identical to that of fixed ions. A cation exchange membrane therefore allows transfer of cations only. Similarly, anion exchange membranes are permeable to anions. The major properties of ion exchange membranes include:³

- high permselectivity.

An ion exchange membrane should be highly permeable to counter ions but impermeable to co-ions.

- low electrical resistance.

A high permeability of ion exchange membrane to counter ions should be achieved under the driving force of electrical gradient.

- good mechanical form stability.

The membrane should be mechanically strong and should have a minimum degree of swelling or shrinking in transition from dilute to concentrated ionic solutions.

- high chemical stability.

The membrane should be stable under pH range of 1-14 and in the presence of oxidising agents.

The properties of ion exchange membranes are determined by the polymer matrix which in turn determines the mechanical, chemical, and thermal stability of the membrane; and concentration of the fixed ionic moiety. The degree of cross-linking of the polymer matrix determines the degree of swelling, chemical and thermal stability, electrical resistance and permselectivity of the membrane.³ An example of an ion exchange membrane is perfluorinated Nafion membrane which is a strong cation exchange membrane with active fluorosulfonic acid groups. This membrane is frequently used in gas diffusion-flow injection analysis systems.

3.1.4 Microporous Membranes

Volatile analytes or gases can be separated from the original matrix by diffusion through a microporous membrane which are typically made from hydrophobic PTFE. Microporous membranes with pore size of more than 100 nm (e.g. PTFE) are used for non-selective diffusional separation. The pores of the PTFE membrane are filled with the gas, which forms the continuous gaseous layer. The species in the gas phase diffuse across the layer defined by the geometry of the pore. Fluoroplastic microporous membranes are versatile diffusion barriers because they can be employed for a variety of gases and volatile compounds.⁴ These membranes offer higher (1-3 order of magnitude) transmembrane transition efficiencies than other types of membranes.

Microporous membranes with pore sizes of less than 100 nm are employed for molecular sieving. This includes pressure driven processes such as ultra-filtration. The smaller the pore size and porosity of the membrane, the higher the resistance to leakage of water across the membrane.¹

Despite the many advantages that can be achieved by using microporous membranes, such as simplicity and enhancement of sensitivity and selectivity in the separation of chemical species, they are susceptible to fouling with particulate matter by adsorption and desorption on the surface or within the membrane, or irreversible changes in the

polarised diffusion layer close to the membrane /liquid or membrane/gas interfaces.¹ These membranes are also sensitive to high pressure applied on the donor or acceptor side, especially when the gaseous phase is used. This may result in gases non-selectively passing through the membrane and causing bubble problems. In addition, the application of high pressures and use of membrane with larger pore size and porosity may allow some non-volatile compounds to pass through the membrane barrier. The structure of microporous membranes may be symmetric (pore diameter not varying over membrane cross section) or asymmetric (pore diameter varying from one side of the membrane to another).

3.2 MEMBRANE SEPARATION PROCESSES

Different membrane processes can be obtained depending on the type of membrane used, driving forces and area of application. The driving forces in membrane separation processes include:

- ◆ hydrostatic pressure gradient (micro- and ultra-filtration, reverse osmosis, or gas separation)
- ◆ concentration gradient (dialysis), and
- ◆ electrical potential gradient (electrodialysis).³

In some membrane processes such as pervaporation, pressure and concentration differences are the driving forces.

3.2.1 Micro-filtration

This is an example of a pressure driven membrane process. The term micro-filtration is used when particles with a diameter of 0.1-10 μm are separated from solvents or other components with molecular masses less than $(0.1-1) \times 10^6$.³ The separation mechanism is based on a sieving effect and particles are separated according to their sizes. Membranes suitable for micro-filtration are of a symmetric microporous structure with pore size of 0.1-10 μm . A hydrostatic pressure of 10- 500 kPa can be used.

3.2.2 Ultra-filtration

Ultra-filtration is a pressure driven process. Molecules or small particles with less than 0.1 μm in diameter are retained by membranes used in ultra filtration.³ The osmotic pressure of feed solution is generally negligibly small and hydrostatic pressures of 0.1-1 MPa are used. Ultra filtration membranes are mostly asymmetrically structured with the skin layer having a pore diameter of 1-10 nm.

3.2.3 Reverse osmosis

This is another example of a pressure driven membrane process. In this membrane process, macromolecules, particles, and low molecular compounds such as salts and sugar are separated from the solvent, usually water. Feed solutions often have a significant osmotic pressure which must be overcome by the hydrostatic pressure applied as the driving force. This limits the practical application of this method.³ The transmembrane flux is a function of hydrodynamic permeability and net pressure.

3.2.4 Gas permeation

Gas permeation is similar to reverse osmosis. In both processes, asymmetric membrane is used and hydrostatic pressure is the driving force. The only difference between the two processes is that in reverse osmosis, liquid mixtures are separated, while in gas permeation, the feed mixture consists of gases or vapours. The membrane selectivity is determined by the solubility and diffusivity of components in the membrane interface.

3.2.5 Dialysis

In dialysis, one or more solutes are transferred from one solution (the feed) to another (the dialysate) through a membrane along the concentration gradient.³ Dialysis depends on the concentration gradient and the flow of solute occurs from the more to less concentrated solution. Microporous membranes are used in dialysis. The purpose

is to achieve separation or purification of the solution in some solutes which are transferred more rapidly than others due to their relative permeability.

3.2.6 Electrodialysis

In electrodialysis, solute ions move across the membranes through the application of an electric field. The driving forces are concentration differences and electrical potential. The direction of transport can occur from more concentrated to less concentrated or vice versa, depending on the field direction.³

The main advantage of using electrodialysis over dialysis is that the external potential can easily be maintained until the desired degree of separation is achieved. In dialysis, the concentration gradient diminishes gradually as a result of mass transport. Ion selective membranes are used in electrodialysis.

3.2.7 Piezodialysis

Piezodialysis (pressure dialysis) is a type of membrane process in which some solutes permeate a membrane preferentially due to a pressure difference applied across the membrane.⁷ In this case, the pressure is equivalent to the electrical potential difference in electrodialysis. The difference between piezodialysis and reverse osmosis is that solutes permeate through the membrane in piezodialysis, whereas in reverse osmosis, solvent is the component that moves across the membrane.

3.2.8 Pervaporation

Pervaporation employs both concentration gradient and pressure as driving forces for separation. Volatile organic compounds are removed from a liquid feed solution through a semi-permeable membrane into the gas phase.³ The separation of components from a liquid mixture is determined by the differences in pressures and their permeation rates through the membrane.

3.2.9 Osmosis

Osmosis is a diffusion process in which solvent permeates through a semi-permeable membrane from the less concentrated side to the more concentrated side.⁷ A build up of hydrostatic pressure (known as osmotic pressure) occurs on the high concentration side of the membrane if that side is sealed to prevent transfer of solvent.

The osmotic pressure of a dilute solution is given by Van't Hoff's equation:

$$\Pi_A = RTC_A \quad (3.1)$$

Where Π_A and C_A are the osmotic pressure and concentration of species A, respectively.

However, in most cases, even for dilute solutions, a small correction is needed to compensate for the slight deviation from an ideal solution so that

$$\Pi_A = aRTC_A \quad (3.2)$$

where a is the osmotic coefficient.

3.3 DIFFUSION

Diffusion is a phenomenon by which matter is transported from one point to another under the driving force of a concentration gradient.⁷ Thus diffusion is mass transport by individual molecular motion.

The mathematical theory of diffusion is based on the fundamental principle of non-equilibrium thermodynamics which states that the diffusion flux is directly proportional to the concentration gradient. The diffusional movement of mass in one direction through a plane is given by Fick's first law. This law states that the flux

(mass per unit time) is equal to the product of driving force (concentration gradient) and a constant (the diffusivity). Fick's first law is mathematically expressed as

$$J_x = -D \frac{dC}{dx} \quad (3.3)$$

where J_x , the diffusional flux, is the mass flow per unit area in the direction of x (in g moles/cm²/s), D , is the diffusion coefficient (in cm²/s) and C is the concentration (g mole cm⁻⁴) in the direction x , which is normal to the plane. The negative sign in the equation indicates that the mass flows in the direction of lower concentration. The law is valid for dilute solutions. The equation can be applied to membrane permeation when the permeation flux is small.⁷

When a membrane is used for separation, additional terms are introduced for the membrane diffusional processes and the permeation flux is given by ⁷

$$N_A = -D \frac{dC_A}{dx} - \frac{D}{2C_M} \frac{d^2 C_A}{dx^2} \quad (3.4)$$

where C_M is the concentration of analyte in the membrane and C_A is the concentration of the analyte on one side of the membrane (e.g. donor stream) and N_A is the permeation flux.

Fick's first law is inadequate to solve most of the diffusional problems because the concentrations are usually unknown. A more convenient expression is Fick's second law, which in one dimension is expressed as

$$\frac{dC}{dt} = D \frac{d^2 C}{dx^2} \quad (3.5)$$

Fick's second law states that the rate of change of concentration is proportional to the spatial rate of change in the direction of the concentration gradient.

For membrane diffusion, a modified form of Fick's second law must be deduced and additional terms introduced since the membrane acts as another component in the diffusion system. The modified Fick's second law of diffusion (applied to membrane separation) can be expressed as

$$\frac{dC_A}{dt} = \frac{d}{dx} \left(D \frac{dC_A}{dx} \right) + \frac{d}{dx} \left(D \frac{C_A}{C_M} \frac{dC_A}{dx} \right) \quad (3.6)$$

Where t is the time.⁷

Equations 3.4 and 3.6 differ from Fick's basic equations, 3.3 and 3.5, in that second terms are added that are due to the presence of the membrane. Generally, in gaseous diffusion processes, the effect of the second term may be negligible.⁷

3.4 GAS DIFFUSION-FLOW INJECTION ANALYSIS (GD-FIA)

3.4.1 Introduction

Converting an analyte to a volatile form is a well established technique for separation and preconcentration. The volatile analyte is produced from a donor stream (which contains the matrix) and is then transported to an acceptor stream which is passed onto a detector. The acceptor stream may be a gas or a liquid and is separated from the donor by a suitable interface. In conventional systems, transport from liquid to gas phase was accomplished in open vessels (e.g. adapted Dreschel bottles), but most modern systems employ membranes as the separation interface.

Gas-liquid separation, in which the analyte in a liquid sample is converted to a gaseous species, has long been used in conventional procedures such as the Kjeldahl distillation for the determination of nitrogen; the cold vapour atomic absorption determination of mercury, and; hydride generation-atomic absorption spectrometry, to enhance both sensitivity and selectivity.⁸ The first FIA diffusion method was reported by Baadenhuijsen and Sauren-Jacobs⁹ for the determination of carbon dioxide in

plasma using a non-porous silicone rubber membrane. A dual phase diffusion cell, consisting of tubular PTFE membrane, was first applied for the separation of arsine generated in a FI system.¹⁰

3.4.2 The transport process

Most flow injection determinations are carried out in aqueous media and therefore the membranes used are normally hydrophobic. Microporous PTFE has been most widely used, in either sheet or tubular form. The tubular form offers larger surface area than the sheet form and is therefore more suitable for rapid and quantitative separation of large amounts of gas from solution.¹¹ Separation of the volatile analyte occurs under isothermal conditions and is usually controlled by the rate of diffusion across the membrane.

3.4.3 Factors affecting the transmembrane rate of transport

In general, the transport mechanism in a membrane involves diffusion of the species from a bulk sample across a static diffusion layer to a solid or fluid interface. Then, transport through the membrane matrix; including adsorption and desorption process on both interfaces, and finally the transport of the analyte into the bulk acceptor fluid across the diffusion layer.⁴

The following deals only with the processes that are relevant to gas diffusion through inert hydrophobic membranes such as microporous PTFE.

Geometry of the membrane

Transport rates across membranes are approximately inversely proportional to the membrane thickness and proportional to the active surface area of the membrane.⁴ The use of thinner wall membranes results in a better peak shape and a shorter response time. It is therefore important that the membrane should be as thin as possible so as to achieve high transport rates.

Flow rates

Enrichment factors depend on the rate of diffusion through the membrane and the relative flow rates of the donor and acceptor streams.¹ A high flow rate of acceptor stream can be used to dilute the analyte whereas a low flow rate, or stop flow mode, can be employed for preconcentration. The concentration of analyte in the acceptor stream is inversely proportional to the acceptor flow rate provided that the mass flux is constant.

Although it is possible to get a very high concentration of chemical species by using very low flow rates of the acceptor stream, stopped flow mode is more suitable. In the latter case, the enrichment factor depends on the permeation rate per unit volume of the membrane device and the time of permeation. The analyte concentration can be controlled by the length of the stopping period.

The amount of chemical species passing across the membrane usually increases with the flow rate of the donor stream. However, the resultant signal may decrease if the flow rate is so high that insufficient contact time leads to inefficient diffusion of the analyte. The contact time is longer at lower flow rates, hence a greater proportion of species pass across the membrane.

Sample size has a similar effect to sample flow rates by controlling contact time and hence peak shape. Increasing the injected sample volume results ultimately in a steady state and broadening of the peak.

Time of exposure

The amount of analyte transported depends linearly on the total sample volume passing through the donor chamber and, in cases when the transport is slow, on the time of exposure, provided that the acceptor stream has sufficient absorption capacity.⁴ Initially a linear relationship exists between the signal and the product of

time of exposure of the membrane to the sample and the concentration of analyte in the sample. Increasing contact time ultimately leads to steady state and broadening of the peak.

Temperature

An increase in temperature causes increase in diffusion rates and affects solubility in the donor and acceptor streams. Depending on the changes in the distribution coefficients, this could result in either positive or negative change in transport efficiency.⁴ The temperature dependence of transport can be controlled by thermostating. Elevated temperature may, on the other hand, be applied to improve the efficiency of transmembrane transport and sensitivity of a procedure.

Pressure

An increase in the pressure decreases transport because of increasing the solubility of the analyte in the liquid phase.

Acidity

Acid/base properties of the analyte significantly influence the membrane separation procedure. The pH discrimination of mass transport through microporous membranes can be used for separation and preconcentration of analytes from aqueous and gaseous samples.⁴ In order to achieve high transport efficiency of the non-ionised analyte through the membrane, the pH of the donor stream should be significantly lower than the pK_a of the acid species. This ensures that the analytes are present mostly in molecular forms. The acceptor stream, on the other hand, should have a pH which is significantly above the pK_a so that the diffused species are immediately ionised. The reverse is true for basic species.

Acceptor stream modifiers

The composition of an acceptor stream determines the quantity of analyte absorbed. For acid/base analytes, the maximum concentration is limited to the amount of absorption agent (acid or base) or by the absorption capacity of the acceptor.⁴ As the analyte is absorbed, an equilibrium is attained when the absorption capacity of the acceptor stream is reached and no further preconcentration takes place. For neutral components, or non-modified acceptor liquid such as water, the enrichment factor is limited to the time taken by the sample/membrane/acceptor to reach the equilibrium. Negative deviation from the linear dependence occurs when the absorption capacity of the acceptor stream is reached. Acids, bases or buffer solutions are recommended as the acceptor media for ionizable species.⁴

3.4.4 Membrane separation devices used for gas diffusion-flow injection analysis

The membrane separation device is the most important part of a GD-FIA manifold. It should have stable and efficient performance which is important for successful development of any separation process. Membrane performance is critical for good signal and baseline stability and signal to noise ratio at the detector.⁴ For the design of an efficient membrane device, the following factors should be considered:

- the membrane material
- the area of membrane exposed to the donor and acceptor streams
- the volume and the geometry of the grooves or the cavities on both sides of the membrane.

The device should continuously separate the analyte from the donor stream with long term stability and over a wide range of flow rates and flow rate ratios. In addition, the device has to prevent additional dispersion, i.e. unwanted dilution and deterioration of the original concentration profile; handle different types of analyte, and operate with a small volume of acceptor stream if preconcentration is desired.⁴ The membrane device can be made from chemically inert materials such as fluoroplastics (PTFE,

PVDF), glass, and stainless steel, to prevent any reaction between the device and the sample, reagent or modifiers. The volume and geometry of the channels are fundamental parameters for the transport process. The volume should be as small as possible with maximum contact area. The membrane area can be increased by making the grooves shallower and wider or longer (or both). This results in an increase in the transport efficiency.

3.4.4.1 *Sandwich membrane device*

Classical sandwich gas diffusion modules with rectangular or circular shaped membranes are the most frequently used designs (Figure 3.1). The device consists of two pieces, each having a groove facing the gas semi-permeable membrane. Identical grooves, or grooves of different volumes, having a constant cross section and of rectangular or circular profile are used. Cells with straight grooves, or spiral grooves are commercially available. Support (perfluorinated PTFE, metallic screen) should be provided to prevent mechanical damage and to improve durability and long term stability of the membrane.

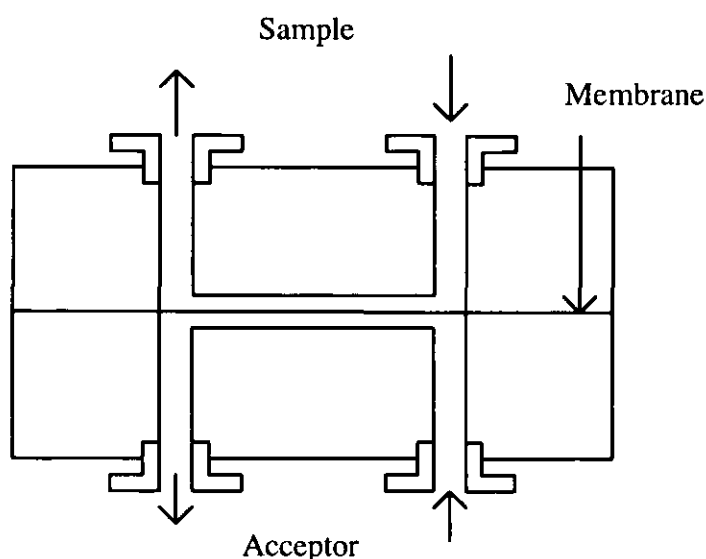


Figure 3.1 Sandwich membrane device.

3.4.4.2 Dual membrane sandwich device

The dual membrane device consists of two identical, or different membranes, placed in two wells in either side of the sample (donor) channel of the central body. The body is sandwiched by two outer pieces, each with a groove just facing the membrane (Figure 3.2)

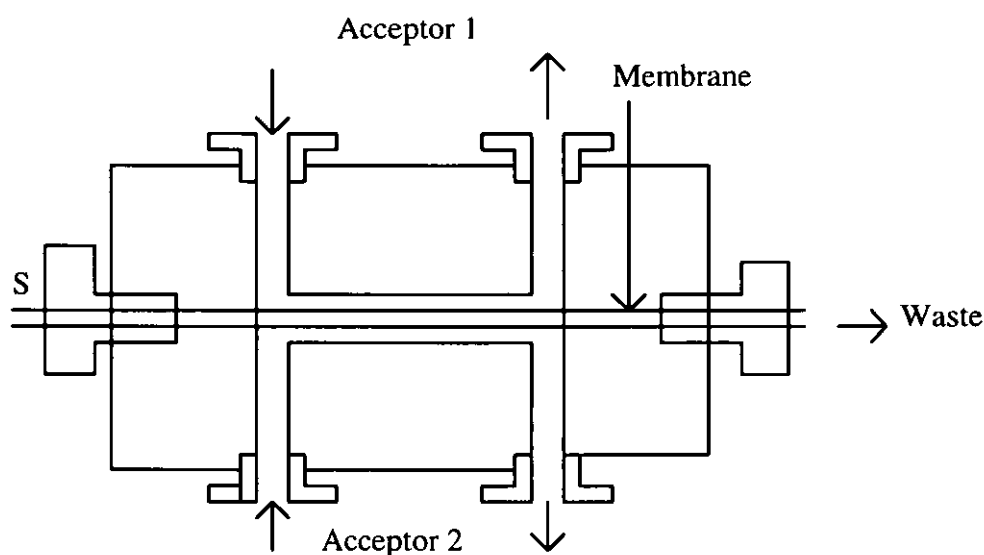


Figure 3.2 Dual sandwich membrane gas diffusion device with rectangular membrane sandwiched between two bodies.

The donor stream flows through the central channel. Chemical species of different properties pass across a particular membrane and are collected in suitable acceptor streams. Selectivity of the separation process can be achieved by differences in composition of the acceptor streams, chemical conditions in the donor stream, or differences in the selectivities of the two membranes.⁴

3.4.4.3 Coaxial device

A coaxial gas diffusion module (a tube in a shell device) is made from membrane tubing with wall thickness ranging from several tenths to hundredths of a millimetre. A single or multiple tubing is inserted into a large tube made of PTFE, glass or other

chemically inert material with a T or Y joint at each end of connection.⁴ A spiral configuration can be used inside the larger diameter outer tube, thus shortening the total length of the device. The donor stream flows in either the annular space or through the central membrane tube (Figures 3.3). The latter configuration has the advantage of minimising the analyte dispersion and preventing potential blockage by any particular matter due to the large volume.

The advantages of using coaxial modules are their resistance to the leakage of liquid and ease of connection to the tubings commonly used in FIA. However, coaxial modules are not yet widely commercially available.

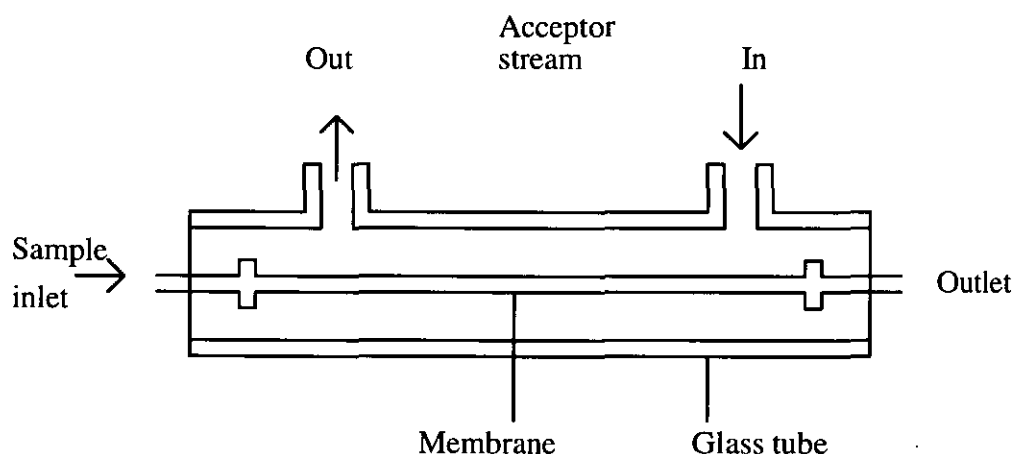


Figure 3.3 A coaxial gas diffusion device.

3.4.4.4 Stationary configuration

Tubular or planar membrane can be inserted into a high-volume reactor for studying transmembrane transport, chemical equilibria in solution and process streams. In these cases, a suitable length of tubular membrane is wound around a support construction (frame) or a special device is used for holding the planar membrane in continuous contact with the reaction mixture. The cell should be stirred so as to prevent the formation of concentration depletion layer at the membrane sample interface. In a stirred device, the response is controlled by diffusion across the wall. In an unstirred device, a depleted layer is formed rapidly around the membrane and response is controlled by diffusion through this layer. The analyte can be collected in

a stationary or continuously flowing acceptor stream. The chemical conditions on both sides of the membrane among other factors govern the amount of analyte in the acceptor stream. Since the chemical reactions taking place in the reactor influence the response, the device is suitable for studying chemical equilibria in solution, dissolution processes and measurement of kinetics.

3.4.4.5 *Devices with open interfaces*

A gas diffusion device without a separation membrane has been described¹² and consisted of a closed chamber holding two silicone rubber sheets supported on parallel plates. The donor and the acceptor streams enter the device and spread along a particular silicone rubber sheet producing a thin film of liquid on the surface of each membrane.⁴ The films are linked to the sheets by liquid-solid adhesion. The films pass the entire length before going out to waste or the detector channel. The liberated analyte from the film of the donor liquid diffuses across the free gaseous interspace to the acceptor stream where it is collected and then sensed directly or through the use of an analytical reagent. The system has been used for the determination of nitrogen in plant materials using potentiometric and photometric measurements of ammonia.¹²

3.4.5 **Flow injection manifolds incorporating separation devices**

Figure 3.4 shows the basic gas diffusion-flow injection analysis system. The system can be used in various modes for the separation, preconcentration and dilution of analytes. This depends largely on the ratio of the flow rate of the sample, acceptor and donor streams. Modification of this system is a stopped flow mode, displayed in Figure 3.5.

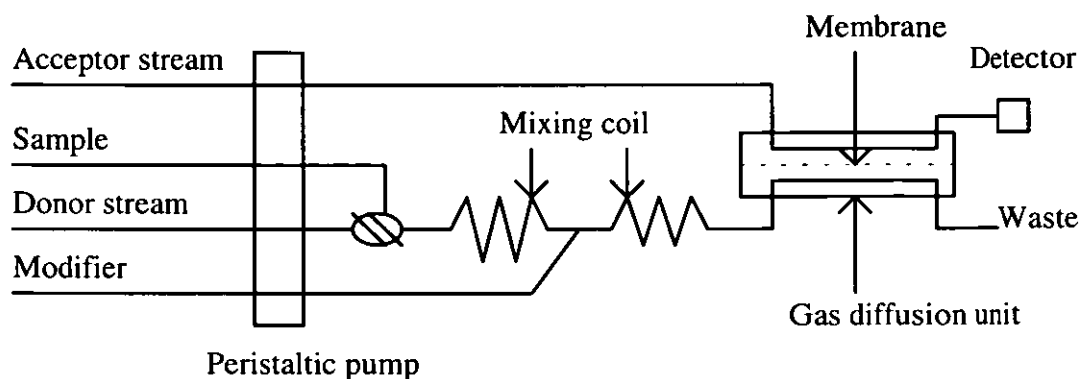


Figure 3.4 Basic gas diffusion-flow injection system.

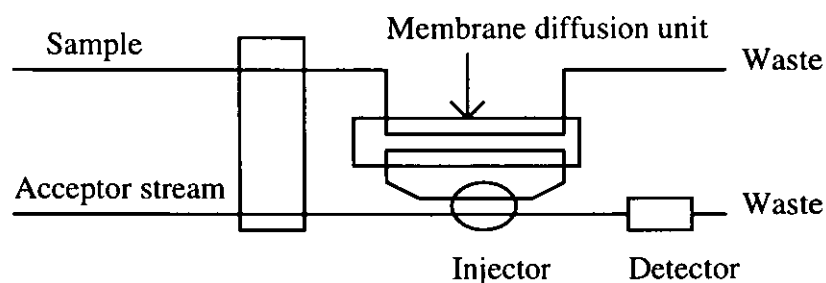


Figure 3.5. FIA manifold for stop flow preconcentration mode.

The extent of preconcentration in the stop flow mode can be exploited to its full potential by stopping the acceptor stream inside the injection loop while a large volume of sample is passed through the unit (Figure 3.5).^{13,14,15}

REFERENCES

1. Noble, R. D., *Separation Science and Technology*, 1987, **22**, 731
2. Moskin, L. N., *J. Anal. Chem. USSR*, 1988, **43**, 449.
3. Strathmann, H., in *Ullmann's Encyclopaedia of Industrial Chemistry*, Ed. Elvers B., Hawkins S., and Schult G., vol. 16, pp. 187-263.
4. Kuban, V., *Crit. Rev. Anal. Chem.*, 1992, **23**, 323.
5. Friedlander, H. Z. and Rickles, R. N., *Anal. Chem.*, 1965, **37**, 26A.
6. Matson S. L., Lopez J. and Quinn J. A., *Chemical Engineering Science*, 1983, **38**, 503.
7. Hwang S. and Kammermeyer K., *Membrane in Separations*, John Wiley and Sons, Interscience, New York, 1975, Vol. VII, pp. 1-41
8. Fang, Z., Zhu, Z., Zhang, S., Xu, S., Guo, L. and Sun, L., *Anal. Chim. Acta*, 1988, **214**, 41.
9. Baadenhuijsen H. and Seuren-Jacobs, H. E. H., *Clin. Chem.*, 1979, **25**, 443.
10. Pacey, G. E., Straka M. R. and Gord J. R., *Anal. Chem.*, 1986, **58**, 502.
11. Aoki T., Uemura, S. and Munemori, M., *Anal. Chem.*, 1983, **55**, 1620.
12. Zagatto, E. A. G., Reis B. F. and Bergamin, F. H. and Krug, F., *J. Anal. Chim. Acta*, 1979, **109**, 45.
13. Zhu, Z. and Fang, Z., *Anal. Chim. Acta*, 1987, **198**, 25.
14. Kuban, V., *Anal. Chim. Acta*, 1992, **260**, 45.
15. Kuban, V., Dasgupta, P. K. and Marx J. N., *Anal. Chem.*, 1992, **64**, 36.

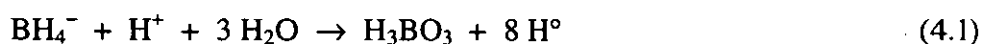
Chapter 4

CHAPTER FOUR

GAS/VAPOUR GENERATION

4.1 HYDRIDE GENERATION.

The potential of hydride generation was first reported by Holak.¹ This technique has become an accepted method for the determination of elements which form volatile hydrides. Metals such as antimony, arsenic, bismuth, germanium, lead, selenium, tellurium and tin form volatile covalent hydrides by reduction of their higher oxidation states using sodium borohydride. Its reaction with the metals is represented by the equations:



where E represents the analyte and m and n may be equal.

The use of sodium borohydride has superseded that of metal-acid reactions for the generation of hydrides because of its superior speed and reduction yield. In addition, it provides less contamination of the blanks and generates hydrides from all the hydride forming elements. However, the method suffers from a drawback, the element has to be in a particular oxidation state before the hydride can be formed. For example, selenium, present as Se (VI), must first be converted to Se (IV) before its reduction to hydrogen selenide can be effected by sodium borohydride.

The hydrides have been determined by atomic absorption spectroscopy because they are easily atomised. Most of the hydride forming elements are comparatively insensitive in the air-acetylene flame and suffer from severe interference problems in certain matrices. Their sensitivity is greatly improved when the hydride generation technique is used instead of flame atomisation.

The original hydride method for the determination of As was carried out using zinc reduction¹⁻⁵ to form arsine. This involved injection of an acidified sample through a septum cap onto a column of zinc metal. The generated hydride was swept through the Zn column by an inert gas, such as nitrogen, into a collection vessel. The method was extended to include other elements by using sodium borohydride as the reducing agent.^{1,3,4} In this method, the acidified sample was placed into a reaction cell and mixed with a solution of sodium borohydride introduced through a side arm. An inert gas was used to purge the generated hydrides.

The first report involving the use of FI for hydride generation AAS was by Astrom.⁶ A carrier stream of 0.2 M hydrochloric acid was merged with a stream of 1% sodium borohydride in 0.1 M sodium hydroxide. The resulting solution was introduced into a Vijan-type¹⁴ U-tube gas liquid separator. The generated hydride was swept by a flow of N₂ or Ar into a quartz tube for atomic absorption detection. Pacey *et al.*⁷ improved the system by incorporating a gas liquid separator into the FI system.

Yamatoto *et al.*⁸ applied the FI technique to generate hydrides of As, Bi, Sb, Se, and Te by means of sodium borohydride. A PTFE reaction tube and a mixing coil were incorporated in the FI system. The hydrides thus generated were separated from the solution and introduced into an atomic absorption spectrometer. Yamatoto *et al.*⁹ used a microporous Teflon tube membrane separator inside a pyrex glass sheath tube. This tubular membrane presented a large surface area for gas diffusion. The system was applied for the determination of As in surface water.

A comparison of hydride FI generation and continuous flow-hydride generation from Sb (III) and Sb (V) with subsequent determination by atomic absorption spectrometry has shown that, where speciation is required, flow injection analysis-hydride generation (FI-HG) is recommended over continuous flow-hydride generation. This was due to lower interference from Sb (V) when FI is employed. The FI and continuous flow-hydride generation AAS

methods were found to have lower detection limits than batch methods.¹⁰

Combination of FI-HG with molecular emission cavity analysis (MECA), for the determination of As, was reported by Burguera and Burguera.¹¹ The sample was injected into a stream of hydrochloric acid before merging with a stream of sodium borohydride. The resultant solution was swept by argon into the gas-liquid separator. The separated hydride was then introduced into the MECA detection system.

Hydride generation has been employed with ICP-AES detection for the determination of volatile elements, in order to achieve lower detection limits.¹²⁻¹⁸ An important point when coupling FI-HG to ICP-AES is to restrict the rate of H₂ generation as this may extinguish the plasma. FI-HG has also been coupled to ICP-MS e.g. for the determination of As, Sb and Hg (cold vapour generation) at ultra-trace level.¹⁹

Sodium borohydride has been applied successfully for the generation of the hydrides of As, Bi, Ge, Sb, Se, Sn, Te²⁰ and Pb.²¹ However, this reducing agent is expensive and is only stable for a few days when stored refrigerated and hence should be prepared daily.²²⁻²⁴ The major disadvantage of employing the hydride generation technique combined with atomic absorption spectroscopy is the interference caused by transition metals, mainly those of Groups 8, 9, 10, and 11.^{16,25-27} To overcome this problem, Lin *et al.*²⁸ developed a flow injection-electrochemical hydride generation technique for AAS which avoids the use of sodium borohydride. In this method, a thin layer type flow cell was used. The PTFE body of the cell consisted of upper (cathode) and lower (anode) blocks, each with solution inlets and outlets, and a cathode or anode embedded in them. These were separated by PTFE gaskets with an ion-exchange membrane in between. The anode was made of platinum. Electrolytic solutions of H₂SO₄, HClO₄, HNO₃ and HCl at various pH values were used to test the efficiency of the hydride generator. The same authors noted that the flow injection-electrochemical-hydride generation technique incorporates most of the advantages of the flow injection analysis-sodium borohydride-hydride generation technique.²⁸

Brockmann *et al.*²⁹ developed a new hydride generation system based on electrolytic reduction. In this method, a peristaltic pump was used to convey electrolyte continuously into the electrochemical cell. The sample solution (400-500 μL), introduced into the catholyte (dilute HCl or H_2SO_4) carrier stream, was propelled to the cell. 2 M H_2SO_4 was used as the anolyte. Hydrides and hydrogen were formed at the cathode; rinsed out of the cell by the catholyte flow and separated from the aqueous solution by a PTFE membrane gas-liquid separator. The hydride was transported by the argon carrier stream to an electrically heated quartz cell and its determination made by atomic absorption spectrometry.

The sensitivity, detection limits and reproducibility of electrochemical hydride generation compared favourably with those obtained using FI hydride generators based on sodium borohydride. The other advantages of using electrochemical generation over sodium borohydride generation are minimum consumption of costly, high purity acids and avoiding the use of sodium borohydride which is difficult to handle. Brockmann *et al.*²⁹ noted that low sample consumption, high sampling frequency and automation can be achieved when the arrangement is constructed as a flow injection system.

4.2 GENERATION OF HYDROGEN SULPHIDE

4.2.1 From sulphide

The main industrial sources of sulphide are paper mills, petroleum refineries, meat processing plants and sewage treatment plants. Industrial waste waters contain inorganic sulphur such as sulphate and sulphite species which may be reduced, under anaerobic conditions, to sulphide. The determination of sulphide in sewerage systems is important because of the potential for toxic atmospheres and corrosion of sewer fabrics due to the action of sulphuric acid, formed biochemically by oxidation of sulphide. There is a general interest in the determination of sulphide since accurate determination of total sulphur in the soil, petroleum products and plants involves conversion of sulphur to sulphide by reduction. Hydrogen sulphide, produced from sulphides on acidification, is an air pollutant due to its

toxicity, unpleasant odour and its reactivity with metals and metal salts. The gas has the effect of tainting potable water.

Several analytical techniques have been used for the determination of sulphides, these include: iodometric titration, UV/VIS spectrophotometry, gas phase molecular absorption spectrometry (GPMAS), MECA, ICP-AES, the sulphide ion selective electrode, and gas chromatography.³⁰⁻⁴⁷

The methylene blue method is the most widely used spectrophotometric method for trace determination of sulphide and is used later in this work. This method involves the reaction between sulphide and an acid solution of *p*-aminodimethylaniline, in the presence of Fe^{3+} , to form a blue complex (methylene blue). Prior to the formation of the blue colour, the hydrogen sulphide produced is usually absorbed in a suitable absorbing solution such as zinc acetate or alkaline suspension of cadmium hydroxide. This results in the formation of zinc sulphide or cadmium sulphide respectively which prevents air-oxidation of the sulphides which takes place rapidly in aqueous alkaline solution. The methylene blue complex is determined by a UV/VIS spectrometer at 670 nm. The absorbance peak however, can vary with conditions. It is therefore important to control the experimental conditions so as to get reproducible results. A limit of detection of $0.008 \mu\text{g l}^{-1}$ sulphide has been achieved by this method.³³ Other sulphur containing compounds such as dimethyl disulphide may interfere as do SO_2 , N_2 and O_3 .

A FIA method has been developed for the determination of sulphide using the methylene blue method.³⁴ A sensitive and automated method has been developed for acid extractable sulphides in environmental samples by employing a gas dialysis separation technique in combination with the methylene blue procedure.

A number of methods have been reported which involve direct determination of H_2S in the vapour phase e.g. gas phase molecular absorption spectroscopy,^{36-40,48} MECA⁴¹⁻⁴⁵ and ICP-AES.⁴⁹ Various types of membrane separators were used including a PTFE membrane.

4.2.2 From sulphate

Total sulphur in real samples such as plants and soils can be determined by converting all the sulphur forms into either sulphate by acid-oxidation or sulphide by reduction. Sulphate can be determined gravimetrically or turbidimetrically or by reduction to hydrogen sulphide.⁵⁰

Conversion of sulphate into a vapour phase compounds, usually hydrogen sulphide is generally considered to be difficult. However, Bogdanski *et al.*⁵¹ determined trace amounts of sulphate by molecular cavity analysis using a vaporisation system.⁵¹ Hydrogen sulphide was generated from sulphate by using an apparatus whose components included a heater, reactor, condenser and MECA detector. A modified tin-orthophosphoric acid reductant was used to reduce sulphate to hydrogen sulphide. A high temperature (300°C) was employed for the generation of hydrogen sulphide from sulphate. The evolved gas was carried by nitrogen to a MECA cavity and the S₂ emission measured as a function of time. It was observed that the conversion of sulphate to hydrogen sulphide began at 198°C.

Sulphate has been determined spectrophotometrically as methylene blue after being reduced by hydriodic and hypophosphorous acids in acetic acid solution to sulphide which was then reacted with *p*-aminodimethylaniline and ferric ions to form a dye.⁵² The results obtained using different reducing mixtures showed that the hydriodic/hypophosphorous acid mixture gave the best precision and lowest blanks as compared to other reducing mixtures such as hydriodic acid-phosphorous, hydriodic acid-phosphorous-acetic acid and hydriodic acid-phosphorous-acetic acid. The effect of temperature on the yield of hydrogen sulphide was studied and the results obtained showed that the reduction performed under boiling gave the highest yield, whereas no reduction could be observed at room temperature. Ti and H₃PO₄ can also be used to reduce sulphate to hydrogen sulphide.⁵²

The determination of sulphate can be performed using the Johnson and Nishita method, which has been found to be accurate, sensitive and precise.^{50,53} In this method, sulphate is reduced by mixture of hydriodic acid-formic acid and hypophosphorous acid to hydrogen sulphide. The gas is absorbed in a zinc acetate solution before being treated with the colour forming agent, *p*-aminodimethylaniline in the presence of ferric ions, resulting in the formation of methylene blue. The intensity of the methylene blue complex is determined by spectrophotometry at 670 nm. This method has been applied for the determination of sulphate in soil as it is capable of converting all the sulphate to sulphide.⁵³

Hydrogen sulphide has also been produced from sulphur in plants and soil by oxidising the samples with sodium hypobromite (NaOBr) solution to form sulphate before reacting with the hydriodic acid-formic acid-hypophosphorus-acid mixture.^{54,55}

4.2.3 From organic sulphur compounds

Grekas and Calokerinus developed the MECA method for determining organic and inorganic sulphur containing compounds as hydrogen sulphide generated by an electrolytic method.⁵⁶ The apparatus used in this method consisted of a MECA detector and the electrolysis unit. The latter consisted of a thermostated cell with platinum electrodes, a d.c. power supply and an on-off switch controlled by a precision timer.⁵⁷ The cell was continuously purged by nitrogen which ensured adequate stirring. The nitrogen was also used to sweep the hydrogen sulphide to the MECA cavity.

4.3 GENERATION OF SULPHUR DIOXIDE

4.3.1 From sulphite

Sulphur dioxide is a major air pollutant in the environment. The gas is released into the atmosphere mainly from the combustion of coal and petroleum, the smelting of sulphur containing ores, the production of sulphuric acid and the paper manufacturing industry. It is

the main cause of increasing acidification of the environment through the generation of acid rain.

Sulphite based preservatives are commonly used in the fruit industries because they are stable, inhibit bacterial growth and act as antioxidants.⁵⁸ Strict control of sulphite concentration is important as large amounts are toxic and can destroy certain vitamins.

Because of the growing concern over sulphite as a food preservative and sulphur dioxide as an important air pollutant, rapid and reliable methods for the determination of these compounds are continually being sought. Sulphite and sulphur dioxide have been determined by a variety of analytical techniques which include: iodometric method,^{32,59} spectrophotometric methods,⁶⁰⁻⁶⁶ gas phase molecular absorption spectrometry (GPMAS),⁶⁷⁻⁷¹ coulometry, conductimetry, gas chromatography with flame photometric detection⁷² and MECA.⁷³⁻⁷⁶

The method used in this work was that due to West and Gaeke.⁶⁰ This employs pararosaniline as the colour forming reagent and formaldehyde as a catalyst. A solution of tetrachloromercurate (II) (TCM) is used for trapping the generated sulphur dioxide⁶⁰ resulting in the formation of dichlorosulphitomercurate (II) (DCSM) according to the equation,



DCSM is very stable and prevents oxidation of SO_2 to SO_3 during sampling and storage.

Interference by heavy metals can be eliminated by adding disodium ethylenediaminetetraacetate ($\text{Na}_2\text{H}_2\text{EDTA}$) to the TCM solution prior to the completion of DCSM formation.^{61,62} Sulphamic acid is used to eliminate the interference of nitrite, produced from the absorption of oxides of nitrogen from the sample.^{63,64} The interference due to ozone may be overcome by delaying the analysis time for about 20 minutes from

the time of sample collection to the addition of reagents. This allows any ozone that remains in the absorbing solution to decay.

A modified form of the West and Gaeke method using purified reagents has been found to improve the sensitivity, reproducibility and working range as compared to the original West and Gaeke method.⁶¹

The West and Gaeke method has become very popular for the determination of sulphite and sulphur dioxide due to its sensitivity and simplicity. The method has been applied to the determination of total sulphur in soils by conversion of soil sulphur into sulphur trioxide and then to sulphur dioxide.⁶⁵ Automated methods employing flow systems and continuous monitors have been developed for this reaction.⁶⁶

A number of methods have been reported which involve direct determination of sulphur dioxide in the vapour phase. These include: GPMAS^{48,67,69} and MECA.⁷³⁻⁷⁶

4.3.2 From sulphur

Sulphur dioxide has been produced by combustion of sulphur, in petroleum products, in a lamp apparatus for light petroleum and by hot tube combustion for heavier fractions.⁷⁷ The sulphur dioxide evolved was trapped in 0.02 M sodium tetrachloromercurate (II)-0.002 M EDTA solution.

4.4 GENERATION OF HALOGENS

Oxidation of halides to generate halogens can be used as a route for their determination. The gaseous halogens formed can be determined by using several methods such as, molecular absorption spectrophotometry, microwave induced plasma emission and mass spectrometry.

4.4.1 Generation of bromine

Nicholson and Syty⁷⁸ generated bromine from bromide using an oxidising mixture of sulphuric acid and potassium permanganate. In this method, the oxidising mixture was introduced into a reaction vessel from a burette attached to a side arm. The bromide sample was injected into the oxidising solution by means of a syringe. Nitrogen, used as a carrier gas, flowed continuously through the reaction vessel. The liberated bromine gas was swept by the nitrogen to an absorption cell. Concentrated sulphuric acid and potassium permanganate are efficient oxidants of bromide.⁷⁸ Varying the concentration of potassium permanganate from 0.001 M to 0.15 M, while holding the concentration of sulphuric acid constant (3.6 M), resulted in an increase in the absorption signal by 19.1 %.

Calzada *et al.*⁷⁹ used microwave induced plasma emission (MIP-AES) to determine bromide after continuously generating bromine using three different oxidant systems: $\text{KBrO}_3\text{-H}_2\text{SO}_4$, $\text{H}_2\text{O}_2\text{-H}_2\text{SO}_4$ and $\text{NaClO-H}_2\text{SO}_4$. The latter system was found to be most effective for generation of the gas.

Oxidising solutions such as potassium persulphate, potassium permanganate, potassium perbromate, potassium dichromate, sodium nitrite and hydrogen peroxide acidified with sulphuric acid have been used for the continuous flow generation of bromine from bromide.⁸⁰ Of these oxidants, potassium persulphate (0.1 M) in sulphuric acid (5 M) was found to be most effective for generating bromine.

4.4.2 Generation of chlorine

The standard procedure for generating chlorine from chloride employs acidified KMnO_4 . This has been reported by Nicolic and Milosavljevic.⁸¹ In this method, a peristaltic pump was used to propel the carrier stream, reagent stream and acceptor solution. A chloride sample was injected into the carrier stream (3 M H_2SO_4) which later merged with the reagent stream (saturated KMnO_4) before entering the mixing coil. The production of chlorine took

place in the flow injection manifold. As the solution passed through the diffusion cell, chlorine gas diffused through the PTFE membrane into the acceptor stream (0.001 M H_2SO_4). The dissolved chlorine in the acceptor stream flowed into the second mixing coil before entering the detector.

4.5 GENERATION OF CARBON DIOXIDE

4.5.1 From organic carbon

The most commonly used method for the determination of total organic carbon involves oxidation of organic material and subsequent measurement of the liberated carbon dioxide.⁸² Oxidation can be done in the gas phase by passing the sample over a catalyst at high temperature (Dumas method) or by wet oxidation.

Wet oxidation methods involving the use of strong oxidising agents have been used to convert organic carbon to carbon dioxide. Some of these strong oxidising agents are chromic and sulphuric acid mixture,^{83,84,85} fuming sulphuric acid and orthophosphoric acid in combination with chromic acid to enhance oxidative power of the digestion medium.^{104,105} Use of dichromate-sulphuric acid mixture,^{86,87,88} and a mixture of permanganate and ceric sulphate⁸⁹ have also been reported. An automated wet oxidation method for the determination of dissolved organic carbon in lake water has been described.⁸² In this method, ultraviolet irradiation or silver-catalysed peroxydisulphate were used. The latter method was found to be more precise and convenient than the former.

Carbon dioxide has been generated from carbon compounds using heat-promoted persulphate oxidation.⁹⁰ In this method, the TOC working standards (0-10 ppm C) were prepared from stock solution of potassium hydrogen phthalate. 5 ml of each working standard was put in chromic acid washed 10 ml glass serum vials and 0.3 ml of saturated

acidified potassium persulphate solution added. The samples were sealed with a Teflon faced septa and an aluminium crimp ring. To maintain a gas tight seal, the sealed samples were inverted and then heated to 80° C for 30 minutes to oxidise completely all organics to carbon dioxide. Solutions with high concentration of chloride (> 0.1 %) were found to significantly slow the persulphate oxidation. Carbon dioxide was collected from the sample by injecting a glass syringe through the Teflon-faced septa into the headspace of the serum vial. Another syringe needle, connected to a low pressure argon source, introduced argon into the sample solution. The sample was purged of its carbon dioxide with argon which was collected by the glass syringe for introduction into ICP-AES.

A distinction between organic and inorganic carbon (carbonate) in a sample can be made by measuring both carbon dioxide generated by acidification and also making total carbon measurement by oxidation methods. The difference between the two measurements represents the organic carbon. The validity of the organic carbon determination depends on whether the stripping operation is complete and volatile organic material is not lost.

Total organic carbon has been recognised as a useful measure of pollution and a number of techniques have since been developed for this non-specific method of analysis. Differences among techniques appear primarily in the procedure used for oxidation and detection of carbon dioxide produced on combustion of organic matter. Techniques for measurement of carbon dioxide evolved upon oxidation of organic matter include; infrared analyser,^{91,92,93} gravimetric,⁹⁴ titrimetric,⁹⁵ conductometric⁹⁶ and gas chromatographic⁹⁷ methods.

Chlorine, oxides of sulphur and nitrogen may interfere with the determination of organic carbon by wet oxidation. Interference by chlorine can be eliminated by using a saturated acidic silver arsenite trap in the oxidation train. Interference from oxides of sulphur and

nitrogen can be solved by passing the gas stream through a solution of barium chloride in hydrochloric acid and through a tube containing silver metal and lead oxide heated at 193°C.

Methods for dry combustion of organic matter in the presence of catalysts such as cuprous oxide, cobaltic oxide and asbestos-supported silver permanganate at a high temperature (900-1000°C) have been described. These methods involve procedures and equipment which are relatively too sophisticated for routine analysis of water.⁸⁹ These methods have drawbacks for the analysis of water which include the use of small samples, due to problems resulting from evolution of a large volume of steam at the high temperature employed for combustion. This may be impractical on the basis of sampling and reproducibility. Incomplete oxidation may also occur when rapid combustion is carried out at high temperature, leading to formation of carbon monoxide rather than carbon dioxide, thus yielding spuriously low results.⁸³

4.6 GENERATION OF NITROGEN FROM NITROGEN CONTAINING COMPOUNDS

Although it is possible to determine ^{15}N abundance of soil or plant derived nitrogen by converting it into any stable molecular weight compound of nitrogen, it is important that this compound is gaseous at room temperature and contains one or two nitrogen atoms.⁹⁸ Elemental N_2 is such a compound; it is stable in conventional ion sources and the mass spectrum of nitrogen is not confused by ions originating from other isotopic elements as in the case of N_2O . The principal requirements for generating nitrogen from nitrogen containing compounds include: quantitative conversion of sample nitrogen to pure N_2 , random pairing of nitrogen atoms during the formation of N_2 and removal of contaminant gases and volatiles, particularly water vapour, carbon dioxide and carbon monoxide.⁹⁸

4.6.1 Methods for generating nitrogen

4.6.1.1 *Direct combustion method*

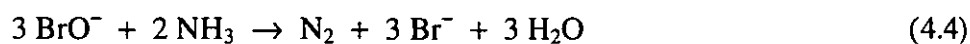
The most widely used method for converting nitrogen containing compounds to nitrogen is the Dumas method. This method involves combustion of sample nitrogen and subsequent conversion to N_2 . The combustion of the sample is achieved in a stream of pure oxygen on an oxidant such as NiO , at a high temperature of about $1000^\circ C$. By using a catalyst such as a sealed tin cup, that holds the sample, the temperature of combustion may be raised to $1700^\circ C$. The combustion products are swept by an inert carrier stream, such as helium, over a reductant such as copper at $700^\circ C$. The nitrogen, water vapour and carbon dioxide carried along in the carrier stream are passed through a column packed with absorbent for removal of carbon dioxide and water vapour. The generated nitrogen can then be introduced into a mass spectrometer, via a stainless steel capillary, for isotopic mass ratio determination. This method has been reported to work well with inorganic and simple organic samples, but not with complex samples such as biological materials which give lower recovery due to incomplete combustion.^{99,100}

4.6.1.2. *Kjeldahl-Rittenberg method (Digestion-distillation-oxidation)*

Most nitrogen containing compounds can be converted to ammonia, which is an easily measurable and extracted form of nitrogen. The extraction of ammonia can be achieved by distillation. The most common method of converting combined nitrogen to ammonium is the Kjeldahl method. In this, inorganic and organic nitrogen present in the sample are oxidised by digestion in sulphuric acid in the presence of catalysts such as mercury (II) oxide, selenium and copper sulphate.¹⁰¹ Carbon and hydrogen are removed as carbon dioxide and water respectively whereas the convertible nitrogen present in the sample is converted and retained in the digest as ammonium ion. The ammonium is separated by steam distillation of NH_3 or microdiffusion in the presence of a strong base such as $NaOH$. The liberated ammonia gas is trapped in dilute acid. Inorganic nitrogen, such as

nitrite and nitrate, present in plant and soil extracts can be converted to ammonium without digestion using Devardas alloy, followed by distillation or diffusion in the presence of a weak base such as MgO.⁹⁸

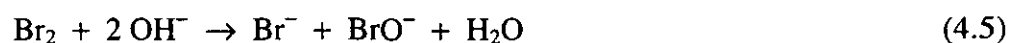
The ammonium-N thus prepared may be oxidised to N₂ by reaction under a vacuum with a degassed solution of alkaline lithium or sodium hypobromite (Rittenberg method), according to the equation,



This is achieved by placing the dried ammonium salt in one arm of the Rittenberg flask and the hypobromite into the other. The flask is attached to an inlet manifold of the mass spectrometer and as the flask is rotated, an excess BrO⁻ is brought into contact with the ammonium salt, liberating N₂. The gas is introduced into the mass spectrometer via a cold trap to remove water vapour and contaminants such as CO₂, Br₂ and N₂O. A modified form of Rittenberg procedure involving drying of ammonium solution in vials, and connection of the vials to a stainless steel inlet system for the mass spectrometer has become popular. In this method, the hypobromite is delivered to the vial from the reservoir placed above the apparatus.¹⁰²

In order to obtain accurate results, the hypobromite solution must be freshly prepared, the pH must be adjusted between 7.5 and 9.5, the temperature should not rise above 18°C and the exposure of the solution to sunlight should be avoided as the solution is quite unstable. The hypobromite solution should therefore be stored in amber bottles at low temperature. Hypobromites of alkali metals can be prepared by the following routes:

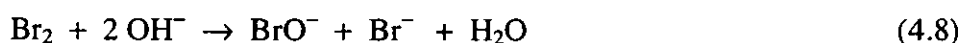
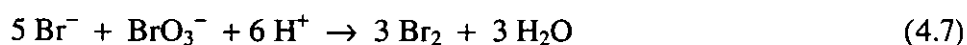
- dissolving bromine in aqueous solution of a suitable base



- adding excess bromide to hypochlorite solution at pH 9-14



- producing bromine by addition of HCl to a solution containing bromide and bromate at a concentration ratio of 5:1, before the addition of alkali. The reaction proceeds according to the following equations;



The nitrogen isotopic analysis can be performed using either a mass spectrometer or an optical emission spectrometer. Both instruments exploit a physical property of the nitrogen molecule, N_2 , to determine the relative amounts of $^{14}\text{N}_2$, $^{14}\text{N}^{15}\text{N}$ and $^{15}\text{N}_2$ species.⁹⁸ In mass spectrometry, charged ions are separated according to their mass to charge (m/z) ratio whereas in optical emission spectrometry, N_2 molecules are separated on the basis of their vibrational properties. The procedures used to convert soil and biological samples to elemental nitrogen for both methods are similar. Since N_2 is usually the material analysed in both instruments, the technique developed for one can frequently be adapted for the other. Optical emission spectrometry is uniquely applicable to the isotopic analysis of nanomole quantities of nitrogen, whereas mass spectrometry is indispensable for the analysis of the extremely small variations in the ^{15}N abundance that occur in nature.¹⁰³ Isotope ratio mass spectrometry was chosen in this study for the determination of $^{15}\text{N}/^{14}\text{N}$ ratio because the accuracy of the method is superior to that of optical emission spectrometry.

REFERENCES

1. Holak, W., *Anal. Chem.*, 1969, **41**, 1712.
2. Pihlar, B. and Kosta, I., *Anal. Chim. Acta*, 1980, **114**, 275.
3. Madsen, R. E., *At. Absor. Newsl.*, 1971, **10**, 57.
4. Dalton, E. F. and Malanoski, H., *At. Absor. Newsl.*, 1971, **10**, 92.
5. Manning, D. C., *At. Absor. Newsl.*, 1971, **10**, 86.
6. Astrom, O., *Anal. Chem.*, 1982, **54**, 190.
7. Pacey, G. E., Streka, M. R. and Gord, J. R., *Anal. Chem.*, 1986, **58**, 502.
8. Yamamoto, M., Yasuda, M. and Yamamoto, Y., *Anal. Chem.*, 1985, **57**, 1382.
9. Yamamoto, M., Obata, Y., Nitta, Y., Nakata, F. and Kamamaru, T., *J. Anal. At. Spectrom.*, 1988, **3**, 579.
10. Guntinas, M. B. de la Calle, Madrid, Y. and Camara, C.; *Anal. Chim. Acta*, 1991, **252**, 161.
11. Burguera, M. and Burguera, J. L., *Analyst*, 1986, **111**, 171.
12. Ruzicka, J. and Hansen, E. H., *Flow Injection Analysis*, John Wiley and Sons, New York, 1988.
13. Betteridge, D., *Anal. Chem.*, 1978, **50**, 832A.
14. Thompson, M., Pahlavanpour, B., Walton, S. J. and Kirkbright, G. F., *Analyst*, 1978, **103**, 568.
15. Thompson, M. and Pahlavanpour, B., *Anal. Chim. Acta*, 1979, **109**, 251.
16. Thompson, M., Pahlavanpour, B., Walton, S. J. and Kirkbright, G. F., *Analyst*, 1978, **103**, 705.
17. Liversage, R. R., Van Loon, J. C. and De Andrade, J. C., *Anal. Chim. Acta*, 1984, **161**, 275.
18. Tioh, N., Israel, Y. and Barnes, R. M., *Anal. Chim. Acta*, 1986, **184**, 205.
19. Stroh, A. and Vollkopf, U., *J. Anal. At. Spectrom.*, 1993, **8**, 35.

20. Fernandez, F. J., *At. Absor. Newsl.*, 1973, **12**, 6.
21. Thompson, K. C. and Thomerson, D. R., *Analyst*, 1974, **99**, 595.
22. Rooney, R. C., *Analyst*, 1976, **101**, 749.
23. Greenland, L. P. and Campbell, E. Y., *Anal. Chim. Acta*, 1976, **87**, 323.
24. Godden, R. G. and Thomerson, D. R., *Analyst*, 1980, **105**, 1137.
25. Smith, A. E., *Analyst*, 1975, **100**, 300.
26. Pierce, F. D. and Brown, H. R., *Anal. Chem.*, 1976, **48**, 693.
27. Welz, B. and Melcher, M., *Spectrochim. Acta, Part B*, 1981, **36**, 439.
28. Lin, Y., Wang, X., Yuan, D., Yang, P., Huang, B. and Zhuang, Z., *J. Anal. At. Spectrom.*, 1992, **7**, 287.
29. Bockmann, A., Nonn, C. and Golloch, A., *J. Anal. At. Spectrom.*, 1993, **8**, 397.
30. Beaton, J. D., Burns, G. R. and Platou J., *Technical Bulletin No 14*, The Sulphur Institute, Washington, D. C., 1968
31. HMSO, *Tentative Method for Examination of Water and Associated Materials*, HMSO, London, 1983.
32. William, W. J., *Handbook on Anion Determination*, 1st Edn., Butterworth, London, 1979.
33. Kart, M., *Methods of Air Sampling Analysis*, 2nd Edn., American Public Health Association, Washington, D.C., 1977.
34. Leggett, D. J., Chen, N. H. and Mahadevappa, D. S., *Anal Chim. Acta*, 1981, **128**, 162.
35. Rees, T.D., Gyllenspetz, A. B. and Docherty, A. C., *Analyst*, 1971, **96**, 201.
36. Cresser, M. S., *Anal Chim Acta*, 1976, **85**, 253.
37. Cresser, M. S. and Isaacson P. J., *Talanta*, 1976, **23**, 885.
38. Cresser, M. S., *Laboratory Practice*, 1978, **27**, 639.
39. Anwar J., and Marr I. L., *J. Chem. Soc., Pakistan*, 1986, **8**, 67.
40. Syty A., *Anal Chem.*, 1979, **51**, 911.

41. Belcher, R., Bogdanski, S. L. and Townshend A, *Anal Chim. Acta*, 1973, **67**, 1.
42. Belcher, R., Bogdanski, S. L., Knowles, D. J. and Townshend, A., *Anal. Chim. Acta*, 1975, **77**, 53.
43. Calokerinos, A. C. and Townshend, A., *Progress in Analytical Atomic Spectroscopy*, 1982, **5**, 62.
44. Burguera M., Bogdanski, S. L. and Townshend, A., *Critical Rev. Anal. Chem.*, 1981, **10**, 185.
45. Burguera, J. L. and Burguera, M., *Anal. Chim. Acta*, 1984, **157**, 177.
46. Stevens, R. K., O'Keefe, A. E. and Krost, K. J., *Anal. Chem.*, 1971, **34**, 837.
47. Hawke, D. J., Lloyd, A., Martinson, D. M., Slater and P. G., Excell, C., *Analyst*, 1985, **110**, 269.
48. Arowolo, T. A., Ph.D. Thesis, *Development and Application Methods For Determination of Selected Sulphur Species*, Aberdeen University, UK, 1992.
49. Lewin, K., Walsh, J. N. and Miles, D. L., *J. Anal. At. Spectrom.*, 1987, **2**, 249.
50. Bardsley, C. E. and Lancaster, J. D., In Black, C. A., *Methods of Soil Analysis: Chemical and Microbiological Properties*, American Society of Agronomy, Madison, Chptr 15, pp.1102-1114.
51. Bogdanski, S. L., Shakir, I. M. A., Stephen, W. I. and Townshend, A., *Analyst*, 1979, **104**, 886.
52. Gustafsson, L., *Talanta*, 1960, **4**, 236.
53. Johnson, C. M. and Nshita, H., *Anal. Chem.*, 1952, **24**, 736.
54. Tabatabai, M. A. and Chae, Y. M., *Agronomy Journal*, 1982, **74**, 404.
55. Tabatabai, M. A. and Bremner, J. M., *Soil Sci. Soc. Amer. Proc.*, 1970, **34**, 62.
56. Atienza, J., Herrero, M. A., Maquieira, A., and Puchades, R., *Critical Rev. Anal. Chem.*, 1991, **22**, 331.
57. Grekas, N. and Calokerinos, A. C., *Anal. Chim. Acta*, 1987, **202**, 241.

58. Bogdanski, S. L., Townshend, A. and Yenegul, B., *Anal. Chim. Acta*, 1980, **115**, 361.
59. Beaton, J. D., Burns, G. R. and Platou, J., *Technical Bulletin No 14*, The Sulphur Institute, Washington, 1968.
60. West, P. W. and Gaeke, G. C., *Anal. Chem.*, 1956, **28**, 1816.
61. Scaringelli, F. P., Saltzman B. E. and Frey, S. A., *Anal. Chem.*, 1967, **39**, 1709.
62. Scaringelli, F. P., Elfers, L., Norris, D. and Hochheiser, S., *Anal. Chem.*, 1970, **42**, 1818.
63. Pate, J. B., Ammons B. E., Swanson, G. A. and Lodge, Jr. J. P., *Anal. Chem.*, 1965, **37**, 942.
64. West P. W. and Ordoveza, F., *Anal. Chem.*, 1962, **34**, 1324.
65. Bloomfield, C., *Analyst*, 1962, **87**, 586.
66. Tanner, R. L., Forrest, J. and Newman, L., in *Sulphur in the Environment Part I: The Atmospheric Cycle*, Ed. Nriagu, J. O., John Wiley and Sons Ltd, New York, 1978, pp. 371-451.
67. Cresser, M. S., *Proc. Anal. Div. Chem. Soc.*, 1978, **15**, 68-69.
68. Syty A., *Anal. Chem.*, 1973, **45**, 1744.
69. Winkler, H. E. and Syty A., *Environmental Science and Technology*, 1976, **10**, 913.
70. Lewis, S. F. and Syty, A., *At. Spectrosc.*, 1983, **4**, 199.
71. Ruschak, M. L. and Syty, A., *Anal. Chem.*, 1982, **54**, 1637.
72. Harrison, R. M., in *Handbook of Air Pollution Analysis*, Eds. Harrison, R. M. and Perry, R., Chapman and Hall, New York, 2nd Edn., 1986, pp. 279-341.
73. Henden, E., Pourreza, N. and Townshend, A., *Progress in Analytical Atomic Spectroscopy*, 1979, **2**, 355.
74. Calokerinos, A. C. and Townshend, A., *Fresenius Z. Anal. Chem.*, 1982, **311**, 214.
75. Kouimtzis, T. A., *Anal. Chim. Acta*, 1977, **88**, 303.
76. Grekas, N. and Calokerinos, A. C., *Analyst*, 1985, **110**, 335.
77. Alder, J. F. and Kargosha, K., *Anal. Chim. Acta*, 1979, **111**, 145.

78. Nicholson, G. and Syty, A., *Anal. Chem.*, 1976, **48**, 1481.
79. Calzada, M. D., Quintero, M. C., Gamero, A. and Cotrino, J., *Talanta*, 1992, **39**, 341.
80. Nakahara, T., Morimoto, S. and Wasa, T., *J. Anal. At. Spectrom.*, 1992, **7**, 211.
81. Nikolic, S. D. and Milosavljevic, E. B., *Analyst*, 1991, **116**, 49.
82. Goulden, P. D. and Brooksbank, P., *Anal. Chem.*, 1975, **47**, 1943.
83. Van Syke, D. D., *Anal. Chem.*, 1954, **26**, 1706.
84. Lindenbaum, A., Schubert, J. and Armstrong, W. D., *Anal. Chem.*, 1948, **20**, 1120.
85. Archer, E. E., *Analyst*, 1954, **79**, 30.
86. Schulz, N. F., *Anal. Chem.*, 1953, **25**, 1762.
87. Moore, W. A., Kroner, R. C. and Ruchhoft, C. C., *Anal. Chem.*, 1949, **21**, 953.
88. Moore, W. A., Ludzack, F. J. and Ruchhoft, C. C., *Anal. Chem.*, 1951, **23**, 1297.
89. Kolthoff, I. M., Elving, P. J. and Stross, F. H., *Treatise on Analytical Chemistry: Part III- Analytical Chemistry in Industry*, John Wiley and Sons, New York, 1971, Vol. 2, pp.477-480.
90. Bondarowicz, J., *Spectroscopy*, 1993, **8**, 30.
91. Pickhardt, W. P., Oemler, A. N. and Mitchell, Jr., J., *Anal. Chem.*, 1955, **27**, 1784.
92. Montgomery, H. A. C. and Thom, N. S., *Analyst*, 1962, **87**, 689.
93. Van Hall, C. E., Safranko, J. and Stenger, V. A., *Anal. Chem.*, 1963, **35**, 315.
94. Allison, L. E., *Soil Sci. Soc. Am. Proc.*, 1960, **24**, 36.
95. Clarke, F. E., *Industrial Engineering Chem.* 1947, **19**, 889.
96. Kreg, J. and Szekiolda, K. H., *Z. Anal Chem.* 1965, **207**, 388.
97. Dugan, G., *Anal. Lett.*, 1977, **10**, 639.
98. Robinson, D. and Smith, K. A., in *Soil Analysis-Modern Instrumental Techniques*, Ed. Smith K. A, Marcel Dekker, New York, 2nd Edn., 1991, Chptr. 11, pp 465-503.
99. Simon, H., Daniel, H. and Kleber, J. F., *Angew. Chem.*, 1959, **71**, 303.
100. Proksch, G., *Plant Soil*, 1969, **31**, 380.

101. Fieldler, R. and Proksch, G., *Anal. Chim. Acta*, 1975, **78**, 1.
102. Ross, P. J. and Martin, A. E., *Analyst*, 1970, **95**, 817.
103. Middelboe, V. and Johansen, H. S., in *Soil Analysis: Modern Instrumental Techniques*, Ed. Smith, K. A., Marcel Dekker, New York, 2nd Edn., 1991, Chptr. 10, pp 433-463.

Chapter 5

CHAPTER FIVE

STRIPPING VOLTAMMETRY

5.1 INTRODUCTION

Heavy metals have been recognised as highly toxic and dangerous environmental pollutants reaching man through respiration and the food chain. Owing to their nonbiodegradable nature, heavy metals accumulate in vital organs in man, thus exerting progressively growing toxic action. Mercury, cadmium, arsenic, thallium, and selenium are the most hazardous heavy metals, some of which have been linked to cancer and heart diseases.¹ Some essential nutrients such as copper, zinc and tin may exert toxic action depending on their concentration levels. A 'concentration window' therefore exists between the toxic and essential levels for these metals. Due to this concentration difference, a reliable method for determining the metal content in various matrices is necessary. The toxicity of some metals is controlled by their physicochemical forms. Speciation studies are therefore required for understanding the role the trace metals play in bio-cycles and human health.

The determination of trace metals has been performed using atomic absorption spectroscopy, plasma emission and mass spectrometry, x-ray fluorescence spectroscopy, stripping analysis and neutron activation analysis. The choice of a suitable analytical method for trace metals depends on the detection limit, instrumental cost, analysis time, sample preparation, sensitivity and selectivity required.

Stripping analysis has gained popularity due to its ability to determine more than one element at sub-ppb levels, using inexpensive instrumentation. The technique compares favourably with non-electrochemical techniques in terms of speed of analysis. In addition, stripping analysis offers the advantage of species characterisation. The technique is also suitable for automatic on-line monitoring and for in situ measurements.

5.2 PRINCIPLES OF VOLTAMMETRY

Voltammetry is a type of electroanalytical techniques in which the current at a working electrode is measured as a function of a potential waveform applied to the electrode.¹ The potential of the working electrode serves as a driving force for the electrochemical reaction (reduction or oxidation) at the surface. The current versus voltage curves are obtained when a gradually changing voltage is applied to a cell containing the solution of interest, a stable reference electrode and a small area working or indicator electrode.² Such curves are called voltammograms. In the special case where the dropping mercury electrode is used as the working electrode, the technique is referred to as polarography, and the current versus voltage curves are called polarograms. In voltammetry, an electron transfer reaction can take place if a suitable potential is applied to the working electrode. The extent of this electron-transfer reaction is determined by the surface concentration of some electroactive species. The resultant current is transient, decaying rapidly unless there is some mechanism to bring a continuously renewed supply of the electroactive material to the surface.

5.3 MASS TRANSPORT

Three main modes of mass transport that occur in voltammetry are diffusion, migration and convection.

5.3.1 Diffusion

Diffusion is the movement of species along a concentration gradient. An electrode reaction converts the starting material to product and this is represented as:



There exists a boundary layer close to the electrode in which the concentration of M^{n+} is a function of the distance from the electrode surface. The concentration of M^{n+} is lower at the surface than in the bulk and it therefore diffuses towards the electrode.

5.3.2 Migration

Migration is the movement of charged species due to a potential gradient. It is the mechanism by which charge passes through the electrolyte. The current of electrons through the external circuit must be balanced by the passage of ions through the solution between the electrodes (cations moving to cathode and anions to anode). Migration is not necessarily an important form of mass transport for the electroactive species, even if charged. The forces leading to migration are purely electrostatic, and hence the charge can be carried by ionic species in solution. Usually electrolysis is carried out in an inert electrolyte which carries most of the charge, and little of the electroactive species is transported to the electrode by migration.

5.3.3 Convection

Convection is the movement of species due to mechanical forces. Voltammetric experiments can be performed under forced convection which may be achieved by stirring or agitating the electrolyte or flowing the electrolyte through the cell. These forced convections may have a large influence on the current density.

In situations where solutions are stirred, the resultant bulk motion of the liquid is the dominant transport mechanism, but diffusion also plays some part. A thin stationary layer of liquid is assumed to be in contact with the electrode and is unaffected by stirring. The mechanism of mass transport across this thin layer is by diffusion.

In a well stirred solution, fresh active material is always available to the electrode, hence the current is proportional to the concentration, which diminishes slowly due to the

charge transfer reaction. The current rolls off exponentially with time at a slow rate. In the absence of stirring, there is no noticeable change of bulk concentration because during all but the first small fraction of the time, the current is very small. However, if the solution is stirred, the current continues at a higher level and appreciable changes in the concentration may take place.

5.4 ELECTRON TRANSFER

Electrolysis, the process of electron transfer, only takes place in a cell with an anode and a cathode because of the need to maintain the overall charge balance. In a voltammetric experiment, the potential is varied in a predetermined manner such as a linear ramp or pulse train and in the presence of electroactive species. A current is recorded when the applied potential becomes sufficiently negative or positive for the electroactive species to be electrolysed. For electron transfer to take place, there must be correspondence between energies of the electron orbitals where electron transfer takes place in the donor and the acceptor. In the electrode, this level is the highest filled orbital which in metals is the Fermi level, while in soluble species it is the valence orbital which accepts or donates electrons.

For systems at equilibrium, the applied potential E controls the concentration of the electroactive species:



at the electrode surface according to the Nernst equation,

$$E = E^0 - \frac{RT}{nF} \ln\left(\frac{a_{\text{red}}}{a_{\text{ox}}}\right) \quad (5.3)$$

where a_{ox} and a_{red} are the activities of the oxidised and reduced form of the electroactive species (Ox and Red) respectively, n is the number of electrons transferred in the reaction, R is the molar gas constant, T is the absolute temperature, F is the faraday constant and E° is the standard electrode potential.

Substituting the activities by concentration terms and using common logarithms and an absolute temperature of 298 K, the Nernst equation becomes:

$$E = E^{o'} - \frac{0.05916}{n} \log\left(\frac{\text{red}}{\text{ox}}\right) \quad (5.4)$$

where $E^{o'}$ is the formal electrode potential defined in terms of concentration instead of activities.

The current resulting from a change in oxidation state of the electroactive species is termed faradaic current as it obeys Faraday's law;

$$q = \int i dt = mnF \quad (5.5)$$

where q is the charge passed during a period t , which is the charge required to convert m moles of starting material to product in an electrode reaction involving the transfer of n electrons per molecule. The faradaic current is a direct measure of the rate of redox reaction taking place at the electrode. This depends mainly on the rate at which the species move from the bulk of the solution to the electrode (mass transport), and the rate at which electrons transfer from the electrode to the solution species and vice versa (charge transfer).

5.5 PRINCIPLES OF STRIPPING VOLTAMMETRY

A detection limit of $10^{-5} \text{ mol dm}^{-3}$ can be achieved by basic electrochemical analytical methods. This limit is governed by the ratio the faradaic current to the background

current. The background current consists of the faradaic currents of impurities, the capacitive current due to charging of the electrical double layer at the electrode surface and the noise of the electronic circuit. A much lower detection limit ($10^{-11} \text{ mol dm}^{-3}$) can be achieved using stripping voltammetry. In this method, an analyte is accumulated onto the working electrode, usually in the form of an amalgam. The analyte is then stripped into the solution by scanning the potential towards more positive or more negative values. Since there is a substantially higher concentration of the analyte within the amalgam than originally present in the solution, the sensitivity of the determination is much greater, allowing a detection limit as low as $10^{-11} \text{ mol dm}^{-3}$ to be achieved. The high sensitivity obtained by stripping voltammetry is also due to compensation of the charging background current. In the case of differential pulse stripping voltammetry, this is achieved by sampling currents twice; once prior to the application of the pulse and then again just before pulse termination. The difference in current is attributed mainly to the faradaic reaction.

Stripping voltammetry is a two step procedure:

The deposition (preconcentration/accumulation) step

The deposition step is usually carried out by employing a controlled potential electrolysis for a specific time and under reproducible hydrodynamic (mass transport) conditions in the solution. This results in the formation of amalgam with the mercury or mercury film working electrode. The electrode reaction that occurs at the mercury working electrode e.g. for measuring the amalgam-forming metals is represented by the equation:



Since the volume of the mercury is small, as compared with the volume of the solution, this step amounts to concentration of the analyte.³

Solid electrodes (without a mercury film) can also be used for measurements of ions with more positive redox potential than mercury. The electrode reaction for solid electrodes is represented by:



resulting in a metallic film on the electrode.

The stripping step

In this step, for metals, the potential is scanned anodically (towards more positive potential), linearly or in another potential-time waveform. The metal analyte is reoxidised back into the solution when the potential reaches the standard potential of the metal - metal ion couple, resulting in a current flow.



5.6 INSTRUMENTATION

5.6.1 Reference electrode

This electrode provides a known and stable potential that is insensitive to the composition of the solution under study and with which the potential of the working electrode is compared.¹ Due to its constant composition, the reference electrode remains unpolarised during the analysis. Silver-silver chloride and saturated calomel electrode (SCE)) are mostly used as reference electrodes in electrochemical analysis. The silver/silver chloride reference electrode was used in this work for the voltammetric determination of Se(IV) due to its lower sensitivity to current loadings compared with other reference electrodes.

5.6.2 Auxiliary electrode

The auxiliary electrode is made of a chemically inert conducting material having a reasonable surface area. The electrode is employed to minimise errors in cell resistance in controlling the resistance of the working electrode. The most commonly used auxiliary electrodes in stripping analysis are platinum wires or graphite rods.¹

5.6.3 Working electrode

The working electrode is where the reaction of interest takes place. In voltammetry, the working electrodes used should have small surface area to enhance polarisation. The depletion of the analyte by electrolysis is minimised by using very small electrodes. Hanging mercury electrodes and mercury film electrodes have been used in stripping analysis.¹ Gold, carbon and platinum can be used as support materials for the formation of a thin film of mercury.

5.6.3.1 *Hanging mercury drop electrode*

The advantages of using the hanging mercury drop electrode (HMDE) in stripping analysis include:

- a fresh surface of mercury is rapidly and reproducibly renewed for each measurement, thus minimising interferences due to carry-over.
- the high overpotential for reduction of hydrogen ion to hydrogen at the mercury electrode makes it possible to work with quite high negative potentials without the unwanted generation of free hydrogen adversely affecting the results.

However, the hanging mercury drop electrode suffers from the following drawbacks:

- use of the electrode as an anode is limited to a positive potential of 0.4 V (versus saturated calomel electrode). This is because Hg is oxidised to Hg(I) at higher potentials, giving a voltammogram that masks those of other oxidizable species.

- the electrode solution may seep into the capillary tube between the glass and the mercury, causing irregularities in the voltammograms. This, however, can be prevented by coating the inside of the capillary with a silicone layer.
- mercury is more or less toxic depending on the form in which it is present. The use of the mercury electrode may lead to the pollution of the working environment with mercury.
- the HMDE has a low surface area to volume ratio. The small area reduces the deposition efficiency and the large volume yields a low concentration of the metals in the mercury electrode. Also, the large volume causes broadening of the stripping peaks.
- the metal analytes may diffuse into the mercury column in the capillary especially if very long deposition period is employed, thus causing further broadening and decreasing of peak current.
- the mercury drop may be dislodged if very high solution stirring rates are used. Moderate stirring rates are therefore recommended to avoid this.
- the electrode has not gained widespread use in flowing stream analysis because of inherent instability and due to practical difficulties.

5.6.3.2 *Mercury film glassy carbon electrode*

The problems encountered with HMDE led to the introduction of glassy carbon as a working electrode. The glassy carbon is plated with a thin film of mercury to produce a mercury film glassy carbon electrode (MFGCE). The electrode shows sensitivities of at least ten times higher than the HMDE when used as a rotating thin film electrode. This is attributed mainly to the different diffusion process occurring in the two electrodes. Sensitivity is related to the electrode's area/volume ratio. The higher the value of this ratio the higher the sensitivity. The very small volume required for the formation of the film makes the mercury film electrode ideal for the determination of toxic metals at the sub-ppb level.

Glassy carbon as a support material for a mercury film suffers from several disadvantages. These include an uneven surface which is not well defined, as compared to the perfectly spherical mercury drop and, passivation of the glassy carbon surface by adsorbed species which may result in an incomplete mercury film being formed. The surface of the glassy carbon electrode should be pre-treated to make it as even as possible. This involves polishing of the electrode on a polishing cloth to a mirror finish using fine alumina powder made into a slurry.

5.6.3.3 *Chemically modified electrode*

Chemically modified electrodes have bound to their surface substances or functional groups that alter the physico-chemical properties of the electrode.⁴ Since the ideal chemically inert electrode does not exist, all real electrodes are to some extent chemically modified electrodes due to presence of various functional groups on their surface and by substances adsorbed from solution. It is therefore difficult to draw a distinct boundary between chemically modified electrodes and the various combined electrodes such as potentiometric enzymes, tissue and bacteria electrodes, and gas sensors.⁴ In this study, a narrow definition of chemically modified electrodes is those electrodes with modifiers bound directly to the electrode surfaces either by chemical bonds or by strong physical interactions.

Modifications of the electrode surface can be employed to improve sensitivity and/or selectivity. Catalytic effects may also be introduced by modifying the electrodes using suitable catalysts.

For the analysis of trace metals using voltammetric methods, no preferred substitute for the mercury electrode has been found despite the development of chemically modified electrodes over the past decade.⁵⁻¹⁰ This is due to the unique ability of mercury to form amalgams with metal ions during the preconcentration step.

5.7 SUPPORTING ELECTROLYTE

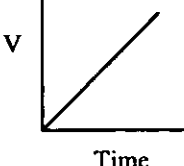

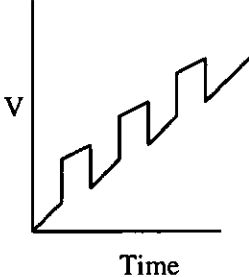
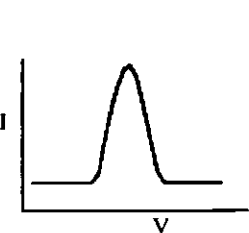
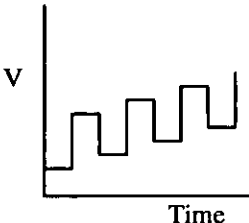
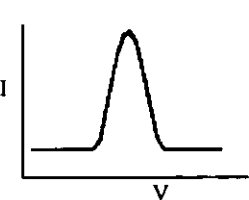
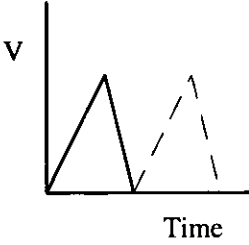
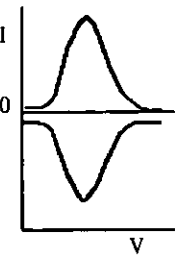
A supporting electrolyte is used in stripping analysis to minimise electrical migration of metal ions caused by the electric field. Besides, it provides the conductive medium that voltammetry requires. Substances that have been used as supporting electrolytes include: inorganic salts (KCl, KNO₃), mineral acids (HCl, HClO₄), bases (NaOH) and buffer systems such as NaHCO₃/Na₂CO₃ and acetate-acetic acid (for pH control).

The control of pH may be necessary because of speciation consideration and because electrode potentials may vary with pH. The composition of the electrolyte may also affect the sensitivity and selectivity of the measurements. An ideal supporting electrolyte should give well shaped and resolved peaks for all the metals simultaneously determined. Supporting electrolytes of concentration range 0.001-1M may be used, however, a concentration of 0.1M is usually used as a compromise between high conductivity and minimum contamination. Consistency of the supporting electrolyte from sample to sample is necessary to avoid changes in the ohmic drop. The reagents used for preparing the supporting electrolytes should be ultra-pure.

5.8 MODES OF STRIPPING VOLTAMMETRY

Various modes of stripping voltammetry are illustrated in Table 5.1.

Table 5.1 Modes of stripping voltammetry

| Type of stripping voltammetry | Potential excitation signal (waveform) | Voltammogram |
|--|---|--|
| <p>Linear scan voltammetry</p> <p><u>Disadvantage</u> It suffers from a significant charging current contribution.</p> <p><u>Detection limit</u>: 10^{-5} - 10^{-4} M</p> | <p>Linear scan</p>  |  |
| <p>Differential pulse voltammetry</p> <p>Pulse of equal magnitude are superimposed on a linear scan.</p> <p>Sampling of current is done before the application of the pulse and just before its termination.</p> <p><u>Advantages</u> It offers higher sensitivity than linear scan voltammetry due to enhancement of faradaic current and decrease in nonfaradaic charging current.</p> <p><u>Detection limit</u> 10^{-8} - 10^{-7} M</p> | <p>Differential pulse</p>  |  |
| <p>Square wave voltammetry</p> <p>Symmetrical square wave pulse is superimposed on a staircase waveform when the forward pulse coincides with the staircase step.</p> <p><u>Advantages</u> It offers great speed (faster than DPSV), higher sensitivity (similar to DPSV) and effective discrimination against charging (capacitive) current. Also, it is insensitive to dissolved oxygen in the sample.¹¹</p> | <p>Square wave</p>  |  |
| <p>Cyclic voltammetry</p> <p>Triangular potential waveform is applied.</p> <p>The potential is first varied linearly then the scan direction is reversed and the potential is returned to its original value.</p> <p><u>Advantages</u> It is an important tool for the study of mechanism and rates of oxidation / reduction processes, in organic and metal-organic systems. Cyclic voltammograms often reveal intermediates in oxidation/reduction reactions.</p> | <p>Triangular</p>  |  |

Applications of different modes of stripping voltammetry for the analysis of electroactive substances are presented in Table 5.2.

Table 5.2 Applications of various modes of stripping voltammetry for the analysis of trace elements and other electroactive substances.

| Electrode type | mode of stripping voltammetry | Analyte | Reference number |
|---|---|--------------------------|------------------|
| Mercury film glassy carbon electrode (MFGCE) electrode modified with pyrogallol | Adsorptive cathodic stripping voltammetry | V | 12 |
| MFGCE modified with 8-hydroxyquinoline and dimethylglyoxime | Square wave adsorptive stripping voltammetry | Cu, Ni | 11 |
| MFGCE modified with catechol complexing agent | Adsorptive stripping | Sn | 13 |
| Nafion coated mercury film electrode modified with dimethylglyoxime | Adsorptive stripping voltammetry | Ni | 14 |
| Nafion coated mercury film electrode | Anodic stripping voltammetry | Cu, Pb | 5 |
| HMDE modified with poly-L-histidine | Cathodic stripping voltammetry | Cu | 15 |
| Platinum coated with anion exchange polymer (poly-4-vinylpyridine) | Stripping voltammetry | Cr (IV) | 16 |
| HMDE modified with poly-L-lysine | Differential pulse cathodic stripping voltammetry | Nitroprusside anion | 17 |
| Gold film electrode | Differential pulse anodic stripping voltammetry | Se | 18 |
| HMDE | Adsorptive stripping voltammetry-differential pulse modulation used | Se in the presence of Cu | 19 |

5.8.1 Differential pulse cathodic stripping voltammetry

In this thesis, the voltammetric technique employed was differential pulse cathodic stripping voltammetry (DPCSV). DPCSV is used for the determination of a wide range of organic and inorganic compounds that form insoluble salts with the electrode material. This involves the application of a relatively positive potential to the working electrode resulting in the formation of an insoluble film of salt on the electrode surface. A mercury working electrode is usually used for such applications, although silver electrodes can be used for some species such as halides and sulphides.

In the deposition step, the reactions that occur are represented as :



where M is the electrode material, A^{n-} is the analyte and MA the insoluble salt forming the film on the electrode. The insoluble salt formed on the working electrode is stripped off during the stripping step by applying a cathodic potential scan (scanning towards more negative potential).



The sensitivity of cathodic stripping voltammetry depends on the amount that can be plated in a given period which is a function of the kinetics of formation and the solubility of the deposited compound, the diffusion coefficient of the reacting ion in the deposited film, and the density of the film.²⁰ The dissociation rate of the insoluble mercury compound also determines the sensitivity of cathodic stripping voltammetry. A high sensitivity is achieved in this method by using electrodes with large surface areas such as

a mercury drop pool. This is in contrast to the use of mercury films in anodic stripping voltammetry to obtain higher amalgam concentration. The use of a mercury pool electrode has been recommended to overcome the problems of lower peak currents and erratic results when an in situ mercury film or HMDE is used.²¹ In this method, the use of highly purified mercury and supporting electrolyte, effective removal of oxygen and separation of auxiliary electrode from the sample were recommended for achieving reproducible results.

5.8.2 Adsorptive stripping voltammetry

Adsorption of organic compounds has been regarded as a problem that limits voltammetric measurements. However, it has been shown that controlled adsorptive accumulation of important compounds on the surface of an electrode can be used to enhance sensitivity and selectivity.

The adsorption process must be reproducible and proceed without passivating the electrode. The amount of analyte accumulated on the electrode surface depends on the solvent, electrode material, ionic strength, pH, mass transport potential and temperature. In contrast to cathodic stripping, the accumulated analyte does not react with the electrode material and there is no charge transfer during the preconcentration step in adsorptive stripping voltammetry. Adsorptive stripping voltammetry involves the formation of a film on the electrode surface. It is therefore not unusual for the calibration graphs to display non-linearity at concentrations higher than 10^{-6} M. However, the reproducibility of these curves is quite good. The linearity of the calibration graphs can be improved via lowered surface coverage by applying shorter accumulation time, lower stirring rates and sample dilution.

5.9 FLOW INJECTION-ELECTROCHEMICAL DETECTION

Flow injection coupled to electrochemical detection lends itself to high precision and low detection limits and sample throughput can be high. This method has been widely used for determination of organic substances, particularly for the direct determination of drugs.^{22,23}

The early development of flow injection-anodic stripping voltammetry was hampered by the difficulties associated with the use of mercury electrodes. With the development of the mercury film electrode (MFE) by Florence,²¹ this situation has changed. Flow injection-anodic stripping voltammetry at MFE is now a well characterised technique that lends itself to routine analysis in a wide range of applications. The mercury film electrodes used in ASV are usually based on a glassy carbon substrate. This is because the substrate allows formation of a stable mercury film without memory effects. It has been suggested that mercury is deposited on glassy carbon in the form of droplets (1 μm) rather than as a uniform film.²³ However, film approximation has been found to be valid for very thin films. Tubular,²⁴ thin layer and wall jet^{25,26} geometries have been used for flow injection-anodic stripping voltammetry.

Usually, application of ASV at a MFE involves the deposition of metal ion into the mercury film under convective diffusion conditions. The solution is brought to rest for a given period and the deposit is stripped under diffusion control. It has now been demonstrated however, that the stripping step can be performed in a flowing carrier stream. This offers the advantage of a simplified and improved experimental procedure especially in regard to electrolyte exchange. When stripping is done in a static solution, concentration effects resulting from high concentration of the oxidised metal in the reaction layer may adversely affect the stripping peak.²⁷ This effect is eliminated when stripping is done in a flowing carrier stream.

In a static system, the use of in situ plated mercury is preferred to preplated mercury film. This is due to the possibility of exposure of preplated mercury film to air, when solutions are manually changed during the plating and stripping steps. With a flow system, preplated films can easily be prepared and may be preferable to in-situ plating of mercury film because it diminishes contamination of the electrode. Gold electrodes have been used for the determination of Se, As, and Hg using ASV on the bare electrodes

DPASV is becoming increasingly popular for metal analysis, in preference to dc ASV, primarily because of its inherently greater sensitivity.⁴⁵ The differential stripping peak current is significantly affected by the flow. However, proper optimisation of instrumental settings and flow conditions, it is possible to obtain reproducible response.²⁶

The advantage of using flow systems such as FI with stripping voltammetry is the convenience it offers in the electrolyte exchange procedure. For instance, the stripping solution can be changed several times during the stripping scan, so that the best complexing medium for each metal of interest can be used.

A practical difficulty encountered in using ASV is the removal of dissolved oxygen. Dissolved oxygen has little effect on the plating process, but has a major effect on the stripping scan. It can lead to instability of the metal amalgam and cause irreproducible background and stripping currents. In FI, the removal of oxygen is effected by purging of the carrier solution reservoir using an inert gas. Purging with inert gas can be restricted to the solution in the detector compartment rather than the entire carrier solution in the reservoir, as has been done by Wang when using a large volume wall jet detector.²⁵

REFERENCES

1. Wang, J., *Stripping Voltammetry-Principles, Instrumentation and Applications*, VCH, Florida, 1985.
2. Cox, J. A. and O'Reilley, J. E., in *Instrumental Analysis*, Eds. Christian, G. D. and O'Reilley, J. E., Allyn and Bacon, Boston, 2nd Ed., 1986, pp. 52-95.
3. Riley, T. and Tomlinson, C., *Principles of Electrochemical Methods*, John Wiley and Sons Ltd, Chichester, 1987, pp.177
4. Zyka J., *Instrumentation in Analytical Chemistry*, Ellis Horwood, New York, 1994, Vol. 2, 13-50.
5. Dalangin, R. R. and Gunasingham H., *Anal. Chim. Acta*, 1994, **291**, 81.
6. Tanaka, S. and Yoshinda H., *Talanta*, 1989, **36**, 1044.
7. Wang, J., Greene B. and Morgan C., *Anal. Chim. Acta*, 1984, **158**, 15.
8. Gao Z., Li P., Dong S. and Zhao Z., *Anal. Chim. Acta*, 1990, **232**, 367.
9. Dong S. and Wang Y., *Anal. Chim. Acta*, 1988, **212**, 341.
10. Gunasingham H., and Dalangin R. R., *Anal. Chim. Acta.*, 1991, **246**, 309.
11. Economou, A. and Fielden P. R., *Anal. Chim. Acta*, 1993, **273**, 27.
12. Adeloju, S. B. O. and Pablo F., *Anal. Chim. Acta*, 1994, **288**, 157.
13. Adeloju S. B. O. and Pablo F., *Anal. Chim. Acta*, 1992, **270**, 143.
14. Zen, J. and Lee M., *Anal. Chem.*, 1993, **65**, 3238.
15. Josino, C. M., Rui Z. and Fogg A. G., *Analyst*, 1990, **115**, 1561.
16. Cox, J. A. and Kulesza, P. J., *Anal. Chim. Acta*, 1983, **154**, 71.
17. Pirzad, R. and Moreira, C., *Analyst*, 1994, **119**, 1.
18. Wu, T. and Xiang, W., *Analyst*, 1988, **113**, 1431.
19. Van den Berg, C. M. G. and Khan, S. H., *Anal. Chim. Acta*, 1990, **231**, 221.

20. Brainina, Kh. Z., *Talanta*, 1971, **18**, 513.
21. Florence, T. M., *J. Electroanal. Chem.*, 1979, **97**, 219.
22. Chan, H. K. and Fogg A.G., *Anal. Chim. Acta*, 1979, **111**, 281.
23. Ivaska, A. and Smyth, F., *Anal. Chim. Acta*, 1980, **114**, 283.
24. Lieberman, S. H. and Zirino, A., *Anal. Chem.*, 1974, **46**, 20.
25. Wang, J. and Dewald, H. D., *Anal. Chem.*, 1984, **56**, 156.
27. Gunasigham, H., Ang, K. P., Ngo, C. C. and Thiak, P. C., *J. Electroanal. Chem.*, 1986, **198**, 27.
28. Almeida Motu, A. C. M., Buffles, J., Kounaves, S. P. and Goncalves, M., *Anal. Chim. Acta*, 1985, **172**, 13.

Chapter 6

CHAPTER SIX

ISOTOPE RATIO MASS SPECTROMETRY

6.1 INTRODUCTION

Mass spectrometry as the name implies separates ions into a spectrum on the basis of their masses or, more precisely, according to their mass-to-charge ratio.¹ The separation of ions is achieved by magnetic or a combination of electrical and magnetic fields. All types of mass spectrometer are equally suitable for routine isotope analysis. However, single-, double-, and triple or multi-collector magnetic sector instruments and to a smaller extent quadrupole mass spectrometers have been used in isotope tracer analysis.²

To determine the isotopic composition of stable elements by mass spectrometer, the analyte is usually converted to a suitable gas.¹ The gas should have a low molecular mass, be simple in structure, easily prepared from organic or inorganic compounds and readily pumped out of the mass spectrometer.

Canham and Pacey (1988) used a mass spectrometer with an electron impact (EI) source in their feasibility study of flow injection-mass spectrometry to determine concentrations of As, Se, Sn and Sb after hydride generation.³ Both single focusing magnetic sector and quadrupole mass spectrometry (GC-MS system) were used. The latter system was used for the quantitative determination of the generated hydrides.

6.2 PRINCIPLES AND INSTRUMENTATION

6.2.1 Ion production by electron impact

Commercially available instruments for mass spectrometry use several types of ion source. Chemical ionisation is widely used in high resolution mass spectrometry of labelled and

unlabelled organic and metabolic intermediates.² Field ionisation and field desorption have also been used for producing ions of organic compounds.⁴ However, isotopic ratio analyses of inorganic gases are usually done using EI.

Neutral molecules must be ionised before they can be separated by the mass spectrometer. In the EI method, the sample molecules in the gaseous phase are bombarded with a stream of accelerated electrons emitted by a thin, red-hot filament usually made of rhenium or tungsten. These electrons may eject electrons from the molecules, leaving positively charged ions, or they may decompose molecules into charged fragments.¹ The energy of this stream of accelerated electrons is usually adjustable from 5 to 80 eV, but by convention usually operates at 70 eV.⁴ The ionisation of the gaseous sample does not have to be quantitative because it is the relative abundance of ions of different mass-to-charge ratios, rather than absolute abundance that is measured in isotope mass spectrometry. The electron beam should, however, have sufficient energy to cause ionisation of gas molecules and for sufficient molecules to be dissociated for the law of probability to hold. The relative abundance of the various ions produced by electron impact of any given molecule under a given set of conditions is constant and hence the method can be used for identification.

For effective ionisation of gas molecules to take place, the ionising region of the mass spectrometer is maintained at low pressure ($<10^{-6}$ Torr) and the electron beam is accelerated through a potential which is considerably above the ionisation potential of the analyte.¹ Most of the positively charged ions are singly charged, a few are doubly charged and rarely, triply charged. The remaining neutral gas molecules are continually removed from the mass spectrometer tube by means of a pump. The positively charged ions produced are constantly drawn out of the ionising region and accelerated in the proper direction by a negative potential applied to an electrode in the ion source. The advantages of using electron impact sources are high efficiency, durability and capability of producing a steady, intense beam of positive ions.

6.2.2 Ion separation

6.2.2.1 *Mass analysis by magnetic sectors*

The ion beam, once outside the ion source, moves down a straight, evacuated tube towards a curved region placed between the poles of a magnet, called a magnetic sector.⁵ The function of the magnetic sector is to disperse the ions in curved paths that depend on their mass-to-charge ratio. A mass spectrometer is operated at low pressure so that the mean path of the ion is large with respect to the geometry of the analyser assembly. Scattering due to ion-ion and ion-molecule collisions would result if this requirement were not met. The low mass ions are deflected most while the heavier mass ions are deflected least.

The kinetic energy (K.E.) of the positively charged ions leaving the source is given by the equation;

$$\text{K.E.} = \frac{mv^2}{2} = Ve \quad (6.1)$$

where m is the mass, v is the velocity, e is the charge and V is the accelerating voltage.

A permanent magnet encloses the analyser such that a homogeneous magnetic field is at right angles to the flight tube (Figure 6.1).

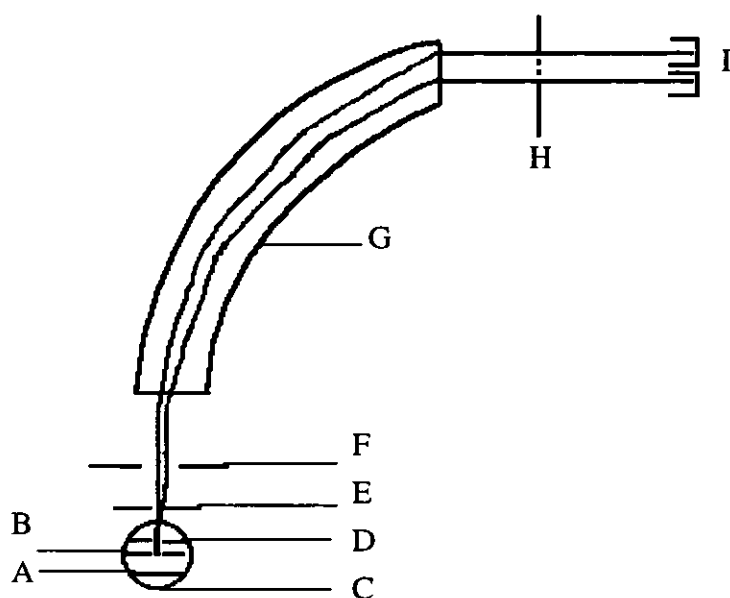


Figure 6.1 Mass separation by magnetic mass spectrometer. A, ion repeller; B, exit slit; C, source magnet; D, source slit, E, Beam centring electrodes; F, alpha plate, G, analyser magnetic field; H, resolving slit; and I, Faraday collectors.

The ion beam is deflected through a fixed angle onto a collector plate.² If the flux density of the magnetic field through which the ion passes is B , the ions in the magnetic field experience a centripetal force of Bev . This force must be balanced by the centrifugal force of ions mv^2/r , where r is the radius of curvature. Thus

$$\frac{mv^2}{r} = Bev \quad (6.2)$$

Substituting $v = Ber/m$ from the K.E. equation 6.1, yields

$$\frac{m}{e} = \frac{B^2 r^2}{2V} \quad (6.3)$$

This is the mass spectrometer equation.

For singly charged ions, the radius is determined by the magnitude of the magnetic and electric fields. A mixture of ions of different mass-to-charge ratio can be analysed by either: varying the magnetic field, while holding the accelerating voltage constant or varying the accelerating voltage and maintaining the magnetic field constant. Magnetic scanning is used in most instruments, since electric field scanning can cause problems, such as, a decrease in sensitivity at high mass.

6.2.2.2 *Quadrupole mass analysers*

The quadrupole mass analyser consists of four parallel rods as shown in Figure 6.2. The quadrupole field into which the ions are accelerated is generated by connecting opposite rods to a direct current and radio frequency voltages, one pair being 180 degrees out of phase with the other.^{2,4} Single charged ions undergo oscillations on entering the quadrupole field which are dependent on the mass of the ion and field parameters. Mass spectra are obtained by varying the direct current and radio frequency components of the voltage supply (while keeping their ratio constant) to the quadrupole assembly hence changing its mass filter.

Quadrupoles have several advantages over magnetic instruments. They are cheaper and more compact than magnetic instruments.⁴ Rapid scans can be achieved with quadrupole instruments since only a change in voltages is required; a spectrum can be produced within a millisecond, but the quality is often poor.

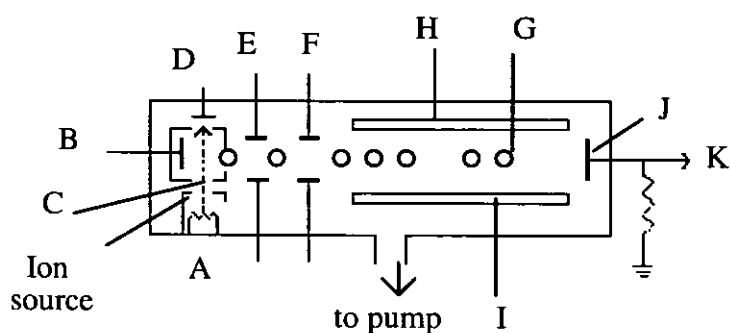


Figure 6.2 Quadrupole mass spectrometer. A, filament; B, ion repeller; C, electron beam; D, electron trap; E and F, ion beam focusing plates; G, ion beam; H and I, two of the four quadrupole rods; J, collector; and K, output.

6.2.2.3 Multi-collector systems

The comparison of two ion currents in a single collector mass spectrometer can be done by measuring them sequentially. Using this procedure can result in a loss of precision. This is because the conditions under which the ions are generated, the pressure and composition of the sample, and characteristic of the measurement systems are all susceptible to fluctuations during analysis.² However, such effects are minimised in a multi-collector systems since two or more ion beams are collected and measured simultaneously. The two ion beams in a dual collector instrument can be compared electronically and the ratio computed directly. For the determination of isotopic-abundance of a single element, the ion beam is divided into two or more beams of different mass-to-charge ratio.¹ If a mass spectrometer with a double ion-collector system is used, the ion beams are focused such that they fall onto two insulated electrodes (collectors) and the ion currents they impart are amplified and measured.

6.2.3 Detection of ions

After ions have been separated according to their mass-to-charge ratio, it is necessary to measure the currents in the individual ion beams.

6.2.3.1 *The Faraday cup*

A beam of positively charged ions is allowed to fall on a plate which is connected to earth potential via a resistor. Voltage amplifiers of high input impedance are used to measure the ion current.⁶ For high sensitivity measurements, the resistance should be as high as 10^{11} Ohms to ensure that a high voltage develops across the resistor. The factors that limit the sensitivity, accuracy and speed with which a spectrum can be scanned are: electrical noise in the resistor, amplifier drift, statistical noise and secondary electrons.⁶ Secondary electrons are emitted when the ion current impinges on the metal plate and these electrons produce the same effect on the measured current as the positive ion arriving. To produce an accurate measurement of the ion current, the emission of secondary electrons must be prevented. This is achieved by replacing the metal plate by a metal box called a Faraday cup, and using an electron suppressor as shown in Figure 6.3. The ion enters the Faraday cup through an aperture in its front surface. An electron suppressor, consisting of a plate to which a negative potential of the order of 50 V is applied in respect to Faraday cup, is used to ensure that no secondary electrons escape through the aperture.

The ion current from the Faraday cup is proportional to the number of incident ions and hence to the partial pressure of corresponding molecular species in the sample gas. This method is used in isotope ratio instruments to measure a major beam due to the most abundant isotope species of a molecule, and minor beams due to less abundant species.

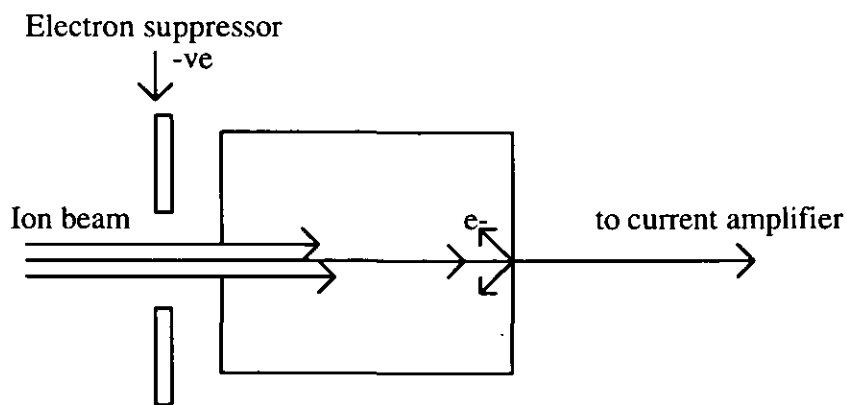


Figure 6.3 Faraday cup detector

6.2.3.2 *Electron multiplier detector*

There are two kinds of multiplier detectors, both of which make use of secondary electron emission. These are the discrete and continuous dynode multipliers.⁶ An example of a discrete multiplier is the "Venetian blind" design which consists of a number of dynodes which are made of special materials, beryllium/copper alloy is commonly used. The basis of choice being high yield of secondary electrons when the surface is bombarded by positive ions or electrons.

In discrete multipliers, the ion beam strikes the first dynode (conversion electrode) and a fraction of the ions causes emission of several electrons. The dynodes are connected to a chain of resistors, across which is connected to a high voltage supply.⁶ Each successive dynode is held at an increasingly positive potential. The last dynode (most positive) is connected to the pulse amplifier. The secondary electrons emitted when the first dynode is bombarded with the ion beam are attracted to the next dynode where they cause further secondary electrons to be emitted. These in turn are attracted to the third dynode and cause further emission of secondary ions. The process is repeated on the surface of successive dynodes until the last dynode is reached, with resultant production of an avalanche of electrons. The final dynode (collector) acts as Faraday cup and is connected to a resistor with high resistance and then to a d.c. amplifier.

In a continuous multiplier, a thin film of semi-conducting material is deposited on the inner surface of an insulating tube.⁶ A potential difference is applied across the end of the tube. The ion beam strikes the semi-conductor near the negative end of the tube with resultant emission of secondary electrons which are accelerated a short distance towards the positive end before bombarding the semi-conductor again. Further emission of electrons takes place on impact. The process is continued along the entire length of the tube, resulting in large current amplification. Multipliers have a fast response and high sensitivity, with gains up to 10^6 .

6.2.4 Resolution

The resolution of mass spectrometer is the capability of the instrument to differentiate between masses. It is given by

$$R = \frac{m}{\Delta m} \quad (6.4)$$

Where Δm is the mass difference between adjacent peaks that are just resolved and m is the nominal peak (or mean mass of the two peaks). The resolution of the isotope ratio mass spectrometer (Optima, Micro Mass, UK) used in this work was 100.

6.2.5 Vacuum system

The use of a vacuum system in a mass spectrometer ensures that ions travelling through the instrument do not suffer collisions with gas molecules that may cause them to be scattered or to lose energy. In addition, the use of the vacuum system prevents contamination of the analyte since the ionisation of the residual gases along with the sample in the ionising chamber gives rise to a higher background current. An operating pressure of $<10^{-6}$ Torr is usually employed for mass spectrometers. Rotary and diffusion

pumps or turbomolecular pumps are used to obtain the low pressures required in isotope ratio mass spectrometers. Heating the source-analyser-collector assembly to 200-300°C is used to increase the rate of outgassing of the vacuum system.

6.2.6 Sample inlet system

In most isotope mass spectrometers, the sample is admitted continuously into the pumped system. It is important that the sample gas is introduced at a constant rate and in extremely small amounts so as to maintain the mass spectrometer at a low pressure.² This is achieved by introducing a flow restrictor (or leak) into the inlet of the mass spectrometer. The gas flow through such a leak can be either molecular or viscous depending on the pressure at the entrance side of the leak and the construction of the leak.

Molecular flow takes place when the pressure at the entrance to the leak is low and the mean free path of the sample molecule is large with respect to the dimension of the leak. Under molecular flow conditions, lighter molecules pass into the source more readily and the sample reservoir becomes enriched in the heavier component of the mixture.² Movement of gases in the source is also molecular and lighter gases are pumped away more quickly. The relative numbers of chemically identical ions generated in the source at any point in time reflect accurately the partial pressure of the parent molecules in the reservoir. For isotope analysis, using a typical molecular leak, the sample reservoir should be large and sample pressure low. Molecular leaks are constructed by sealing a plug of porous materials into the sample inlet tube close to its connection with the mass spectrometer. Microporous, refractive and chemically inert materials used for this purpose are sintered silicon carbide, quartz and glass.

Gas flow is viscous at higher pressure. A viscous leak is usually constructed by crimping a capillary inlet tube to the point of entry to mass spectrometer. As the pressure falls across the restriction, gas flow changes from viscous to molecular hence the overall characteristic of the leak depends on its construction and operating pressure. Viscous

inlets are generally preferred for isotope ratio measurement because gaseous samples are conveniently handled in small volumes at relatively high pressure (5-10 kPa). Many commercially available isotope mass spectrometers, however, use molecular leaks. In this work, a viscous leak was employed.

6.3 CALCULATIONS AND CORRECTIONS

6.3.1 Enrichment delta

Enrichment is the excess of any particular isotope species in the sample compared to the same isotopic species in a reference. The enrichment delta expresses this excess as a fraction of the particular isotopic species in the reference. It is usually quoted in parts per thousand and written as ‰ or per mil. Thus enrichment delta is given by the formula;

$$\delta = \left[\frac{R_{sam} - R_{ref}}{R_{ref}} \right] 1000 \quad (6.5)$$

where R_{sam} and R_{ref} are the sample and reference ratios of minor to major beam as measured on the isotope ratio instrument. Enrichment delta notation can be used to express results for all species of gases measured.

6.3.2 Isotopic abundance (Atom %)

Isotopic abundance expresses the number of atoms of a particular isotope of an element in the sample as a fraction of the total number of atoms of that element present. It is usually expressed as a percentage and noted as Atom % or At %.

$$\text{Atom\%} = \frac{\text{number of atoms of one isotope of an element}}{\text{number of atoms in all the isotopes in that element}} \times 100 \quad (6.6)$$

For example, the isotopic abundance for ^{15}N can be defined as:

$$\text{Atom \%} = \left[\frac{\text{number of } ^{15}\text{N atoms}}{\text{number of } ^{15}\text{N atoms} + \text{number of } ^{14}\text{N atoms}} \right] 100 \quad (6.7)$$

The results can also be expressed as atom % excess (atom % enrichment in excess of a reference gas) which is defined as the following:

$$\text{Atom \% excess (enrichment)} = \text{sample atom \%} - \text{reference atom \%} \quad (6.8)$$

6.3.3 Instrument corrections

The correction factors which are of concern in isotope ratio measurements include:

- a tail contribution from major to minor peak
- a background gas peak at the minor isotope mass
- the cross mixing of sample and reference gases due to seat leakage in the changeover valve.

6.3.4.1 Carbon dioxide corrections (*Craig*⁷)

In the determination of CO_2 , different isotopic species of the same element can produce a contribution at certain masses. A correction must therefore be made. The international CO_2 PDB has a contribution (about 6%) at mass due to ^{17}O isotope. Similarly, 2% of mass 46 is derived from isotopic species containing ^{13}C and ^{17}O but not ^{18}O . The abundances for masses higher than 46 are negligible.

For a triple collector instrument measuring a sample close to PDB, the correction formulae are⁷:

$$\delta^{13}\text{C} = 1.0676 \delta(45/44) - 0.0388 \delta^{18}\text{O} \quad (6.9)$$

and

$$\delta^{18}\text{O} = 1.0010 \delta(46/44) - 0.0021 \delta^{13}\text{C} \quad (6.10)$$

6.3.4.2 Nitrogen corrections

An interfering peak at mass 30 due to trace of nitrous oxide (NO) may occur when nitrogen is analysed at low enrichments. This, if not taken into account, may affect the resultant calculation of N atom %.

A formula modified from the standard formula is used when the enrichments are low (<5%)

A standard formula for high enrichment is given by:

$$^{15}\text{N atom \%} = \frac{R_{29} + R_{30}}{2(1 + R_{29} + R_{30})} \times 100 \quad (6.11)$$

while a modified formula for low enrichment is given by:

$$^{15}\text{N atom \%} = \frac{R_{29}}{2 + R_{29}} \times 100 \quad (6.12)$$

where R_{29} = 29/28 mass ratio and R_{30} = 30/28 mass ratio.

REFERENCES

1. Bremner, J. M., in *Methods of Soil Analysis-Part 2 Chemical and Microbiological Properties*, Ed. Black, C. A., American Society of Agronomy, Madison, 1965, pp. 1256-1286.
2. Robinson, D. and Smith, K. A., in *Soil Analysis-Modern Instrumental Techniques*, Ed. Smith K. A., Marcel Dekker, 2nd Edn., New York, 1991, pp. 465-503.
3. Canham, J. S. and Pacey, G., *Anal. Chim. Acta*, 1988, **214**, 385.
4. Millard, B. J., *Quantitative Mass Spectrometry*, Heyden, London, 1978, pp.1-23.
5. Gross, M. L., *Instrumental Analysis*, Eds. Bauer, H. H., Christian, G. D. and O'Reilley, J. E., Allyn and Bacon, Boston, 1978, pp. 443-482.
6. Beynon, J. H. and Brenton, A. G., *An Introduction to Mass Spectrometry*, University of Wales Press, Cardiff, 1982, pp. 1-56.
7. Micro Mass, Instrument Manual SIRA Series II, Manchester, U.K.

Chapter 7

CHAPTER SEVEN

DETERMINATION OF SULPHUR SPECIES

In this chapter, DPGD-FI interfaces were employed for the generation of H₂S or SO₂ from sulphur species (organic and inorganic sulphur) and separation of these gases from the liquid stream. The ultimate aim was to couple the DPGD-FI system to MS for the isotopic ratio determination of sulphur (e.g. ³⁴S/³²S). However, a UV/VIS spectrophotometer was used for the detection of the generated H₂S or SO₂ due to the unavailability of an isotope ratio mass spectrometer in our laboratory. Additionally, the DPGD-FI system was interfaced with a thermal conductivity detector for the generation, separation and subsequent determination of H₂S or SO₂. The thermal conductivity detector could be used on-line with MS for the determination of total sulphur.

7.1 PRELIMINARY EXPERIMENTS

7.1.1 DETERMINATION OF SAMPLE INJECTOR LOOP VOLUME

7.1.1.1 Procedure

Potassium permanganate standards of 0.52, 1.58, 2.63, 3.5 and 7.0 ppm were prepared. Absorbance measurements were made at 521 nm using a UV/VIS spectrophotometer (Unicam 8700 series, ATI Unicam, Cambridge, UK). The stock solution of potassium permanganate was loaded in the loop and then injected into the FI system employing de-ionised water as the carrier stream. The injected solution was received in a 50 ml calibrated flask, after passing through the FI system, and made up to the mark with de-ionised water. The absorbance of this solution was also measured. The procedure was repeated for each of the other two loops employed.

7.1.1.2 Results and Discussion

The results obtained were used to construct a calibration graph of absorbance versus volume of potassium permanganate, as shown in Figure 7.1. The volumes of loops A, B, and C were obtained by interpolation from the calibration graph and these are tabulated in Table 7.1

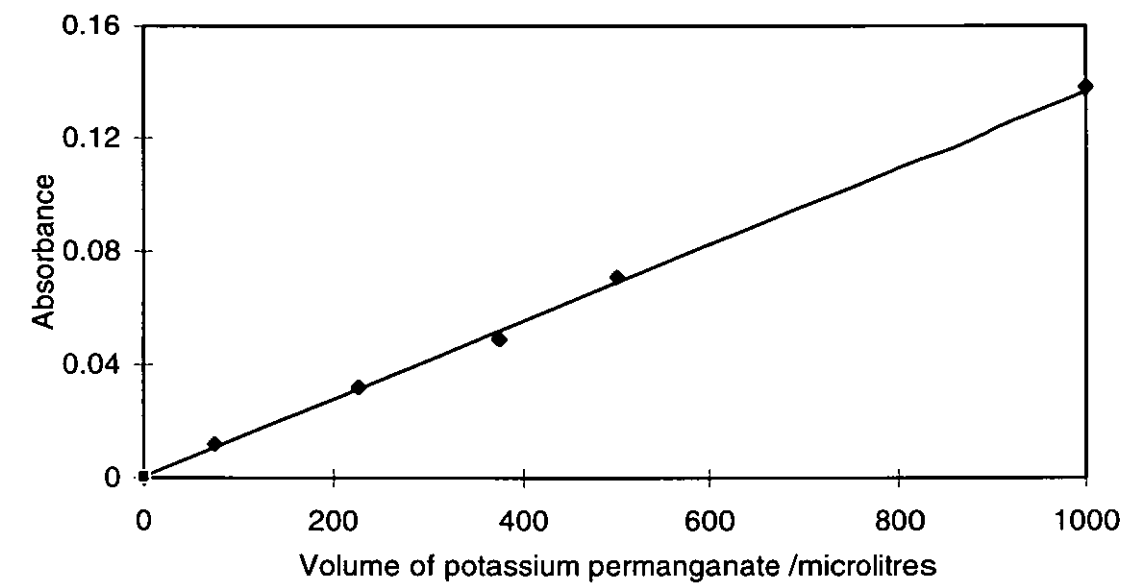


Figure 7.1 Calibration graph of absorbance of potassium permanganate standards for determining sample loop volume in FI system

Table 7.1 Sample injection loop volumes obtained from the calibration graph and by calculation.

| Injection loop | Absorbance | Experimental volume (μl) | Theoretical volume (μl) (0.8 mm i.d. tube used) |
|--------------------------|------------|--------------------------|---|
| Loop volume A (177.8 cm) | 0.105 | 770 | 890 |
| Loop volume B (87.3 cm) | 0.053 | 390 | 440 |
| Loop volume C (24.0 cm) | 0.017 | 120 | 120 |

7.1.2 CALIBRATION OF PERISTALTIC PUMPS

7.1.2.1 Procedure

A peristaltic pump (Gilson Minipuls 2) was used to propel solutions in the FI system. The flow rates of water, when pump tubes with internal diameters of 1.65 mm and 1.14 mm were used, were determined for each pump setting. This involved the collection of water passing through the end of the pump tube into a previously weighed beaker for three minutes. At the end of the collection period, the beaker with its contents were weighed. The mass of water collected was obtained by difference in the two measurements. The same procedure was repeated with a Gilson Minipuls 3 peristaltic pump.

7.1.2.2 Results and Discussion

The results obtained using the peristaltic pumps, Gilson Minipuls 2 and 3, are displayed in Figures 7.2 and 7.3 respectively.

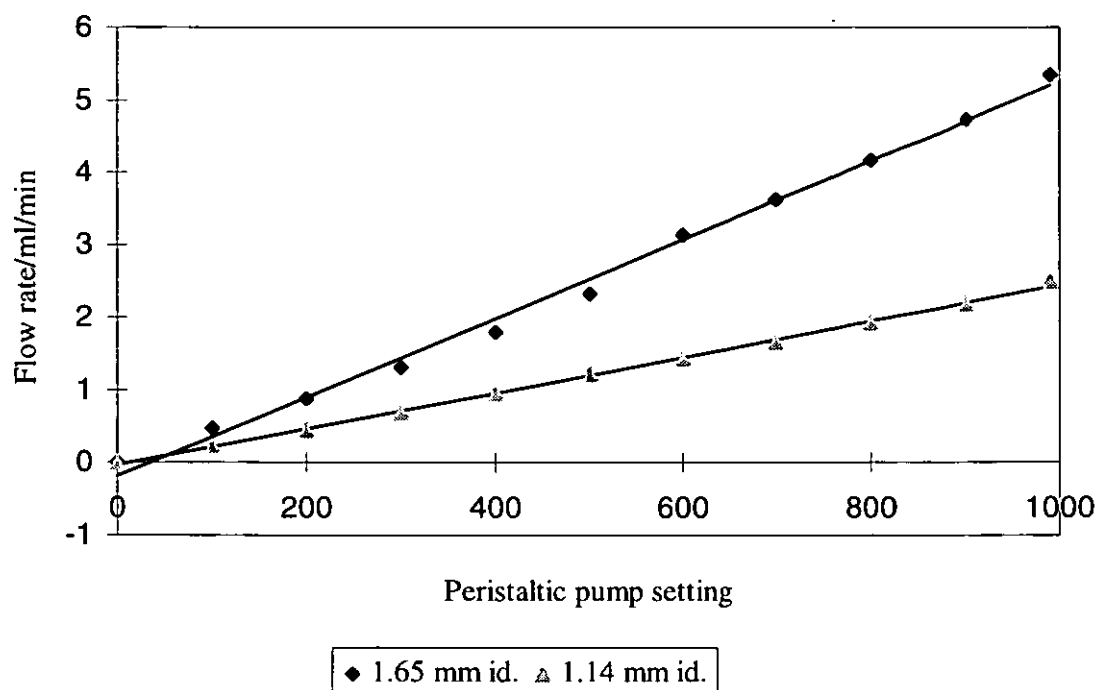


Figure 7.2 Calibration graph of flow rates in the FI system at different settings of a Gilson Minipuls 2 pump using pump tube with internal diameters of 1.14 and 1.65 mm.

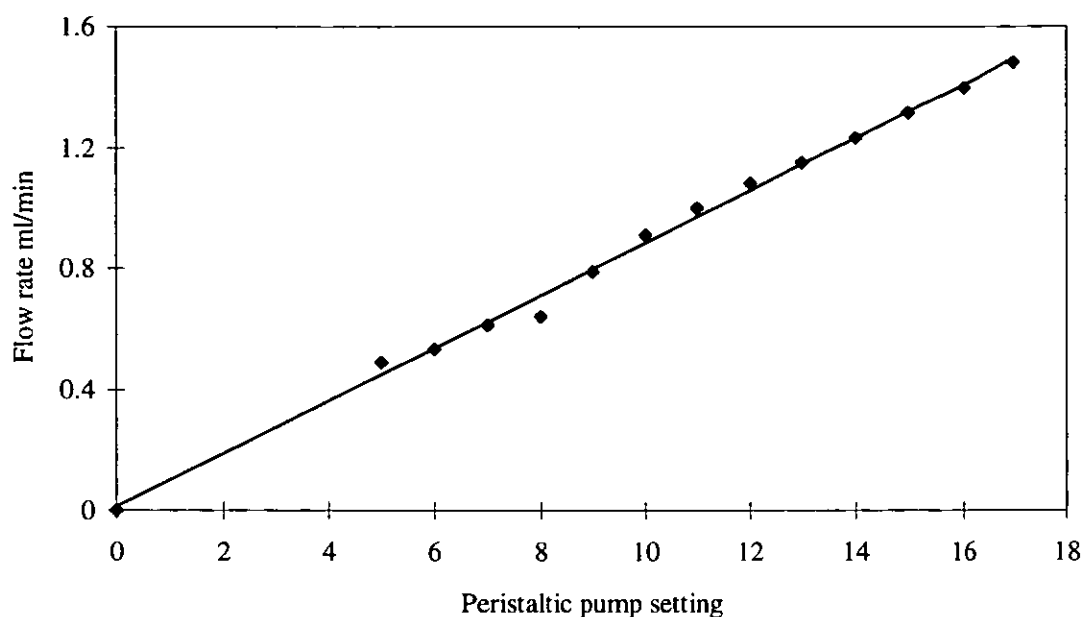


Figure 7.3 Calibration graph of flow rate in the FI system at different settings of a Gilson Minipuls 3 peristaltic pump with pump tube with internal diameter of 1.14 mm.

7.2 DETERMINATION OF SULPHIDE

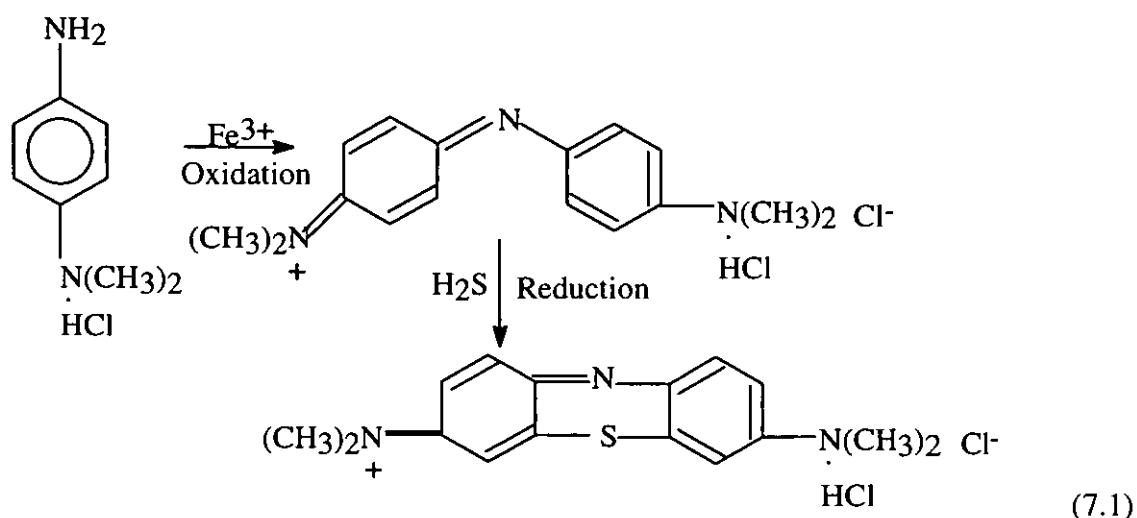
7.2.1 SPECTROPHOTOMETRIC DETERMINATION OF HYDROGEN

SULPHIDE/SULPHIDE BY METHYLENE BLUE METHOD

7.2.1.1 Introduction

The most widely used spectrophotometric method for the trace determination of sulphide is the methylene blue method. In this method, sulphide reacts with an acid solution of *p*-aminodimethylaniline in the presence of ferric chloride to form methylene blue. At first the solution is red, but later turns to blue as the dye is formed.¹ Hydrogen sulphide is generated by the action of acid on sulphide. Before developing the methylene blue colour, the hydrogen sulphide can be absorbed into zinc acetate solution resulting in the precipitation of zinc sulphide. An alkaline suspension of cadmium hydroxide can also be used as an

absorption medium for hydrogen sulphide. Ammoniacal cadmium chloride solution has also been used for absorbing hydrogen sulphide. The reaction of *p*-aminodimethylaniline in the presence of ferric chloride is represented by the following equation:



The absorbance of the methylene blue complex can be determined using a UV/VIS spectrophotometer set at 670 nm. However, the peak absorption wavelength has been found to vary with conditions, hence strict control is required to obtain reproducible results.

Sulphur containing compounds such as dimethyl sulphide may interfere with the determination of sulphide/hydrogen sulphide by the methylene blue method since they can also react with *p*-aminodimethylaniline in the presence of Fe^{3+} to form methylene blue. It is therefore important that appropriate conditions are selected to eliminate the potential interferences. Other interfering compounds are strong reducing agents, such as sulphur dioxide, which inhibit the blue colour formation of the dye. This interference can be eliminated by using 2-6 drops of Fe^{3+} instead of only one drop for colour development. Nitrogen dioxide and ozone have been found to give slight negative interferences.

The methylene blue method has been used for the determination of sulphide in stream water,² gaseous sulphide in the environment,^{3,4} acid volatile sulphide in sediments,⁵ hydrogen sulphide in industrial atmospheres, workplace air and sewage plants⁶ and sulphide and total sulphur in soils and plants.⁷

7.2.1.2 Experimental

Reagents

All chemicals were of analytical grade.

Sulphide stock solution (500 ppm H₂S) was prepared by dissolving 3.53 g of sodium sulphide, Na₂S.9H₂O (Fisons, Loughborough, UK), in 1 litre of de-ionised water.

Zinc acetate absorption solution (0.09 M) was prepared by dissolving 20 g of zinc acetate dihydrate (Fluka, Dorset, UK) and 10 g of sodium acetate trihydrate (Fluka, Dorset, UK) in de-ionised water and diluting to 1 litre.

Amine-sulphuric acid stock solution was prepared by adding 50 ml of concentrated sulphuric acid to 30 ml of de-ionised water and then allowing the solution to cool before adding 12 g of *p*-aminodimethylaniline (Fluka, Dorset, UK).

Amine-sulphuric acid test solution was prepared by diluting 25 ml of amine-sulphuric stock solution with 1:1 sulphuric acid.

Ferric chloride solution (3.72 M) was prepared by dissolving 50 g of ferric chloride hexahydrate (Aldrich, Dorset, UK) in 50 ml de-ionised water.

7.2.1.3 FI-Hydrogen sulphide generation

The DPGD-FI system used for the generation and separation of H₂S is shown in Figure 7.4.

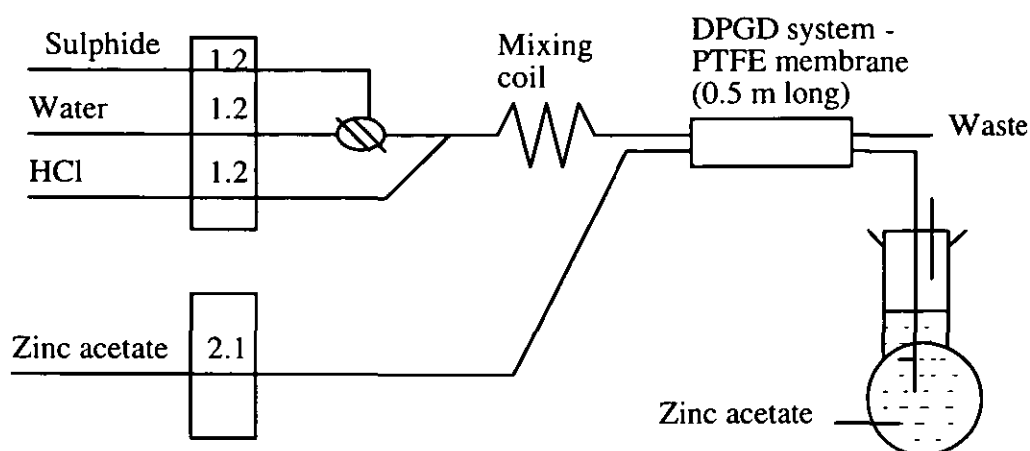


Figure 7.4 DPGD-FI manifold used for generation and separation of hydrogen sulphide

Two peristaltic pumps (Gilson Minipuls 1 and 2) were used to propel the sample and reagents in the FI system. The valve injector used was fitted with a 0.39 ml loop. A dual phase gas diffusion (DPGD) unit, interfaced with the FI system, consisted of a tubular microporous PTFE membrane (0.5 m long) inserted into a glass tube with a bore size of 2.5 mm. The gas diffusion unit had connections that allowed the liquid stream to run through the core of the tubing and the generated gas to pass into the zinc acetate acceptor stream flowing round the membrane.

Zinc acetate absorbing solution as an acceptor stream.

500 ppm H_2S stock solution was injected into the water carrier stream. This stream was then merged with the reagent stream (HCl) and the resultant solution was passed to the mixing coil and the tubular microporous PTFE membrane. The generated H_2S was separated from the liquid carrier stream by the microporous PTFE membrane. The zinc acetate absorption solution, employed as the acceptor stream was received into a 25 ml volumetric flask (Figure 7.4) for a 10 minute period after injection. To the collected zinc acetate solution, 0.6

ml of the amine-sulphuric acid test solution and one drop of ferric chloride were added. The volume was made up to the mark with zinc acetate solution.

7.2.1.4 Results and Discussion

The zinc acetate solution, collected from the FI system following the injection of 500 ppm H_2S , did not form the methylene blue complex on treatment with the amine-sulphuric acid test solution in the presence of ferric chloride. This was confirmed by the absence of the blue colour. However, the characteristic offensive smell of hydrogen sulphide was detected, an indication that the gas must have been generated in the FI system, but did not leave the diffusion unit to be absorbed into the zinc acetate acceptor stream. In an attempt to solve this problem, the following steps were taken:

- the replacement of the PTFE membrane with a new one in case the pores of the membrane used earlier had been blocked, preventing the generated gas from diffusing through the membrane into the zinc acetate acceptor stream. It was found that even with the new PTFE membrane connected to the FI system, the solution collected in the receiver from the system did not give positive results with the methylene blue method.
- the reduction of the flow rates of carrier and reagent streams by changing the pump rate settings. This was expected to increase the reaction time of the sample and the reagent (HCl), with subsequent production of higher amounts of hydrogen sulphide in the FI system. However, no positive result was achieved.
- prolonging of the time of collection of zinc acetate solution from the acceptor stream to increase the chances of collecting most of the generated H_2S . Again there was no methylene blue complex formed.
- the increase in the hydrochloric acid concentration from 3 M to 6 M and sulphide concentration from 500 to 1000 ppm H_2S . No blue complex was obtained.

The zinc acetate solution appeared not to be a satisfactory absorber for use in a DPGD-FI system. This is because the zinc acetate reacted with the H_2S at the PTFE membrane/zinc acetate interface to form zinc sulphide precipitate, which immediately blocked the pores of PTFE membrane. The zinc sulphide precipitate did not leave the diffusion unit, and hence was not collected in the receiver.

The problem of formation of sulphide precipitate on the membrane surface in the DPGD-FI system may be overcome by substituting zinc acetate with an absorption solution which efficiently absorbs hydrogen sulphide, but does not form a precipitate with it. Alternatively, an acceptor gas stream such as nitrogen or helium can be used to sweep the generated hydrogen sulphide from the dual phase gas diffusion unit into a vessel containing zinc acetate absorption solution for a specific period before carrying out the methylene blue test. This is discussed later and in any case more closely resembles the interface that would be used for MS where He would be the preferred carrier.

7.2.2 GENERATION OF H_2S IN A DPGD-FI SYSTEM AND ITS DETERMINATION BY THERMAL CONDUCTIVITY DETECTOR AFTER MICROPOROUS PTFE MEMBRANE SEPARATION

The DPGD-FI system used for the generation of H_2S is shown in Figure 7.5.

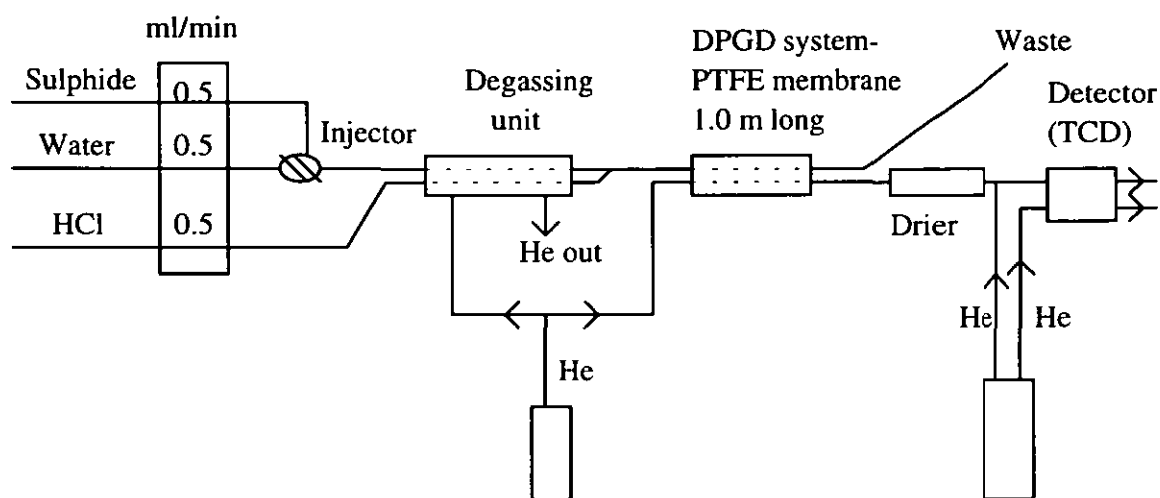


Figure 7.5 DPGD-FI interface coupled to a thermal conductivity detector used for the generation, separation and determination of H_2S .

The dual phase gas diffusion (DPGD) unit was as described previously (Section 7.2.1.3) except that a 1 m long PTFE membrane was used.

In addition, in this manifold, a PTFE microporous membrane degassing unit was used to remove dissolved gases in the reagent and carrier streams. This was found to be necessary when employing MS detection for N_2 (see Section 9.5) and was therefore incorporated as a standard feature in the manifold. The degassing unit had two pieces of tubular PTFE membrane, through which the carrier and reagent streams passed before mixing. These two pieces were enclosed in a single glass tube through which helium passed so that both streams could experience a similar physical environment, thus degassing to the same extent.

The drying chamber used consisted of a glass column, 10 cm long and 7 mm i.d. and was filled with magnesium perchlorate to dry the gaseous analyte before reaching the thermal conductivity detector. This prevented moisture from reaching the detector which could have caused damage to the detector filaments.

7.2.2.1 Experimental

Reagents

500 ppm H_2S stock solution was prepared by dissolving 3.53 g of sodium sulphide, $\text{Na}_2\text{S} \cdot 9\text{H}_2\text{O}$, (analytical grade, Fisons, Loughborough, UK) in 1 litre of de-ionised water. The working standards (20-300 ppm H_2S) were prepared from the sodium sulphide stock solution.

2 M, 3 M, 4 M, 5 M and 6 M HCl were prepared from concentrated HCl (Spectrosol grade, BDH, Poole, UK).

7.2.2.2 Influence of HCl on the generation of H_2S

Procedure

The concentration of HCl was varied from 2 M to 6 M and each was used for producing H_2S from the sulphide working standards injected into the FI system. Flow rates of 0.49 ml/min were employed for the sulphide, water carrier and HCl reagent streams.

Results and Discussion

The peak height and area measurements for the signals obtained when various concentrations of HCl were employed for generating H_2S in the FI system were used for constructing the calibration graphs in Figures 7.6 and 7.7.

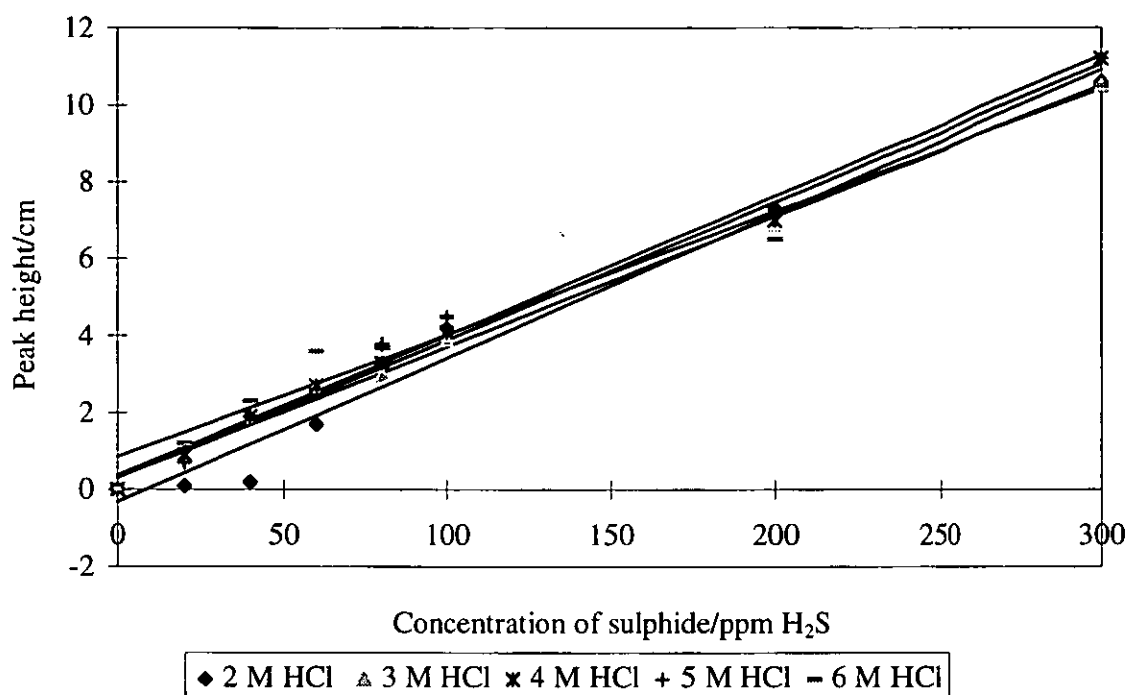


Figure 7.6 Calibration graphs of peak height against concentration of sulphide standards used for the generation of H_2S employing 2-6 M HCl.

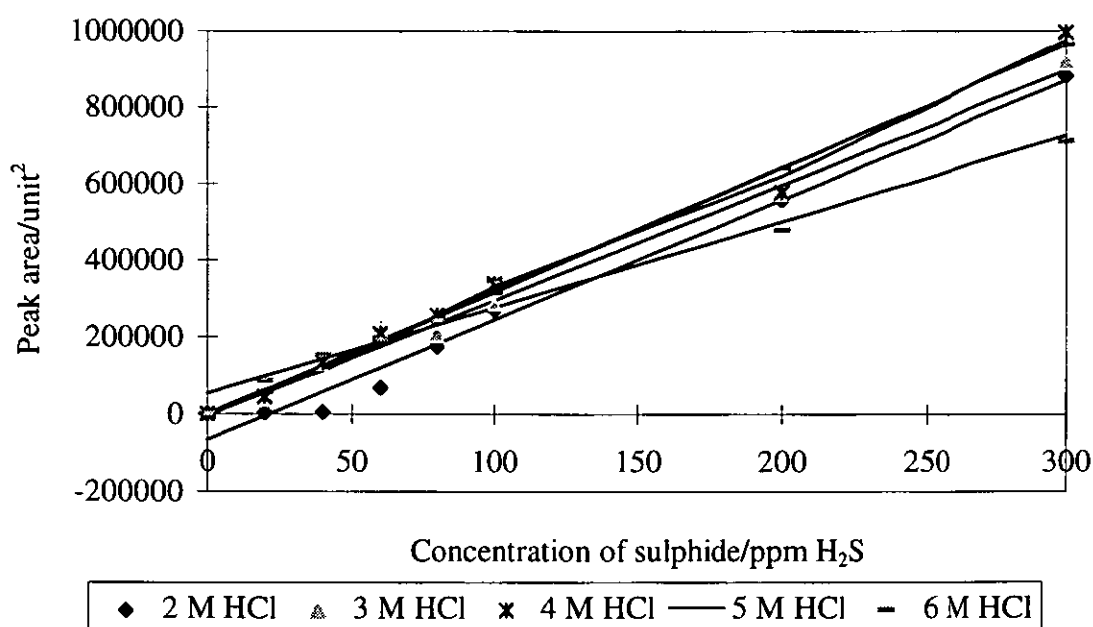


Figure 7.7 Calibration graphs of peak area against concentration of sulphide standards used for the generation of H_2S employing 2-6 M HCl.

Peak area or peak height, as a measure of the signal, was proportional to the concentration of the analyte. Peak area measurements, at low concentrations of analyte, may not be accurate due to failure of the integrator to correctly determine the starting and end points of the peak profile. However, for high concentrations of the analyte, peak area measurements tend to be more reliable than those of peak height.

From the calibration graphs (Figures 7.6. and 7.7), it was found that, on the basis of sensitivity and correlation coefficient, better results were achieved when either 3 M, 4 M or 5 M HCl were used. 3 M was chosen on the basis of minimising reagent consumption, safety and pump tube life time. Application of higher concentration of the acid as a reagent stream resulted in slight charring of the pump tubes.

7.2.2.3 Influence of temperature on the generation of hydrogen sulphide

Procedure

The FI system used and conditions were the same as those used previously except that the tubular microporous PTFE membrane was immersed in a water-bath set at 25°C, 40°C or 50°C. The sulphide standards, concentration range 0-100 ppm H₂S, were prepared and each was injected into the FI system. The H₂S, generated from each standard, was determined by the thermal conductivity detector and the signal peak height measured.

Results and Discussion

The calibration graphs of peak height versus concentration of sulphide standards injected into the FI system at 25°C, 40°C or 50°C were constructed and are shown in Figure 7.8. It was found from these calibration graphs that no significant increase in H₂S generation

was obtained when temperatures higher than 25°C were used. This was shown by the regression lines whose slopes (see Table 7.2) were not significantly different from one another at the 95 % confidence level. Thus the sensitivity was not significantly increased at higher temperature, but the correlation coefficient improved considerably at higher temperature. The parameters of the regression lines are presented in Table 7.2.

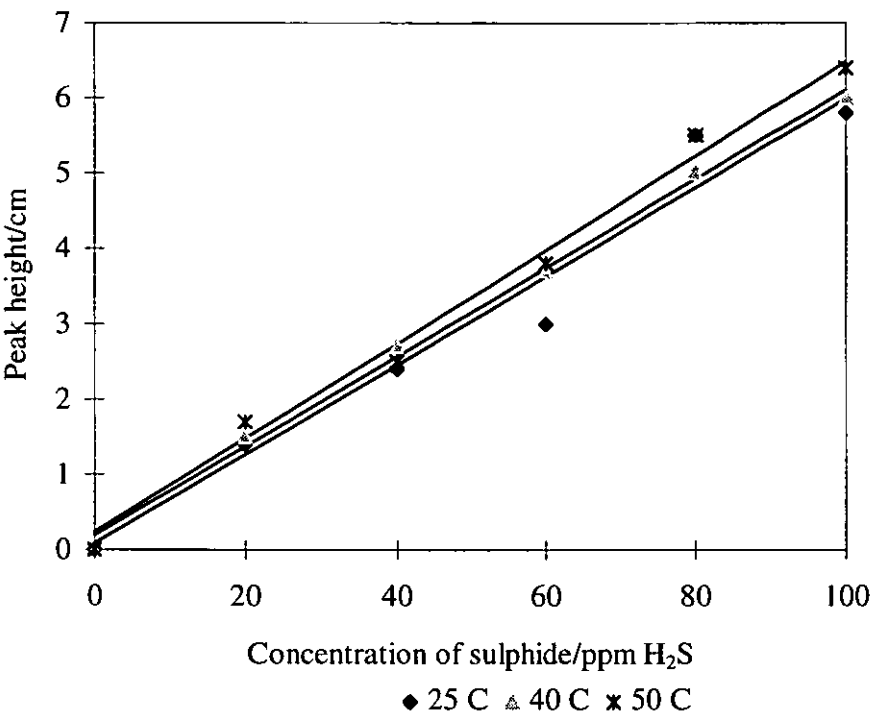


Figure 7.8 Calibration graphs of peak height against concentration of sulphide for the generation of H₂S in the FI system at 20°C, 40°C and 50°C, as determined by a thermal conductivity detector.

Table 7.2 Characteristics of calibration curves obtained when 25°C, 40°C, and 50°C were employed for generating H₂S.

| Characteristics of regression curves | 25°C | 40°C | 50°C |
|--|-------|-------|-------|
| slope | 0.059 | 0.059 | 0.063 |
| y-intercept | 0.081 | 0.193 | 0.233 |
| regression coefficient | 0.969 | 0.997 | 0.990 |
| Calculated t-value for each slope | 0.047 | 0.042 | 0.087 |
| Null Hypothesis: No significant difference of each slope from the true value (mean value). | | | |
| Mean, $\mu = 0.0603$, standard deviation, $s = 1.9348$, $n = 3$, and $n-1 = 2$. | | | |
| The calculated t-value was obtained using the equation: | | | |
| $t = (x_i - \mu)(n/s)^{0.5}$ | | | |
| The critical value at the 95 % confidence level = 4.3 | | | |
| The calculated t-value for each of the slopes is less than the critical value at the 95 % confidence level, hence the null hypothesis is retained. | | | |

Generally, increase of temperature has the effect of:

- increasing the rate of chemical reactions. Since ionic reactions are usually fast, as in the case of acidification of sulphide to form H₂S, an increase in temperature was not expected to have much influence on the rate of reaction between the sulphide and hydrogen ions.
- lowering the solubility of H₂S in the aqueous donor stream. As the temperature for the generation of H₂S in the FI system was increased, a decrease in the solubility of the gas

was expected in the donor stream, and hence more H_2S was expected to diffuse through the PTFE membrane into the acceptor stream. The experimental results obtained, however, showed that even at high temperature (40°C and 50°C), there was no significant increase in H_2S transferred. This is as an indication that the microporous PTFE membrane (1 m long) was an efficient separation device for H_2S , even at a low temperature.

- increasing the diffusion coefficient of the gas. As the diffusion coefficient of the gas is expected to increase at high temperature, more of the H_2S was expected to diffuse through the membrane. However, again no benefit was realised.

A temperature of 25°C was therefore selected for the remainder of the work.

7.2.2.4 Optimisation of flow rate

The DPGD unit was immersed in a water-bath set at 25°C . The flow rate was varied using different settings of the peristaltic pump (Gilson Minipuls 3). An 80 ppm H_2S standard was used to study the effect of changing flow rate.

As the flow rate was increased from 0.490 to 1.083 ml/min, it was observed that the peaks obtained became narrower, showing that the dispersion of the sample in the FI system decreased with the increase in the flow rate as expected. The graph of peak height versus flow rate is shown in Figure 7.9.

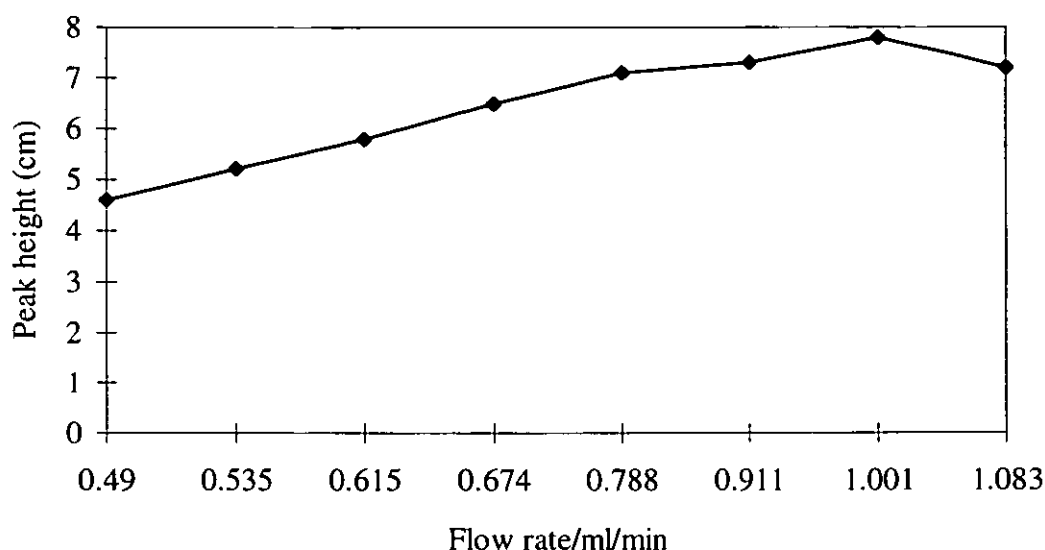


Figure 7.9 Graph of peak height of TCD signals versus flow rates of carrier and reagent streams.

As the flow rate was increased from 0.490 to 1.083 ml/min, there was a general increase in the peak height until a maximum value of 7.8 cm was reached at a flow rate of 1.001 ml/min. Further increase of the flow rate resulted in a decrease of the peak height. This was an indication that the H_2S generated was being given insufficient time to diffuse from the liquid and through the membrane.

The optimum flow rate of reagent and carrier stream was therefore taken as 1.0 ml/min. This was used for all subsequent experiments.

7.2.2.5 Calibration using optimised conditions

The calibration experiments were carried out under the previously optimised conditions. H_2S standards with concentrations ranging from 10 to 100 ppm were injected into the FI

system, using a fixed sample loop volume of 0.5 ml. The generated H_2S was detected by the thermal conductivity detector.

Results and Discussion

Using peak height measurements, a calibration graph of peak height versus concentration of sulphide standards was constructed as shown in Figure 7.10. A detection limit of 5.0 ppm H_2S (3σ above the blank) was achieved.

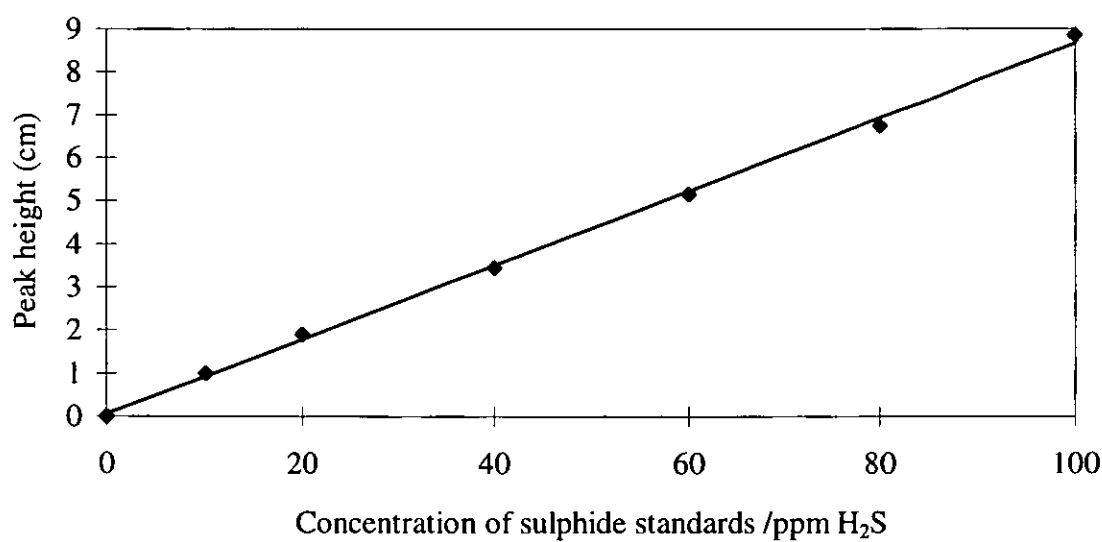


Figure 7.10 Calibration graph of peak height of signals for H_2S obtained from a thermal conductivity detector. Slope, 0.086; y-intercept, 0.063; and correlation coefficient, 0.999.

7.2.3 SEPARATION EFFICIENCY OF THE MICROPOROUS PTFE MEMBRANE FOR H_2S

7.2.3.1 Procedure

Using a 0.5 m long PTFE membrane

The FI system used is shown in Figure 7.11.

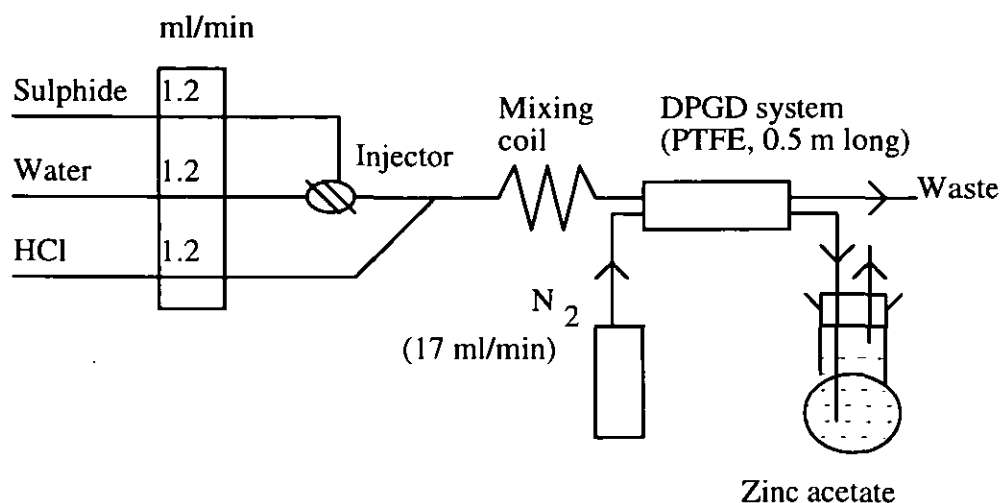


Figure 7.11 FI manifold used for determining the separation efficiency of the PTFE membrane for H_2S .

A PTFE membrane (0.5 m long) was used to separate the generated H_2S from the liquid donor stream. Nitrogen gas, flowing at 17.0 ml/min, was used as an acceptor stream. The generated H_2S , after diffusing through the membrane, was swept into a 25 ml calibrated flask containing zinc acetate solution (25 ml). The flask was sealed with a rubber stopper through which a short tube and the tubing from the gas-liquid separator passed.

Working standards (0-2ppm) were prepared from 500 ppm H_2S standard stock solution by transferring, in each case, an appropriate volume of stock solution into a 25 ml volumetric flask. This was followed by addition of 0.6 ml amine-sulphuric acid solution and one drop of ferric chloride solution. The volume was made up to the mark with de-ionised water. The absorbance of each standard was determined at 666 nm.

40, 60, 200 and 300 ppm H_2S standards (used as samples) were each injected into the FI system using a fixed sample loop volume of 0.5 ml. The separated H_2S gas was received into a 25 ml volumetric flask containing 15 ml of zinc acetate solution for a period of 10 minutes. To this solution, 0.6 ml of amine-sulphuric acid and one drop of ferric chloride

were added. The volume was made up to the mark with the zinc acetate solution. The blank solution was prepared by transferring 0.6 ml amine-sulphuric acid solution and one drop of ferric chloride to a 25 ml volumetric flask and the volume made to the mark with the zinc acetate solution. The absorbance of each solution was measured against the blank solution using a UV/VIS spectrophotometer.

7.2.3.2 Results and Discussion

The calibration graph shown in Figure 7.12, was drawn using the absorbance of methylene blue complex derived from the generated H_2S . The detection limit (3σ above the blank) obtained for the determination of sulphide by methylene blue method (off-line method) was 0.19 ppm H_2S .

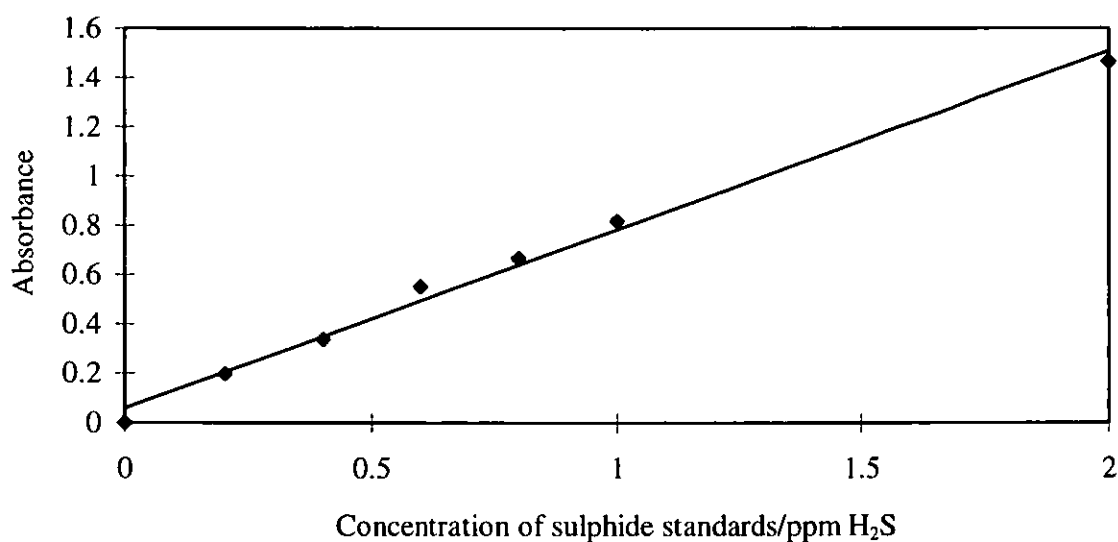


Figure 7.12 Calibration graph of absorbance of methylene blue complex derived from hydrogen sulphide, determined by the UV/VIS spectrophotometric method. Slope, 0.725 ppm^{-1} ; y-intercept, 0.059; and correlation coefficient, 0.992.

The separation efficiency of the membrane for H₂S was calculated for each sample injected into the FI system and the values obtained are shown in Table 7.3

Table 7.3 Separation efficiency of the PTFE membrane (0.5m long) for H₂S.

| Concentration of sulphide injected into the FI system (ppm H ₂ S) | Absorbance at 666.4 nm | Separation efficiency of PTFE membrane (0.5 m long) for H ₂ S |
|--|------------------------|--|
| 40 | 0.220 | 27.8 |
| 60 | 0.299 | 27.6 |
| 100 | 0.437 | 26.1 |
| 200 | 0.866 | 27.8 |
| 300 | 1.185 | 25.9 |
| | | MEAN, 27.0 ; RSD, 3.5 % |

From the calibration graph in Figure 7.12, an absorbance of 0.220 was obtained which corresponded to 0.2226 ppm H₂S. For 100% separation efficiency, the final concentration of sulphide in the final 25 ml volume should have been 0.8 µg/ml. The separation efficiency of the 0.5 m long PTFE membrane for H₂S, obtained when 40 ppm H₂S standard was injected into the FI system, was 27.8%. Similarly, the efficiencies for H₂S, obtained when other sulphide standards were injected into the manifold were calculated. The separation efficiency of the PTFE membrane (0.5 m long) for hydrogen sulphide was 27.0 ± 3.5 %.

Using a 1 m long PTFE membrane

The procedure for determining the separation efficiency of the tubular membrane for H₂S was repeated with a 1.0 m long PTFE tubular membrane using the method previously

described. Sulphide standards of concentrations 50 and 100 ppm H_2S were used for generating H_2S in the FI system.

The separation efficiency of the PTFE membrane (1 m long) for H_2S obtained when 50 and 100 ppm H_2S standards were injected into the FI system were 37% and 38% respectively. The separation efficiency of the membrane for H_2S was therefore taken as $37.5 \pm 0.7 \%$.

The separation efficiencies for both PTFE membranes (0.5 and 1 m long) were found to be rather low. This may have been due to an inefficient collection of the generated H_2S , as some of the gas may have escaped from the receiver without being absorbed in the zinc acetate solution. However, better separation efficiency was achieved when the longer membrane was used. This can be explained by the larger surface area which allowed more of the generated gas to diffuse from the liquid donor stream to the nitrogen acceptor stream

7.3 DETERMINATION OF SULPHITE

7.3.1 *DETERMINATION OF SULPHITE AS SULPHUR DIOXIDE BY A SPECTROPHOTOMETRIC METHOD*

Sulphur dioxide is one of the major pollutants of the atmosphere.⁸ The gas has an irritating smell that affects the upper respiratory tract and can cause physical discomfort or death. The maximum allowable concentration of the gas is 10 ppm. However, concentrations of 2 or 3 ppm may be toxic to vegetation and 1 ppm of the gas may corrode metallic materials.⁹ Thus under certain circumstances, concentrations lower than the maximum allowable value may be highly objectionable and even dangerous. The main source of sulphur dioxide in the atmosphere is the combustion of sulphur containing coals and petroleum. The occurrence of

the gas in air may result from its use in bleaching, fumigation, refrigeration and the manufacture of sulphuric acid. Also, the gas is released into the atmosphere during the manufacture of paper by the sulphite process and in the synthesis of phenol.⁹ Several methods have been employed for the determination of sulphur dioxide. These methods apply to the analysis of air and the determination of total sulphur in many organic and inorganic materials that can be ignited at a high temperature in an atmosphere of oxygen to liberate sulphur dioxide.⁸ The methods commonly used for the determination of high concentrations of sulphur dioxide and sulphite are titration methods. These include: the reaction with iodine followed by titration of excess iodine with thiosulphate, reaction with standard alkali followed by titration of excess base with acid, or oxidation of sulphuric acid followed by the usual methods of determination of sulphate⁸ such as the turbidimetric methods. Polarographic, conductometric, fluorescence, coulometric, flame photometric and nephelometric techniques have also been used for the determination of both species.⁸

The para-rosaniline colorimetric method, described by West and Gaeke⁹ and modified by Scaringelli *et al.*,¹⁰ is the most widely used because of its simplicity, specificity and sensitivity for sulphur dioxide. This is the reference method adopted by the United States Environmental Protection Agency for the determination of atmospheric concentrations of sulphur dioxide.¹¹

Tetrachloromercurate II (TCM) solution is used for trapping the SO₂ according:

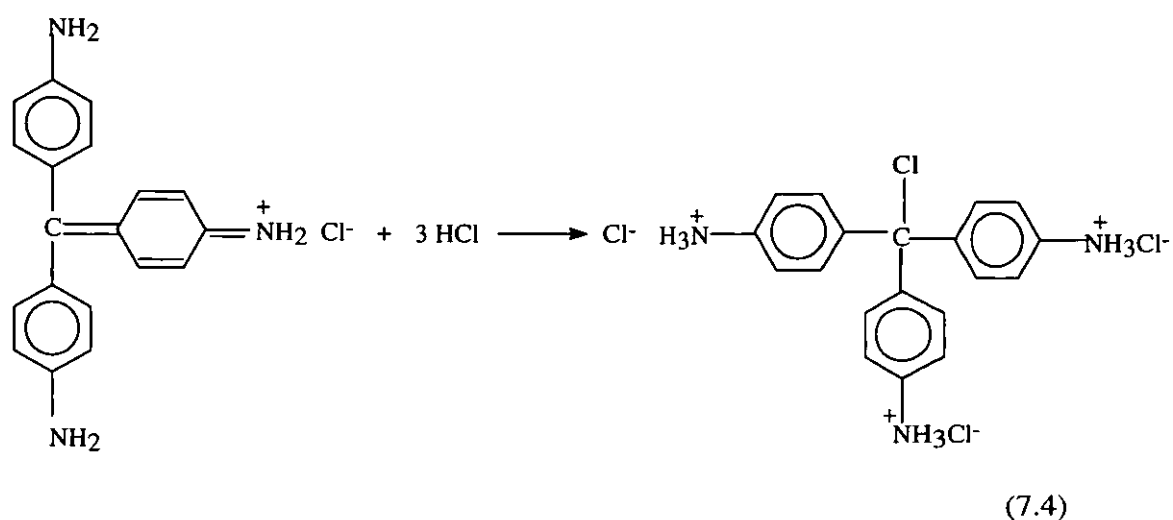


The resulting dichlorosulphitomercurate II (DCSM) is remarkably stable and prevents the oxidation of sulphur dioxide to sulphur trioxide.⁹ Dichlorosulphitomercurate II is stable

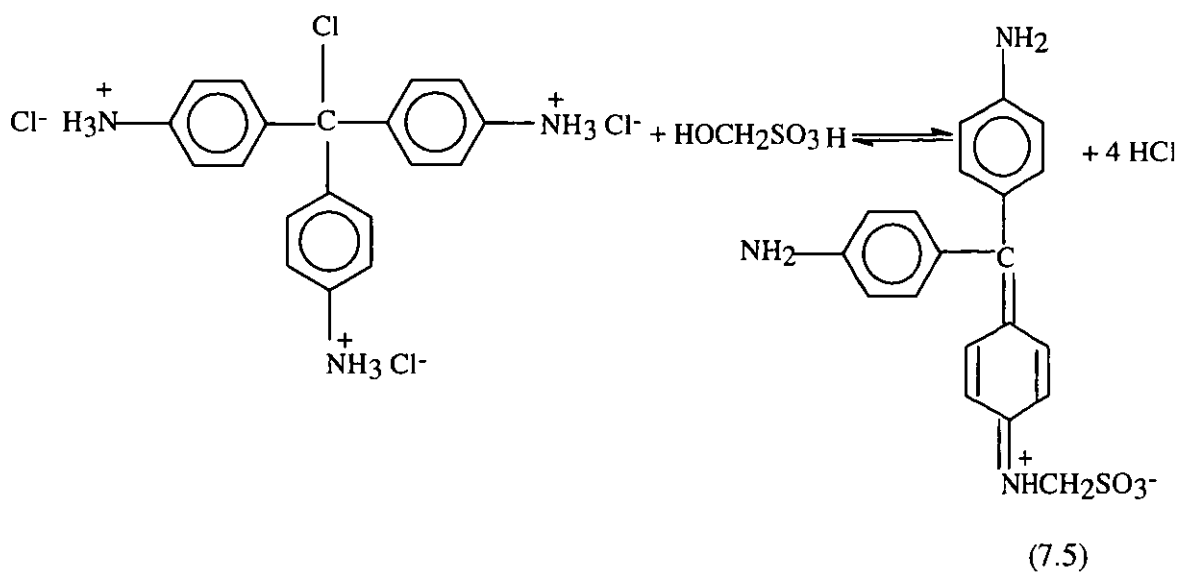
towards ozone and oxides of nitrogen. It reacts with formaldehyde according to the following chemical equation;



Para-rosaniline reacts with hydrochloric acid as shown in the equation below.



Finally, a red-violet complex is formed by the reaction shown in equation 7.5.³



This method was used in preliminary studies involving the optimisation of the operating conditions of the FI system for the determination of sulphite as SO_2 .

Experimental

Apparatus

UV/VIS spectrophotometer (Unicam 8700 series, ATI Unicam, Cambridge, UK).

Reagents

All the reagents used were of analytical grade. De-ionised water was used throughout.

Sulphite stock solution (500 ppm) was prepared by dissolving 0.394 g of anhydrous sodium sulphite (Fisons, Loughborough, UK) in 500 ml of anti-oxidant solution. The working standards were prepared daily by diluting appropriate volumes of the sulphite stock solution with anti-oxidant solution (0.04 M TCM).

Sodium tetrachloromercurate II (0.04 M TCM) (anti-oxidant solution) was prepared by dissolving 10.86 g of mercury chloride , 4.68 g of sodium chloride (Fisons, Loughborough, UK), 0.066 g of disodium EDTA (Fisons, Loughborough, UK) and 0.06 g of sulfamic acid (Fisons, Loughborough, UK) in a 1 litre volumetric flask with de-ionised water. The volume was made up to the mark with de-ionised water. The sulfamic acid was used to destroy any nitrogen dioxide present, thus removing interferences by NO_2 or NO_2^- .

7.3.2 SEPARATION EFFICIENCY OF THE MICROPOROUS PTFE MEMBRANE FOR SO_2

Using a 0.5 m long PTFE membrane

The FI system used for this experiment is shown in Figure 7.13.

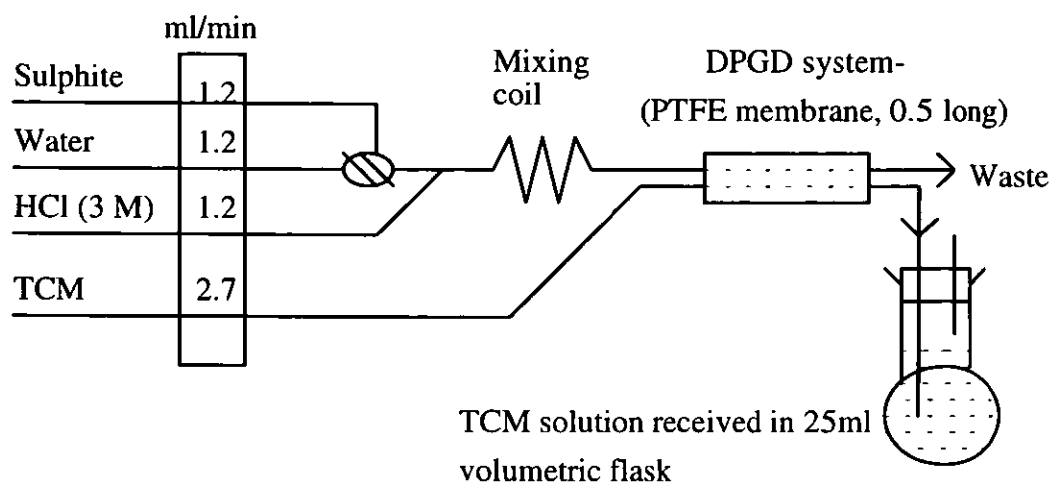


Figure 7.13 FI system for studying the effect of varying the length of PTFE membrane.

7.3.2.1 Calibration procedure

Working standards (0-2 ppm) were prepared from the stock sulphite standard solution (500 ppm). 0.04 M TCM solution was used to dilute the standards to appropriate volumes. To 20 ml of each standard in a 25 ml volumetric flask, 1 ml of para-rosaniline and 1 ml of formaldehyde were added and the volume made to the mark using 0.04 M TCM. The absorbance of each standard was measured off-line using the UV/VIS Spectrophotometer set at a wavelength of 551 nm. The sulphite standards of concentrations 200, 300 and 500 ppm were each injected into the FI system using a sample loop volume of 0.39 ml. The TCM acceptor stream solution (0.04 M) carrying the para-rasaniline and formaldehyde reagents, was pumped by a peristaltic pump through the space between the microporous PTFE tube and the outer glass tube. The donor stream containing the analyte of interest (SO_2) was passed inside the PTFE tube. As the donor stream passed inside the tubular microporous PTFE membrane, SO_2 diffused through the membrane into the outer liquid acceptor stream (TCM). The acceptor stream was received into a 25 ml volumetric flask for a period of 6.5 minutes.

7.3.2.2 Results and Discussion

The calibration graph (Figure 7.14) was constructed using the absorbance values determined off-line for various sulphite standards. A detection limit (at 3σ of the blank) of 0.24 ppm of sulphite was obtained. From the regression equation of this calibration graph, the separation efficiency of the membrane for SO_2 was calculated for each sulphite standard (sample) injected into the FI system (Table 7.4).

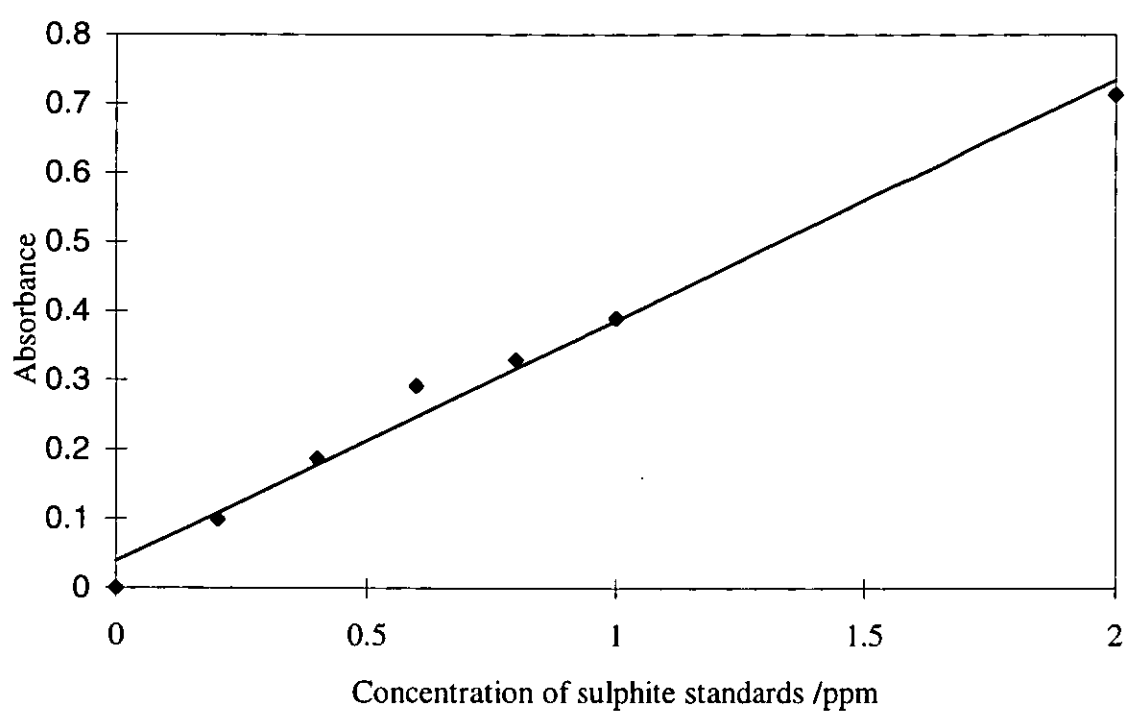


Figure 7.14 Calibration graph of absorbance of pararosaniline complex derived from sulphite standards determined by the UV/VIS spectrophotometric method. Slope, 0.347; y-intercept, 0.039; and correlation coefficient, 0.987.

Table 7.4 Separation efficiency of 0.5 m long PTFE membrane for SO₂

| Concentration of sulphite (ppm) | Absorbance | Concentration of absorbed SO ₂ in TCM (experimental) (ppm) | Calculated Sulphite concentration (ppm) | Separation efficiency (%) |
|---------------------------------|------------|---|---|---------------------------|
| 200 | 0.279 | 0.691 | 3.096 | 22.3 |
| 300 | 0.433 | 1.144 | 4.644 | 24.6 |
| 500 | 0.681 | 1.874 | 7.740 | 24.2 |
| | | | | MEAN, 23.7; RSD, 1.2 |

The separation efficiency of the 0.5 m long PTFE membrane for SO₂ was 23.7 ± 1.2 .

Using 1 m long PTFE membrane

The FI manifold used was the same as that in Figure 7.13 except that the 0.5 m long PTFE membrane was substituted with the one of 1.0 m length. In addition, only a 300 ppm sulphite standard was used for generating SO₂ in the FI system. The absorbance of the solution of SO₂, absorbed in the TCM solution, following its treatment with pararosaniline and formaldehyde, was measured using the UV/VIS spectrophotometer. An absorbance of 0.530 was obtained.

The efficiency was determined by the method previously outlined and was found to be 30.5%.

7.3.3 SPECTROPHOTOMETRIC DETERMINATION OF SULPHUR DIOXIDE GENERATED FROM SULPHITE

7.3.3.1 Calibration procedure

The sulphite working standards (0-5 ppm) were prepared from the stock sulphite standard solution (500 ppm). This involved transferring appropriate volumes of the stock standard solution into 25 ml volumetric flasks followed by addition of about 20 ml of 0.04 M TCM. 1 ml of para-rosaniline and 1 ml of formaldehyde were added and the volume made up to the mark with 0.04 M TCM. The absorbance of each standard was measured using the UV/VIS spectrophotometer.

Two manifolds were employed, one without heating of the reaction vessel (see Figure 7.15) and one with heating (see Figure 7.16).

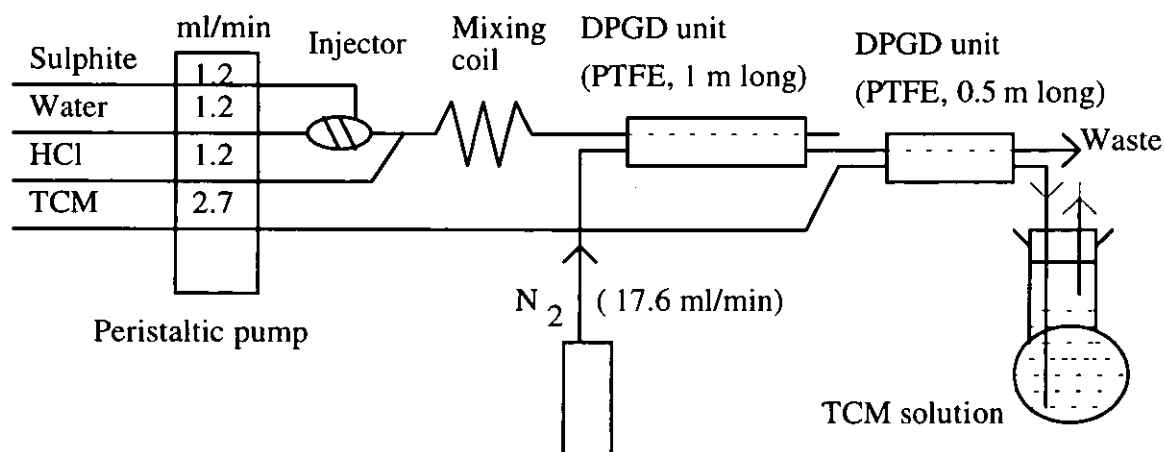


Figure 7.15 FI system for generating sulphur dioxide involving no heating.

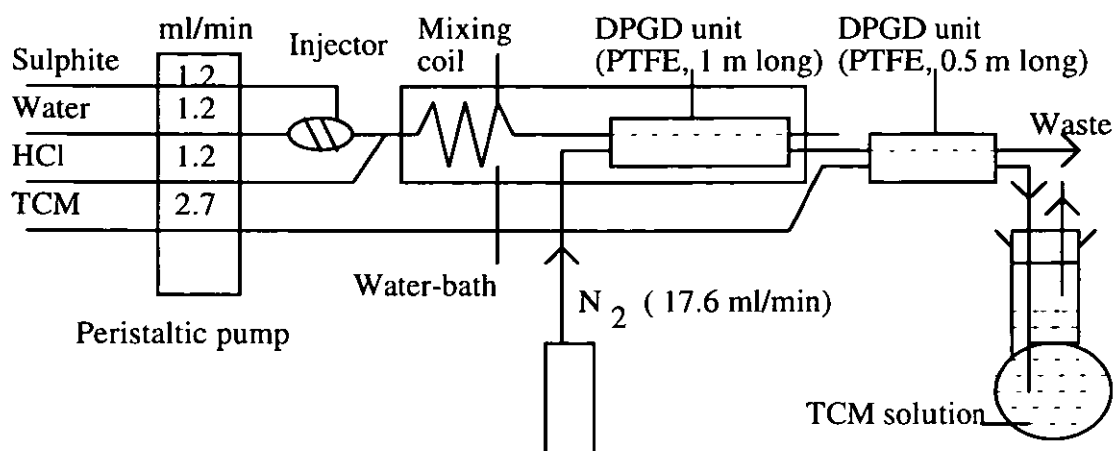


Figure 7.16 FI system used for the generation of SO_2 which involves the warming of mixing coil and PTFE membrane (1 m long) in water-bath maintained at 50°C .

In these experiments, a second membrane was used to trap the gaseous analyte into the absorption medium, rather than the conventional bubble trap. Thus, SO_2 generated from 500 ppm of sulphite standard injected into the FI system was separated by the microporous PTFE membrane (1 m long). The gas diffused from the donor liquid stream into the nitrogen acceptor stream which was then passed to the second PTFE membrane (50 cm long). The SO_2 gas diffused through this membrane from the donor N_2 stream into the acceptor liquid stream (0.04 M TCM). The outlets from this separator were led into a 25 ml volumetric flask where the solution containing the analyte was collected for a period of 10.5 minutes after the sample injection. The volume of the collected solution was made up to the mark with 0.04 M TCM solution. The UV/VIS spectrophotometer was used to measure the absorbance of the unknown concentration.

7.3.3.2 Results and Discussion

The concentration of the sulphide sample was obtained by interpolation from the calibration graph in Figure 7.17, and the transport efficiency of the dual membrane system for SO_2 was subsequently calculated. This is shown in Table 7.5

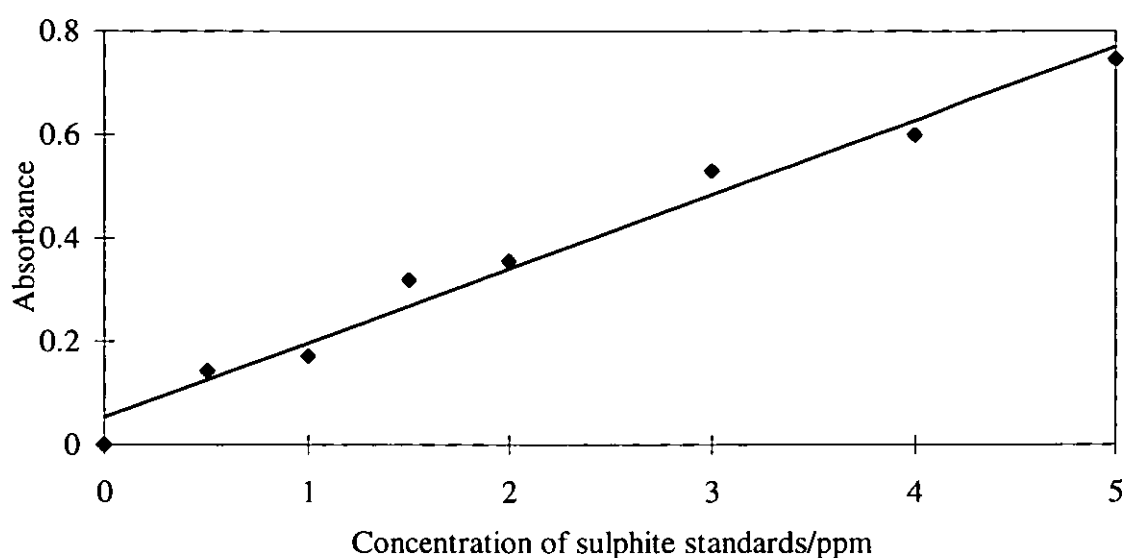


Figure 7.17 Calibration graph of absorbance of pararosaniline complex derived from sulphite standards determined by the UV/VIS spectrophotometric method. Slope, 0.143 ppm^{-1} ; y-intercept, 0.054; and correlation coefficient, 0.974.

Table 7.5 Transport efficiency of the PTFE membranes for sulphur dioxide in case in which heating and no heating were involved.

| Concentration. of sulphite injected into FI system (ppm) | Treatment of mixing coil and membrane | Absorbance | Conc. of sulphite from calibration graph (ppm) | Calculated sulphite conc. (ppm) | Transport efficiency (%) |
|--|---|------------|--|---------------------------------|--------------------------|
| 500 | Not heated | 0.299 | 1.713 | 7.74 | 22.1 ± 2.1 |
| 500 | Heated in water-bath at 50°C | 0.720 | 4.657 | 7.74 | 60.2 ± 4.9 |

A higher concentration of SO_2 was obtained with warming the mixing coil and the PTFE membrane (1 m long) than in the case where no heating was applied. As the temperature of the coil was increased, the rate of reaction between sulphite and hydrochloric acid was increased, resulting in an increase in the amount of SO_2 generated in the system. SO_2 is a very soluble gas, but its solubility in aqueous media decreases with the increase in temperature.¹² Thus a high temperature was required to overcome the problem of solubility, but then the transport efficiency of the dual membrane system was very good. The heated membrane interfaces were used in subsequent experiments.

Effects of using a mixing coil in the FI system

Using the FI system shown in Figure 7.16, but with the mixing coil disconnected, 500 ppm of sulphite standard was injected into the system. The SO_2 absorbed in the TCM solution was determined by the pararosaniline colorimetric method as before. A 45.4 % transport efficiency was achieved. This value is significantly different from the 60.2 %, previously obtained, at the 95 % confidence level. This is because the null hypothesis that the two transport efficiencies are not significantly different is rejected since the calculated t value of 33.3 is greater than the critical t value of 12.71 at the 95 % confidence level. The difference in these separation efficiencies can be explained by the fact that better mixing of the injected sulphite and the HCl reagent stream was achieved when the mixing coil was incorporated into the FI system. Although it might seem obvious that a mixing coil is required, this is not always the case. It is necessary to avoid bubble formation as these can pass through the membrane separator without being exchanged. Therefore, for water soluble gases, reactions within the separator is preferred.

Effect of changing the concentration of HCl on the generation of SO₂

Procedure

Different concentrations of HCl (2-6 M) were each used as the reagent stream in the FI system to react with the injected sulphite sample in the carrier stream. 500 ppm of sulphite sample was injected into the FI system after the concentration of HCl was changed.

Results and Discussion

Figure 7.18 displays the results obtained when various concentrations of HCl were used to produce SO₂ from sulphite. The graph shows that no significant increase in SO₂ was obtained above 3 M HCl and therefore this was the preferred acid concentration.

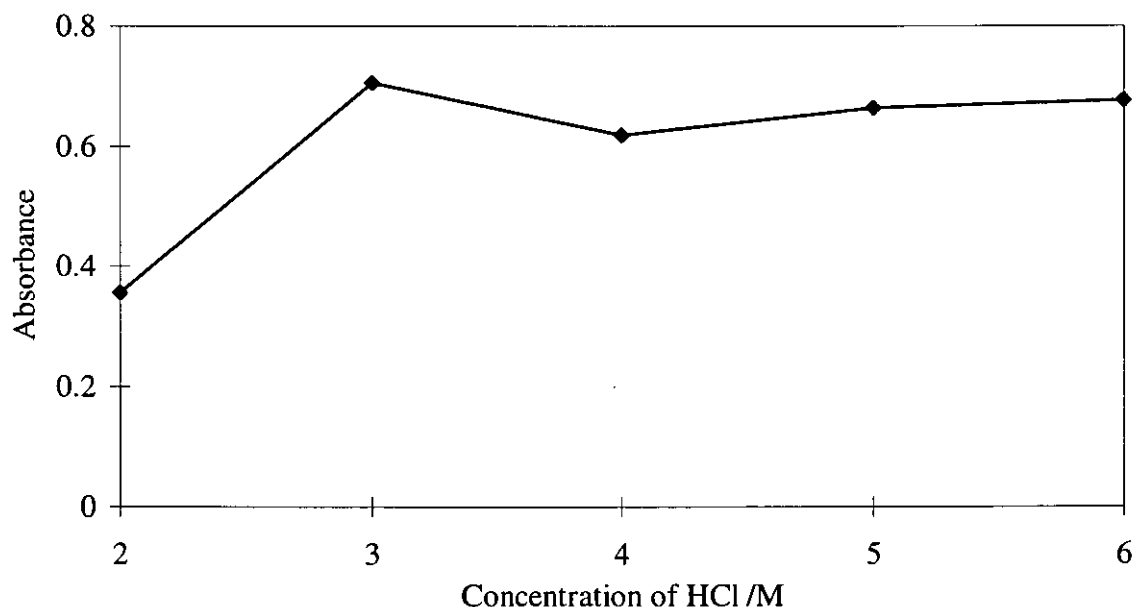


Figure 7.18 Influence of hydrochloric acid concentration on generation of sulphur dioxide.

7.3.4 CALIBRATION OF SULPHUR DIOXIDE GENERATION USING OFF-LINE DETERMINATION OF THE GAS BY UV/VISIBLE SPECTROPHOTOMETRY.

Procedure

Sulphite standards (0-500 ppm) were injected into the FI system employing an injection valve with a loop which had a volume of 0.39 ml. The manifold and operating conditions was as described previously.

Results and Discussion

The calibration graph of absorbance versus concentration of sulphite injected is shown in Figure 7.19. A detection limit (at 3σ above the blank) of 108.9 ppm of sulphite injected into the FI system was achieved by this method.

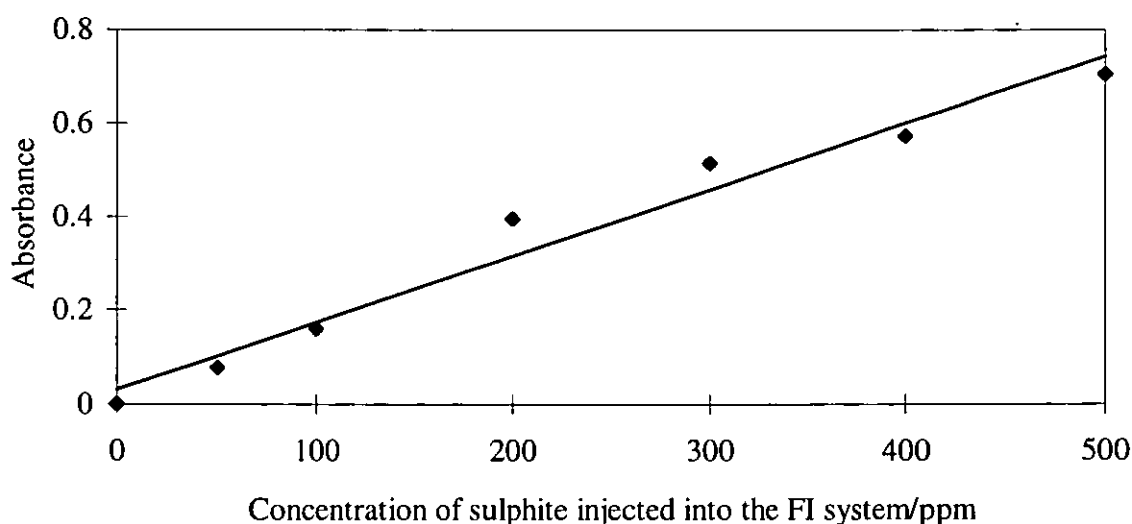


Figure 7.19 Calibration graph of sulphite standards injected in the gas diffusion-flow-injection system. Slope, $1.424 \times 10^{-3} \text{ ppm}^{-1}$; y-intercept, 0.031 and regression coefficient, 0.969.

Effects of changing the flow rate on the acceptor stream

Although TCM is the accepted trapping medium, it is not an environmentally friendly material. It was therefore decided to see if the consumption could be reduced and therefore two lower TCM flow rates were investigated, 1.8 and 1.3 ml/min. A 23.5% transport efficiency of the combined membrane was obtained when a flow rate of TCM of 1.3 ml/min was employed and the generation of the gas conducted without heating. This was higher than the 22.1% obtained earlier when a TCM flow rate of 2.7 ml/min was employed.

7.3.5 GENERATION OF SULPHUR DIOXIDE FROM SULPHITE IN A GAS DIFFUSION-FLOW INJECTION SYSTEM INTERFACED TO A THERMAL CONDUCTIVITY DETECTOR

A schematic diagram of the FI system used is shown in Figure 7.20.

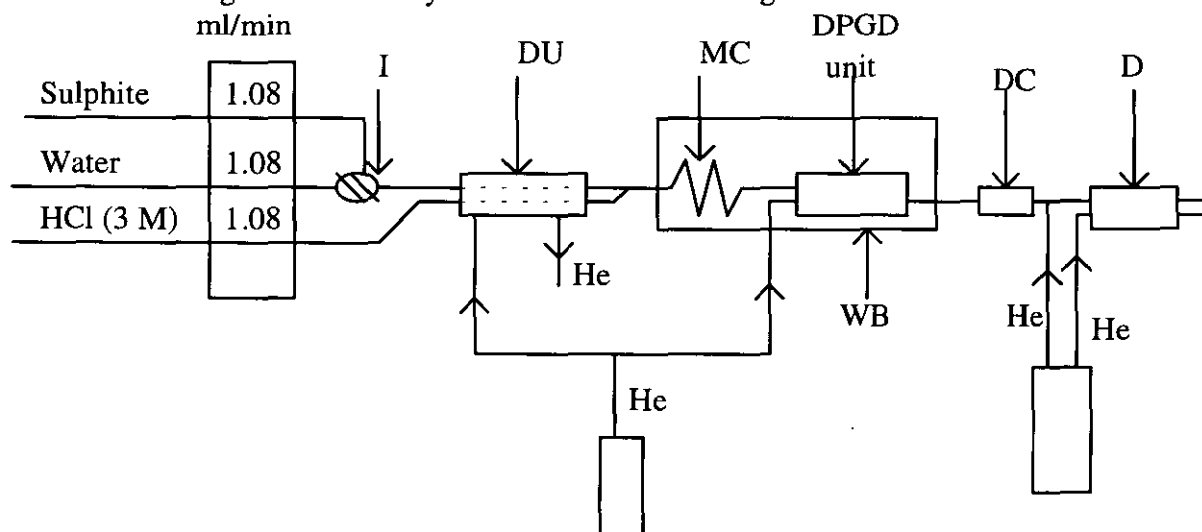


Figure 7.20 FI system with thermal conductivity detector used for generating sulphur dioxide. S, sample (sulphide); C, carrier stream (water); R, reagent (HCl); I, injector; DU, degassing unit; MC, mixing coil; DPGD, dual phase gas diffusion unit (PTFE membrane, 1.0 m long); DC, drying chamber ($\text{Mg}(\text{ClO}_4)_2$); WB, water-bath and D, detector (TCD).

Effect of using drying agent in the FIA system on SO₂ signal

Magnesium perchlorate Mg(ClO₄)₂

The magnesium perchlorate drying agent (BDH Ltd, Poole, Dorset, UK) was packed into the drying chamber. Sulphite standards of concentrations 100-500 ppm were each injected into the FI system in which the mixing chamber and the DPGD unit were immersed in a water-bath set at 50°C (Figure 7.20). The generated SO₂ was detected by the thermal conductivity detector and the signals thus obtained were presented in the form of peaks. The peak height measurements obtained were used for plotting the calibration graph shown in Figure 7.21. The detection limit offered by this method was 104.9 ppm SO₃²⁻ (at 3 σ above the blank).

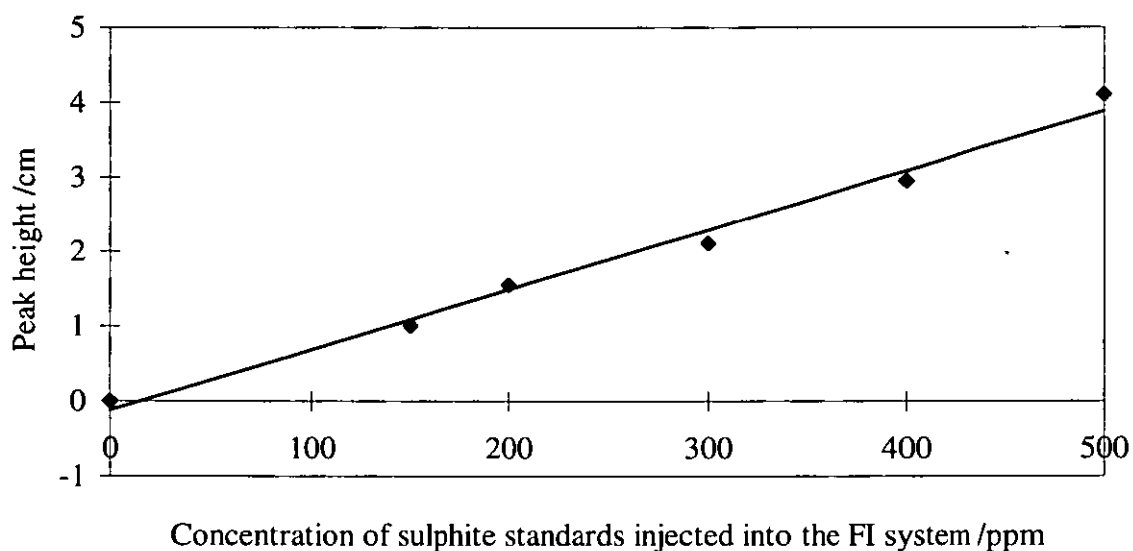


Figure 7.21 Calibration graph of peak height of signal due to sulphur dioxide derived from sulphite standards injected in the FI system. Slope, 0.008 cm/ppm; y-intercept, -0.118 cm; correlation coefficient, 0.988.

Addition of the drying tube in the FI system caused a small 12 % loss in signal.

Optimisation of flow rate on the carrier and reagent streams

Pump tubes with i.d. of 1.14 mm, 3 M HCl, water bath temperature of 50°C, magnesium perchlorate drying agent and 500 ppm of sulphite standard were used in the FI system. The results obtained are presented in Figure 7.22. 0.911 ml/min was taken as the optimum flow rate since the highest peak height was obtained at this flow rate.

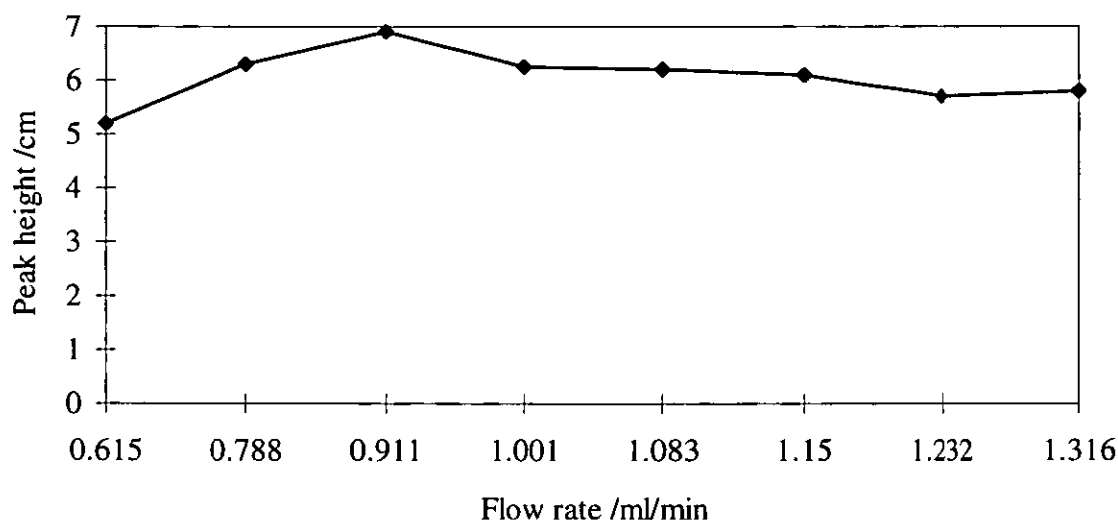


Figure 7.22 Influence of flow rate of carrier and reagent streams on peak height of TCD signal.

Influence of temperature on generation of sulphur dioxide

Using the same conditions as given above, the water bath temperature was varied over the range from ambient to 60° C. 500 ppm of sulphite was injected into the FI manifold. The results obtained are shown in Table 7.6.

Table 7.6 Peak height of signal due to sulphur dioxide generated at different temperatures in the FI system and determined by the thermal conductivity detector.

| Temperature of water-bath (° C) | Peak height (cm) |
|---------------------------------|------------------|
| No heating (20°C) | 2.6 |
| 45 | 6.4 |
| 50 | 7.2 |
| 60 | 7.2 |

This confirms the previous results obtained without the drying tube. However, the drying tube would be essential for MS experiments, particularly at high temperatures when the water vapour flux through the membrane is much higher.

Generation of SO₂ using optimised conditions

An optimum flow rate of 0.911 ml/min was employed for both reagent and carrier streams, 3 M HCl and magnesium perchlorate drying agent were used in the FI system shown in Figure 7.20. Sulphite standards (50-500 ppm) were each injected into the FI system. Water bath temperature was set at 50°C. The generated SO₂ was determined by the thermal conductivity detector after being separated by the 1.0 long PTFE membrane.

Calibration graphs of peak height and peak area against concentration for SO₂ generated at 50°C are shown in Figures 7.23 and 7.24. Detection limits of 30 ppm and 62 ppm were obtained when the TCD signals were measured as peak heights and peak areas respectively.

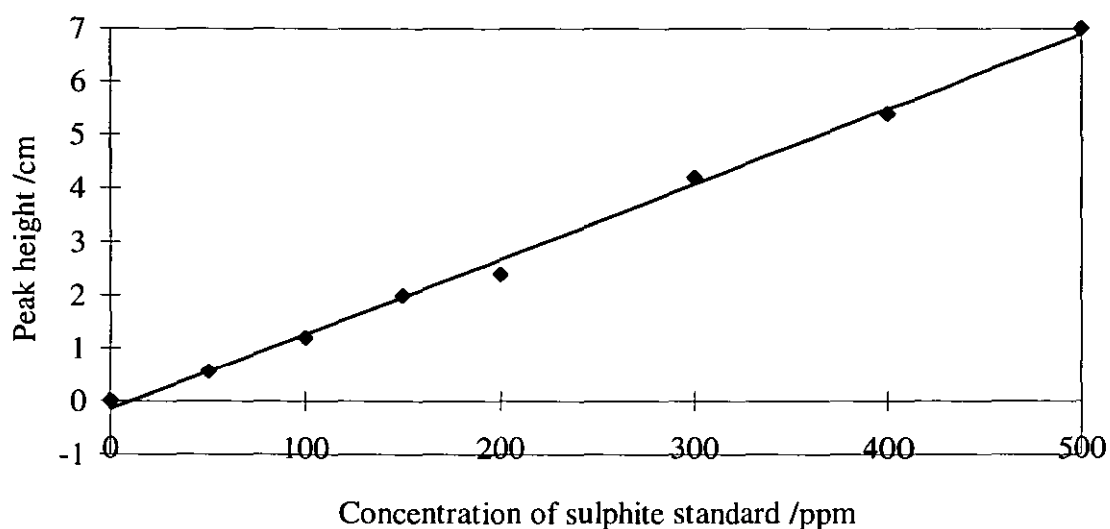


Figure 7.23 Calibration graph for sulphur dioxide generated from sulphite standards and subsequently detected by the thermal conductivity detector. Slope, 0.014 cm/ppm; y-intercept, -0.152 cm; and correlation coefficient, 0.997.

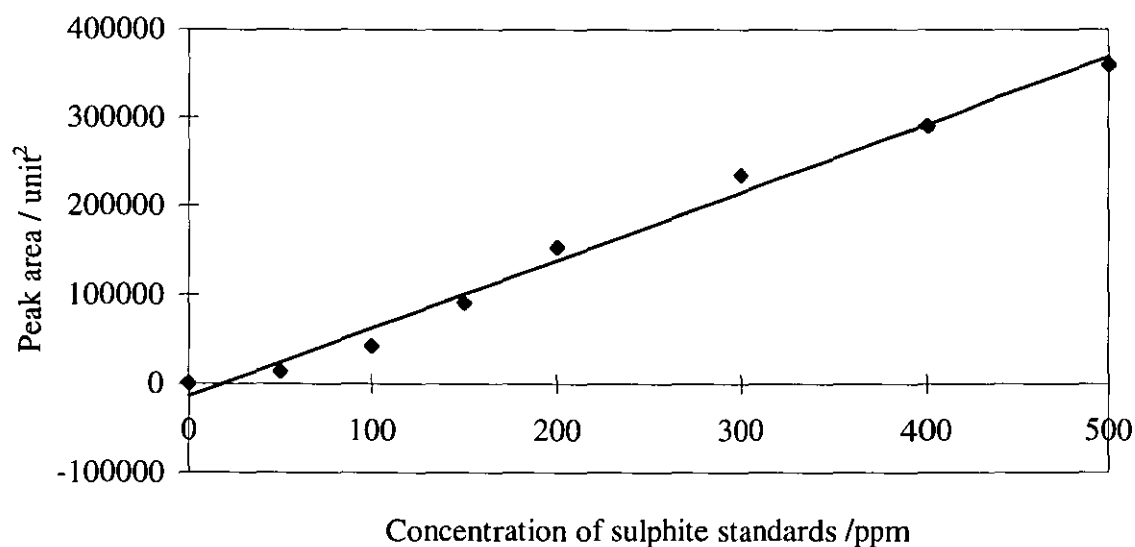


Figure 7.24 Calibration graph of peak area for sulphur dioxide generated from sulphite followed by detection by the thermal conductivity detector. Slope, 767.0 unit²/ppm; y-intercept, -14554 unit²; and correlation coefficient, 0.986.

7.3.6 GENERATION OF HYDROGEN SULPHIDE FROM SULPHITE IN THE DPGD-FI SYSTEM USING SODIUM BOROHYDRIDE AND ITS DETERMINATION BY THE METHYLENE BLUE METHOD

Reagents

All the reagents used were of analytical grade and were prepared as shown in Section 7.2.1.2. Sulphite working standards of concentrations 50-250 ppm SO_3^{2-} were prepared from 500 ppm sulphite standards.

7.3.6.1 Procedure

50 ppm of SO_3^{2-} working standard was injected into the FI system shown in Figure 7.25.

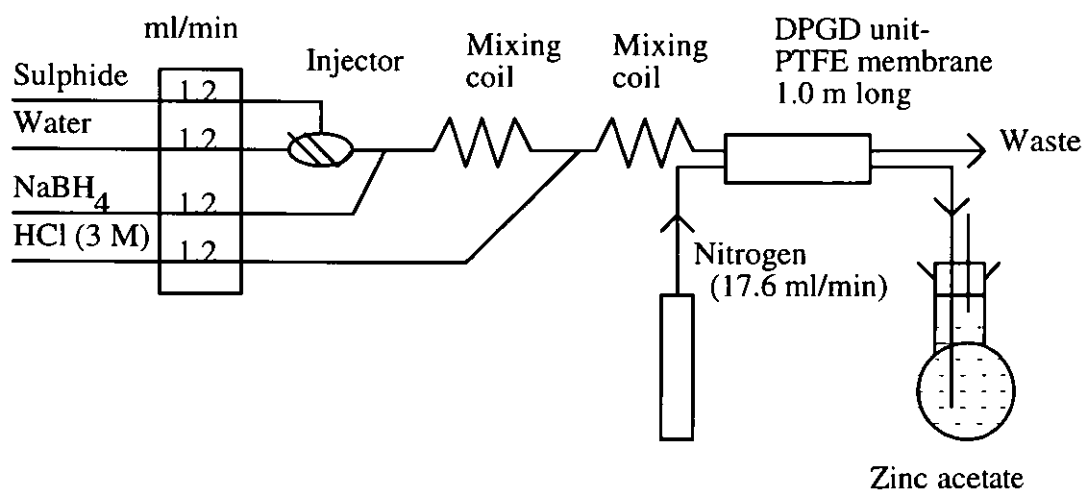


Figure 7.25 FI manifold for generating hydrogen sulphide from sulphide standards using sodium borohydride.

The generated H_2S diffused through the microporous PTFE membrane (1 m long) into the nitrogen carrier (acceptor) stream which was then bubbled through the zinc acetate solution

(20 ml), contained in a 25 ml volumetric flask, for a period of 10 minutes. The solution was then treated with 0.6 ml amine-sulphuric acid and one drop of ferric chloride. The solution was made up to the mark with the zinc acetate solution. The same procedure was applied to the other sulphite working standards.

7.3.6.2 Results and Discussion

The absorption spectra obtained showed that the maximum absorbance occurred at 656.6 nm. A shoulder peak appeared at 613.2 nm when high concentrations of sulphite were injected into the FI system. The peak at 656.6 nm was due to the methylene blue complex. The results obtained are presented in the calibration graph in Figure 7.26. A detection limit of 36 ppm of sulphite (at 3σ above the blank) was achieved.

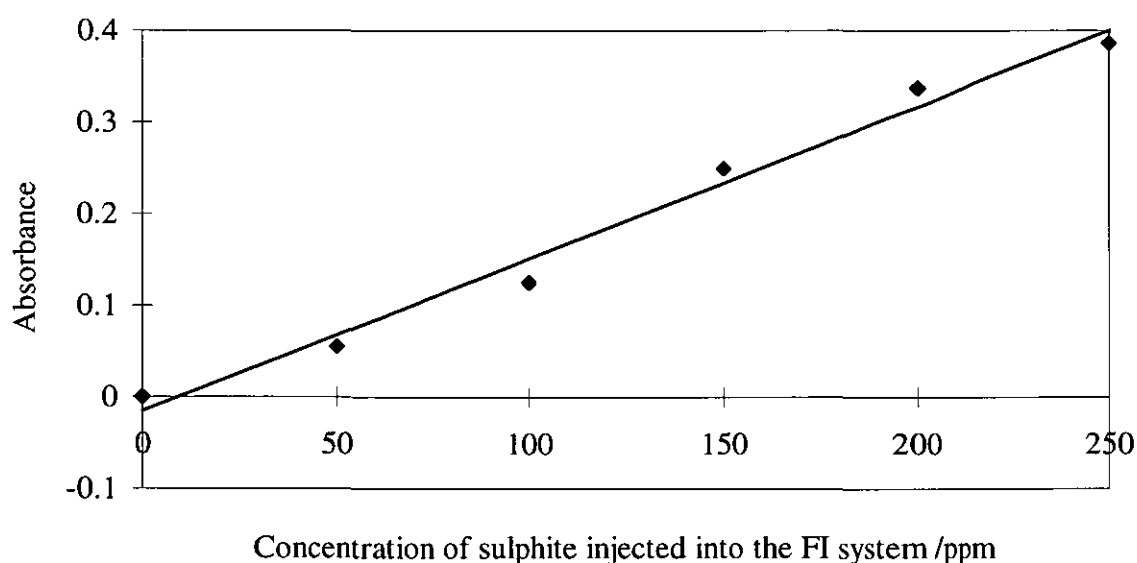


Figure 7.26 Calibration graph of absorbance of methylene blue complex versus concentration of sulphite injected for the generation of H_2S by the action of NaBH_4 reductant. Slope, $1.659 \times 10^{-3}/\text{ppm}$; y-intercept, -0.015 ; and regression coefficient, 0.984.

This experiment shows that when sodium borohydride was used in the FI system, sulphite was reduced to H_2S . The oxidation state of sulphur changed from +6 to -2 when SO_3^{2-} was converted to H_2S . This provides an alternative route for the determination of sulphite and one which may be preferred for mass spectrometry experiments. This is because the H_2S route overcomes the problems of handling SO_2 for mass spectrometry. These include: high solubility of SO_2 in aqueous media and its adsorption onto moist surfaces.

7.4 DETERMINATION OF SULPHATE

7.4.1 GENERATION OF H_2S FROM SULPHATE IN THE DPGD-FI SYSTEM AND ITS DETERMINATION BY UV/VIS SPECTROPHOTOMETRIC METHOD

7.4.1.1 Introduction

Unsuccessful attempts were made to generate H_2S by reduction of sulphate in the FI system using orthophosphoric acid previously heated with activated charcoal, phosphoric acid, stannous chloride in concentrated orthophosphoric acid and hydriodic acid. In all these cases, a water-bath in which a mixing coil and a PTFE membrane were immersed, was maintained at 80° C.

Reduction of sulphate to H_2S has been achieved by a hydriodic acid-formic acid-hyphosphorous acid reducing mixture, Johnson and Nshita method.⁷ In this method, the sample and reagents are heated to 115°C for a period of 2 hours. Attempts to implement this method employing the FI manifold was unsuccessful. Problems of leakage and irregular flow of liquid occurred at such high temperatures due to high pressure build up in the system.

The reduction of sulphate to H_2S by the Johnson and Nshita method can be done off-line and the generated gas absorbed in a solution such as zinc acetate or alkaline cadmium

chloride. The absorbed H_2S can then be used as a sample to generate H_2S in the FI manifold. The gas can subsequently be introduced into a mass spectrometer for isotopic ratio measurements, or any other suitable detector, following PTFE membrane separation.

It was therefore necessary to establish whether H_2S could be regenerated from absorbed H_2S in zinc acetate solution by acidification.

7.4.2 REGENERATION OF HYDROGEN SULPHIDE FROM ABSORBED HYDROGEN SULPHIDE IN ZINC ACETATE SOLUTION BY ACIDIFICATION

H_2S was generated in the FI system in Figure 7.27 by acidification of 1000 ppm H_2S standard.

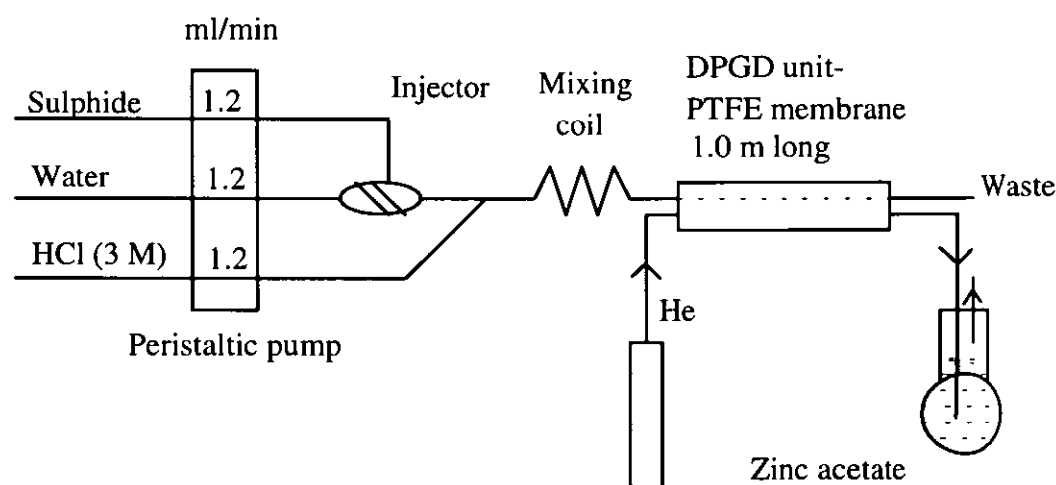


Figure 7.27 FI system used for generation of H_2S in zinc acetate by acidification.

7.4.2.1 Procedure

1000 ppm of H_2S standard was injected into the FI system. The generated gas was swept by a helium acceptor stream into 20 ml zinc acetate solution contained in a 25 ml volumetric flask. The methylene blue test was carried out by adding 0.6 ml *p*-aminodimethylaniline and

one drop of ferric chloride. After the volume was made to the mark using the zinc acetate solution, the resulting solution was left standing on the bench for 20 minutes. The absorption spectrum of the collecting solution is shown in Figure 7.28 and shows the characteristic spectrum of the methylene blue complex.

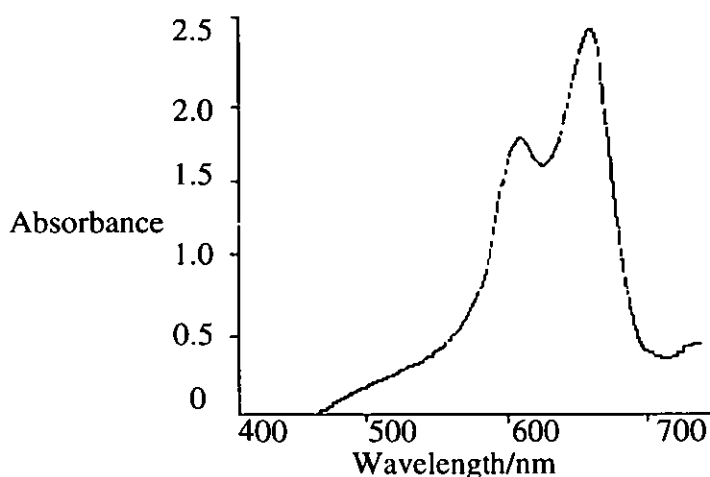


Figure 7.28 Absorption spectrum of methylene blue complex derived from H_2S generated from sulphide standard solution (1000 ppm H_2S) injected into the DPGD-FI system.

The sulphide standard (1000 ppm H_2S) was injected again into the DPGD-FI system and the generated H_2S was absorbed in zinc acetate solution for 10 minute as previously. This solution was then thoroughly mixed and one loop volume (0.56 ml) was then injected into the FI system. The H_2S thus formed on-line was carried by the helium acceptor stream after diffusing through the microporous PTFE membrane into the zinc acetate collector solution. The absorption spectrum of the final solution is shown in Figure 7.29 confirming the regeneration of H_2S .

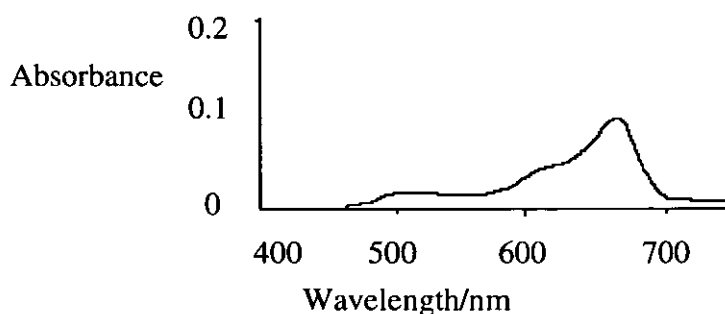


Figure 7.29 Absorption spectrum of methylene blue derived from the absorbed H_2S in zinc acetate solution following the injection of 0.56 ml of sulphide standard (1000 ppm H_2S) into the DPGD-FI system.

An attempt was also made to generate H_2S continuously from the H_2S trapped in zinc acetate solution as shown in Figure 7.30.

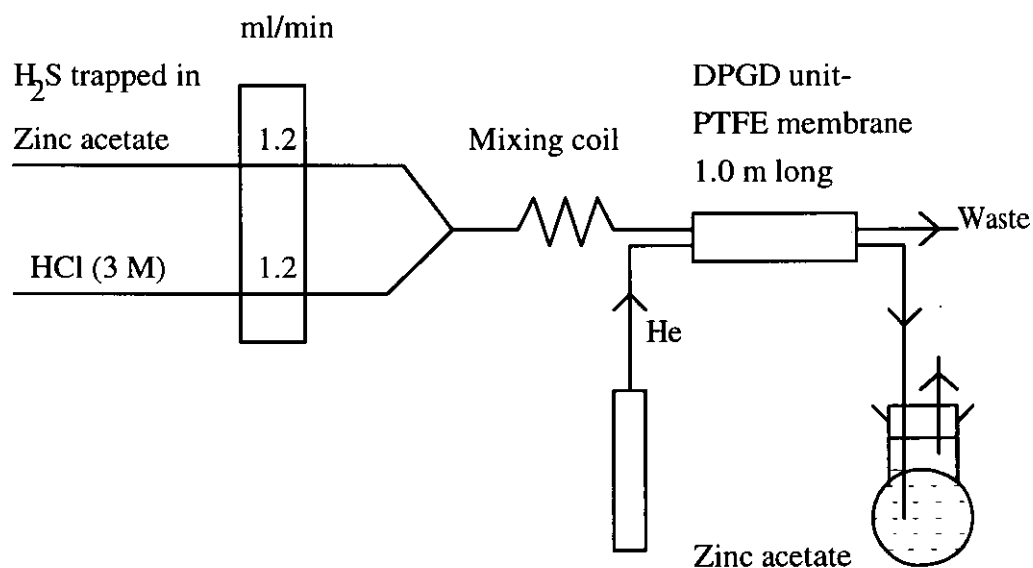


Figure 7.30 Continuous flow generation of hydrogen sulphide in DPGD-FI system.

This involved using the absorbed H_2S in the zinc acetate solution following the injection of one loop volume (0.56 ml) of 1000 ppm H_2S standard into the DPGD-FLA system. The absorbed gas in the zinc acetate solution was allowed to react with 3 M HCl in a continuous flow system (Figure 7.30) to generate H_2S which was absorbed again in the zinc acetate solution. The solution of the re-absorbed H_2S was treated with *p*-aminodimethylaniline and ferric chloride as described earlier. An absorbance of 0.694 for the methylene blue complex was obtained by the UV/VIS spectrophotometric detector at 666 nm.

7.4.2.2 Results and Discussion

From these experimental results, it was established that the H_2S can be regenerated from H_2S absorbed in the zinc acetate solution by acidification (using 3 M HCl). The use of zinc acetate solution for the absorption of H_2S should be limited to low concentration of H_2S because very high concentrations of H_2S lead to the formation of a thick white precipitate of zinc sulphide. This precipitate can easily block the FI system tubes and also causes leakage of the liquid stream at the connection points on the FI manifold.

The conversion of sulphate directly to H_2S is a difficult process; as it involves using a high temperature and a long period of heating which cannot easily be accommodated in a FI system. The following steps are recommended for the determination of sulphate as H_2S .

- The sulphate should be reduced by the hydriodic acid-formic acidic-hypophosphorous acid (or red phosphorous) reducing mixture (Johnson and Nshita method) to H_2S outside the FI system.
- the generated H_2S should be trapped in zinc acetate solution.
- the H_2S absorbed in the zinc acetate solution should then be injected into the FI system and regenerated by acidification.

- the regenerated H_2S , having diffused through the membrane, can be swept by the acceptor gas stream to suitable detectors such as an isotope mass spectrometer or a thermal conductivity detector.

7.5 DETERMINATION OF ORGANIC SULPHUR (L-CYSTEINE AND METHIONINE AMINO ACIDS)

7.5.1 Introduction

Sulphur is present in all cells, primarily in proteins and biomolecules. The principal sulphur containing amino acids in living organisms are methionine and cysteine.¹³ These amino acids serve as components of proteins and as starting materials for the biosynthesis of other molecules. Methionine is an active participant in general biomolecular synthesis due to the presence of an active terminal methyl group, close to the molecule's sulphur atom, which can be transferred to other molecules. Cysteine, on the other hand, plays an important role in the three dimensional structures of proteins. Cysteines can bind individual protein chains to one another or stabilise the complex three dimensional structures as they twist or fold back on themselves. They are able to achieve this when interspersed among other amino acids by linking to one another through sulfhydryl groups (-SH) and forming disulphide bridges between neighbouring cysteine residuals.

Cephalosporins in drug formulations have been determined by an air segmented flow-visible spectrophotometric method involving alkaline degradation to hydrogen sulphide and methylene blue complex formation using *p*-aminodimethylaniline and ferric chloride.¹⁴ Penicillin was not found to interfere with the determination of cephalosporin by this method as sulphide is not a primary degradation product. The yield of sulphide obtained depended on the cephalosporin used and varied from 14-64.5 %. This method was applied for the determination of both cysteine and methionine.

7.5.2 DETERMINATION OF L-CYSTEINE AS HYDROGEN SULPHIDE BY THE METHYLENE BLUE SPECTROPHOTOMETRIC METHOD FOLLOWING THE GENERATION AND SEPARATION OF THE GAS IN THE DPGD-FI SYSTEM

Reagents

Ferric chloride, *p*-aminodimethylaniline, zinc acetate and HCl (3 M) solutions were prepared according to the procedure given in Section 7.2.1.2.

Sulphide stock solution (1000 ppm H₂S) was prepared by dissolving 0.7377 g of sodium sulphide, Na₂S.9H₂O (Fisons, Loughborough, UK) in 100 ml of de-ionised water.

L-cysteine (1124 ppm) was prepared by dissolving 0.4 g of L-cysteine (Aldrich, Dorset, UK) in 100 ml of 0.1 M NaOH (Fisons, Loughborough, UK), to which 1 g of ascorbic acid sodium salt (analytical grade, Fisons, Loughborough, UK) was added. The solution was heated gently at 100° C in a water-bath for 1 hour. At the end of this period, the solution was allowed to cool.

7.5.2.1 Procedure

The L-cysteine sample, previously alkaline degraded in the presence of ascorbic acid to sulphide was injected into the FI system (Figure 7.11). Hydrogen sulphide was produced on-line by acidification before being separated from the liquid carrier stream by the microporous PTFE membrane (1.0 m long). The separated gas was swept by helium gas into the zinc acetate solution. The solution was treated with *p*-aminodimethylaniline and ferric chloride as outlined earlier in section 7.2.3. A similar procedure was applied to the sulphide standards of concentration range 0-100 ppm H₂S.

7.5.2.2 Results and Discussion

The results obtained for the sulphide standards were used for constructing the calibration graph in Figure 7.31. The mean absorbance of methylene blue complex derived from H₂S

produced from L-cysteine sample was 0.268. From the calibration graph, this absorbance corresponded to a concentration of 58.83 ppm H_2S . Assuming 100 % conversion of L-cysteine sample to H_2S , the concentration of the L-cysteine sample was expected to be 1124 ppm. The % conversion of L-cysteine to hydrogen sulphide was therefore 5.1%.

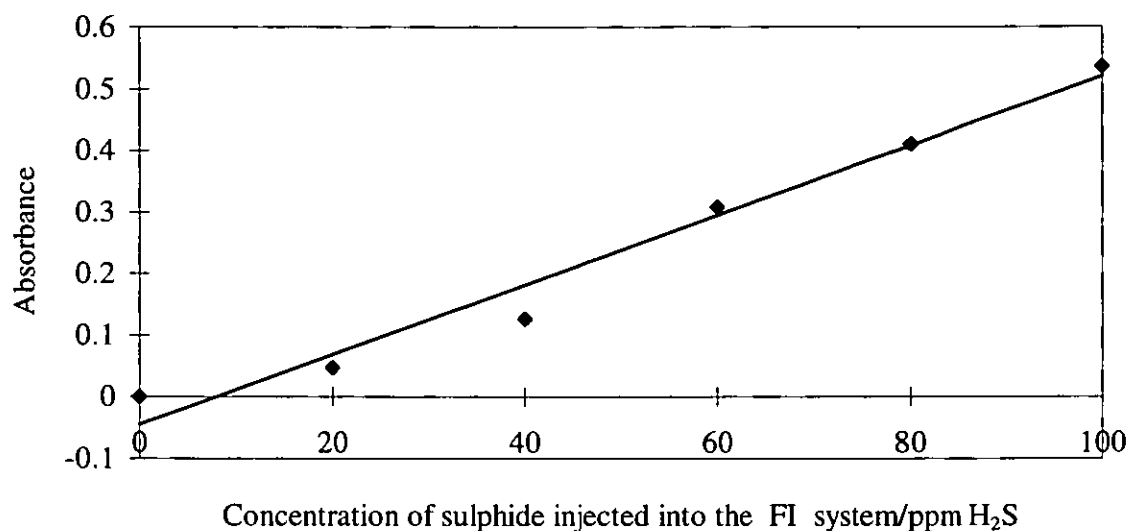


Figure 7.31 Calibration graph of absorbance of methylene blue complex versus concentration of sulphide injected into the FI system.

The low conversion efficiency of L-cysteine to H_2S may be attributed to several factors. These include:

- incomplete degradation of L-cysteine when it was heated in NaOH and ascorbic acid solution.
- low absorption efficiency of zinc acetate for H_2S . Some of the H_2S may have inevitably escaped from the vessel containing the zinc acetate solution before being absorbed.
- low efficiency of the PTFE membrane for separating the H_2S generated in the FI system.

Despite the low conversion efficiency of L-cysteine to H_2S , the method is suitable for applications in isotope ratio mass spectrometry where quantitative conversion of L-cysteine to H_2S is not a requirement.

7.5.3 GENERATION OF HYDROGEN SULPHIDE FROM METHIONINE IN THE DPGD-FI SYSTEM AND ITS DETERMINATION BY THE METHYLENE BLUE SPECTROPHOTOMETRIC METHOD

The same procedure and FI manifold used for producing hydrogen sulphide from L-cysteine were applied to D-methionine (Aldrich, Dorset, UK). When *p*-aminodimethylaniline and ferric chloride were added to the zinc acetate absorption solution, following the injection of methionine (previously heated with alkaline and ascorbic acid), the characteristic blue colour of the methylene blue complex was not observed. This served as an indication that methionine was not degraded to sulphide by sodium hydroxide on the application of heat and hence no hydrogen sulphide was produced following the injection of the resultant solution in the FIA system.

7.6 CONCLUSIONS

The DPGD-FI system was used for the generation of hydrogen sulphide from sulphide, sulphite and L-cysteine, and sulphur dioxide from sulphite. The DPGD-FI interface was coupled to a thermal conductivity detector. A UV/VIS spectrophotometer was also used for the detection of these gases (off-line).

The separation efficiency of the microporous PTFE membrane for SO_2 and H_2S varied with the length of the membrane used in the DPGD unit. The longer the membrane the higher the separation efficiency. This was due to a larger surface area being available for the gases to diffuse through. The separation efficiencies of the 0.5 m long PTFE membrane for the separation of H_2S and SO_2 were $27.3 \pm 2.2 \%$ and 23.7% respectively.

For the 1 m long PTFE membrane, the separation efficiencies for H_2S and SO_2 were $37.3 \pm 0.7 \%$ and 30.5% , respectively.

Two DPGD units, one consisting of a 0.5 m long PTFE membrane and the other a 1 m long PTFE membrane, were connected in series in the FIA system for the separation of SO_2 generated from sulphite. This arrangement was used as an alternative to bubbling the SO_2 through the trapping solution. The transport efficiency of the combined membranes, when the longer membrane was heated in a water-bath maintained at 50°C was $60.2 \pm 4.9 \%$ whilst in the case where no heating was involved it was $22.1 \pm 2.1 \%$. The application of high temperature influenced the rate of transport of SO_2 across the membrane from the donor stream to the acceptor stream. This was essential because of the high solubility of SO_2 in aqueous media at ambient temperatures.

The low separation efficiencies in all these cases may in part have been due to the manner of absorption of H_2S and SO_2 . For example, zinc acetate was employed for the absorption of H_2S while TCM solution was used for SO_2 . The absorption of these gases was carried out off-line. It was assumed that the absorption efficiencies of zinc acetate for H_2S and TCM solution for SO_2 were 100 %. In practice, this assumption may not hold as some of the gas could have escaped from the container without being trapped in the absorbing solutions.

The detection limit obtained for the determination of H_2S generated from sulphide, and detected by the TCD was 5 ppm H_2S (at 3σ above the blank). For the determination of SO_2 , generated from sulphite, by the UV/VIS spectrophotometric method, involving the use of the two membranes connected in series (0.5 and 1 m long PTFE membrane), the detection limit was 109 ppm SO_3^{2-} . However, when the DPGD-FI system was interfaced with a TCD, a detection limit of 30 ppm SO_3^{2-} was achieved. For the generation of H_2S from sulphite, using NaBH_4 reducing agent, and subsequent determination by the UV/VIS spectrophotometric method (methylene blue method), the detection limit obtained was 36 ppm SO_3^{2-} .

The determination of L-cysteine (as an example of organic S) through the H₂S route was achieved by the degradation of this amino acid to sulphide by NaOH and ascorbic acid involving heating off-line. The DPGD-FI system was used for the generation of H₂S from the resultant solution by acidification followed by its determination by the UV/VIS spectrophotometric method. A 5 % conversion efficiency of L-cysteine to H₂S was obtained. The low overall conversion efficiency might have been due to incomplete degradation of L-cysteine coupled with the transport efficiency of the PTFE membrane previously shown to be 37.5 % for H₂S. The method was not successfully applied for the generation of H₂S from methionine. This is due to absence of a terminal H directly joined to the sulphur atom (HS group) in methionine. It has a CH₃ terminal group instead and therefore does not give H₂S as the degradation product.

The attempted generation of H₂S from sulphate in the DPGD-FI system was not successful. This was due to the high temperature (115°C) required for the conversion to take place. The reducing mixture employed was that used in the Johnson and Nshita method i.e. hydriodic acid, hypophosphorous acid and formic acid reducing mixture. At this temperature, problems of leakage of liquid at the connection points due to build up of pressure and irregular flow of the liquid in the FI manifold were encountered. In addition, copious quantities of water vapour passed through the PTFE membrane, which on cooling condensed in the acceptor stream leading to the TCD. This had the potential danger of damaging the filaments of the TCD.

REFERENCES

1. Arowolo, T. A., Ph.D. Thesis, *Development and Application Methods for Determination of Selected Sulphur Species*, Aberdeen University, 1992, pp.1-256
2. Rees, T. D., Gyllenspetz, A. B. and Docherty, A. C., *Analyst*, 1971, **96**, 201.
3. Marr, I. L. and Cresser, M. S., *Environmental Chemical Analysis*, 1983, International Textbook Company, New York, 1983, pp.97.
4. Zutshi, P. K. and Mahadevan, T. N., *Talanta*, 1970, **17**, 1014.
5. Davidson, W. and Lishman, J. P., *Analyst*, 1983, **108**, 1235.
6. Waernbaum, G. and Wallin, I., *Scandinavian J. Work Environment Health*, 1979, **5**, 31.
7. Johnson C. M. and Nishita, H., *Anal. Chem.*, 1952, **24**, 736.
8. Syty, A., *Anal. Chem.*, 1973, **45**, 1744.
9. West, P. W. and Gaeke, G. C., *Anal. Chem.*, 1956, **28**, 1816.
10. Scaringelli, F. P. Saltzman, B. E. and Frey, S. A., *Anal. Chem.*, 1967, **39**, 1709.
11. Huitt, H. A. and Lodge, J. P., *Anal. Chem.*, 1964, **36**, 1305.
12. Lide, D. R., *Handbook of Chemistry and Physics*, 73 rd Ed., CRC Press, Boca Raton, 1992.
13. Greyson, J., *Carbon, Nitrogen and Sulphur Pollutants and their Determination in Air and Water*, Marcel Dekker, New York, 1990, pp. 76-78.
14. Abdalla, M. A. and Fogg, A. G., *Analyst*, 1983, **108**, 53.

Chapter 8

CHAPTER EIGHT

DETERMINATION OF CARBON AS CARBON DIOXIDE

8.1 INTRODUCTION

In this chapter, a DPGD-FI system was employed for generating carbon dioxide from organic and inorganic carbon by wet chemical methods. Heat-promoted persulphate¹ and potassium permanganate oxidation in the presence of acid were employed for the generation of CO₂ from potassium phthalate and sodium oxalate (organic carbon) respectively in the DPGD unit. For inorganic carbon (sodium carbonate), HCl and persulphate were used for the on-line production of the gas. The generated CO₂ was absorbed in phenolphthalein colour forming agent. A UV/VIS spectrophotometer was used for measuring the absorbance of the phenolphthalein before and after the absorption of CO₂. The relationship between the difference in absorbance and the amount of CO₂ generated was proportional and linear over a limited range. In addition, the DPGD-FI system was interfaced to an isotope ratio mass spectrometer which was employed for the determination of the ¹³C/¹²C ratio and δ¹³C.

8.2 GENERATION OF CARBON DIOXIDE FROM ORGANIC CARBON IN DPGD-FI SYSTEM AND ITS DETERMINATION BY UV/VIS SPECTROPHOTOMETRIC METHOD (TOTAL ORGANIC CARBON (TOC) DETERMINATION)

Experimental

Reagents

All the reagents were of analytical reagent grade.

Potassium hydrogen phthalate solution(10000 ppm C)

2.125 g of potassium hydrogen phthalate (Fisons, Loughborough, UK) was dissolved in 100 ml of de-ionised water.

Potassium persulphate solution (4% w/v)

10 g of this compound (Fisons, Loughborough, UK) in 200 ml of de-ionised water in a 250 ml volumetric flask. This solution was mixed with a magnetic stirrer and then diluted to the mark with de-ionised water.

Sodium carbonate solution (0.1 M)

2.65 g of sodium carbonate (Fisons, Loughborough, UK) was dissolved in 200 ml of de-ionised water in a 250 ml volumetric flask. The volume was made up to the mark with the de-ionised water.

Sodium bicarbonate solution (0.1 M)

2.1 g of sodium bicarbonate (Fisons, Loughborough, UK) was dissolved in 250 ml of de-ionised water in a 250 ml calibrated flask.

Carbonate-Bicarbonate buffer

150 ml of 0.1 M sodium carbonate was mixed with 300 ml of 0.1 M sodium bicarbonate.

Phenolphthalein solution (1%)

1 g of phenolphthalein (BDH, Poole, UK) was dissolved in 100 ml of ethanol.

Phenolphthalein colour reagent

1.0 ml of 1% phenolphthalein solution was transferred into a 1000 ml volumetric flask containing about 800 ml de-ionised water. 15 ml of carbonate-bicarbonate buffer mixture was pipetted into the solution resulting in formation of pink colour. The volume was made up to the mark with de-ionised water.

3 M HCl

Prepared from concentrated hydrochloric acid.

Procedure

The FI system used for the generation of carbon dioxide from organic carbon is shown in Figure 8.1

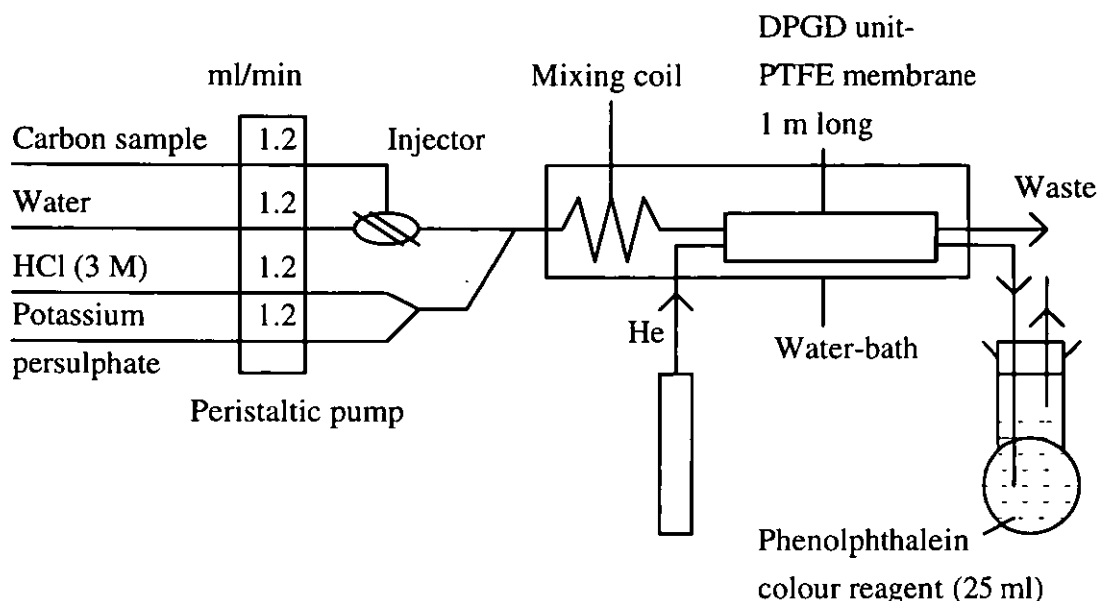


Figure 8.1 Flow injection system for generating carbon dioxide from organic carbon

The working standards of organic carbon (50–1000 ppm) were prepared from the TOC stock solution. Each standard was injected into the FI system. A fixed sample loop volume of 0.56 ml was used. The mixing coil and PTFE membrane separator were immersed in a water bath maintained at 80° C. 25 ml phenolphthalein colour reagent was used to receive the CO_2 gas for a period of 5 minutes after injection.

The absorption spectrum of the phenolphthalein colour reagent was scanned, using the UV/VIS spectrophotometer, (Unicam 8700 series, ATI Unicam, Cambridge, UK), to obtain the wavelength at which maximum absorption occurred. This was found to be 553 nm. The absorbance of the phenolphthalein colour reagent, in which CO_2 generated from each working standard was absorbed, was measured. The decrease in the absorbance of the phenolphthalein was proportional to the concentration of carbon in the sample.

Results and Discussion

A problem of irregular flow rate of the donor stream was encountered when heat promoted persulphate digestion at 80°C was used to generate CO₂ from organic carbon. The pink colour of phenolphthalein turned colourless even when only de-ionised water was injected. This indicated that the colour change of phenolphthalein was not only due to carbon dioxide, but was also possibly due to acid vapour, especially when HCl was used instead of sulphuric acid. Leakage of liquid in the FI system at the connection points also took place when heating of the mixing coil and the PTFE membrane was carried out in the water bath set at 80°C.

The problems could perhaps be overcome by using UV irradiation in the presence of an oxidising agent such as H₂O₂ to generate the carbon dioxide.

GENERATION OF CARBON DIOXIDE FROM SODIUM OXALATE

One terminal product typically found to be present after wet oxidation of organic matter, e.g. by microwave digestion, is oxalate. This was therefore chosen as a model compound for organic carbon. It is well known that oxalate is a standard for the standardisation of KMnO₄ and therefore acidified KMnO₄ was chosen as the oxidising reagent. The oxidation of oxalate by KMnO₄ occurs at a faster rate at high temperatures. A temperature of 65°C is usually employed for this reaction.

Reagents

1000 ppm C standard stock solution

Prepared by dissolving 5.583 g of sodium oxalate (analytical grade, Fisons, Loughborough, UK) in 1 litre of de-ionised water. The carbon working standards (200-800 ppm) were prepared from the stock solution.

5×10^{-2} M KMnO_4 solution

Prepared by dissolving 3.95 g of KMnO_4 in 500 ml de-ionised water.

Procedure

The FI manifold employed for generating CO_2 from sodium oxalate was similar to the one shown in Figure 8.1 except that sodium oxalate was used as the sample stream, potassium permanganate and sulphuric acid were used as the reagent streams, each flowing at 0.5 ml/min. Also, only the mixing coil was heated in the water-bath which was set at 65°C .

Sodium oxalate working standards were successively injected into the DPGD-FI system. The solutions of phenolphthalein used to trap the generated CO_2 were determined at 553 nm by the UV/VIS spectrophotometric method. The absorbance of the blank was also measured after water had been injected into the FI system.

Results and Discussion

The calibration graph, constructed using the results obtained, is presented in Figure 8.2. The slope and the y-intercept of the graph were 6.28×10^{-4} and 3.90×10^{-3} , respectively. A regression coefficient of 0.978 and a detection limit (3σ above the blank) of 127.3 ppm C were obtained.

This method can be employed for generating CO_2 from easily oxidised organic compounds and residual oxalate from wet digests. However, the method was found to be ineffective in oxidising potassium hydrogen phthalate due to the presence of the benzene ring, which is too stable to be affected by the acidified KMnO_4 .

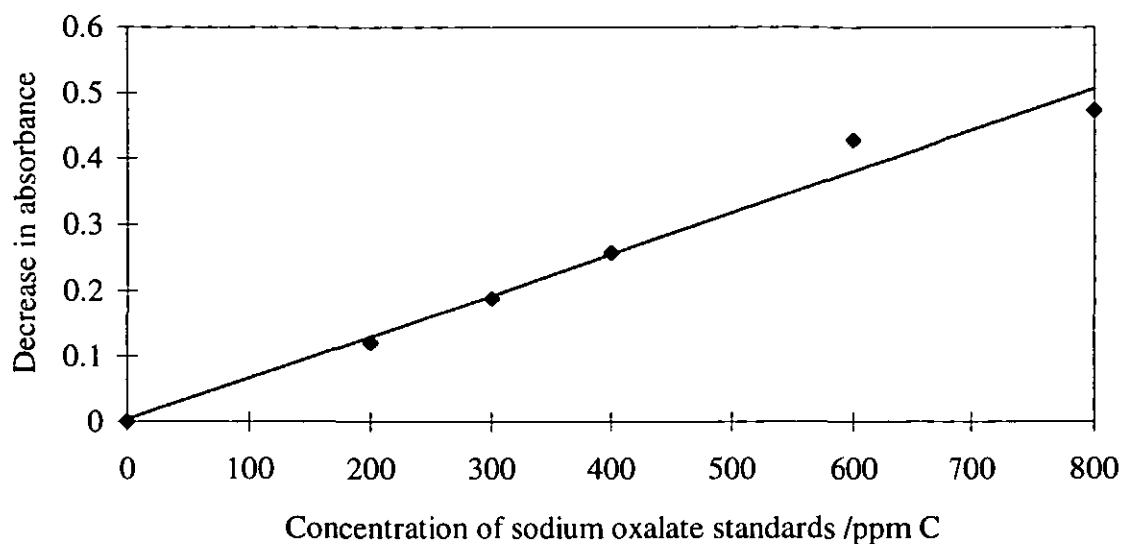


Figure 8.2 Calibration graph of decrease in absorbance of phenolphthalein due to carbon dioxide absorbed versus concentration of sodium oxalate standards.

8.3 UV/VIS SPECTROPHOTOMETRIC DETERMINATION OF TOTAL INORGANIC CARBON (TIC) AS CARBON DIOXIDE GENERATED AND SEPARATED IN DPGD-FI SYSTEM

Total inorganic carbon can be determined in a similar way to total organic carbon except that no heating is employed in the persulphate digestion (Section 8.2). Under such conditions, CO_2 is generated only from inorganic carbon and not from organic carbon which requires heat for its digestion.

Experimental

Reagents

Sodium carbonate standard stock solution (4000 ppm C) was prepared by dissolving 8.83 g of sodium carbonate in 250 ml of de-ionised water.

Phenolphthalein colour reagent, potassium persulphate and 3 M HCl were prepared as in Section 8.2.

Procedure

For the determination of total inorganic carbon by the phenolphthalein method, the water bath that had been used for total organic carbon was excluded from the FI system shown in Figure 8.1. Microporous PTFE membranes of 0.5 m and 1.0 m in length were used to separate the generated CO₂.

For calibration of the method, sodium carbonate standards (250-3000 ppm C) were prepared from the 4000 ppm C stock solution. Each standard was injected into the FI system. Carbon dioxide gas was generated and separated by the microporous PTFE membrane before being swept by helium into 25 ml phenolphthalein reagent for a period of 5 minutes. This solution was determined at 553 nm by the UV/VIS spectrophotometer. The absorbance of the phenolphthalein colour reagent which had not been used for the absorption of CO₂ was measured off-line.

Results and Discussion

The results obtained when PTFE membranes of 0.5 m and 1.0 m length were used are displayed in the calibration graphs in Figure 8.3. The detection limits (3 σ above the blank) obtained when the 0.5 and 1.0 m long PTFE membranes were employed in the DPGD unit were 579 and 408 ppm C respectively.

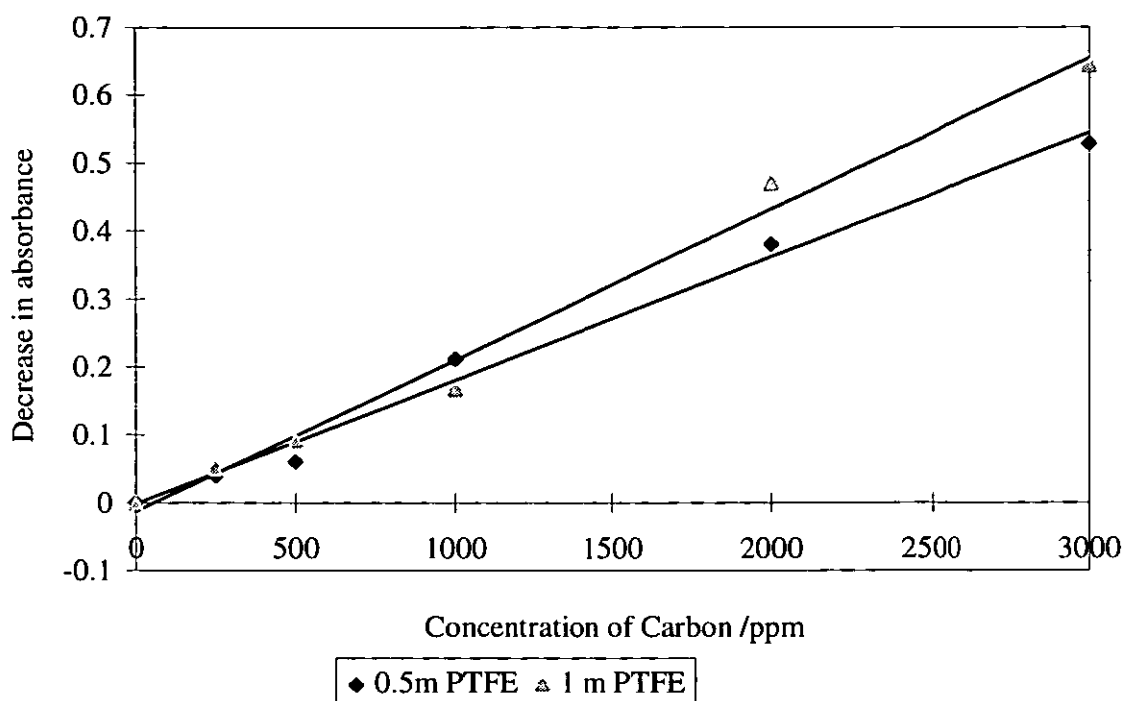


Figure 8.3 Calibration graph of difference in absorbance of phenolphthalein due to CO₂ generated in the DPGD-FI system versus concentration of inorganic carbon standards injected in the system (0.5 m and 1 m long PTFE membranes used).

A slope of $1.73 \times 10^{-4} \text{ ppm}^{-1}$; a regression coefficient of 0.980 and a y-intercept of 0.0661 were obtained when 0.5 m PTFE membrane was employed in the DPGD interface while a slope of $2.22 \times 10^{-4} \text{ ppm}^{-1}$; a y-intercept of -0.0133 and a regression coefficient of 0.989 were obtained when 1 m long PTFE membrane was used.

For further improvement of the method, de-ionised water was injected into the FI system in which the 1.0 m long PTFE membrane was used as a gas-liquid separator. This provided a more realistic blank for measuring the baseline high absorbance of the phenolphthalein and takes account of any acid vapour that might be transported with the CO₂, and dissolved CO₂. Carbon standards with concentrations ranging from 250 to 2000 ppm were injected into the FI system and the calibration procedure repeated.

The absorbance of the phenolphthalein colour reagent in the case in which de-ionised water was injected into the FI system, hence no carbon dioxide was generated, was determined by the instrument. The difference between this absorbance and the one obtained for each carbon standard injected in the FI system was due to the CO₂ generated in the system. The results obtained are displayed in the calibration graph in Figure 8.4.

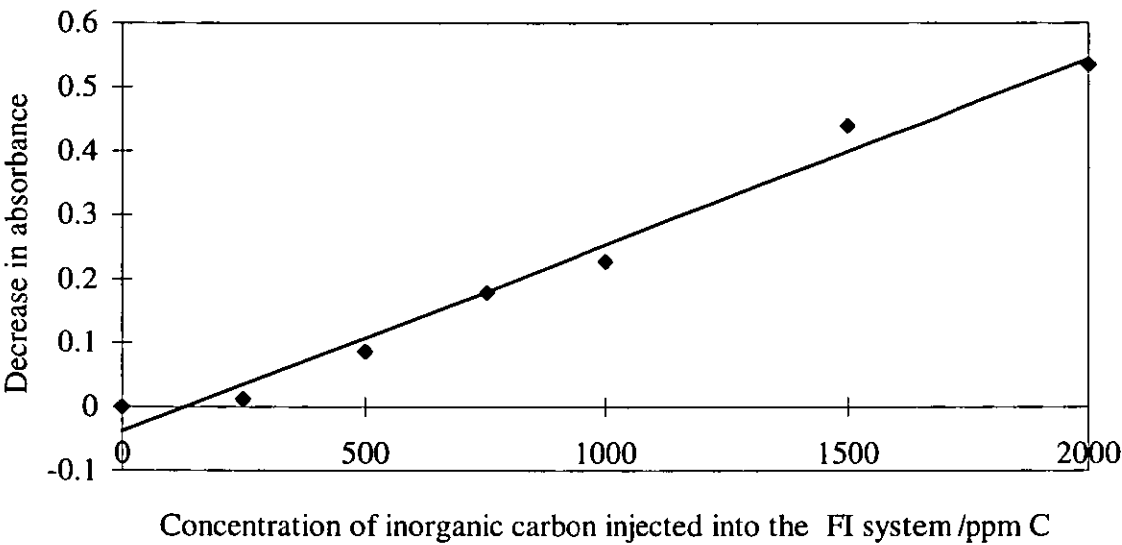


Figure 8.4 Calibration graph of difference in absorbance of phenolphthalein due to CO₂ generated in the FI system versus concentration of inorganic carbon standards injected in the system. Slope, $2.90 \times 10^{-4} \text{ ppm}^{-1}$; y-intercept, -0.039 and regression coefficient, 0.981 .

This method offered a lower detection limit of 320 ppm C (3σ above the blank).

GENERATION OF CARBON DIOXIDE FROM INORGANIC CARBON USING HYDROCHLORIC ACID

The FI system shown in Figure 8.5 was employed for the production of CO₂ by the action of HCl acid on inorganic carbon.

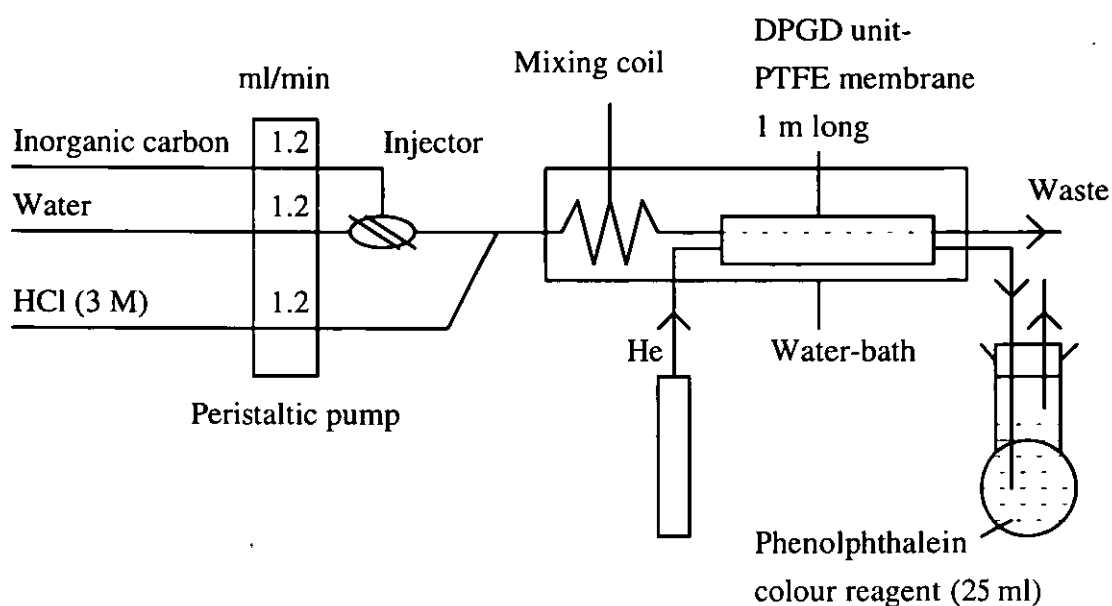


Figure 8.5 FI manifold for carbon dioxide generation from inorganic carbon using HCl.

Procedure

In this method, only HCl was used to produce CO_2 from inorganic carbon (no persulphate reagent used). Inorganic carbon (carbonate) standards of concentration ranging from 250 to 2000 ppm were injected into the FI system. The calibration procedure described previously, employing an injected water blank, was used.

Results and Discussion

The results obtained are presented in the calibration graphs shown in Figures 8.6 The detection limits (3σ above the blank) obtained was 337.6 ppm C.

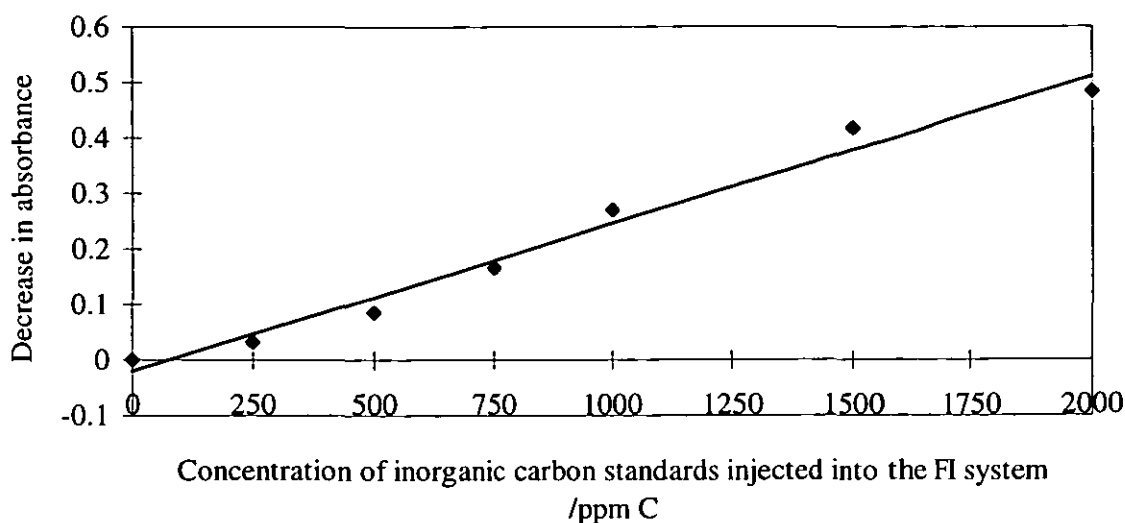


Figure 8.6 Calibration graph of absorbance of phenolphthalein due to CO_2 generated from inorganic carbon Slope, $2.65 \times 10^{-4} \text{ ppm}^{-1}$; y-intercept, -0.0196 , and regression coefficient, 0.979 .

8.4 DETERMINATION OF $^{13}\text{C}/^{12}\text{C}$ RATIO BY ISOTOPE RATIO MASS SPECTROMETRY

Measurements of $^{13}\text{C}/^{12}\text{C}$ ratios have revealed that the value obtained depends on the origin of the carbon. Since ^{13}C represents only 1 % of the total carbon present and the maximum relative variation in the $^{13}\text{C}/^{12}\text{C}$ is only 5 %, it is important that the measurements should have high precision.³ For the determination of the $^{13}\text{C}/^{12}\text{C}$ ratio, a mass spectrometer with several collectors, and standards with known $^{13}\text{C}/^{12}\text{C}$ ratio are required. Isotopic ratio determination of carbon has been applied in archaeology, geochemistry, food chemistry and medicine.

The carbon in the sample is usually converted to carbon dioxide prior to the $^{13}\text{C}/^{12}\text{C}$ ratio being determined by mass spectrometry. This may involve direct combustion of the sample or the use of wet chemical oxidation in either batch or continuous flow systems. Taking advantage of the benefits offered by FI to perform chemistries and separate the

analyte from complex matrices, a DPGD-FI system was employed in this work for generation of the carbon dioxide.

8.4.1 Apparatus for generation of carbon dioxide

The manifold used is shown in Figure 8.7.

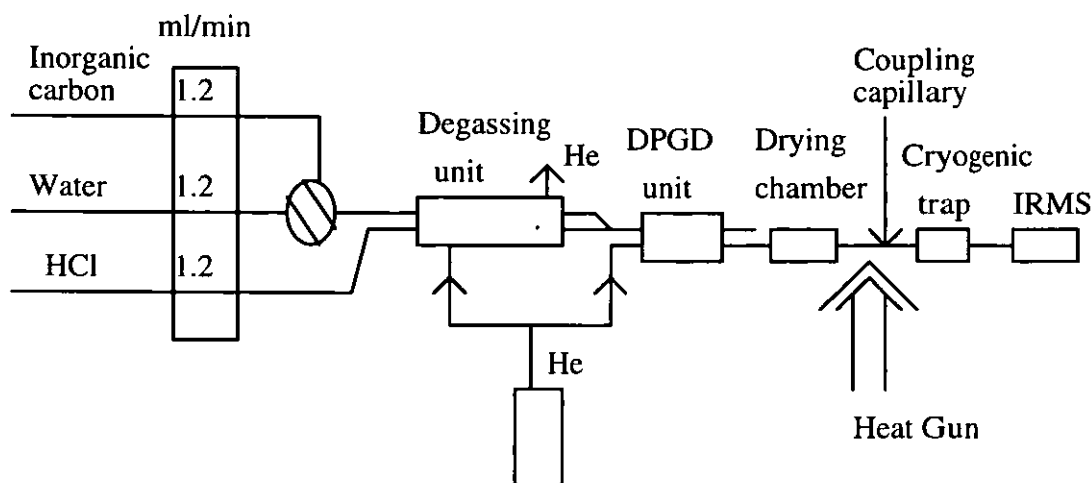


Figure 8.7 A DPGD-FI system coupled with an isotope ratio mass spectrometer (IRMS) for the generation, separation of CO₂; and determination of ¹³C/¹²C ratio.

It was found that the drying trap alone was not sufficient to remove all the water and acidic vapours from the sample carrier gas. Therefore, the interface capillary was heated with a heat gun and then a cryogenic trap was placed before the inlet to the MS to remove all but the CO₂.

8.4.2 Reagents and procedure

4000 ppm C stock solution was prepared by dissolving 8.83 g of sodium carbonate in 250 ml de-ionised water.

Working standards (5-80 ppm C) were prepared from the stock solution.

The working standards were each injected four times into the FI system and the $^{13}\text{C}/^{12}\text{C}$ ratio determined by the isotope ratio mass spectrometer (Optima, Micro Mass, UK).

8.4.3 Method of calculation

For the determination of the $^{13}\text{C}/^{12}\text{C}$ ratio, the ratio of signal intensities for molecular isotopes, $^{13}\text{C}^{16}\text{O}_2/^{12}\text{C}^{16}\text{O}_2$ (45/44) and $^{13}\text{C}^{16}\text{O}^{17}\text{O}/^{12}\text{C}^{16}\text{O}_2$, (46/44) are measured. A correction must therefore be made to convert from molecular deltas to atomic δ , this is accomplished using the Craig correction formulae⁴:

$$\delta^{13}\text{C} = 1.0676 \delta (45/44) - 0.0338 \delta^{18}\text{O} \quad (8.1)$$

and

$$\delta^{18}\text{O} = 1.0010 \delta (46/44) - 0.0021 \delta^{13}\text{C} \quad (8.2)$$

and therefore, eliminating $\delta^{18}\text{O}$ yields:

$$\delta^{13}\text{C} = 1.0677 \delta (45/44) - 0.0388 \delta (46/44) \quad (8.3)$$

$\delta^{13}\text{C}$ is also given by:

$$\delta^{13}\text{C} = 1000 \left[\frac{\left(\frac{^{13}\text{C}}{^{12}\text{C}} \right)_{\text{sample}}}{\left(\frac{^{13}\text{C}}{^{12}\text{C}} \right)_{\text{standard}}} - 1 \right] \quad (8.4)$$

where $(^{13}\text{C}/^{12}\text{C})$ is the ratio of the number of ^{13}C to ^{12}C atoms in the analyte. $\delta^{13}\text{C}$ is therefore the difference in parts per thousand between the $^{13}\text{C}/^{12}\text{C}$ ratios for the sample and standard, referred to the standard.

The Craig formula applies on the assumption that the instrument accurately measures the molecular isotopic ratios. However, mass bias, peak detection and other instrumental sources of error mean that the recorded beam intensity ratio will not accurately correspond to the expected value for a known ratio standard. A standard is therefore used, usually CO₂ gas, to calibrate the instrument response. However, such standards are always secondary standards and are referred to the international standard which is based on the published isotopic ratio of PDB (P.D. BELENITE). The instrument therefore takes as its input value for the gas standard, the atomic $\delta^{13}\text{C}$ value for the gas referred to PDB. Unfortunately for the experiments carried out here, the manufacturers were unable to provide an accurate $\delta^{13}\text{C}$ value, but suggested that -40 per mil would be a close and reasonable working assumption.

The following steps were used for calculation of the $^{13}\text{C}/^{12}\text{C}$ ratio for various samples injected into the DPGD-FI system:

- Using the Craig equation (see equation 8.1), the molecular delta 45/44 for the reference CO₂ gas was calculated by substituting $\delta^{13}\text{C} = -40$ per mil and $\delta^{18}\text{O} = -18$ per mil. The $\delta(45/44)$ for the reference CO₂ gas was found to be -36.897 per mil.
- The sample delta ($\delta 45/44$) obtained in the experiment was converted to the delta with respect to the international standard. This was done using the following formula:

$$\delta(\text{sample})_{\text{international}} = \delta(\text{sample}) + \delta(\text{reference})_{\text{international}} + \frac{\delta(\text{sample}) \times \delta(\text{reference})_{\text{international}}}{1000}$$

- The sample delta (45/44) with respect to the international standard was substituted in the Craig formula to obtain $\delta^{13}\text{C}$. It was assumed that the $\delta^{18}\text{O}$ for the sample was -18 per mil.

- The $\delta^{13}\text{C}$ value, calculated from the Craig formula, was applied to equation 8.4 using $(^{13}\text{C}/^{12}\text{C})_{\text{CO}_2 \text{ gas}} = 1.11223 \times 10^{-2}$ for the reference gas to obtain the $^{13}\text{C}/^{12}\text{C}$ ratio.

8.4.4 Results and Discussion

The mass spectra obtained are displayed in Figure 8.8 and the results extracted from these spectra are tabulated in Table 8.1. There was no significant difference among the data of atom % obtained at different concentrations of C standards injected into the DPGD-FI system, at the 95 % confidence level (see Table 8.2). A mean value of 1.0935 and RSD of 0.31 % for isotopic abundance (atom %) of ^{13}C was achieved. The mean $\delta^{13}\text{C}$ value over the whole concentration range was -5.96 per mil. The inorganic sample was not analysed on the combustion system due to lack of time. It was therefore not possible to compare the results obtained from the DPGD-FI-IRMS and IRMS/combustion systems. However, the mean $\delta^{13}\text{C}$ value obtained in this experiment was reasonable because it was slightly outside the range of -5 to + 5 per mil for inorganic carbon by only a few parts per mil.

The DPGD-FI interface coupled to MS was successfully employed for the generation, separation and subsequent detection of CO_2 for the determination of the isotopic abundance of ^{13}C (atom %), $^{13}\text{C}/^{12}\text{C}$ ratio and $\delta^{13}\text{C}$.

Table 8.1 $^{13}\text{C}/^{12}\text{C}$ ratio and $\delta^{13}\text{C}$ obtained for carbon dioxide generated in the DPGD-FI system using the isotope ratio mass spectrometer.

| Concentration ppm | $\delta(45/44)$ | International scale $\delta(45/44)$ | $\delta^{13}\text{C}$ CRAIG | $^{13}\text{C}/^{12}\text{C}$ Ratio ($\times 10^{-2}$) | Atom % |
|----------------------|-----------------|---|--------------------------------|---|--------|
| 5 | 29.05 | -8.9192 | -8.9137 | 1.1023 | 1.090 |
| 5 | 29.53 | -8.4569 | -8.4202 | 1.1029 | 1.091 |
| 5 | 30.17 | -7.8405 | -7.7621 | 1.1036 | 1.092 |
| 10 | 31.5 | -6.5596 | -6.3946 | 1.1051 | 1.093 |
| 10 | 30.61 | -7.4168 | -7.3097 | 1.1041 | 1.092 |
| 10 | 30.41 | -7.6094 | -7.5154 | 1.1039 | 1.092 |
| 10 | 31.5 | -6.5596 | -6.3946 | 1.1051 | 1.093 |
| 15 | 30.67 | -7.3590 | -7.2480 | 1.1042 | 1.092 |
| 15 | 31.75 | -6.3188 | -6.1376 | 1.1054 | 1.093 |
| 15 | 32.56 | -5.5387 | -5.3047 | 1.1063 | 1.094 |
| 20 | 36.54 | -1.7056 | -1.2124 | 1.1109 | 1.099 |
| 20 | 37.43 | -0.8484 | -0.2973 | 1.1119 | 1.100 |
| 20 | 37.45 | -0.8291 | -0.2768 | 1.1119 | 1.100 |
| 40 | 35.39 | -2.8131 | -2.3949 | 1.1096 | 1.097 |
| 40 | 34.13 | -4.0266 | -3.6904 | 1.1081 | 1.096 |
| 40 | 33.65 | -4.4889 | -4.1840 | 1.1076 | 1.095 |
| 60 | 32.7 | -5.4039 | -5.1608 | 1.1065 | 1.094 |
| 60 | 33.53 | -4.6045 | -4.3074 | 1.1074 | 1.095 |
| 60 | 31.57 | -6.4922 | -6.3226 | 1.1052 | 1.093 |
| 80 | 27.53 | -10.3831 | -10.4766 | 1.1006 | 1.089 |
| 80 | 27.43 | -10.4794 | -10.5794 | 1.1005 | 1.088 |
| 80 | 27.19 | -10.7106 | -10.8262 | 1.1002 | 1.088 |
| MEAN | | | -5.9604 | | 1.093 |
| % RSD | | | | | 0.308 |

Table 8.2 Treatment of data for atom % of ¹³C using the statistical student t test

| | | | | | | |
|---|--------------------|------------|--|--|--|--|
| Concentration (ppm C) | atom % | t-value | | | | |
| 5 | 1.091 | 0.13 | | | | |
| 10 | 1.093 | 0.04 | | | | |
| 15 | 1.093 | 0.04 | | | | |
| 20 | 1.1 | 0.26 | | | | |
| 40 | 1.096 | 0.09 | | | | |
| 60 | 1.094 | 0 | | | | |
| 80 | 1.088 | 0.26 | | | | |
| | | | | | | |
| Mean | 1.09E+00 | | | | | |
| s | 3.78E-03 | | | | | |
| n | 7 | | | | | |
| n-1 | 6 | | | | | |
| Critical t-value level | 2.45 at the 95% | confidence | | | | |
| Null hypothesis: No significant difference between the individual atom % | | | | | | |
| and the mean value of atom % (1.094) | | | | | | |
| | | | | | | |
| $t = (x-\mu)(n/s)^{0.5}$ | | | | | | |
| The null hypothesis is retained since the observed value of t is less than | | | | | | |
| the critical | value (2.45) | | | | | |

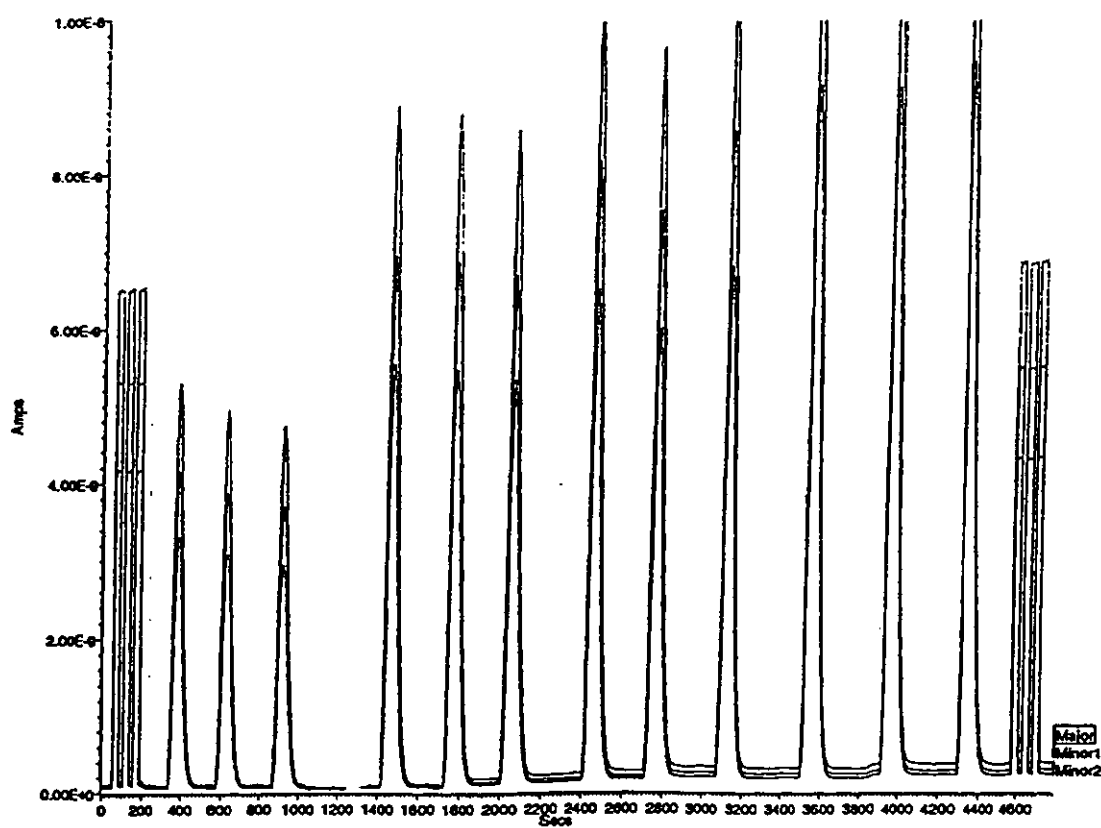


Figure 8.8 Isotopic mass spectra for carbon dioxide generated from 20, 40, 60 and 80 ppm C in the DPGD-FI system interfaced with the isotope ratio mass spectrometer

8.5 CONCLUSIONS

DPGD-FI interfaces were successfully employed for the generation of CO₂ from organic and inorganic carbon. Difficulties were encountered when an attempt to generate CO₂ from aromatic carbon (potassium hydrogen phthalate) using heat-promoted persulphate oxidation was employed. In the absence of not having a mass spectrometer, colorimetric detection was used, based on the discoloration of phenolphthalein. However, acid fumes from HCl were transported across the membrane and it was not possible to determine whether CO₂ was being generated in significant quantities. It would have been possible to investigate this further e.g. using spectroscopic techniques to look for CO₂ or residual aromatic residues in solution. However, because there was insufficient time, it was decided to use a system that was known to work. The generation of CO₂ using permanganate oxidation of aliphatic carbon (sodium oxalate) was employed. There were still some problems with background acidity, but this was compensated for by running water blanks.

For the generation of CO₂ from oxalate in the DPGD-FI system and its subsequent determination by the phenolphthalein spectrophotometric method, a detection limit of 127 ppm C (at 3 σ above the blank) was obtained. The detection limits obtained when CO₂ was generated from sodium carbonate by heat-promoted persulphate oxidation were 579 ppm C and 408 ppm C for the 0.5 m and 1.0 m long PTFE membranes respectively. A lower detection limit of 320 ppm C was achieved when the absorbance was measured (using the 1 m membrane) with respect to a water blank. A detection limit of 312 ppm C was obtained when CO₂ was produced from inorganic carbon by the action of HCl alone.

The DPGD-FI system, interfaced with IRMS, was employed for the determination of the ¹³C/¹²C ratio, abundance (atom % ¹³C) and $\delta^{13}\text{C}$ of various concentrations of inorganic carbon standards. The atom % ¹³C values obtained for various C standards injected into the DPGD-FI system were not significantly different from one another at the 95 % confidence level. In fact a mean value of 1.0935 and RSD of 0.31 % of atom % ¹³C over

the whole range of concentration was obtained. These results compare favourably with the values usually quoted for inorganic carbon. The DPGD-FI interface coupled to IRMS can therefore be used as an alternative method to IRMS/combustion system for the determination of the $^{13}\text{C}/^{12}\text{C}$ ratio, abundance (atom % ^{13}C) and $\delta^{13}\text{C}$. The use of the DPGD-FI interface allows the determination of various species of C to be determined as opposed to the use of IRMS/combustion system which does not distinguish between organic and inorganic carbon.

A dual phase degassing unit was efficiently used for the removal of dissolved gases in the carrier and reagent streams, thus reducing the background. This was shown by the small variation in $\delta^{13}\text{C}$ as the concentration of C injected in the manifold was changed. The background was therefore not contaminated with atmospheric CO_2 due to the high efficiency of the degassing unit.

REFERENCES

1. Bondarowicz, J., *Spectroscopy*, 1993, **8**, 30.
2. Technicon Industrial Method, No 455-76W/A.
3. Constantin, E. and Schnell, A., *Mass Spectrometry*, Ellis Horwood, New York, 1990, pp.61.
4. Micro Mass, Instrument Manual SIRA Series II, Manchester, U.K.

Chapter 9

CHAPTER NINE

NITROGEN CONTAINING COMPOUNDS

9.1 INTRODUCTION

A dual phase gas diffusion-flow injection (DPGD-FI) system was developed to generate N_2 from nitrogen containing compounds and to separate the generated gas from the liquid stream by the PTFE membrane. The nitrogen gas was measured with a thermal conductivity detector and a mass spectrometer for total nitrogen and the $^{15}N/^{14}N$ isotopic ratio, respectively. This work further develops the system first described by Jacob.¹

The direct coupling of the DPGD-FI system to a mass spectrometer presents several advantages. These include: the low detection limit of the mass spectrometer enabling it to detect very small amounts of volatile analytes; and the high precision attainable in isotope ratio measurements.

9.2 CONVERSION OF AMMONIUM-N COMPOUNDS TO NITROGEN

For both DPGD-FI-TCD and DPGD-FI-MS techniques, the ammonium-N compounds were converted to nitrogen by the Rittenberg method. The method is applied to ammonium ions previously formed from nitrogen containing compounds using Kjeldahl digestion. In the Rittenberg method, hypobromite solution is used to oxidise NH_4^+ to N_2 . However, hypobromite is a rather unstable compound and its full oxidising power has been reported to last for only one week, even when stored at low temperature.² This makes the reagent unsuitable for use in FI for the production of nitrogen for quantitative analysis. To overcome the problem of instability, the hypobromite reagent was generated on-line by reacting bromate/bromide with HCl to produce bromine which was in turn reacted with NaOH to produce BrO^- .¹ These reactions are shown in equations 4.7 and 4.8.

9.3 PRINCIPLES OF $^{15}\text{N}/^{14}\text{N}$ ISOTOPIC RATIO MEASUREMENT

The ^{14}N and ^{15}N atoms in the sample are paired to form nitrogen molecules, $^{14}\text{N}_2$, $^{14}\text{N}^{15}\text{N}$ and $^{15}\text{N}_2$. The mass spectrometer provides output signals which are proportional to the numbers of these three types of molecules.

The ^{15}N % abundance is given by:^{2,3}

$$\text{Atom \% } ^{15}\text{N} = \left[\frac{^{14}\text{N}^{15}\text{N} + 2 \text{ } ^{15}\text{N}_2}{2 \text{ } ^{14}\text{N}_2 + 2 \text{ } ^{14}\text{N}^{15}\text{N} + 2 \text{ } ^{15}\text{N}_2} \right] 100 \quad (9.1)$$

For atmospheric N_2 , the abundance (atom % ^{15}N) is 0.3663 ± 0.0004 . The enrichment (excess) or depletion of ^{15}N with respect to atmospheric ^{15}N is given by,

$$\text{atom \% } ^{15}\text{N} (\text{enrichment or depletion}) = [^{15}\text{N \% abundance of sample} - 0.3663] \quad (9.2)$$

In terms of mass spectrometer beam currents, i , ^{15}N % abundance is given by

$$\text{Atom \% } ^{15}\text{N} = \left[\frac{i_{29} + 2 i_{30}}{2 (i_{28} + i_{29} + i_{30})} \right] 100 \quad (9.3)$$

Small variations in ^{15}N abundance are usually measured in terms of parts per thousand difference ($\delta^{15}\text{N}$) from a reference gas, usually atmospheric nitrogen.

$$\delta \text{ } ^{15}\text{N} = \left[\frac{R_{\text{sample}} - R_{\text{reference}}}{R_{\text{reference}}} \right] 1000 \quad (9.4)$$

where R_{sample} is the $^{15}\text{N}/^{14}\text{N}$ ratio for the sample and $R_{\text{reference}}$ is the $^{15}\text{N}/^{14}\text{N}$ ratio for the reference.

$^{15}\text{N}/^{14}\text{N}$ ratio can be obtained from ^{15}N % abundance. Thus

$$\frac{^{15}\text{N}}{^{14}\text{N}} = \frac{A}{100 - A} \quad (9.5)$$

where A represents the abundance of ^{15}N in %.

9.4 THE GENERATION OF NITROGEN GAS AND ITS DETERMINATION BY THERMAL CONDUCTIVITY DETECTOR.

A flow injection system was used to generate nitrogen by a wet chemical method. This involved the reaction of hypobromite with ammonium-N to produce N_2 .

A dual phase gas diffusion unit consisting of a 1.0 m long PTFE membrane was used to separate the generated nitrogen gas from the liquid acceptor stream. The separation of nitrogen from the liquid stream also allows the gas to be directly introduced to the TCD or MS detectors.

The effect of using a degassing unit, to remove atmospheric N_2 from standards and samples, on the TCD signal was investigated.

Reagents

3.6×10^{-2} M KBrO_3 /0.2 M KBr solution was prepared by dissolving 6 g of potassium bromate and 20.5 g of sodium bromide (Fisons, Loughborough, UK) in 1 litre of de-ionised water.

2.5 M NaOH solution was prepared by dissolving 25 g of sodium hydroxide pellets (Fisons, Loughborough, UK) in 250 ml of de-ionised water.

1000 ppm N stock solution was prepared by dissolving 2.36 g of ammonium sulphate (Fisons, Loughborough, UK) in 500 ml of de-ionised water.

Working standards of concentration 10-80 ppm N were prepared from the stock solution.

9.4.1 Procedure

Degassing unit not incorporated in the FI system

The DPGD-FI system, with no degassing unit connected, used for the generation and separation of nitrogen gas, is shown in Figure 9.1.

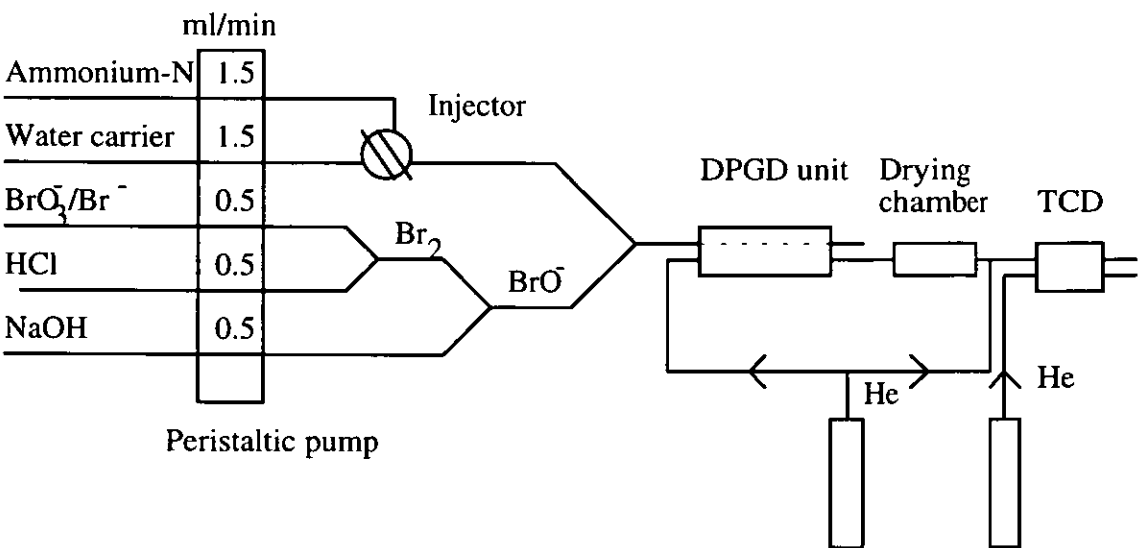


Figure 9.1 DPGD-FI system used for the generation and separation of N₂.

10 ppm N solution was injected into the FI system using an injector loop volume of 0.5 ml. The generated N₂ was separated from the donor stream using the 1.0 m long PTFE membrane and then swept to the detector by a flow of He (25 ml/min). A drying chamber containing Mg(ClO₄)₂ was used to remove water vapour. The peak height of the TCD signal was measured. The procedure was repeated for the other working standards prepared.

Degassing unit included in DPGD-FI system

The experiment was repeated with a degassing unit incorporated into the DPGD-FI system as shown in Figure 9.2.

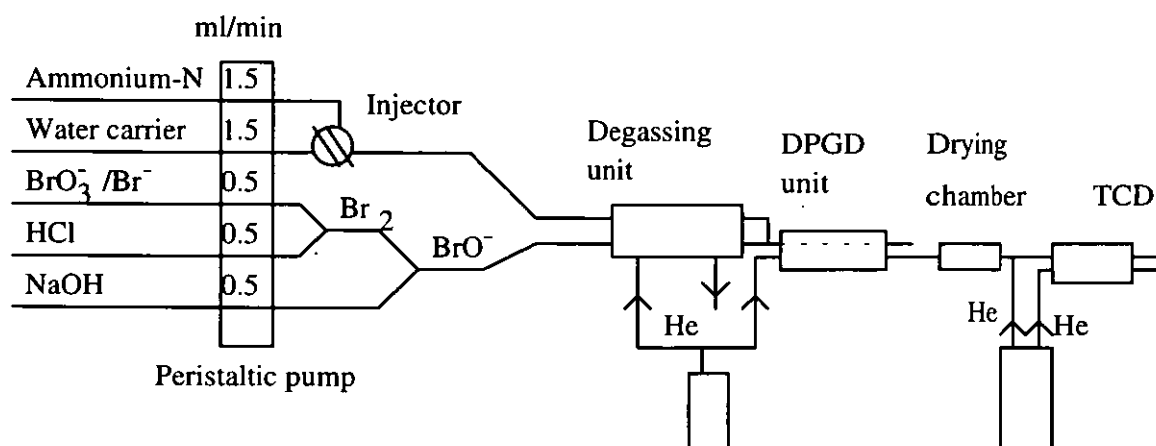


Figure 9.2 DPGD-FI system incorporating a degassing unit, for the generation and separation of N_2 .

9.4.2 Results and Discussion

The results obtained when the degassing unit was incorporated into the DPGD-FI system, and when it was excluded, are shown in the calibration graph of TCD signal (peak height) versus concentration of N_2 in Figure 9.3. For the case in which the sample and the reagents were undegassed, a slope of 0.145 cm/ppm, y-intercept of 0.208 cm and regression coefficient of 0.996 were obtained. A detection limit (3σ above the blank) of 6.0 ppm was achieved. In the case where the degassing system was included, the calibration curve obtained has a slope of 0.101, a y-intercept of 0.196 and a regression coefficient of 0.997. A detection limit of 4.8 ppm (at 3σ above the blank) was achieved. A calibration graph based on peak area measurements is shown in Figure 9.4. A detection limit of 4.5 ppm (at 3σ above the blank) was obtained.

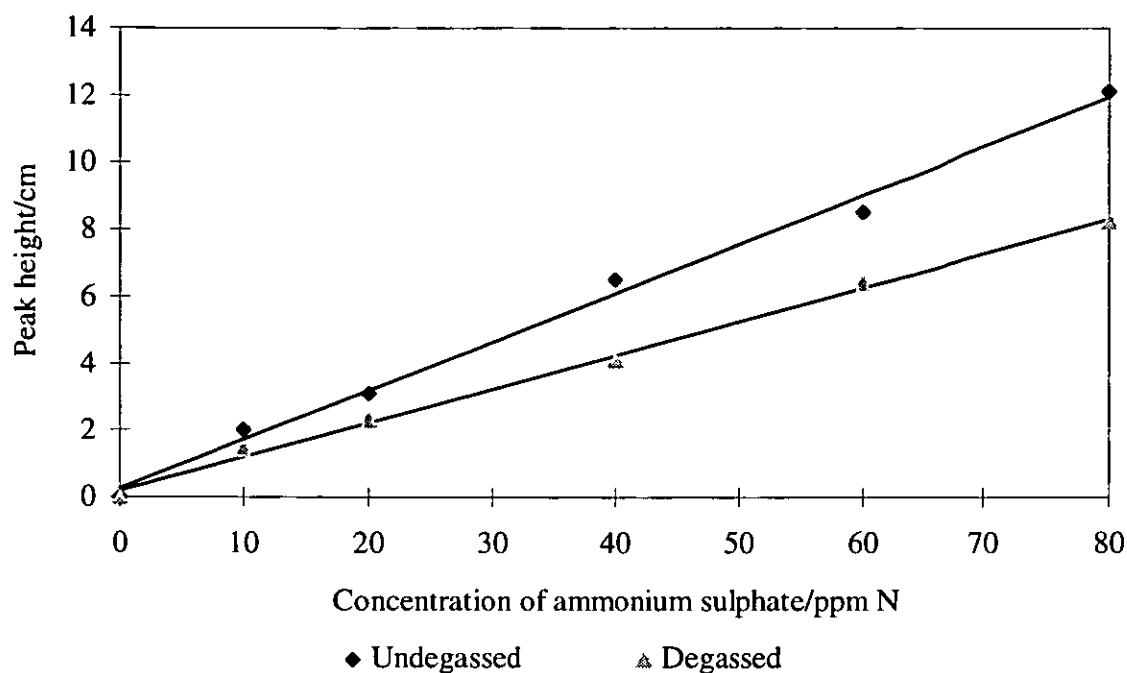


Figure 9.3 Calibration graph of peak height measurement of TCD signal against concentration of nitrogen standards injected into the DPGD-FI system.

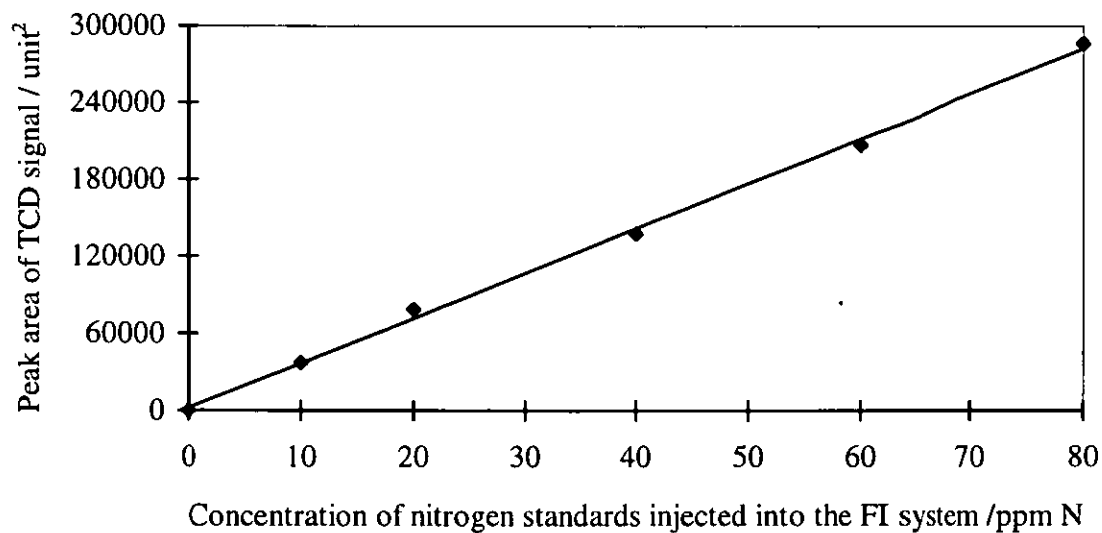


Figure 9.4 Calibration graph of peak area of TCD signal versus concentration of nitrogen injected (with degassing unit). Slope, 3503.5 unit²/ppm; y-intercept, 1975.5 units²; and regression coefficient, 0.998.

9.5 THE DETERMINATION OF $^{15}\text{N}/^{14}\text{N}$ USING THE DPGD-FI SYSTEM INTERFACED TO AN ISOTOPE RATIO MASS SPECTROMETER

The DPGD-FI system, interfaced to an isotope ratio mass spectrometer (Optima, Micro Mass, UK) is shown in Figure 9.5. The reagents and liquid flow rates were the same as described in Section 9.4. The flow rates of helium flowing to the degassing system and dual phase gas diffusion unit were 100 ml/min and 24 ml/min, respectively. A heat gun was used for heating the end of the fused silica capillary tube near the position where it was connected to the drying chamber. This was done to prevent the condensation of the vapour which could have blocked the capillary tube, thus preventing nitrogen from reaching the detector. A cryogenic trap using liquid nitrogen at -196°C was placed between the drying chamber and the detector to freeze out any gas other than nitrogen.

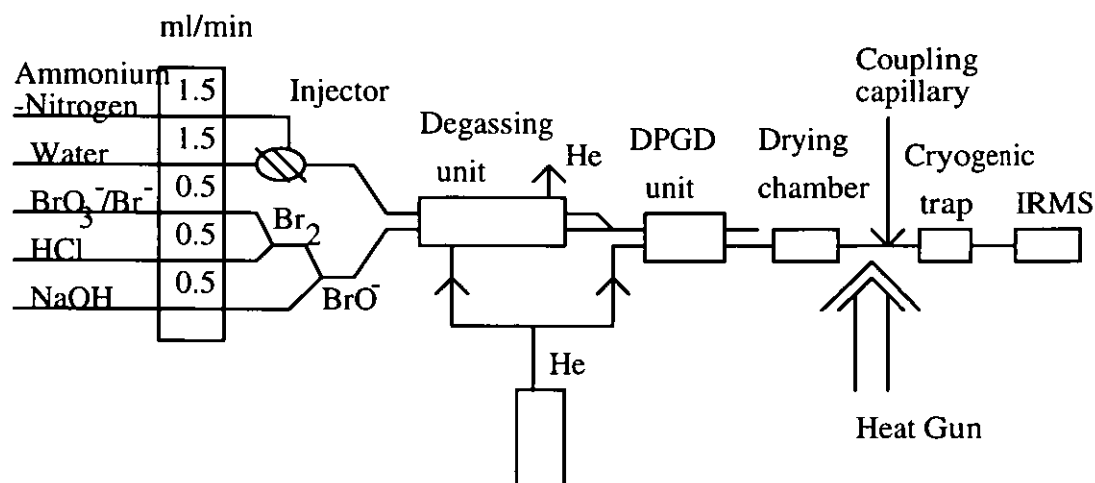


Figure 9.5 DPGD-FI system coupled to MS for $^{15}\text{N}/^{14}\text{N}$ ratio determination.

The system was checked for gas leaks and serious leaks of He were found to be occurring at the connection points. This resulted in a higher background current, due to nitrogen from the atmosphere, being recorded by the detector. In an attempt to solve this problem, the connections were tightened further, but with no significant reduction of leaks, and hence no significant change in the background current. The problem of leakage was finally overcome by replacing the PTFE tubes for delivering helium to the degassing and DPGD units with the stainless steel tubes of the same dimensions. The DPGD unit and

the drying chamber were also connected by stainless steel tubes. The final interface to the mass spectrometer was made by inserting the inlet fused silica capillary into the stainless steel tube coming from the drying unit and applying a sealant at the joint.

Measurement of the ion currents from the reference gas was made to ascertain whether the isotope mass spectrometer was working well. The total current background from the FI system when water was flowing in the manifold was 1.6×10^{-9} A. With the pump off, no water flowing, a background current of 7.11×10^{-11} A was obtained.

9.5.1 Precision of measurements by isotope ratio mass spectrometer

80 ppm N solution was injected into the DPGD-FI system and the $^{15}\text{N}/^{14}\text{N}$ isotope ratio determined. The procedure was repeated four times.

Results and Discussion

The results obtained are shown in Table 9.1

Table 9.1 Reproducibility of $\delta^{15}\text{N}$, abundance (atom %) and $^{15}\text{N}/^{14}\text{N}$ ratio obtained using isotope ratio mass spectrometer.

| Injection of 80 ppm N | $\delta^{15}\text{N}$ (reported by instrument) | Abundance (Atom %) (reported by instrument) | $^{15}\text{N}/^{14}\text{N}$ ratio (calculated) |
|-----------------------|--|---|---|
| 1st | 3.29 | 0.3675 | 3.689×10^{-3} |
| 2nd | 2.84 | 0.3673 | 3.687×10^{-3} |
| 3rd | 2.84 | 0.3674 | 3.688×10^{-3} |
| 4th | 2.89 | 0.3674 | 3.688×10^{-3} |
| 5th | 2.87 | 0.3673 | 3.687×10^{-3} |
| | MEAN 2.86 % RSD 0.86 | MEAN 0.3674 % RSD 1.6×10^{-2} | MEAN 3.688×10^{-3} % RSD 1.6×10^{-2} |

The results obtained for the first injection of 80 ppm N standard, were higher than those obtained for the subsequent injections. This may have been due to the memory effect from the previous determination. When water was then injected in triplicate into the FI system, a peak was obtained corresponding to the first injection while no peaks were obtained for the other injections. This showed that there was a memory effect from the previous injection of 80 ppm N. For this reason data from the first injection of each series of standards was discarded.

9.5.2 Calibration procedure

5-200 ppm N working standards (prepared from ammonium sulphate) were injected into the DPGD-FI system and the $^{15}\text{N}/^{14}\text{N}$ ratio determined by the IRMS.

Results and Discussion

The mass spectra of nitrogen isotopes obtained for various concentrations of ammonium sulphate injected into the FI system are shown in Figure 9.6. The results of $\delta^{15}\text{N}$, abundance (Atom %) and $^{15}\text{N}/^{14}\text{N}$ are shown in Table 9.2. As shown previously, there are a variety of methods by which isotopic ratios can be calculated and the results of using these different approaches are shown in Table 9.3. The values of a few ppm obviously correspond to low enrichment and one of the low enrichment or Craig formula gives values closest to those reported by the instrument.

Generally, there was a decrease in the experimental $\delta^{15}\text{N}$ as the concentration of the injected N sample was increased from 5 to 200 ppm N. Ideally; the $\delta^{15}\text{N}$ should not vary with the concentration of the analyte. This variation in the $\delta^{15}\text{N}$ values might have been due to the effect of nitrogen background arising from the atmospheric nitrogen which passed through the PTFE tubing employed in the FIA system, into the liquid stream containing the N sample. The effect was greater at lower concentration of the analyte. The

sample of $(\text{NH}_4)_2\text{SO}_4$ used was not analysed on the combustion system, but a previous sample from the same source had ^{15}N abundance of 0.3672 %, $^{15}\text{N}/^{14}\text{N}$ ratio of 3.6855×10^{-3} and $\delta^{15}\text{N}$ of 2.46.¹ The experimental results of ^{15}N abundance, $^{15}\text{N}/^{14}\text{N}$ ratio, and $\delta^{15}\text{N}$ obtained for various concentrations of $(\text{NH}_4)_2\text{SO}_4$ using DPGD-FI-IRMS (see Table 9.2) were very close to these values. The method can be improved by employing high quality plumbing, e.g. stainless steel tubing, to reject the atmospheric N_2 .

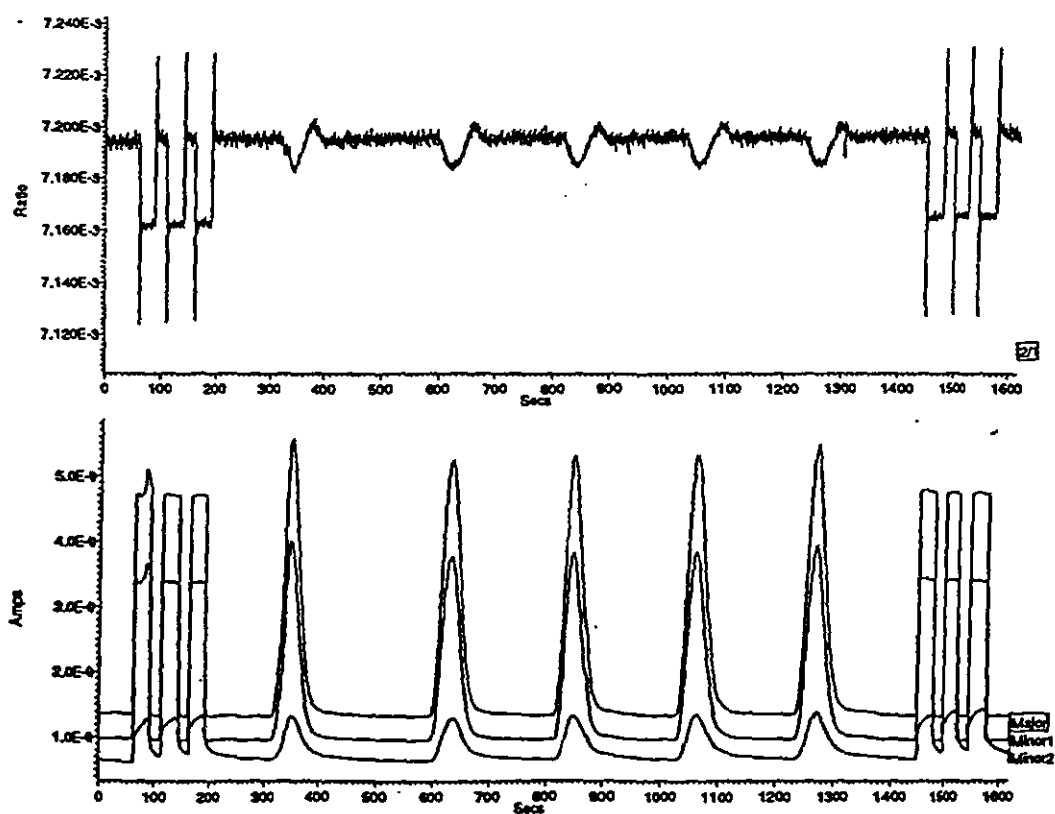


Figure 9.6 Isotopic mass spectra for nitrogen generated from 80 ppm N in the DPGD-FI interfaced with the IRMS.

Table 9.2 Experimental isotopic abundance of ^{15}N (atom %) and $\delta^{15}\text{N}$ determined by DPGD-FI-IRMS, and calculated $^{15}\text{N}/^{14}\text{N}$ ratio and $\delta^{15}\text{N}$.

| Concentration of N injected (ppm N) | Experimental abundance (Atom %) | Experimental $\delta^{15}\text{N}$ | Calculated $^{15}\text{N}/^{14}\text{N}$ Ratio* ($\times 10^{-3}$) | Calculated $\delta^{15}\text{N}$ |
|-------------------------------------|---------------------------------|------------------------------------|--|----------------------------------|
| 5 | 0.3700 | 10.23 | 3.714 | 10.14 |
| 5 | 0.3701 | 10.5 | 3.715 | 10.41 |
| 5 | 0.3700 | 10.11 | 3.714 | 10.14 |
| 5 | 0.3710 | 12.86 | 3.724 | 12.88 |
| 10 | 0.3709 | 12.7 | 3.723 | 12.60 |
| 10 | 0.3704 | 11.18 | 3.718 | 11.23 |
| 10 | 0.3705 | 11.37 | 3.719 | 11.51 |
| 10 | 0.3726 | 14.43 | 3.740 | 17.26 |
| 20 | 0.3691 | 7.59 | 3.705 | 7.67 |
| 20 | 0.3692 | 8.05 | 3.706 | 7.95 |
| 20 | 0.3694 | 8.45 | 3.708 | 8.49 |
| 20 | 0.3693 | 8.25 | 3.707 | 8.22 |
| 40 | 0.3684 | 5.8 | 3.698 | 5.75 |
| 40 | 0.3686 | 6.22 | 3.700 | 6.30 |
| 40 | 0.3685 | 6.12 | 3.699 | 6.03 |
| 40 | 0.3685 | 6.04 | 3.699 | 6.03 |
| 60 | 0.3689 | 7.17 | 3.703 | 7.12 |
| 60 | 0.3688 | 6.86 | 3.702 | 6.85 |
| 60 | 0.3686 | 6.36 | 3.700 | 6.30 |
| 60 | 0.3685 | 6.04 | 3.699 | 6.03 |
| 80 | 0.3675 | 3.29 | 3.689 | 3.29 |
| 80 | 0.3673 | 2.84 | 3.687 | 2.74 |
| 80 | 0.3674 | 2.87 | 3.688 | 3.01 |
| 80 | 0.3674 | 2.89 | 3.688 | 3.01 |
| 80 | 0.3673 | 2.87 | 3.687 | 2.74 |
| 100 | 0.3679 | 4.29 | 3.693 | 4.38 |
| 100 | 0.3683 | 5.5 | 3.697 | 5.48 |
| 100 | 0.3681 | 4.92 | 3.695 | 4.93 |
| 100 | 0.3678 | 4.17 | 3.692 | 4.11 |
| 200 | 0.3672 | 2.49 | 3.686 | 2.47 |
| 200 | 0.3672 | 2.46 | 3.686 | 2.47 |
| 200 | 0.3670 | 1.99 | 3.684 | 1.92 |
| 200 | 0.3671 | 2.14 | 3.685 | 2.19 |
| MEAN | 0.3691 | | 3.702 | |
| % RSD | 0.37 % | | 0.37 % | |

* Isotopic abundance of ^{15}N (atom %) for N_2 reference gas was assumed to be 0.3663%.

Table 9.3 Comparison of methods for calculating N isotopic abundance.

| Conc (ppm N) | Beam 29/28 | Beam 30/28 | Atom % (NC/HE) | Atom% (NC/LE) | Experimental atom% | Experimenta l $\delta^{15}\text{N}$ | Corrected $\delta^{15}\text{N}$ (Craig) |
|-----------------|---------------|---------------|-------------------|------------------|-----------------------|---|---|
| 5 | 7.25E-03 | 7.72E-04 | 0.4363 | 0.3613 | 0.37 | 10.23 | 9.46 |
| 5 | 7.26E-03 | 2.65E-04 | 0.3864 | 0.3615 | 0.3701 | 10.50 | 9.82 |
| 5 | 7.25E-03 | 7.32E-04 | 0.4324 | 0.3614 | 0.37 | 10.11 | 9.51 |
| 5 | 7.27E-03 | 8.61E-04 | 0.4462 | 0.3624 | 0.371 | 12.86 | 12.37 |
| 10 | 7.27E-03 | 7.66E-04 | 0.4367 | 0.3624 | 0.3709 | 12.70 | 12.32 |
| 10 | 7.26E-03 | 8.547E-4 | 0.4450 | 0.3619 | 0.3704 | 11.18 | 10.92 |
| 10 | 7.27E-03 | 8.72E-04 | 0.4469 | 0.3620 | 0.3705 | 11.37 | 11.20 |
| 10 | 7.29E-03 | 1.15E-04 | 0.3731 | 0.3631 | 0.3716 | 14.43 | 14.34 |
| 20 | 7.21E-03 | 1.00E-04 | 0.3677 | 0.3591 | 0.3691 | 7.59 | 6.42 |
| 20 | 7.21E-03 | 4.43E-04 | 0.4018 | 0.3593 | 0.3692 | 8.08 | 7.00 |
| 20 | 7.216E-3 | 5.92E-04 | 0.4167 | 0.3595 | 0.3694 | 8.45 | 7.54 |
| 20 | 7.22E-03 | 9.62E-04 | 0.453 | 0.3595 | 0.3693 | 8.25 | 7.49 |
| 40 | 7.20E-03 | 8.69E-04 | 0.4433 | 0.3587 | 0.3684 | 5.80 | 5.21 |
| 40 | 7.20E-03 | 8.80E-04 | 0.4446 | 0.3589 | 0.3686 | 6.22 | 5.77 |
| 40 | 7.20E-03 | 8.09E-04 | 0.4375 | 0.3589 | 0.3685 | 6.12 | 5.80 |
| 40 | 7.20E-03 | 6.67E-04 | 0.4236 | 0.3589 | 0.3685 | 6.04 | 5.87 |
| 60 | 7.17E-03 | 1.50E-03 | 0.5043 | 0.3572 | 0.3689 | 7.17 | 7.61 |
| 60 | 7.17E-03 | 1.18E-03 | 0.4727 | 0.3571 | 0.3688 | 6.86 | 7.29 |
| 60 | 7.16E-03 | 8.62E-04 | 0.4408 | 0.3569 | 0.3686 | 6.38 | 6.78 |
| 60 | 7.16E-03 | 4.79E-05 | 0.3602 | 0.3568 | 0.3685 | 6.04 | 6.39 |
| 80 | 7.19E-03 | 1.02E-03 | 0.4576 | 0.3580 | 0.3675 | 3.29 | 2.69 |
| 80 | 7.18E-03 | 1.06E-03 | 0.4613 | 0.3579 | 0.3673 | 2.84 | 2.39 |
| 80 | 7.18E-03 | 1.05E-03 | 0.4604 | 0.3579 | 0.3674 | 2.87 | 2.53 |
| 80 | 7.19E-03 | 1.08E-03 | 0.4633 | 0.3580 | 0.3674 | 2.89 | 2.65 |
| 80 | 7.19E-03 | 1.06E-03 | 0.4617 | 0.3580 | 0.3673 | 2.87 | 2.74 |
| 100 | 7.15E-03 | 4.92E-04 | 0.4035 | 0.3561 | 0.3679 | 4.29 | 4.62 |
| 100 | 7.16E-03 | 2.18E-03 | 0.5708 | 0.3565 | 0.3683 | 5.50 | 5.71 |
| 100 | 7.15E-03 | 1.24E-03 | 0.4773 | 0.3563 | 0.3681 | 4.92 | 5.10 |
| 100 | 7.15E-03 | 6.10E-04 | 0.4151 | 0.3560 | 0.3678 | 4.17 | 4.31 |
| 200 | 1.17E-04 | 1.38E-03 | 0.1440 | 0.0059 | 0.3672 | 2.49 | 4.54 |
| 200 | 7.11E-03 | 1.46E-03 | 0.4977 | 0.3544 | 0.3672 | 2.46 | 3.97 |
| 200 | 7.11E-03 | 1.30E-03 | 0.4809 | 0.3541 | 0.367 | 1.99 | 3.01 |
| 200 | 7.10E-03 | 1.07E-03 | 0.4586 | 0.3540 | 0.3671 | 2.14 | 2.72 |

Atom % (NC/HE) = Atom % using nitrogen correction for high enrichment

Atom % = $(R_{29}+R_{30}) \times 100 / (2(1+R_{29}+R_{30}))$

Atom % (NC/LE = Atom % using nitrogen correction for low enrichment

Atom % = $(R_{29} \times 100) / (2+R_{29})$

9.5.3 Isotopic enrichment/depletion

$^{15}\text{N}/^{14}\text{N}$ ratio for solutions made up of natural and depleted ammonium sulphate.

Reagents

347.88 ppm N stock solution was prepared by dissolving 0.164 g of ammonium sulphate (natural abundance = 0.3672 %) in 100 ml de-ionised water.

114.33 ppm N was prepared by dissolving 0.0539 g of the depleted ammonium sulphate (abundance = 0.2 %) in 100 ml de-ionised water.

Working standards for isotopic ratio determinations were prepared by mixing known volumes of the natural and depleted ammonium sulphate stock solutions as shown in Table 9.3.

Procedure

The working standards were injected into the DPGD-FI-MS system and the isotope ratio measurements performed using the isotope ratio mass spectrometer.

Results and Discussion

The results obtained and the calculated $\delta^{15}\text{N}$ are tabulated in Table 9.3. A regression plot of the experimental $\delta^{15}\text{N}$ against the expected (calculated) $\delta^{15}\text{N}$ is presented in Figure 9.7. The graph has a slope of 1.029, a y-intercept of 8.598 parts per thousand and a regression coefficient of 0.999.

Table 9.3 Isotopic ratio standard preparation, experimental atom % and $\delta^{15}\text{N}$; and calculated $\delta^{15}\text{N}$.

| volume of 347.88 ppm N (atom % = 0.3672) (ml) | Volume of 114.33 ppm N (atom %= 0.2) (ml) | Total volume after dilution (ml) | Experime- ntal abundance (Atom %) | Experime ntal $^{15}\text{N}/^{14}\text{N}$ Ratio ($\times 10^{-3}$) | Experime- ntal $\delta^{15}\text{N}$ | Calculated $\delta^{15}\text{N}$ from known abundance |
|--|---|--|--|--|---|--|
| 10 | 0 | 100 | 0.3702 | 3.7158 | 10.62 | 2.46 |
| | | | 0.3701 | 3.7147 | 10.54 | |
| | | | 0.3702 | 3.7158 | 10.58 | |
| | | | 0.3701 | 3.7147 | 10.52 | |
| 9 | 1 | 100 | 0.3641 | 3.6543 | -5.93 | -13.70 |
| | | | 0.3639 | 3.6523 | -6.59 | |
| | | | 0.3643 | 3.6563 | -5.60 | |
| | | | 0.3640 | 3.6533 | -6.30 | |
| 8 | 2 | 100 | 0.3574 | 3.5868 | -24.47 | -32.33 |
| | | | 0.3576 | 3.5888 | -23.74 | |
| | | | 0.3578 | 3.5908 | -23.17 | |
| 7 | 3 | 100 | 0.3492 | 3.5042 | -46.74 | -53.96 |
| | | | 0.3499 | 3.5113 | -44.93 | |
| | | | 0.3496 | 3.5083 | -45.84 | |
| | | | 0.3505 | 3.5173 | -43.39 | |
| 6 | 4 | 100 | 0.3397 | 3.4086 | -74.76 | -79.71 |
| | | | 0.3398 | 3.4096 | -72.71 | |
| | | | 0.3391 | 3.4025 | -74.61 | |
| | | | 0.3381 | 3.3925 | -77.29 | |

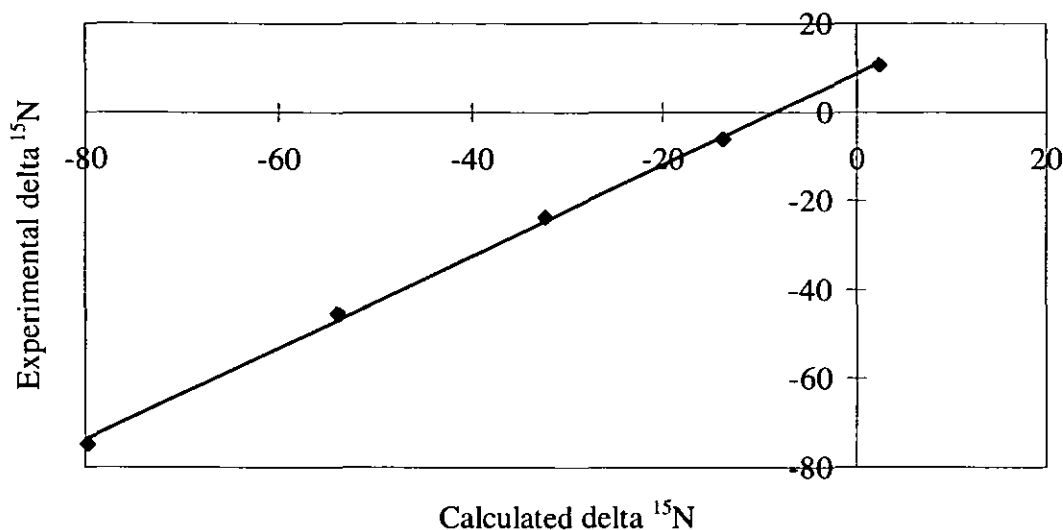


Figure 9.7 A graph showing a comparison between experimental and calculated $\delta^{15}\text{N}$. A degassing system, incorporated in the DPGD-FIA system, was employed for degassing the reagent and the sample streams.

A perfect correlation between the experimental and calculated $\delta^{15}\text{N}$ value was obtained. The regression line, however, did not pass through the origin but this showed a bias of only 8.6 parts per thousand. This might have been due to the background due to atmospheric N_2 which passed through the PTFE tubing for the FIA system into the liquid stream containing the analyte. As indicated previously, the method could be improved by employing a very high quality plumbing to reject the atmospheric N_2 .

9.6 CONCLUSIONS

The DPGD-FI system was employed for the generation of nitrogen from nitrogen containing compounds by using hypobromite generated on-line. A thermal conductivity detector was used for the detection of the generated nitrogen. A comparison was made between the DPGD-FI system in which the degassing system was included and the one in which it was excluded. The DPGD interface employed for the separation of nitrogen from the liquid donor stream consisted of 1 m long PTFE membrane. The detection limit

obtained when the dual phase PTFE membrane degassing unit was incorporated into the DPGD-FIA system was 4.8 ppm N while that obtained without the inclusion of the degassing unit was 6 ppm N (at 3 σ above the blank). However, a higher sensitivity was obtained when the dual phase PTFE membrane degassing unit was not incorporated into the DPGD-FI system. This was due to the fact dissolved gases in the reagent and carrier streams contributed to the enhanced signal from the TCD.

The $^{15}\text{N}/^{14}\text{N}$ ratio, abundance (atom %) ^{15}N , and $\delta^{15}\text{N}$ for nitrogen standard solutions were determined by DPGD-FI interfaces coupled to IRMS. The results of $^{15}\text{N}/^{14}\text{N}$ ratio, abundance (atom %) ^{15}N , and $\delta^{15}\text{N}$ obtained for nitrogen standards injected into the DPGD-FIA system compared favourably with those reported for a previous sample from the same source.¹

Different methods of calculation of isotopic ratios were used. These are low enrichment, high enrichment and Craig correction formulae. The results obtained using low enrichment and Craig correction formula were closest to those reported by the combustion technique. The data for $\delta^{15}\text{N}$ obtained for various N standards injected into the DPGD-FI system appeared to decrease with increase in concentration of N. Under ideal conditions, the $\delta^{15}\text{N}$ should be independent of the concentration of N injected into the manifold. The variation of $\delta^{15}\text{N}$ might have been due to the background contamination. Although the degassing system was employed for the removal of dissolved N_2 in the liquid streams, some atmospheric N_2 might have entered the manifold through the PTFE tubings which were extensively used as connection tubes. The data for $\delta^{15}\text{N}$ was good at high concentration, but poor at low concentration because of the background contamination.

REFERENCES

1. Jacob S. C, *Studies of a Microporous Membrane for Analyte Preconcentration and Separation*, PhD Thesis, Loughborough University, UK, 1994.
2. Fieldler, R. and Proksch G., *Anal. Chim. Acta.*, 1975, **78**, 1.
3. Robinson, D. and Smith, K. A., in *Soil Analysis-Modern Instrumental Techniques*, Ed. Smith, K. A., Marcel Dekker, 2nd. Edn., New York, 1991, pp 465-503.

Chapter 10

CHAPTER TEN

DETERMINATION OF HALIDES

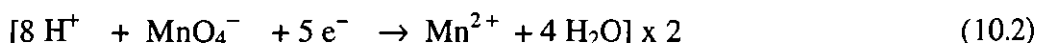
10.1 INTRODUCTION

The versatility of the FI system as a powerful analytical tool for carrying out chemical reactions was demonstrated by using the system for the generation of bromine and chlorine from liquid samples of bromide and chloride, respectively. FI systems were developed for the generation of these gases employing potassium permanganate (oxidant) and sulphuric acid as the reagent streams. A DPGD unit, consisting of microporous PTFE membrane, was used to separate the gases from the liquid donor stream. The ultimate aim was to interface the DPGD-FI system with MS, but due to lack of an isotope ratio mass spectrometer in our laboratory, the generated halogens were determined by UV/VIS spectrophotometry. The gases were swept by helium into various colour forming reagents prior to their determinations by the UV/VIS spectrophotometric methods. The reagents used were phenol red,^{1,2} N-N-dimethy-*p*-phenylenediamine sulphate and phenolphthalein.

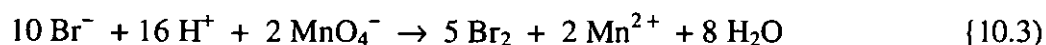
10.2 GENERATION OF BROMINE IN THE FI SYSTEM AND ITS DETERMINATION BY SPECTROPHOTOMETRIC METHODS AFTER PTFE MEMBRANE SEPARATION.

10.2.1 PHENOLPHTHALEIN METHOD

The generation of bromine using MnO_4^- and H_2SO_4 takes place according to the following equations:



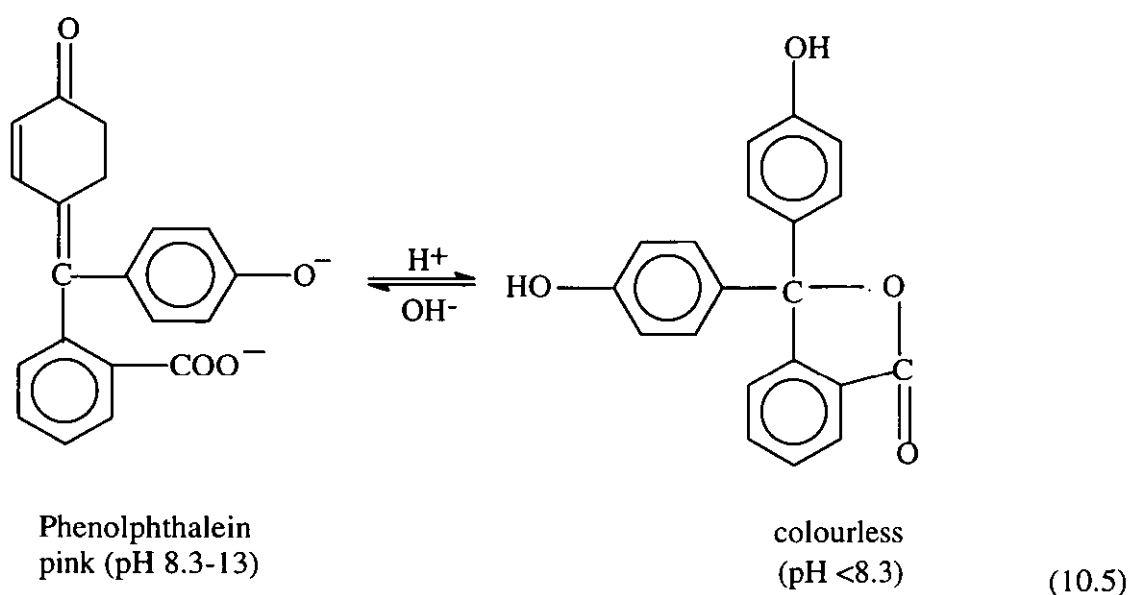
giving an overall reaction



Bromine reacts with water according to the equation:³



Phenolphthalein indicator then reacts with H^+ as shown in the equation below.



The phenolphthalein method is based on the decoloration of phenolphthalein indicator by bromine. The decrease in absorbance of phenolphthalein due to absorption of the generated bromine was used as the basis for determining the concentration of bromide.

Experimental

Reagents

All chemicals were of analytical grade.

Bromide standard stock solution (10000 ppm Br⁻) was prepared by dissolving 3.723 g of potassium bromide (Fisons, Loughborough, UK) in 250 ml of de-ionised water.

Potassium permanganate solution (10⁻² M) was prepared by dissolving 1.58 g of KMnO₄ (Spectrosol grade, BDH, Poole, UK) in 1 litre of de-ionised water.

Sulphuric acid (3 M) was prepared by diluting 40.8 ml of concentrated sulphuric acid in a 250 ml volumetric flask with de-ionised water.

Phenolphthalein colour reagent (BDH, Poole, UK) was prepared as described in Section 8.2.

Procedure

Working bromide standards (1000-10000 ppm Br⁻) were prepared by dilution of appropriate volumes of bromide stock solution. Each bromide standard was injected into the FI system shown in Figure 10.1.

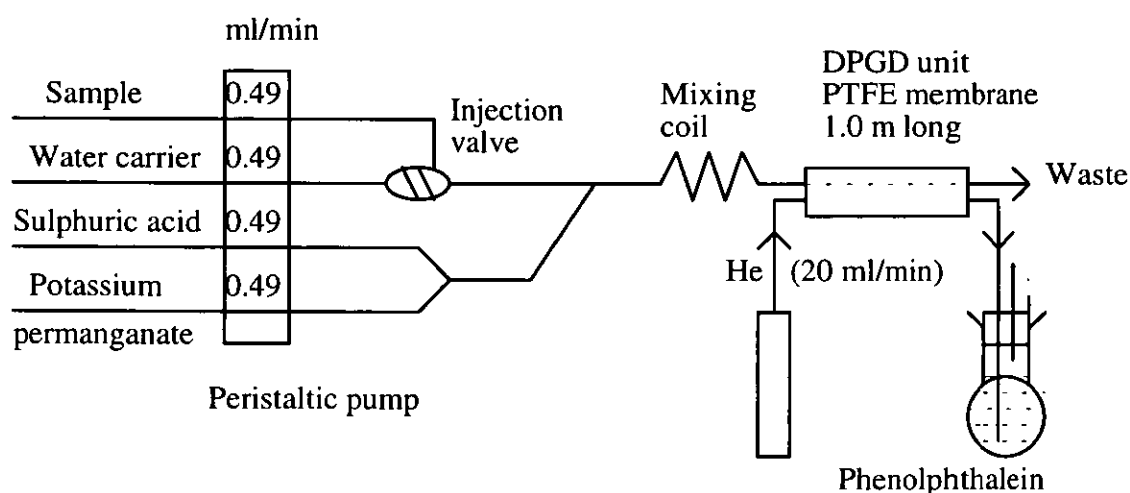


Figure 10.1 FI system for generating bromine from bromide

The generated gas was received in 25 ml phenolphthalein colour reagent after PTFE membrane separation. The absorbance of the resultant solution was determined by a UV/VIS spectrophotometer, (Unicam 8700 series, ATI Unicam, Cambridge, UK). When bromine was swept by helium into phenolphthalein colour reagent, the pink colour of the indicator

faded. This was marked by a decrease in absorbance when it was run in the UV/VIS spectrophotometer.

Results and Discussion

The results obtained are presented in Figure 10.2.

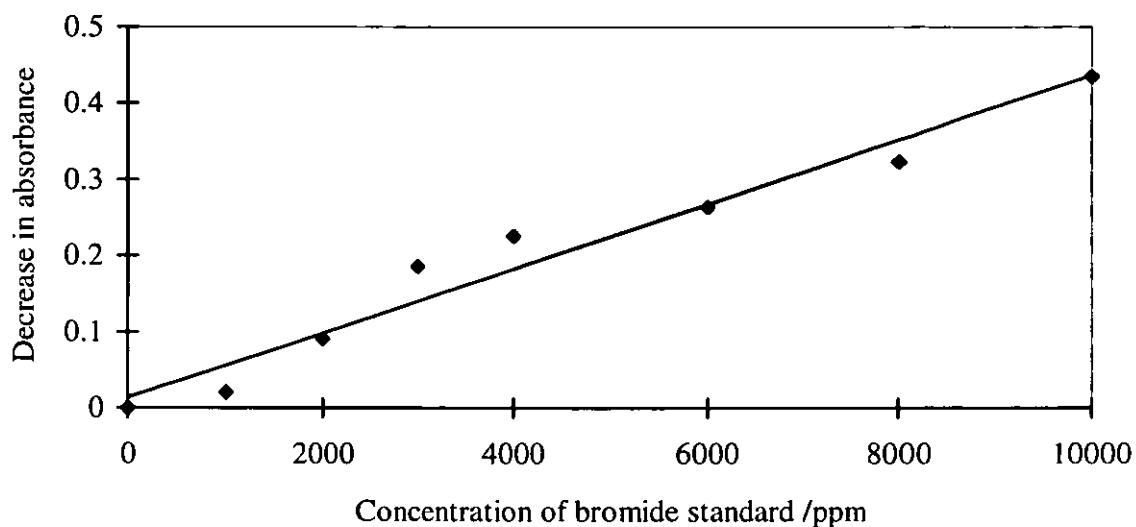
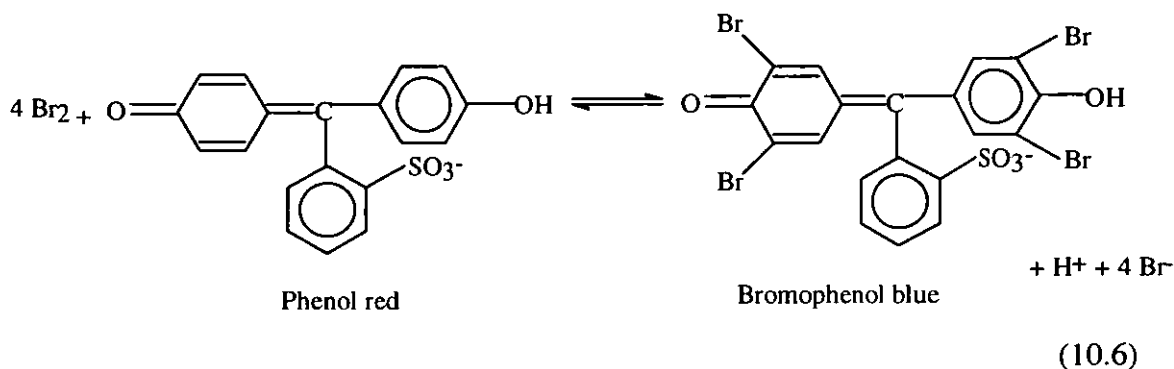


Figure 10.2 Calibration graph of decrease in absorbance of phenolphthalein due to absorption of bromine against concentration of bromide standards. Slope, $4.25 \times 10^{-5}/\text{ppm}$; y-intercept, 1.37×10^{-2} ; and regression coefficient, 0.960.

The spectrophotometric method using phenolphthalein as colour forming reagent has been used for the determination of carbon dioxide in Chapter 8. The method was applied to the determination of bromine generated in the FI system. A linear graph was obtained for concentrations of 1000-10000 ppm Br^- standards. A detection limit of 2385 ppm Br^- (3σ above the blank) was achieved. Because of lack of time, there was no opportunity to attempt to improve the quality of the calibration graph. However, it is unlikely that this would have improved the limit of detection which is rather high for this method.

10.2.2 PHENOL RED METHOD

The generated bromine was determined by a spectrophotometric method based on electrophilic substitution of the gas on phenol red to produce bromophenol blue.⁶ This reaction is represented by:



Experimental

Reagents

Bromide stock solution (8000 ppm Br^-) was prepared by dissolving 2.98 g of potassium bromide in 250 ml of de-ionised water.

Working bromide standards (100-8000 ppm Br^-) were prepared by diluting appropriate volume of bromide stock solution with de-ionised water.

Potassium permanganate solution (0.33 M) was prepared by dissolving 13 g of potassium permanganate in 250 ml of de-ionised water.

Sulphuric acid (3 M).

Phenol red stock solution was prepared by dissolving 2 g of phenol red (Fisons, Loughborough, UK) in 100 ml ethanol.

Dilute phenol red solution was prepared by transferring 1 ml of phenol red stock solution into a 100 ml calibrated flask and adding sodium acetate/acetic acid buffer (pH 5.3) up to the mark.

Procedure

Each bromide working standard was injected into the FI manifold which was similar to that shown in Figure 10.1 except that phenolphthalein was substituted with dilute phenol red solution. After the generated bromine had been separated by the PTFE membrane (1 m long), it was swept by the helium acceptor stream (flow rate of 10.9 ml/min), for 7 minutes, into a solution of 10 ml of dilute phenol red in a 10 ml calibrated flask. The solutions were run on the UV/VIS spectrophotometer at 592 nm.

Results and Discussion

A calibration graph of absorbance versus concentration of bromide drawn is shown in Figure 10.3. The method offered a detection limit of 242 ppm Br^- (3σ above the blank).

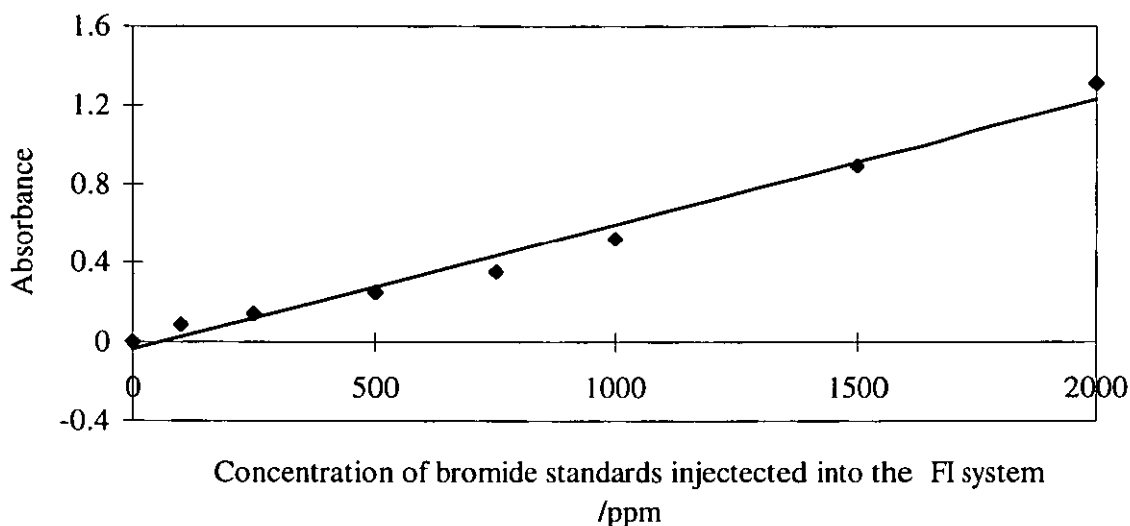


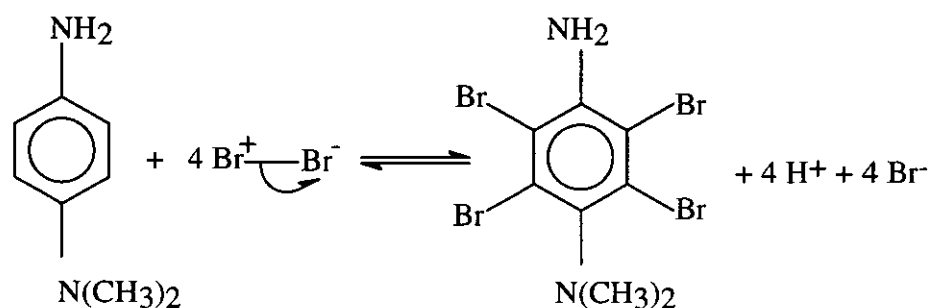
Figure 10.3 Calibration graph of absorbance of bromophenol compound derived from bromine against concentration of bromide injected into the FI system. Slope, $6.32 \times 10^{-4}/\text{ppm}$; y-intercept, -0.0369 , and regression coefficient, 0.981 .

The phenol red method was found to be a more sensitive reagent than phenolphthalein for the generation of bromine. Chlorine has been reported to interfere with the determination of bromine using phenol method. It was, however, found that no response was obtained when

2000 ppm of chloride was injected into the same FI system, an indication that no significant chlorine gas was generated, hence no absorbance obtained. When a higher concentration of chloride was used (10000 ppm), the absorbance change due to presence of chlorine became significant.

10.2.3 *N,N*, DIMETHYL-*p*-PHENYLENYLENEDIAMINE SULPHATE METHOD

The reaction of bromine with *N,N*-dimethyl-*p*-phenylenediamine (bromination) is an electrophilic substitution reaction and this occurs according to the following reaction:



(10.7)

Experimental

Reagents

3 M H_2SO_4 and 0.33 M KMnO_4 were prepared as in Section 10.2.2.

N,N-dimethyl-*p*-phenylenediamine sulphate solution was prepared by adding 0.1 g of *N,N*-dimethyl-*p*-phenylenediamine sulphate (Fluka, Dorset, UK) to 1 ml of 3 M H_2SO_4 acid in a 100 ml volumetric flask, and making up the volume to the mark with de-ionised water.

8000 ppm Br^- stock solution (Fisons, Loughborough, UK) was prepared as in Section 10.2.2.

Working bromide standards (100-1000 ppm Br^-) were prepared by diluting appropriate volumes of 8000 ppm of bromide stock solution with de-ionised water.

Procedure

Working standards were each injected into the FI manifold similar to that shown in Figure 10.1, except that phenolphthalein was substituted with N,N-dimethyl-*p*-phenylenediamine sulphate. The generated bromine gas was separated by the gas-liquid separator in which the PTFE membrane (1 m long) was used. The membrane allowed the bromine gas to diffuse into the helium acceptor stream (flow rate 10.9 ml/min) which swept the gas into 10 ml N,N-dimethyl-*p*-phenylenediamine sulphate. The resultant solution was run on the UV/VIS spectrophotometer at 552.4 nm (maximum absorption wavelength obtained by scanning the absorption spectrum)

Results and Discussion

The results obtained were used to construct the calibration graph shown in Figure 10.4.

The detection limit (3σ above the blank) obtained by this method was 68 ppm Br^- .

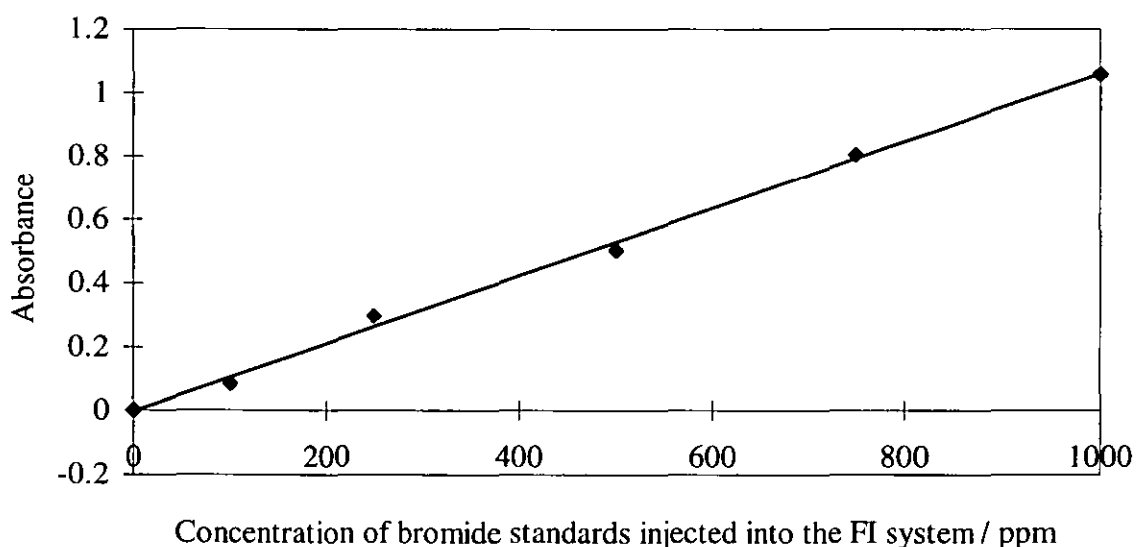


Figure 10.4 Calibration graph of absorbance of complex formed from bromine and N,N-dimethyl-*p*-phenylenediamine sulphate against concentration of the injected bromide standards. Slope, $1.062 \times 10^{-3}/\text{ppm}$; y-intercept, -3.21×10^{-3} ; and regression coefficient, 0.997.

The method was more sensitive than either phenolphthalein or phenol red methods for the determination of the generated bromine gas.

10.3 SEPARATION EFFICIENCY OF PTFE MEMBRANE (1 M LONG) FOR BROMINE GENERATED IN THE FIA SYSTEM.

Procedure

Calibration outside the FIA system (off-line)

Bromide working standards (8-40 ppm Br^-) were used to generate bromine as shown in Figure 10.5.

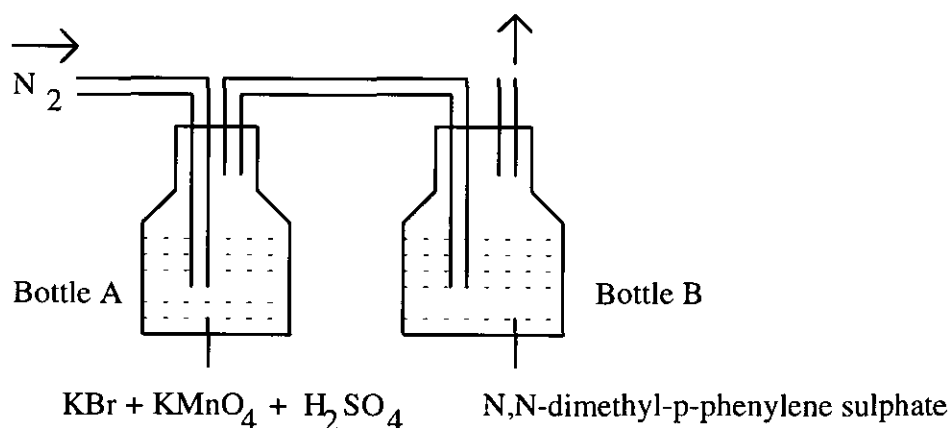


Figure 10.5 Generation of bromine outside FI system

Each standard (100 ml) was transferred, one at a time, into bottle A to which 25 ml of 3 M H_2SO_4 and 25 ml of 0.33 M KMnO_4 solution were added. 100 ml of $\text{N,N-dimethyl-p-phenylenediamine sulphate}$ was transferred into the bottle B. The bottles were immediately closed. Nitrogen gas was passed into the solution containing the bromide sample (bottle A). After 4 minutes, the solution in the bottle B was determined by the UV/VIS spectrophotometer. The procedure was repeated for all the working standards.

determination of sample

4000 ppm of bromide (stock solution) was injected into the FI system shown in Figure 10.6.

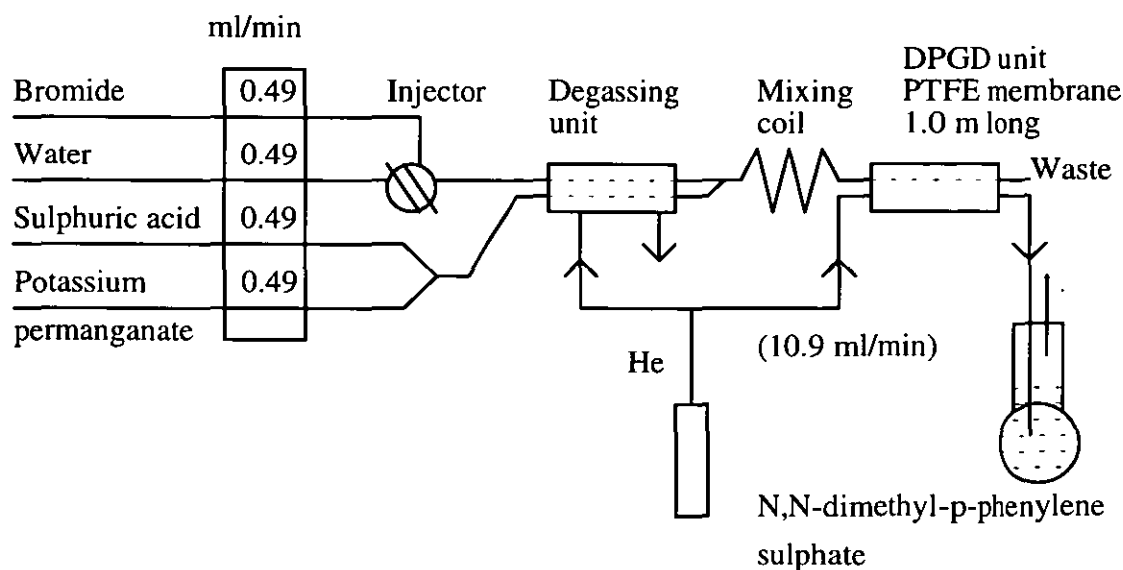


Figure 10.6 FI system for generating bromine

Bromine was generated in the system and was separated by PTFE membrane (1 m long). Thus the generated gas diffused through the membrane from liquid donor stream into the gas acceptor stream (He). Bromine gas was swept by the He stream into 100 ml of N,N-dimethyl-*p*-phenylenediamine sulphate for a period of 9 minutes from the time of injection. The colour of the resultant solution began to turn reddish after 5 minutes. The final solution was run in the UV/VIS spectrophotometer.

Results and Discussion

From the calibration graph (Figure 10.7) the concentration of bromide in the sample was obtained by interpolation. The limit of detection obtained by this method, involving the off-line production of bromine from bromide, was 9.2 ppm Br⁻.

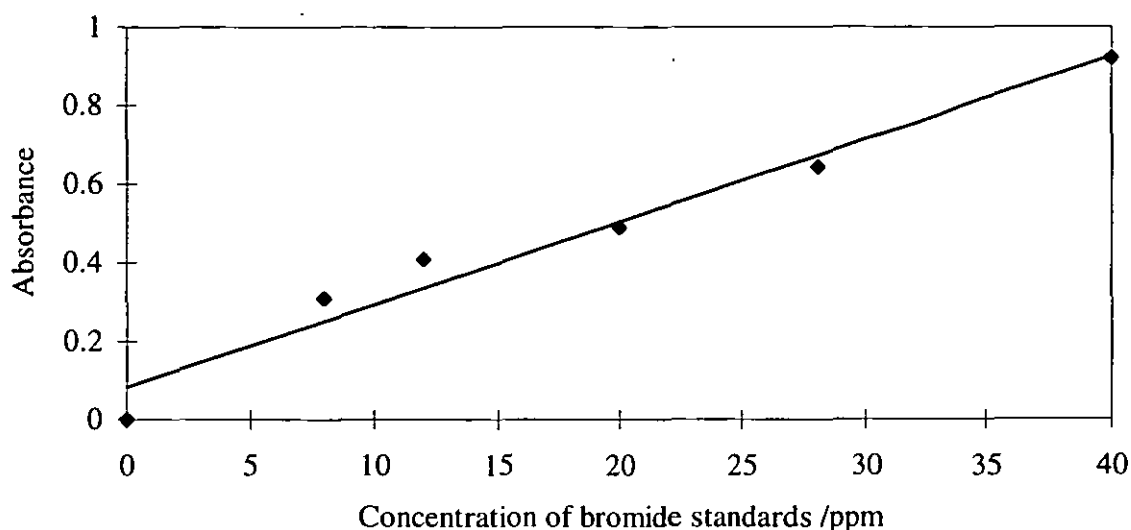


Figure 10.7 Calibration graph of absorbance of complex formed in the reaction of bromine and N,N-dimethyl-*p*-phenylenediamine sulphate against concentration of bromide standards used for generating bromine. Slope, 0.0211 ppm⁻¹; y-intercept, 0.0818, and regression coefficient, 0.966.

Table 10.1 Separation efficiency of the PTFE membrane for bromine.

| Sample injected (bromide) | Absorbance | Concentration from calibration graph (ppm) | Calculated amount of Br ⁻ (µg/ml) | Separation Efficiency (%) |
|---------------------------|------------|--|--|---------------------------|
| 4000 ppm | 0.479 | 18.83 | 20.0 | 94.2 |

The separation efficiency obtained was very high (94.2 %), certainly higher than that obtained for other gases. This may have been due to the erroneous assumption that almost all the generated bromine was absorbed in the N,N-dimethyl-*p*-phenylenediamine sulphate. Some of the gas may have escaped through the outlet in the bottle B, resulting in a low absorbance value for the calibration solution.

10.4 GENERATION OF CHLORINE IN THE DPGD-FI SYSTEM AND ITS DETERMINATION BY A SPECTROPHOTOMETRIC METHOD

10.4.1 PHENOLPHTHALEIN METHOD

The passage of chlorine into the phenolphthalein colour reagent caused the solution to be decolorised. The decrease in absorbance of phenolphthalein due to the absorption of chlorine was the basis for the determination of the concentration of chloride.

Experimental

Reagents

Potassium permanganate (0.33 M) and 3 M H₂SO₄ were prepared as in Section 10.2.2.

Potassium chloride solution (10000 ppm Cl⁻) was prepared by dissolving 10.495 g of potassium chloride (Fisons, Loughborough, UK) in 500 ml of de-ionised water.

Procedure

The FI system used was the same as that shown in Figure 10.1. 4000 ppm and 10000 ppm of chloride were each injected into the FI system to generate chlorine. The gas was passed through phenolphthalein colour reagent and the solution finally determined by the UV/VIS spectrophotometer

Results and Discussion

The pink colour of phenolphthalein faded when 4000 ppm of chloride was injected into the system, but turned colourless on injection of 10000 ppm, indicating that chlorine gas was generated in the system. Thus the method was sensitive to high concentrations of chloride,

but these might not be available in real samples. Calibration of the method was not therefore carried out.

10.4.2 PHENOL RED METHOD

Chlorine was generated by the reaction of Cl^- with $\text{MnO}_4^-/\text{H}^+$. The detection of Cl_2 by spectrophotometric method was based on electrophilic substitution of the gas on phenol red to produce chlorophenol blue. This reaction occurs in a similar manner as previously shown in equation 10.6.

Experimental

Reagents

Chloride stock solution (10000 ppm Cl^-), 3 M H_2SO_4 and 0.33 M KMnO_4 were prepared as in Section 9.2.4.1.

Phenol red solution was prepared as described in Section 10.2.2.

Procedure

The FI system used for generating chlorine was similar to that in Figure 10.1. 2000 ppm of chloride was injected into the FI system. The generated gas was swept into dilute phenol red solution. The absorbance of the resultant solution was determined by the UV/VIS spectrophotometer. The procedure was repeated for 10000 ppm of chloride.

Results and Discussion

The results obtained are shown in Table 10.2.

Table 10.2 Absorbance of chlorophenol compound formed from the reaction of phenol red and chlorine as determined by the UV/VIS spectrophotometer.

| Concentration of chloride (ppm) | Absorbance at 592 nm |
|---------------------------------|--------------------------|
| 2000 | Below limit of detection |
| 10000 | 0.211 |

Chloride concentrations of up to 2000 ppm could not be detected by this method. However, significant absorbance was obtained when a higher concentration of chloride (10000 ppm) was injected into the FI system. The phenol red method has been used for the determination of bromine. However, the presence of chloride has been reported to interfere with the determination of bromine. From the results obtained, it can be concluded that concentrations of chloride of less than 2000 ppm do not significantly interfere with the determination of bromine, using phenol red as colour forming agent. But for higher concentration of chloride, the interference of chloride becomes significant as shown by the absorbance obtained when 10000 ppm of chloride was injected in the system. The method is therefore not suitable for determination of low concentration of chloride in samples. This is due to less chlorination of phenol red compared to bromination of phenol red.

10.4.3 *N, N-DIMETHYL-*p*-PHENYLENEDIAMINE SULPHATE METHOD*

The electrophilic substitution of Cl_2 on *N,N*-dimethyl-*p*-phenylenediamine sulphate takes place in a similar manner as previously shown for bromine (see equation 10.7).

Experimental

Reagents

3 M H_2SO_4 and 0.33 M KMnO_4 and *N,N*-dimethyl-*p*-phenylenediamine sulphate were prepared as in Section 10.2.3.

Chloride stock solution (20000 ppm Cl^-). This was prepared by dissolving 10.6 g of potassium chloride in 250 ml of de-ionised water.

Procedure

The FI manifold used was the same as that in Figure 10.1. N,N-dimethyl-*p*-phenylenediamine sulphate was used as colour forming reagent instead of phenolphthalein. Working standards (0-15000 ppm Cl^-), prepared from chloride stock solution, were each injected into the FI system. The chlorine gas generated from each standard was swept, for 8 minutes, into 10 ml solution of N,N-dimethyl-*p*-phenylenediamine sulphate. The resultant solution was run on the UV/VIS spectrophotometer at 552.4 nm. The procedure was repeated for all the chloride standards.

Results and Discussion

The calibration graph constructed from these results is shown in Figure 10.8. A detection limit of 1759 ppm of chloride (3σ above the blank) was achieved.

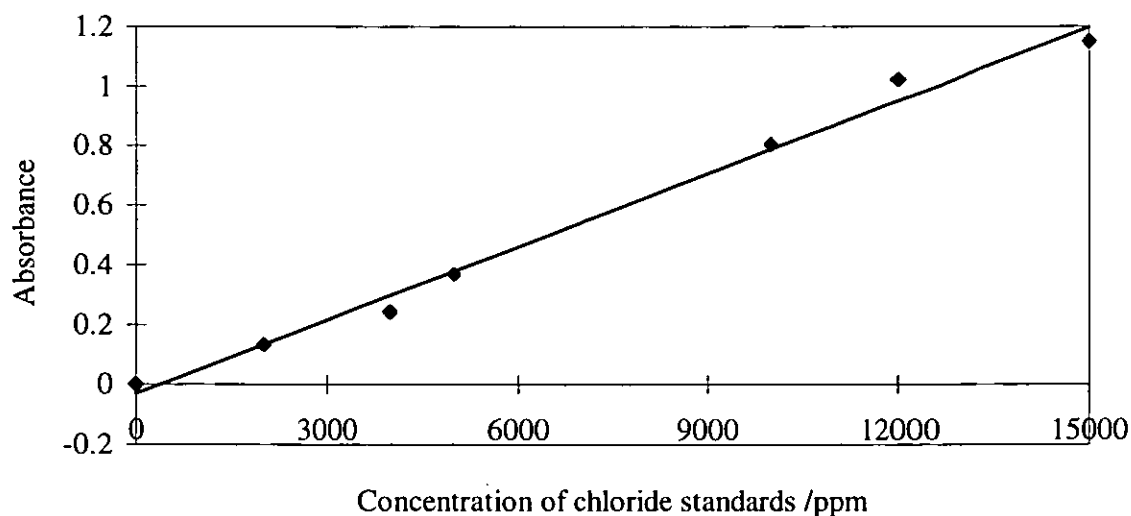


Figure 10.8 Calibration graph of absorbance due to complex formed by chlorine and N,N-dimethyl-*p*-phenylenediamine sulphate against concentration of chloride standards. Slope, $8.19 \times 10^{-5} \text{ ppm}^{-1}$; y-intercept, -0.03002 ; and regression coefficient, 0.991.

10.5 SEPARATION EFFICIENCY OF THE PTFE MEMBRANE (1 M LONG) FOR CHLORINE GENERATED IN THE FI SYSTEM

Experimental

Reagents

Potassium permanganate (0.33 M), sulphuric acid (3 M) and N,N-dimethyl-*p*-phenylenediamine sulphate were prepared as in Section 10.2.3.

Chloride stock solution (4000 ppm Cl⁻) was prepared by dissolving 2.114 g of potassium chloride in 250 ml of de-ionised water.

Procedure

The procedure that was used for determining the separation efficiency of the PTFE membrane (1.0 m long) for chlorine was similar to that applied for bromine earlier. Chloride working standards (0-800 ppm) prepared from the chloride stock solution were used to generate chlorine.

Results and Discussion

The separation efficiency of the PTFE membrane for chlorine was calculated using the concentration of chloride obtained by interpolation on the calibration graph in Figure 10.9. The detection limit achieved using the experimental apparatus shown in Figure 10.5 was 94 ppm of chloride.

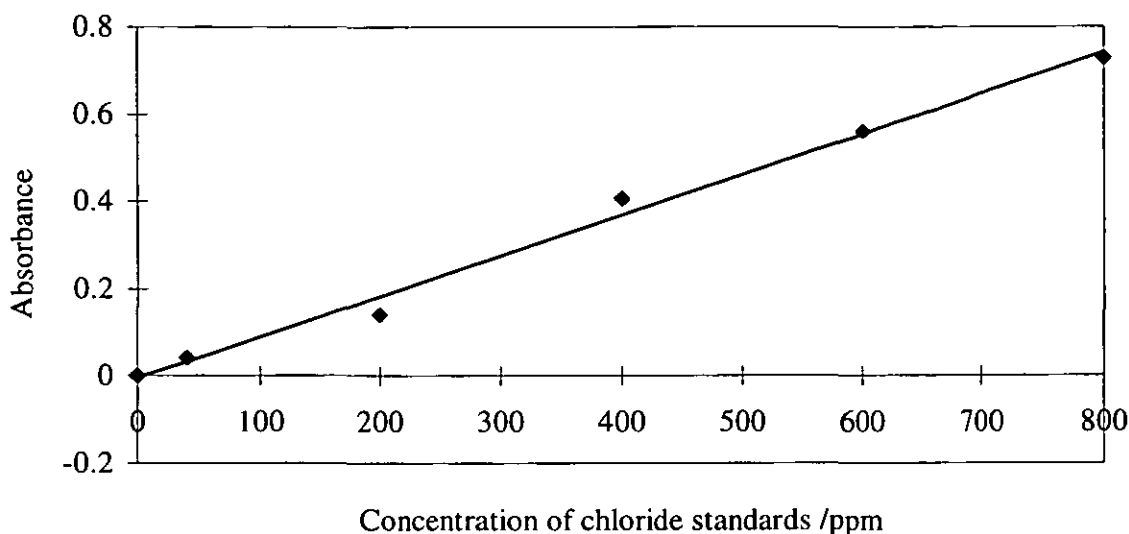


Figure 10.9 Calibration graph of absorbance of complex formed from chlorine and N,N-dimethyl-*p*-phenylenediamine sulphate against concentration of chloride standards. slope, $9.33 \times 10^{-4}/\text{ppm}$; y-intercept, 4.32×10^{-3} ; and regression coefficient, 0.992

A separation efficiency of 76.8 % obtained in this method was based on the generation of chlorine from chloride standards outside the FI system. This was based on the assumption that the chloride standards were quantitatively converted to chlorine and that all the gas was absorbed by N,N-dimethyl-*p*-phenylenediamine sulphate. This assumption is not completely true since chlorine could have been lost through the outlet in the bottle B in Figure 10.5. Loss of chlorine would result in the low absorbance value for each standard, hence high value for separation efficiency of the membrane for chlorine.

10.6 CONCLUSIONS

The DPGD-FI system was employed for the production of bromine from bromide using potassium permanganate oxidising agent and H_2SO_4 and subsequent separation of the gas from the liquid donor stream. The same DPGD-FI system was also applied for the generation of chlorine from chloride. The ultimate aim was to interface the DPGD-FI system with the MS for the isotopic ratio determination of bromine or chlorine. But due

to lack of an isotope ratio mass spectrometer in our laboratory, spectrophotometric methods based on phenolphthalein, phenol red and N,N-dimethyl-*p*-phenylenediamine sulphate for the detection of bromine or chlorine generated in the DPGD-FI system were employed.

The spectrophotometric method based on N,N-dimethyl-*p*-phenylenediamine sulphate gave the highest sensitivity for the detection of bromine or chlorine. The separation efficiency of 1 m long PTFE (component of DPGD unit) for bromine was 94.2 % while that for chlorine was 76.8 %. These high separation efficiencies might have been due to the erroneous assumption made, that all the generated bromine or chlorine was absorbed in the N,N-dimethyl-*p*-phenylenediamine sulphate solution. Some of the generated bromine or chlorine might have escaped from the absorbing solution because of the inefficient manner of trapping the gases, thus resulting in a low absorbance for the calibration solution.

REFERENCES

1. Anagnostopoulou, P. I. and Koupparis, M. A., *Anal. Chem.*, 1986, **58**, 322.
2. Anfalt, T. and Twengstrom, S., *Anal. Chim. Acta*, 1986, **179**, 453.
3. Lee, J. D., *Concise Inorganic Chemistry*, Chapman and Hall, London, 4th Edn., 1991, pp. 596.
4. Morrison, R. T. and Boyd, R. N., *Organic Chemistry*, Allyn and Bacon, Inc., Boston, 2nd Edn., 1966, pp. 915.
5. Fessenden, R. J. and Fessenden, J. S., *Organic Chemistry*, Brookes/Cole, California, 4th Edn., 1990, pp. 867.
6. Basel C. L. and Defreese J. D., *Anal. Chem.*, 1982, **54**, 2090.

Chapter 11

CHAPTER ELEVEN

DETERMINATION OF SELENIUM BY DPGD-FI/STRIPPING VOLTAMMETRY

11.1 INTRODUCTION

In this chapter, stripping voltammetry is investigated as a technique for the determination of Se, following its separation as H_2Se , and once again as an alternative to MS.

Selenium exists in +6 and +4 oxidation states in inorganic species, +4 and +2 as organo selenium compounds, 0 as elemental selenium and -2 as hydrogen selenide.¹ The element is an essential nutrient at trace levels, but toxic in excess amounts in animals and humans. As an essential element, Se acts as the active centre of glutathione peroxidase, an enzyme which is mainly involved with the removal of peroxide from cells to prevent oxidative damage.^{2,3} Excessive amounts of Se produce selenosis, leading to toxic symptoms and death, while deficiency in this element results in a variety of diseases. Introduction of selenium into the environment may represent a health hazard, hence there is need to improve on the sampling and determination of low concentrations of Se in a variety of systems such as, atmospheres, water and biological tissues. The determination of Se is also of interest because it tends to weaken the toxic action of some heavy metals in animals and plants.⁴ Sources of Se in the atmosphere include fossil fuels and coal.

The importance of Se in the metabolism of plants, animals and humans has stimulated the development of a variety of analytical methods. Its occurrence at very low levels (ng/kg) in environmental matrices requires the development of sensitive instrumental methods. A number of analytical methods have been used for its determination. These include the

spectrophotometric and fluorometric methods involving the formation of the selendiazole complex of selenium and 3,3'-diaminobenzidine.^{5,6,7} These procedures have drawbacks such as being time consuming and sensitive to oxidants and reductants and metal ions such as Fe^{3+} and Cu^{2+} .⁸ Other analytical methods that have been used include neutron activation analysis, gas chromatography, X-ray fluorescence.⁹ Atomic absorption spectroscopy (AAS) has also been used to determine Se (as hydrogen selenide) generated by reduction of higher oxidation states of Se with Sn (II), Ti (III) and sodium borohydride.^{10,11,12} Iron has been found to interfere with the determination of Se by HG-AAS by interacting with Se, thus preventing its volatilisation.

The ICP-MS technique has gained popularity for the determination of metals at trace level due to its potential for multi-element analyses at high sensitivity. However, its application to Se determination still needs to be improved.¹³ The main problems associated with the determination of Se by ICP-MS include: the formation of polyatomic ions in the plasma, arising from combination of argon atoms and light elements, with total mass equal to that of the various Se isotopes. Polyatomic species such as $^{40}\text{Ar}_2$ at m/e 80 will overlap with the most abundant Se isotope, ^{80}Se , while $^{40}\text{Ar}^{37}\text{Cl}$, $^{40}\text{Ar}^{38}\text{Ar}$ and $^{40}\text{Ar}_2\text{H}_2$ interfere with ^{77}Se , ^{78}Se , and ^{82}Se , respectively, if these isotopes of lower natural abundance are used for the determination.¹⁴ The other limiting factor for sensitivity is its high ionisation potential which results in poor ionisation yield in the plasma (33 %). These problems can be partially solved by using HG as a means of introducing Se into the ICP-MS instrument. The HG method offers several advantages: allowing separation of the analyte from the sample matrix, thus reducing some interferences associated with the liquid sample introduction mode, and complete introduction of the analyte in the gaseous state, thereby avoiding desolvation effects and resulting in increased sensitivity.¹⁵ Sample introduction with FI and HG, interfaced with ICP-MS, offers several advantages such as a small initial liquid sample volume, low reagent consumption, less interference due to

introduction of Se as a gas and ease of automation of the system.¹⁵ Despite such improvements in sample introduction, some polyatomic interferences still remain and the sensitivity is often too low to determine Se in environmental samples.¹⁴ Further improvement in sensitivity has been achieved by adding nitrogen, methane, and oxygen to the nebulizer gas to overcome these interferences. Addition of alcohols, such as ethanol and propan-2-ol, has been found to considerably reduce polyatomic interferences.¹⁴

Although ICP-AES is now widely accepted as the method of choice for the determination of trace elements, it is not suitable for Se because the principal emission lines of this element are weak and in the ultraviolet region of the spectrum where photomultipliers and monochromator gratings usually exhibit less than optimal performance.¹⁷

Electrochemical reduction of Se(IV) has been employed for the quantitative determination of Se.⁵ Cathodic stripping voltammetry has been used for the determination of Se(IV) on a mercury working electrode and a detection limit of 8 ppb was achieved.¹² The sensitivity of the method has been extended by electrodeposition of Se (IV) and stripping from a gold disc electrode.¹⁸ In this method metal ions such as Cu^{2+} , Pb^{2+} and Cd^{2+} may interfere.

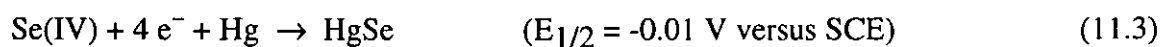
The speed of analysis of atomic spectrometric techniques has made them the method of choice for the determination of trace metals. However, electrochemical techniques provide an excellent alternative and have the advantages of high sensitivity and low cost, albeit with a lower speed of determination. The use of electrochemical techniques, such as stripping voltammetry, allows the differentiation of chemical species to be achieved on the basis of shifts in deposition and analytical peak potentials. This, in addition to the high sensitivity, makes them ideal for speciation work and trace metal analysis in general.

Cathodic stripping voltammetry involves sample preconcentration by means of potentiostatic deposition of the metal onto a working electrode. The metal is stripped from the sample solution by sweeping the voltage to the more negative direction. The determination of Se(IV) by the polarographic technique has been reported using an acidic supporting electrolyte such as, hydrochloric acid or perchloric acid.¹⁹ Electroreduction of Se(IV) at a mercury electrode takes place in acidic solution with the formation of a deposit on the electrode surface. There is some uncertainty about the nature of this deposit which is thought to correspond to mercury selenide or elemental selenium.^{4,19,20}

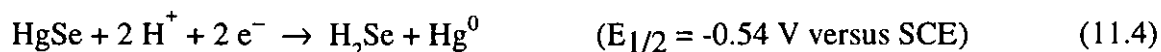
The polarographic reduction of Se(IV) in HCl exhibits two waves at -0.01 and -0.54 V (versus SCE)²¹ which are attributed to the following reactions:^{9,22}



with the overall reaction

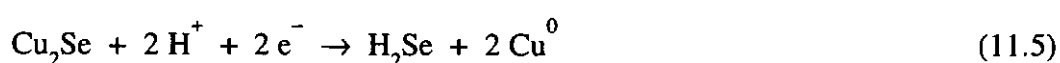


and



Differential pulse cathodic stripping voltammetry, on a HMDE, has been applied for the determination of Se(IV) in biological samples and industrial materials such as gallium arsenide.^{23,24}

Addition of copper (II) ions in the determination of Se by cathodic stripping voltammetry has been found to enhance sensitivity.^{9,25} This enhancement of sensitivity has been suggested to be due to the formation of copper selenide which is more soluble in the mercury drop than mercury selenide.⁹ In the absence of Cu, the peak due to reductive dissolution of HgSe appeared at -0.56 V. As the concentration of Cu was increased another peak was formed at -0.63 V (Ag/AgCl). This was attributed to the reduction of Cu₂Se as shown below.



11.2 DETERMINATION OF SELENIUM BY DIFFERENTIAL PULSE CATHODIC STRIPPING VOLTAMMETRY ON A HANGING MERCURY DROP ELECTRODE

11.2.1 Introduction

In this Section, experimental conditions for the determination of Se(IV) in a static system by DPCSV on a HMDE were optimised so as to obtain the maximum peak current for each determination. The effect of varying the deposition time, concentration of HCl, copper concentration, deposition potential and scan rate were investigated. Se(IV) was then determined in the presence or absence of added Cu by DPCSV on a HMDE in both static and flow systems using optimised conditions. An analytical method involving the generation of hydrogen selenide in the FI system, the separation of this vapour in the DPGD unit (consisting of a PTFE membrane) followed by oxidation back to Se(IV) by Ce(IV) and subsequent determination of Se(IV) by DPCSV was developed. The reason for using HG-DPGD was to separate the generated H₂Se from the liquid sample matrix which could have caused interference problems.

Reagents

0.5 M HCl supporting electrolyte.

Apparatus

A Metrohm instrument, model 626 Polarecord with a model 663 three electrode stand was used. Ag/AgCl (3 M KCl), HMDE and glassy carbon electrodes served as the reference electrode, working electrode and auxiliary electrode, respectively. A pulse height of 50 mV was used throughout this work.

11.2.2 Effect of varying deposition time

The accumulation time for Se on the HMDE was varied from 1 to 5 minutes. This was followed by a voltage sweep from -0.4 to -0.8 V. 4 ppb of Se (IV) was determined by DPCSV in the presence of added copper sulphate of effective concentration of 2×10^{-4} M.

Results and Discussion

The results obtained are presented in Figure 11.1

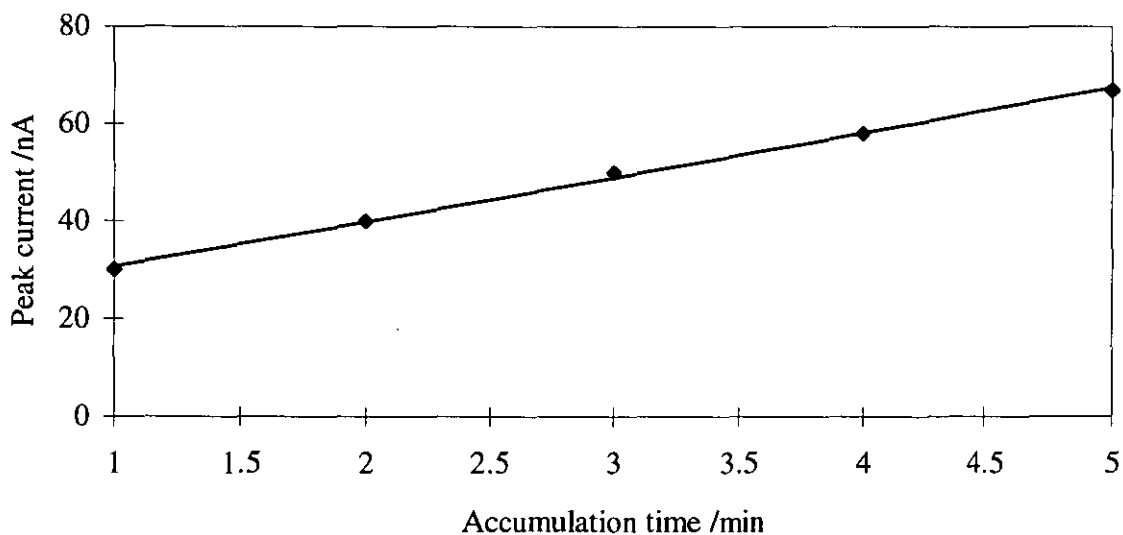


Figure 11.1 Graph of peak current versus accumulation time

It was found that the peak current increased with increase of accumulation time, but with the penalty of longer analysis time. Although an accumulation time of 1 minute resulted in a relatively lower current, it was chosen in the subsequent experiments in order to reduce the analysis time. This is important as analysis time should be as short as possible, especially when dealing with a large number of samples.

11.2.3 Influence of concentration of HCl (supporting electrolyte) on peak current

HCl concentrations ranging from 0.1 to 0.5 M were used as supporting electrolytes. To 25 ml of 0.1 M HCl, 4 ppb Se(IV) and 2×10^{-4} M of copper sulphate (effective concentrations) were added to the electrochemical cell and the determination of the analyte made by the DPCSV. The procedure was repeated with the other concentrations of HCl.

Results and Discussion

The results obtained are displayed in Table 11.1

Table 11.1 Influence of concentration of HCl on the Cu_2Se peak current.

| Concentration of HCl (M) | Peak current (nA) |
|--------------------------|-------------------|
| 0.1 | 17.7 |
| 0.2 | 24.7 |
| 0.3 | 22.3 |
| 0.4 | 17.0 |
| 0.5 | 20.7 |

Distorted peaks were obtained when 0.1-0.4 M HCl were employed. A sharp peak was obtained with 0.5 M HCl supporting electrolyte, hence this was used in subsequent experiments.

11.2.4 Effect of using copper in the determination of Se(IV) by DPCSV

4 ppb Se(IV) (effective concentration) was added to the electrochemical cell to which 25 ml of 0.5 M HCl had been added. Se(IV) was then determined for added Cu^{2+} concentration covering the range from 3.85×10^{-5} to 2.86×10^{-4} M.

Results and Discussion

The results obtained are shown in Figure 11.2.

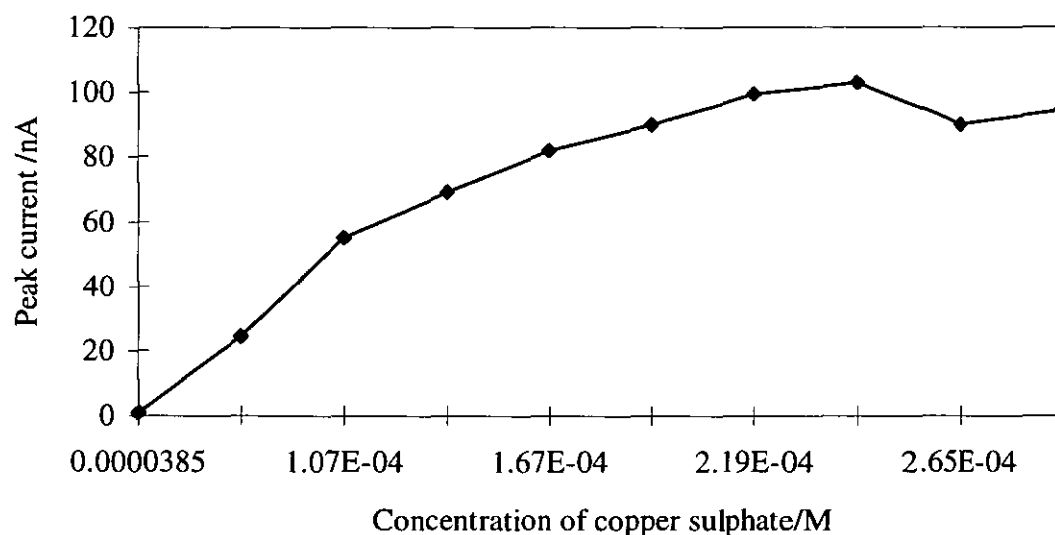


Figure 11.2 Influence of copper concentration on peak current in the determination of Se(IV) by DPCSV on HMDE

For the determination of Se(IV) by DPCSV in the absence of Cu, the maximum peak current occurred at a stripping potential of -0.51 V. On addition of Cu to the electrochemical cell, a shift of peak voltage took place towards a more negative potential. This shift was from -0.51 V to -0.69 V. Sensitivity was enhanced when copper was used in the determination of Se.

In all cases, the current increased as the concentration of copper was increased until a concentration of 2.42×10^{-4} M of copper sulphate had been added. Further increase in the concentration of Cu^{2+} resulted in a slight decrease of peak current and a splitting of the current peak which may have been due to overloading of the mercury drop with copper.

11.2.5 Effects of change of deposition potential on peak current

16.7 ppb of Se(IV) and 2.42×10^{-4} M of copper sulphate (effective concentration) were added to the electrochemical cell containing 25 ml of 0.5 M HCl. The polarising voltage was varied from -0.2 V to -0.5 V and the effect caused by varying the deposition potential on signal current was studied.

Results and Discussion

The results obtained are shown in Table 11.2.

Table 11.2 Effect of changing deposition potential on stripping peak of Cu_2Se .

| Deposition potential (V) | Peak current (nA) |
|--------------------------|-------------------|
| -0.2 | 7 |
| -0.25 | 6 |
| -0.3 | 5 |
| -0.35 | 4.5 |
| -0.4 | 5 |
| -0.45 | 4 |
| -0.5 | 3.5 |

As the deposition potential was increased, there was a general broadening of the peaks. There was also a general decrease in peak current as the deposition potential was made

more negative. The most reproducible peaks were obtained at -0.4 V (versus Ag/AgCl) and therefore this was used as the deposition potential in further work. Also, scanning from lower potentials to a specific higher negative potential (in this case -0.8 V), took a relatively longer period. For the analysis of a large number of samples to be completed within the shortest time possible, it is necessary that the total analysis time per determination should be as short as possible.

11.2.6 Effects of changing scan rate on peak current

16.7 ppb Se(IV) and 2×10^{-4} M of copper sulphate (effective concentration) were used in the electrochemical cell containing 25 ml of 0.5 M HCl. The determination of the analyte was done by DPCSV as outlined earlier.

Results and discussion

The graph of peak current versus scan rate (Figure 11.3) was constructed from the results obtained. There was an increase of peak current as the scan rate was increased. However, at higher scan rates, particularly at -25 mV/s and -50 mV/s, the voltammograms obtained were distorted and asymmetrical hence they could not be used for quantitative analysis. Thus a scan rate of -5 mV/s was used in all subsequent voltammetric determinations of Se (IV).

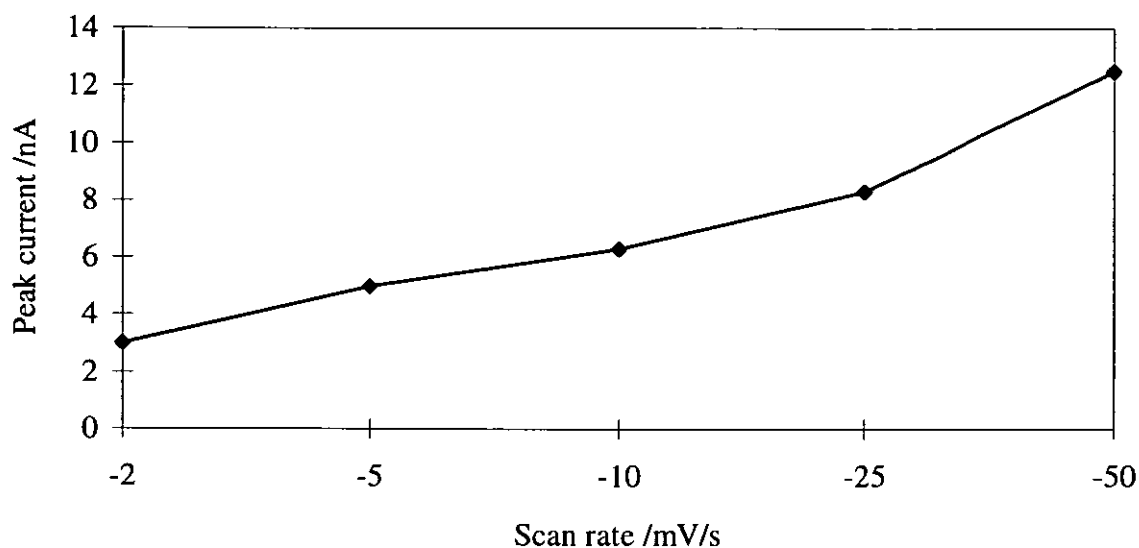


Figure 11.3 Peak current due to stripping peak of Cu_2Se with the variation of scan rate.

11.2.7 Calibration-case in which Cu was not added (static system)

Reagents

0.5 M HCl (supporting electrolyte)

1 ppm Se(IV) standard solution

This solution was prepared by diluting 1 ml of 1000 ppm of Se stock solution to 100 ml using 0.5 M HNO_3 . 10 ml of this solution was pipetted into a 100 ml volumetric flask and the volume made up to the mark with 0.5 M HNO_3 .

Instrumental conditions were those previously determined as optimal (scan rate of -5 mV/s, 2.42×10^{-4} M copper sulphate, deposition potential of -0.4 V, deposition time of 1 min, and drop size dial position 3).

Procedure

25 ml of 0.5 M HCl (supporting electrolyte) was added to the electrochemical cell, the solution was stirred using a PTFE stirrer and was deaerated using nitrogen gas for 10

minutes. The deaeration of the solution was done to remove oxygen which otherwise could interfere with the determination. After 10 minutes, deaeration of the solution was stopped, but stirring was continued. A determination was carried out on the blank and then the procedure repeated for added Se concentration range from 4 to 45.8 ppm.

Results and Discussion

The results obtained were used for constructing the calibration graph shown in Figure 11.4. A detection limit (3σ above the blank) of 6.8 ppb and sensitivity of 6.1 nA/ppb were obtained.

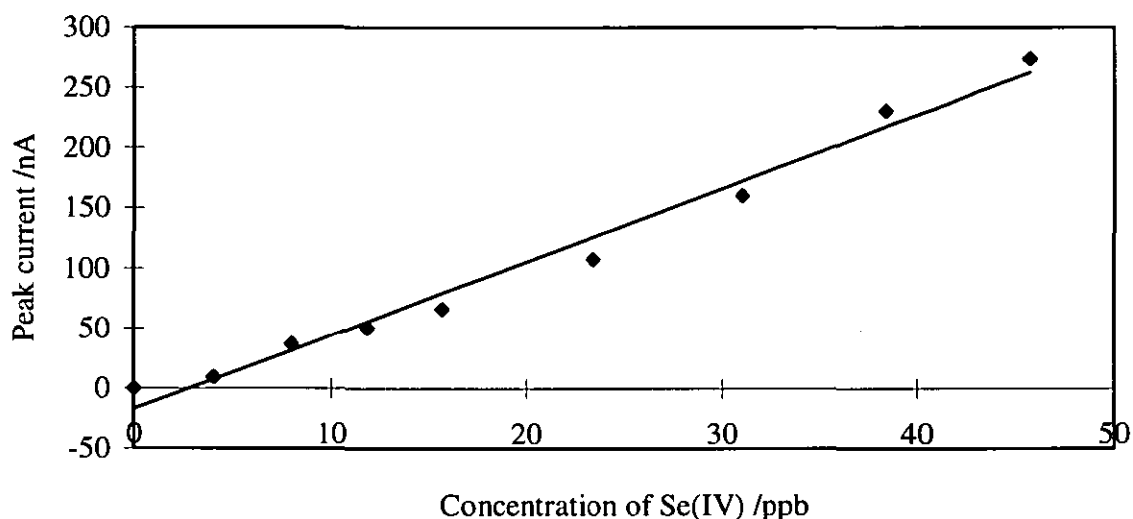


Figure 11.4 Calibration graph of peak current versus concentration of Se (IV) standards by DPCSV on HMDE (copper not added for sensitivity enhancement). Slope, 6.102 nA/ppb; y-intercept, -16.995 nA and regression coefficient, 0.983.

11.2.8 Calibration-case in which Cu was added to enhance sensitivity (static system)

Reagents

Copper sulphate (10^{-2} M) solution was prepared by dissolving 0.249 g of $\text{CuSO}_4 \cdot 5\text{H}_2\text{O}$ in 100 ml de-ionised water.

1 ppm Se(IV) standard was prepared from 1000 ppm of Se stock provided.

Procedure

100 μ l of 1 ppm Se (IV) was pipetted into the electrochemical cell containing 2.42×10^{-4} M copper sulphate solution. Se(IV) was determined by DPCSV on a HMDE using the optimised conditions stated earlier. More volumes of 1 ppm selenium standard were added into the cell and the procedure for determination repeated.

Results and Discussion

The results obtained in this work are presented in the calibration graph shown in Figure 11.5.

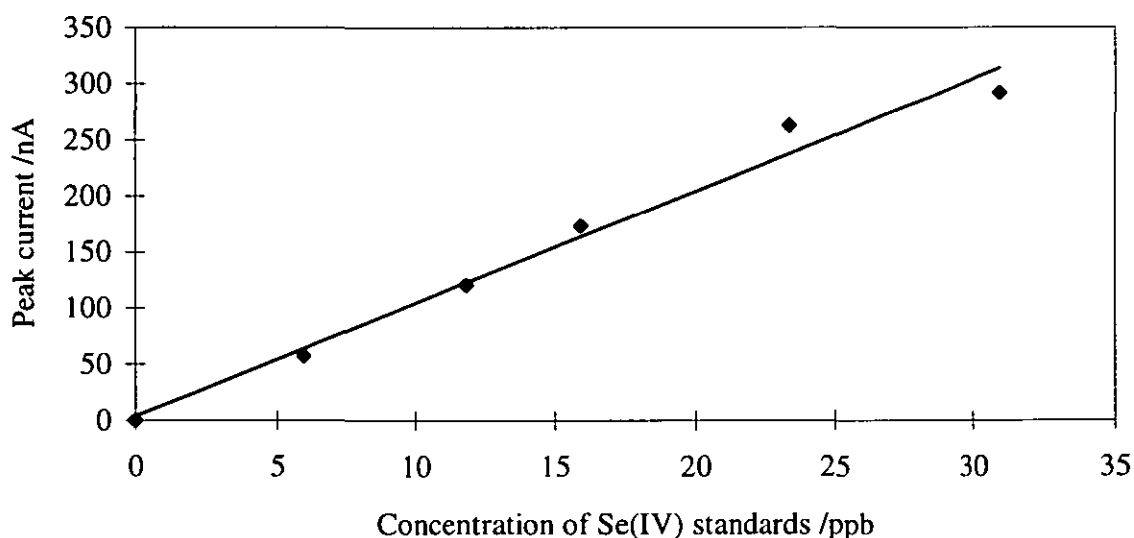


Figure 11.5 Calibration graph of peak current versus concentration of Se(IV) standards as determined by DPCSV in the presence of added copper. Slope, 10.0 nA/ppb; y-intercept, 4.143 nA; regression coefficient, 0.981.

A detection limit (3σ above the blank) of 5.40 ppb and sensitivity of 10.0 nA/ppb were achieved. This represents a modest improvement on the performance without Cu, but the shift in peak voltage from 0.51 to 0.69 V (versus Ag/AgCl) has other benefits in terms of

removing or reducing interferences. For example, in ammonium sulphate buffer, the interference of Zn(II) is completely removed whereas that due to Cd(II) is considerably reduced by using added Cu in the presence of added EDTA in the determination of Se(IV) by DPCSV.⁹ This is not a particular advantage in this case as any interference will be removed at the HG step. The sensitivity, however, was enhanced by a factor of 1.6.

11.2.9 Flow injection-selenium hydride generation and its determination by DPCSV on a HMDE after PTFE membrane separation (Cu not added)

The FI system used is shown in Figure 11.6

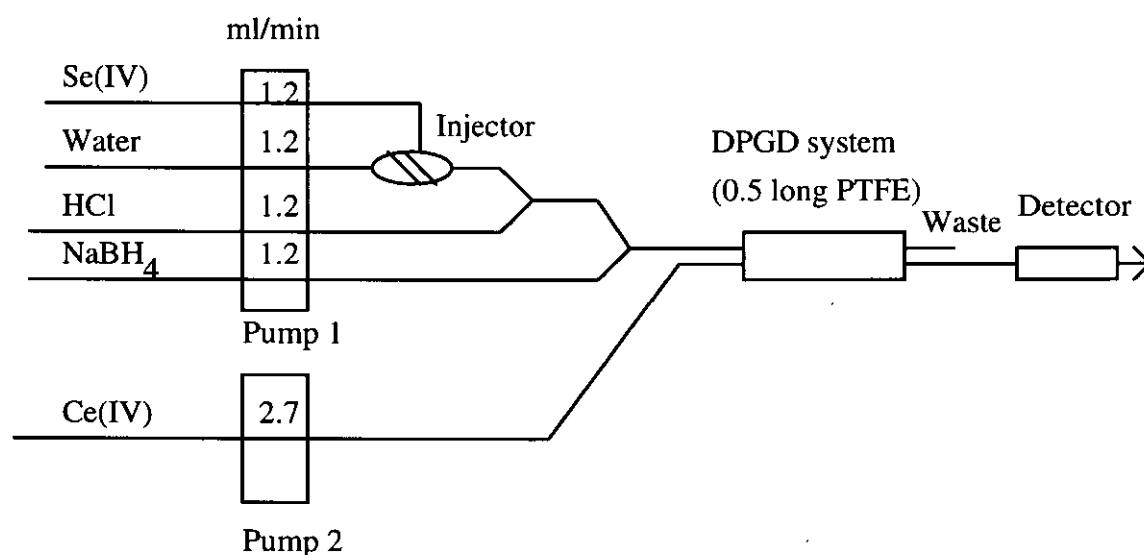


Figure 11.6 DPGD-FI system for generating selenium hydride.

The instrumental conditions for the DPCSV were as described previously.

Selenium (IV) working standards (10-100 ppm) were prepared from 1000 ppm of Se (IV) stock solution. Each selenium standard was prepared in 0.5 M nitric acid.

Sodium borohydride (5.26×10^{-2} M) was prepared by dissolving 2 g of sodium borohydride (Spectrosol reagent, BDH, UK) and 0.5 g of sodium hydroxide pellets (Fisons, Loughborough, UK) in 1000 ml de-ionised water.

Ce(IV) (3.01×10^{-4} M) solution was prepared by dissolving 0.1 g of ceric sulphate ($\text{Ce}(\text{SO}_4)_2$) (Fisons, Loughborough, UK) in 1 litre of 0.5 M HCl.

Procedure

Each Se(IV) standard was injected into the FI system using a sample loop volume of 0.5 ml. Selenium hydride was generated on-line. The hydride was separated from the liquid donor stream by a 0.5 m long PTFE membrane. The separated selenium hydride diffused through the membrane into an acceptor stream of Ce(IV) solution which oxidised Se(-II) to Se(IV). The solution of Se(IV) formed in the Ce(IV) stream was received in the electrochemical cell containing 25 ml of 0.5 M HCl (supporting electrolyte) for 8 minutes. At the end of this period, the total volume of the solution in the cell was 37.2 ml. While the peristaltic pump was stopped, the solution was purged with nitrogen for 10 minutes and Se(IV) finally determined by DPCSV using the optimised conditions. Se(IV) was accumulated on the HMDE by applying a deposition potential of -0.4 V while the stirrer was on, but deaeration of the solution stopped. In the stripping step, the voltage was scanned from -0.4 V to -0.8 V. The peak height of each voltammogram was measured and the peak current calculated.

Results and Discussion

A calibration graph of stripping peak current against concentration of Se(IV) standard injected into the DPGD-FI system was constructed (Figure 11.7). The limit of detection (at 3σ above the blank) and the sensitivity obtained were 11 ppm and 1 nA/ppm, respectively. The same procedure was repeated after replacing the 0.5 m PTFE membrane with the one having a length of 1.0 m. The calibration graph is shown in Figure 11.8. A detection limit (3σ above blank) of 7.7 ppm and sensitivity of 3.7 nA/ppm were obtained with the 1.0 m long PTFE membrane. These results show that higher sensitivity and a lower detection limit were obtained when the longer PTFE membrane was used. This is attributed to the larger surface area presented by the longer membrane. Both graphs show a positive intercept which suggests that some contamination may have been present.

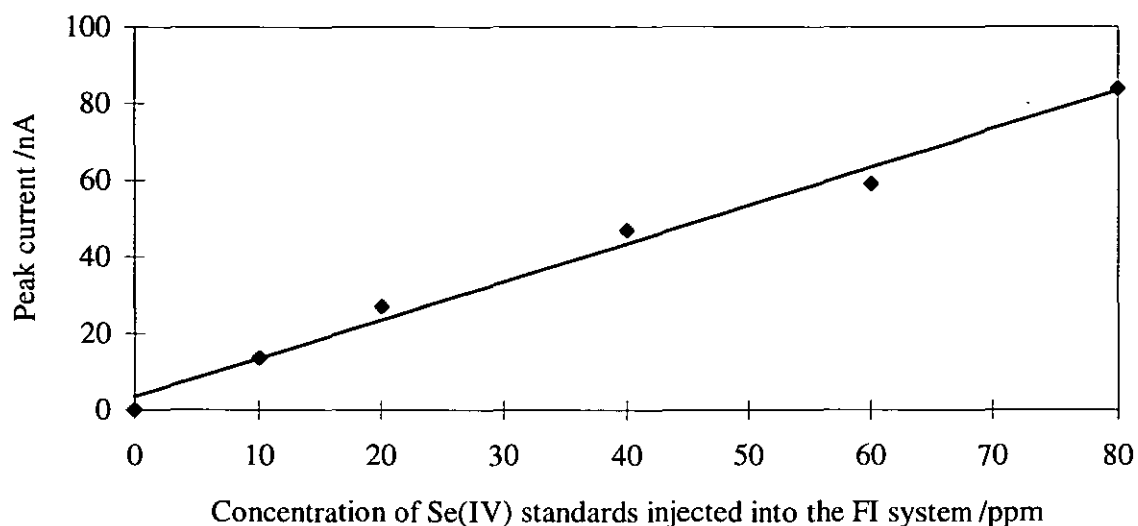


Figure 11.7 Calibration graph of peak current determined by DPCSV on a HMDE versus concentration of Se(IV) injected into the DPGD-FI system (0.5 m long PTFE membrane). Slope, 0.998 nA/ppm; y-intercept, 3.505 nA; and regression coefficient, 0.988.

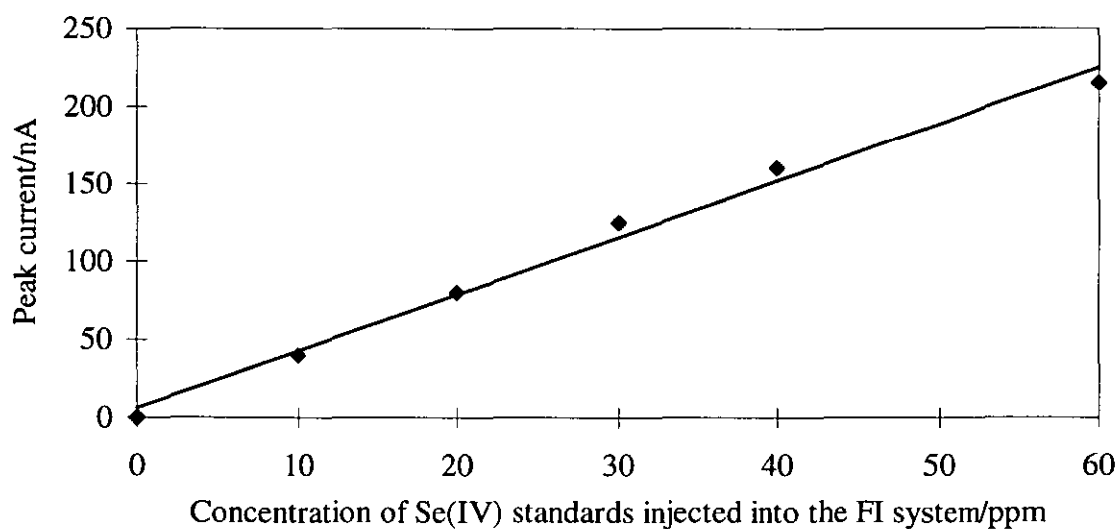


Figure 11.8 Calibration graph of stripping peak current versus concentration of Se(IV) injected into the DPGD-FI system (1.0 m long PTFE membrane). Slope, 3.65 nA/ppm; y-intercept, 6.0 nA; and regression coefficient, 0.990.

Separation Efficiencies of the PTFE membranes

The separation efficiencies of 0.5 m and 1.0 m long PTFE membranes for selenium hydride generated in the FI system were calculated and the results are tabulated in Table 11.3. The calibration graph in Figure 11.4 was used to determine the mass of Se collected in the cell after the separation process.

Table 11.3 Separation Efficiencies of PTFE membranes for hydrogen selenide generated in the FI system.

| Length of PTFE (m) | Se(IV) concentration injected into the FI system (ppm) | Peak current (nA) | Concentration Se(IV) from calibration graph in Fig. 11.4 (ppb) | Concentration of Se(IV) (calculated) (ppb) | Separation Efficiency (%) |
|--------------------|--|-------------------|--|--|---------------------------|
| 0.5 | 60 | 59 | 12.5 | 807 | 1.5 |
| 0.5 | 80 | 84 | 16.6 | 1076 | 1.5 |
| 1.0 | 40 | 179 | 32.1 | 538 | 6.0 |
| 1.0 | 60 | 208 | 36.9 | 807 | 4.6 |

The efficiencies are very poor and further work is required to resolve this problem.

A determination of membrane transport efficiency was carried out using this method and slightly higher efficiencies were obtained i.e. 10.5 %. Sensitivity does not affect efficiency and it is probable that the experimental conditions were more favourable in these runs, but the reason for this is not clear.

11.3 DETERMINATION OF SELENIUM (IV) IN THE PRESENCE OF COPPER BY DIFFERENTIAL PULSE CATHODIC STRIPPING VOLTAMMETRY AT MERCURY FILM GLASSY CARBON ELECTRODE

In the determination of Se(IV) on a HMDE in the flow system previously described, the injected Se(IV) sample was eventually diluted by a factor of 74.4 in the final solution in the cell. Such a large dilution of the sample causes loss of sensitivity. In addition, the separation efficiency of the PTFE membrane (1 m long) for H_2Se was only 10.4 %. The extensive dilution contributed to the poor overall detection limit (11 ppm). To improve the sensitivity of DPCSV for the determination of Se(IV) in a flow system, the HMDE was replaced by a mercury film glassy carbon electrode (MFGCE) in a wall jet configuration. The mercury film electrode is known to offer higher sensitivity than a HMDE due to a larger surface area to volume ratio (at least three orders of magnitude).²⁶ A larger amount of the analyte is therefore preconcentrated on the mercury film than on a HMDE. The other reason for using a MFGCE in a wall jet configuration was to ensure that the transport of the analyte as it approaches the electrode was diffusion controlled rather than being controlled by convective forces which may destroy the mercury film due to turbulent flow.

The principle of a wall jet electrode is that the liquid stream strikes a wall perpendicularly and flows radially over its surface. The requirements for the design of a flow through cell that exhibits characteristics of a true wall jet are:²⁷

- the jet of a liquid passing through the inlet should not break before impinging on the electrode. In general, the jet remains intact for up to 10 mm from the inlet.
- There should be no interference with the development of the boundary layer. For this reason, the auxiliary electrode, reference electrode, back wall, the nozzle body should not be so close to the working electrode that the boundary layer is disturbed.
- the electrode diameter should be at least ten times larger than the inlet diameter.

Experimental conditions for the determination of Se(IV) using this method were optimised so as to obtain the maximum peak current for each determination. The effects of varying the deposition potential, scan rate, stirring of the solution in the electrochemical cell and concentration of copper on peak current were studied.

11.3.1 Effect of varying deposition potential on peak current

An Ag/AgCl reference electrode, platinum foil secondary electrode and mercury film glassy carbon electrode (working electrode) were used in the electrochemical cell.

Mercury film formation

The surface of the glassy carbon electrode was pre-treated by polishing the electrode on a polishing cloth to a mirror finish using fine alumina powder made up in a slurry. The polishing was done by using gentle circular strokes for a short period (10-15 seconds). The electrode was then rinsed with de-ionised water to remove particles embedded into the electrode which would otherwise interfere with the determination of the analyte. The electrode was repolished for a few seconds on a new wet polishing cloth free of alumina. It was then chemically cleaned using dilute HCl for 2-3 minutes and finally rinsed thoroughly with de-ionised water.

200 μl of 1000 ppm of $\text{Hg}(\text{NO}_3)_2$ was pipetted into the cell containing 25 ml of 0.1 M KNO_3 (supporting electrolyte). Mercury was accumulated onto the pre-treated glassy carbon electrode for 10 minutes at a potential of -1.0 V (versus Ag/AgCl).

4.0×10^{-6} M of Cu and 0.08 ppb Se(IV) (effective concentrations) were added to the electrochemical cell. The determination of Se(IV) was done by DPCSV, starting with a deposition potential of -0.2 V. The procedure was repeated using deposition potentials of -0.25, -0.3, -0.35, -0.4 and -0.45 V (versus Ag/AgCl). In each case an accumulation period of 1 minute and a rest period of 23 seconds were employed.

Results and Discussion

A graph of peak current versus deposition potential is shown in Figure 11.9

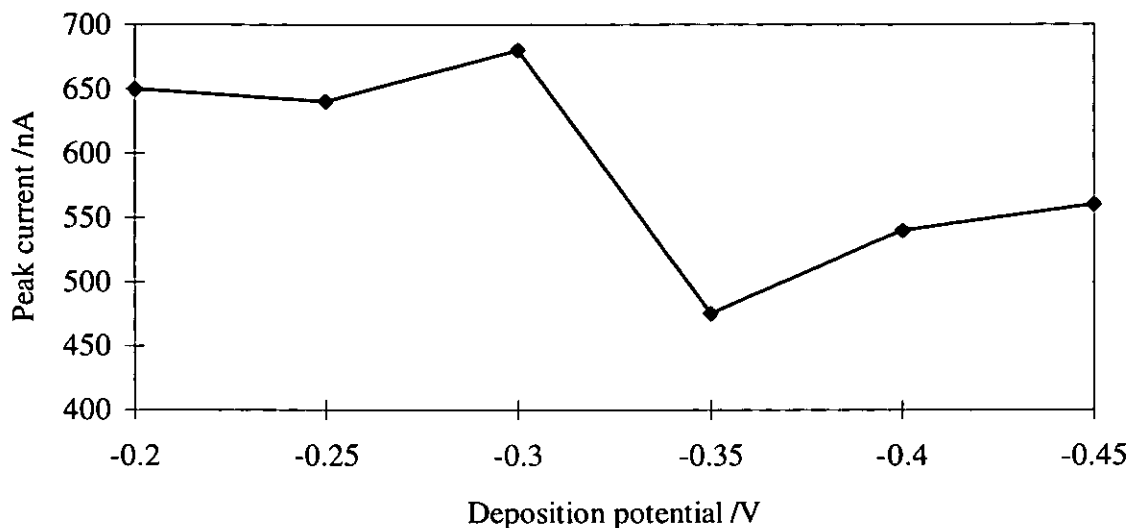


Figure 11.9 Relationship between deposition potential on peak current

A deposition potential of -0.30 V gave the highest stripping current and was taken as the optimum deposition potential for Se(IV) using the MFGCE. This deposition potential was used throughout in the subsequent studies. It is not clear why the optimum deposition potential was different for the film, but it may be that there was incomplete coverage of the carbon.

11.3.2 Effect of varying scan rate on peak current

A deposition potential of -0.3 V (versus Ag/AgCl) was used for depositing Se (IV) onto the mercury film on the glassy carbon support. In the stripping step, the potential was scanned from -0.3 V to -0.8 V.

The determination of 0.08 ppb Se(IV) in the presence of added 4×10^{-6} M $\text{CuSO}_4 \cdot 5\text{H}_2\text{O}$ (effective concentration) was done using DPCSV on the MFGCE as the scan rate was varied from -2 mV/s to -50 mV/s. A graph showing the effect of varying scan rate on peak current (Figure 11.10) was constructed from the results obtained. As the scan rate was increased, there was a general increase in the peak current. However, the peak profile was distorted for scan rates of more than -5 mV/s. A scan rate of -5 mV/s, which gave a very good symmetric peak, was therefore taken as the optimum scan rate.

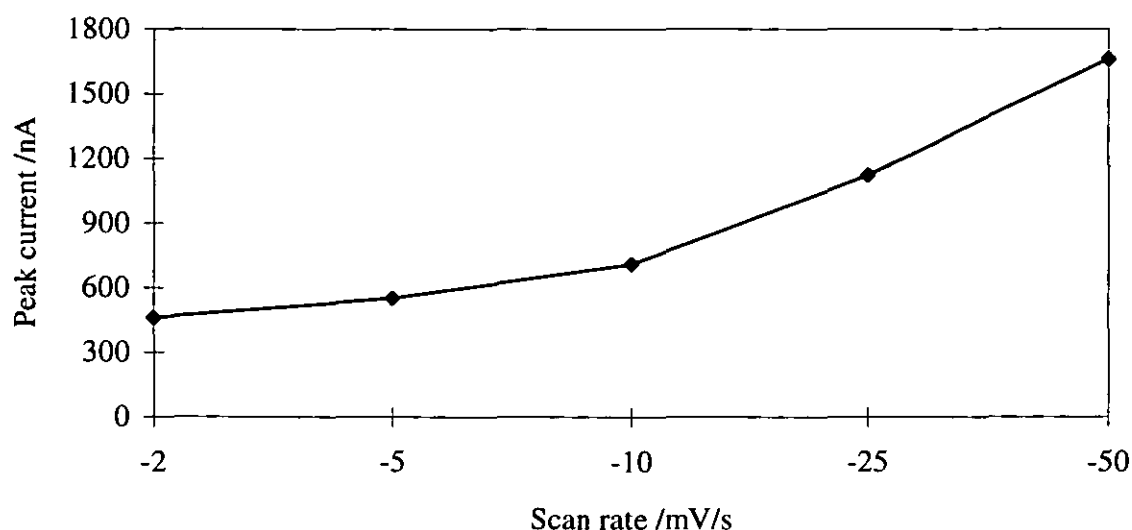


Figure 11.10 Graph of peak current versus scan rate determined by DPCSV at MFGCE

11.3.3 Effect of varying Cu concentration on peak current

The experimental conditions used were: scan rate, -5 mV/s; stirrer position, 3; deposition period, 1 min; deposition potential, -0.3 V (versus Ag/AgCl); and voltage sweep from -0.3 V to -0.8 V.

0.08 ppb of Se(IV) (effective concentration) was transferred into the electrochemical cell containing 25 ml of 0.1 M KNO_3 , supporting electrolyte. Concentration of Cu varying

from 4×10^{-6} M to 8.0×10^{-5} M was added to the cell. The determination of Se(IV) by DPCSV at MFGCE was carried out as described in the preceding section.

Results and Discussion

The results obtained are presented in Figure 11.11. There was no general trend in peak current as the concentration of copper was increased. The lowest concentration studied i.e. 4×10^{-6} M was therefore used in subsequent experiments.

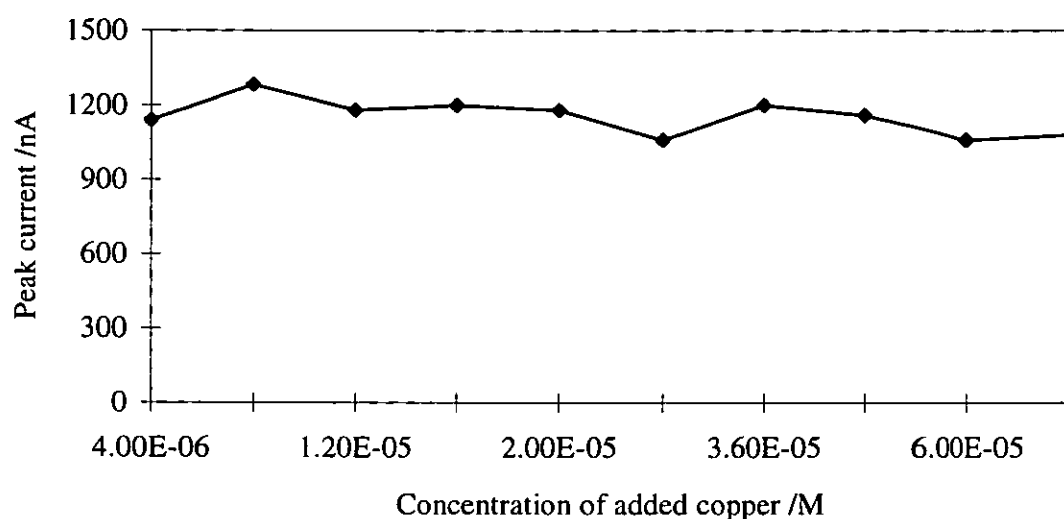


Figure 11.11 Graph of peak current against copper concentration used in the determination of Se(IV) by DPCSV at MFGCE.

11.3.4 Calibration

Reagents

0.1 M KNO_3 solution was prepared by dissolving 5 g of potassium nitrate in 500 ml of 0.01 M HNO_3 .

0.2 ppm Se(IV) standard solution was prepared from 1000 ppm Se(IV) stock solution.

0.01 M of copper sulphate solution was prepared as in Section 11.2.5.

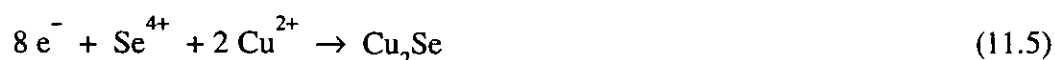
The optimised conditions were used for calibration of the method.

Procedure

2.47×10^{-5} M $\text{Hg}(\text{NO}_3)_2$ was used for preparing the mercury film on the glassy carbon support. Hg was deposited on the glassy carbon for 10 minutes at a potential of -1.0 V.

Accumulation step

$10\ \mu\text{l}$ of 0.2 ppm $\text{Se}(\text{IV})$ was added to the electrochemical cell. $\text{Se}(\text{IV})$ was accumulated on the mercury film on the glassy carbon electrode support for 1 minute at a potential of -0.3 V. The reaction that occurred in the accumulation step is given by:



Stripping step

After $\text{Se}(\text{IV})$ had been accumulated on the mercury film electrode for 1 minute, stirring of solution was stopped. The solution was allowed to rest for a period of 23 seconds so that measurements could be made under quiescent conditions. The stripping reaction is shown below.



Results and Discussion

The results obtained are shown in the calibration graph of peak current versus concentration of $\text{Se}(\text{IV})$ as shown in Figure 11.12. A limit of detection of 0.2 ppb (at 3σ above the blank) and sensitivity of 1030 nA/ppb were achieved. The sensitivity obtained by this method was found to be ten times better than that obtained when a HMDE was

used for the determination of Se(IV) in the presence of added Cu. However, this method suffered from a problem of reproducing the film.

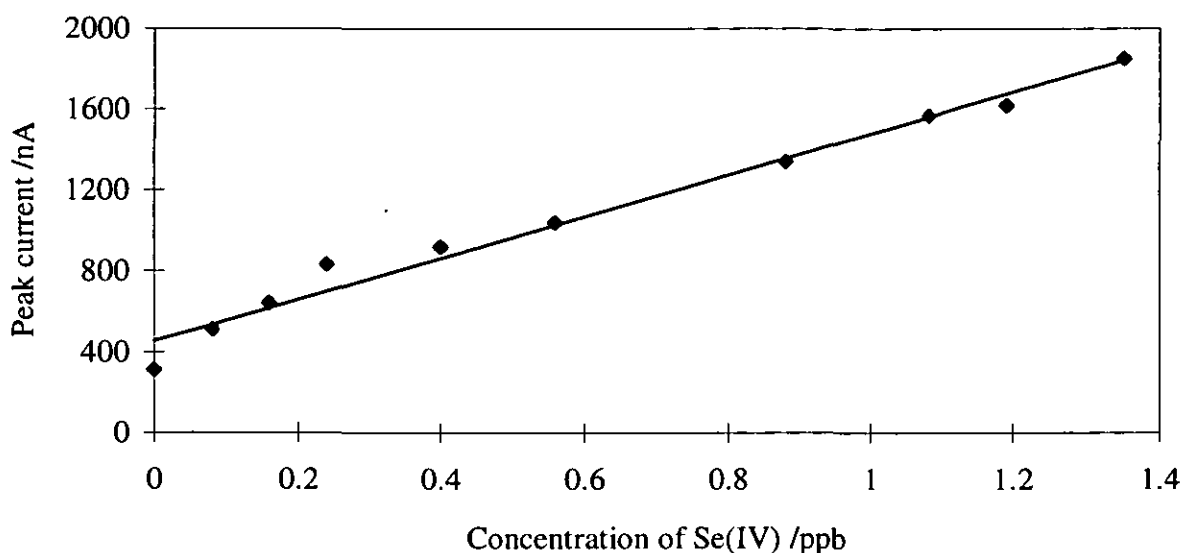


Figure 11.12 Calibration graph of peak current versus concentration of Se(IV) standards determined by DPCSV at MFGCE. Slope, 1029.1 nA/ppb, y-intercept, 451.7 nA; and regression coefficient, 0.981.

11.3.5 On-line generation of selenium hydride in the DPGD-FI system followed by its oxidation to Se(IV) by Ce(IV) and subsequent determination of Se(IV) by DPCSV at MFGCE (wall jet electrode)

Reagents

Ceric sulphate solution (3.01×10^{-4} M) and sodium borohydride (5.26×10^{-2} M) were prepared as in Section 11.2.9.

Copper sulphate (4.97×10^{-4} M)/ Potassium nitrate (0.20 M) was prepared by dissolving 0.062 g of copper sulphate (analytical reagent grade, BDH) and 10 g of potassium nitrate in 500 ml of de-ionised water.

0.1 M KNO_3 was prepared by dissolving 5 g of KNO_3 in 500 ml of 0.01 M nitric acid.

Mercury nitrate solution (50 ppm) was prepared by diluting 5 ml of 1000 ppm mercury nitrate in 100 ml of 0.1 M KNO_3 solution.

10 ppm Se(IV) was prepared from 1000 ppm selenium stock solution provided.

Apparatus

The system used is shown in Figure 11.13.

Mercury film formation

25 ml of 0.1 M KNO_3 (supporting electrolyte) was transferred into an electrochemical cell. The solution was stirred and deaerated with nitrogen for 10 minutes to eliminate the interference of oxygen. $\text{Hg(NO}_3)_2$ was continuously passed through the wall jet electrode (glassy carbon electrode). Accumulation of mercury was done at a deposition potential of 1.0 V (Ag/AgCl) for 15 minutes.

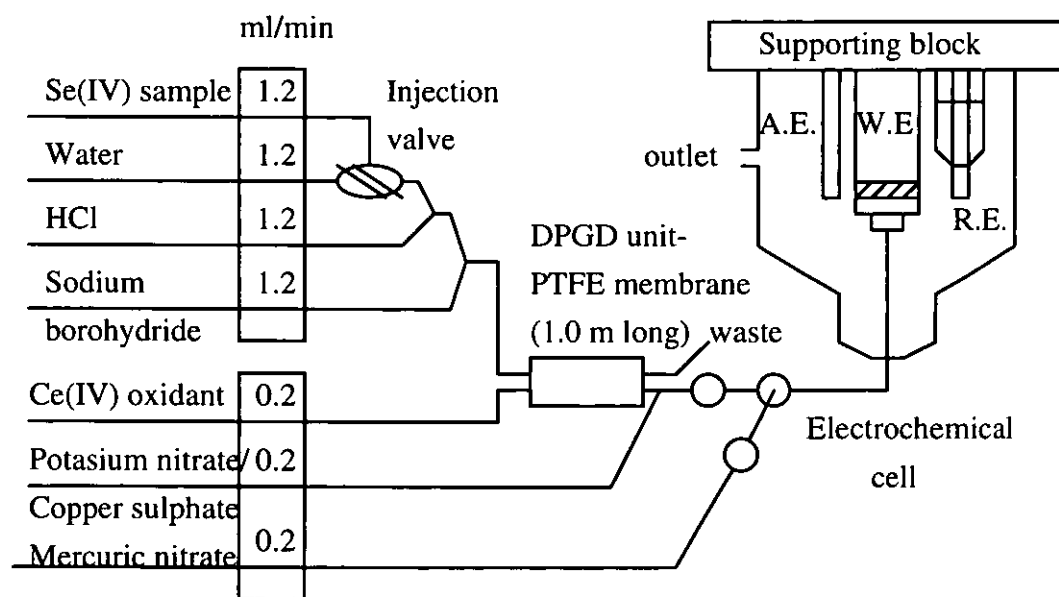


Figure 11.13 On-line detection of Se(IV) by DPCSV at MFGCE following FI-Selenium hydride generation and subsequent oxidation to Se(IV) by Ce(IV) . R.E., reference electrode (Ag/AgCl); A.E., auxiliary electrode (Pt) and W.E., working electrode (MFGCE-wall jet electrode).

Sample injection into FIA

10 ppm of Se(IV) standard was injected into the FI system using a sample loop volume of 0.5 ml. The generated selenium hydride was separated from the liquid donor stream by the PTFE membrane (163 cm long). The selenium hydride diffused into the Ce(IV) acceptor stream. The H_2Se was oxidised to Se(IV) by Ce(IV). Se(IV) was carried by the acceptor stream and was mixed with $\text{KNO}_3/\text{CuSO}_4$ mixture at a point of confluence using a T-piece, before passing through the wall jet electrode (MFGCE).

Measurement

DPCSV measurement of Se(IV) was made in the normal way using the following experimental conditions: deposition potential of -0.3 V (Ag/AgCl), voltage sweep from -0.3 V to -0.85 V , accumulation period of 10 minutes from the time of injection, rest period of 23 s and scan rate of -5 mV/s

Results and Discussion

The voltammogram obtained is shown in Figure 11.14.

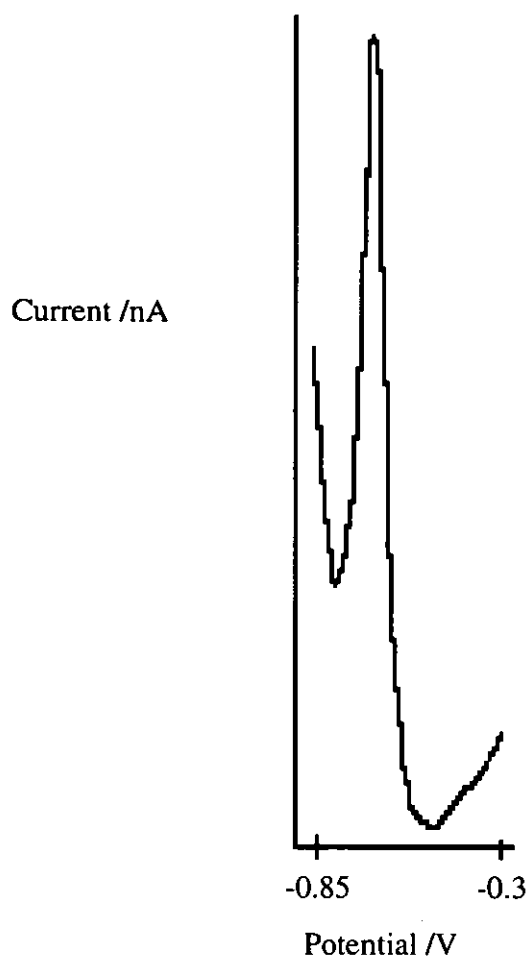


Figure 11.14 Stripping peak of Cu₂Se obtained in the determination of Se(IV) by DPCSV at MFGCE following the generation of H₂Se in the DPGD-FI system.

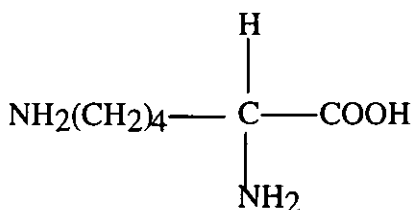
Although an initial peak was obtained, it was not possible to obtain peaks with any subsequent injection. The cause of this was instability in the film which appeared to be destroyed or made inactive after the first injection.

11.4 DETERMINATION OF Se(IV) BY DIFFERENTIAL PULSE CATHODIC STRIPPING VOLTAMMETRY AT A Hg-Cu FILM ON A GLASSY CARBON ELECTRODE (STATIC SYSTEM)

An attempt was made to form a Hg-Cu film on a glassy carbon electrode. This was made by mixing an effective concentration of 3.92×10^{-5} M $\text{Hg}(\text{NO}_3)_2$ and 4×10^{-5} M $\text{CuSO}_4 \cdot 5\text{H}_2\text{O}$ in the electrochemical cell and applying a deposition potential of -1.0 V. At this potential, Hg^{2+} and Cu^{2+} were reduced to Hg^0 and Cu^0 , respectively on the glassy carbon electrode. Subsequent attempts to use this method for the determination of Se(IV) were unsuccessful because the deposition potential of the Se(IV) was too close to the hydrogen cut off potential in the 0.1 M KNO_3 supporting electrolyte. An attempt was made to reduce the H^+ concentration by replacing KNO_3 with $\text{NaHCO}_3/\text{Na}_2\text{CO}_3$ buffer (pH 10). However, three analytical peaks were obtained instead of one. The experiment was therefore abandoned since the peaks did not have any dependence on the concentration of Se(IV).

11.5 DIFFERENTIAL PULSE CATHODIC STRIPPING VOLTAMMETRIC DETERMINATION OF SELENIUM (IV) ON HANGING MERCURY DROP ELECTRODE MODIFIED WITH POLY-L-LYSINE

Poly-l-lysine is a polymer of the amino acid lysine. The chemical structure of lysine is shown below.



Poly-L-lysine is essentially positively charged at low pH and negatively charged at high pH. An investigation was done to determine whether the sensitivity of detecting Se(IV) by the DPCSV could be significantly enhanced by employing poly-L-lysine as a modifier for a HMDE.

11.5.1 Without poly-L-lysine modifier.

Reagents

0.1 M HCl.

1 ppm Se(IV) was prepared from 1000 ppm Se(IV) stock solution.

Experimental conditions

HMDE, Ag/AgCl and glassy carbon electrode were used as the working, reference and auxiliary electrodes respectively. An accumulation potential of -0.35 V, accumulation period of 1 min, voltage scan from -0.35 V to -0.8 V, scan rate of -5 mV/s, and drop time of 0.5 s were employed.

Procedure

An effective concentration of 3.98 ppb of Se(IV) standard was added to the electrochemical cell in which 25 ml of 0.1 M HCl electrolyte had been added. The analyte was determined by the DPCSV in two steps after the solution had been de-aerated with nitrogen for 10 minutes.

Se(IV) was accumulated on the HMDE at a potential of 0.35V for 1 minute. The stripping peak was obtained by scanning the voltage from -0.35 V to -0.8 V after allowing a rest period of 23 seconds following the accumulation step. The procedure was repeated after each additional volume of the standard was transferred into the cell.

Results and Discussion

The results obtained are presented in the calibration graph shown in Figure 11.15. The calibration graph had a slope of 5.9 nA/ppb, y-intercept of -29.5 nA, and regression coefficient of 0.984. A sensitivity of 5.9 nA/ppb and a detection limit of 9.3 ppb (3σ above the blank) were obtained for the determination of Se (IV) by this method. These were similar to those obtained previously (see Section 11.2.3) and therefore this showed that the system was working reliably.

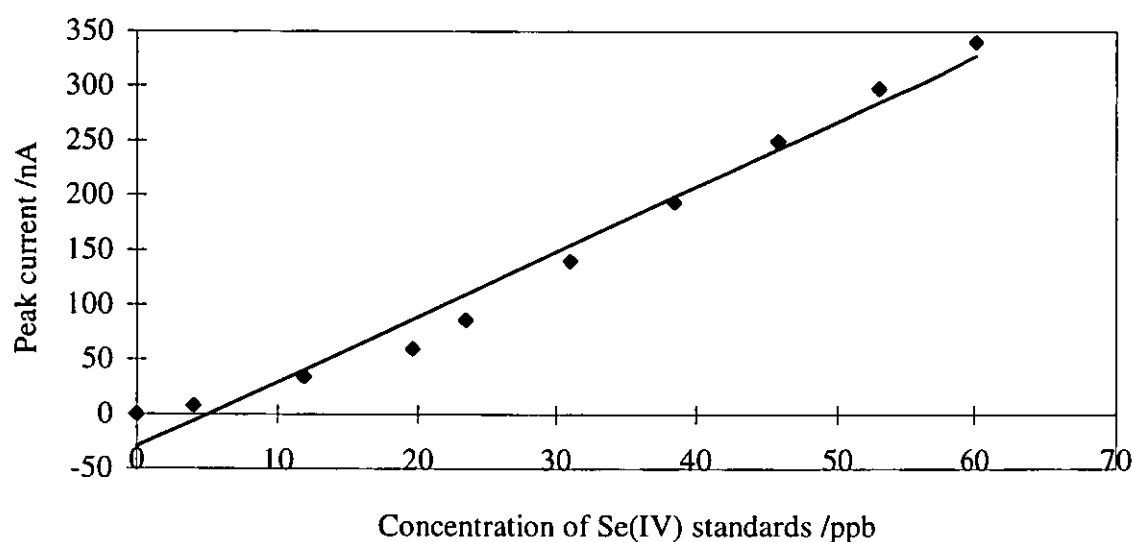


Figure 11.15 Calibration graph of peak current versus concentration of Se(IV) standard, determined by DPCSV on HMDE.

11.5.2 With poly-L-lysine and copper

Reagents

10^{-2} M $\text{CuSO}_4 \cdot 5\text{H}_2\text{O}$

1000 ppm of poly-L lysine (molecular mass of 61,800).

10 ppm Se(IV) standard.

0.1 M HCl.

Experimental conditions

The experimental conditions applied were similar to those used in the case where poly-L-lysine was not used as the modifier.

Procedure

Effective concentrations of 15.8 ppb of Se(IV), 7.9 ppm of poly-L-lysine and 3.95×10^{-5} M copper sulphate solution were added to the cell containing 25 ml of 0.1 M HCl, supporting electrolyte. The determination of Se(IV) by DPCSV was carried out as before.

Results and Discussion

The calibration graph shown in Figure 11.16 had a slope of 3.78 nA/ppb, y-intercept of -16.44 nA and regression coefficient of 0.993. A detection limit of 6.6 ppb and sensitivity of 3.78 nA/ppb were achieved. The results were similar to those obtained with added Cu, but without poly-l-lysine, and hence there was no advantage of using poly-l-lysine for modifying the HMDE for the determination of Se(IV) by the DPCSV.

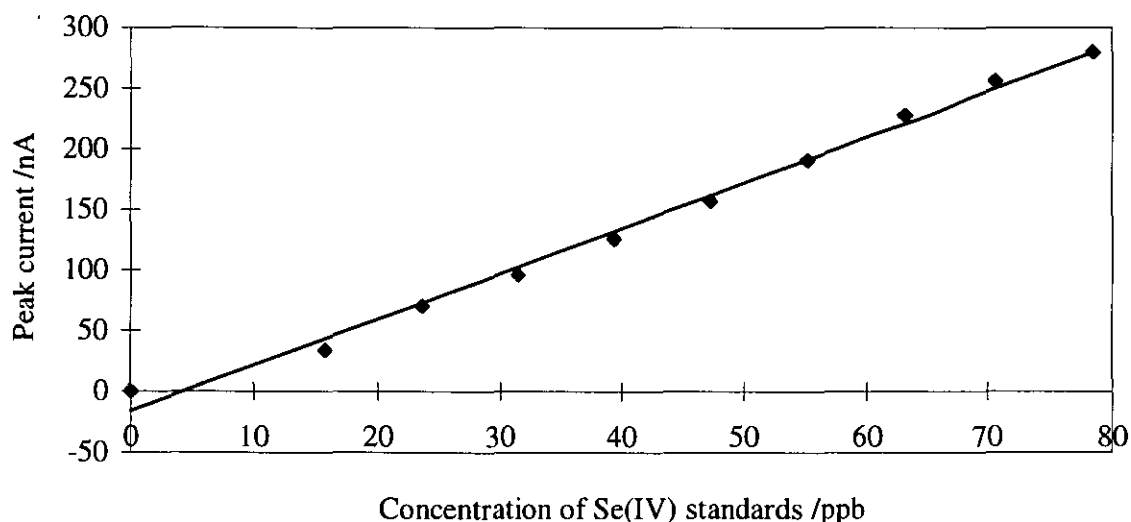


Figure 11.16 Calibration graph of peak current of Se(IV) standards, determined by DPCSV on chemically modified HMDE using poly-L-lysine.

11.6 PRELIMINARY EXPERIMENTS PERFORMED USING A CHEMICALLY MODIFIED MERCURY FILM ELECTRODE

Mercury film electrode and a chemically modified film electrode were employed so as to increase the sensitivity of the DPCSV method for the determination Se(IV) in both static and flow systems.

The formation mercury film on a solid support is usually carried out at a deposition potential of -1.0 V (versus Ag/AgCl). However, at this potential, there is a problem of hydrogen evolution which may be responsible for irreproducibility of the film formation and instability of the film in use. Thus, a study was carried out to ascertain the optimum potential at which the mercury would be formed on a glassy carbon electrode and on a modified glassy carbon electrode using DC voltammetry. The modifiers chosen were TCM (HgCl_4^{2-}) (negatively charged) and hexadecyltrimethyl ammonium bromide (positively charged). It was found that the maximum deposition current when $\text{Hg}(\text{NO}_3)_2$ was used for the formation of mercury film directly onto glassy carbon electrode occurred at -0.7 V. When the TCM solution was used for forming the Hg film on the glassy carbon electrode coated with hexadecyltrimethyl ammonium bromide, the maximum deposition potential occurred at -0.5 V. In the case where the mercury film was formed from $\text{Hg}(\text{NO}_3)_2$ on the glassy carbon electrode coated with hexadecyltrimethyl ammonium bromide, the maximum deposition current was obtained at -0.7 V.

The TCM based mercury film formed by applying a deposition potential of -0.5 V to the glassy carbon electrode which had been coated with hexadecyltrimethyl ammonium bromide, was then used as a working electrode for the determination of Se(IV) (no added Cu) in 0.1 M KNO_3 (pH 2.1) by the DPCSV method. A calibration graph (see Figure 11.17) with a linear range of 0-28 ppb Se(IV) was obtained. A sensitivity of 9.4 nA/ppb was achieved. This sensitivity was not significantly different from that obtained without using the quaternary ammonium salt and Cu.

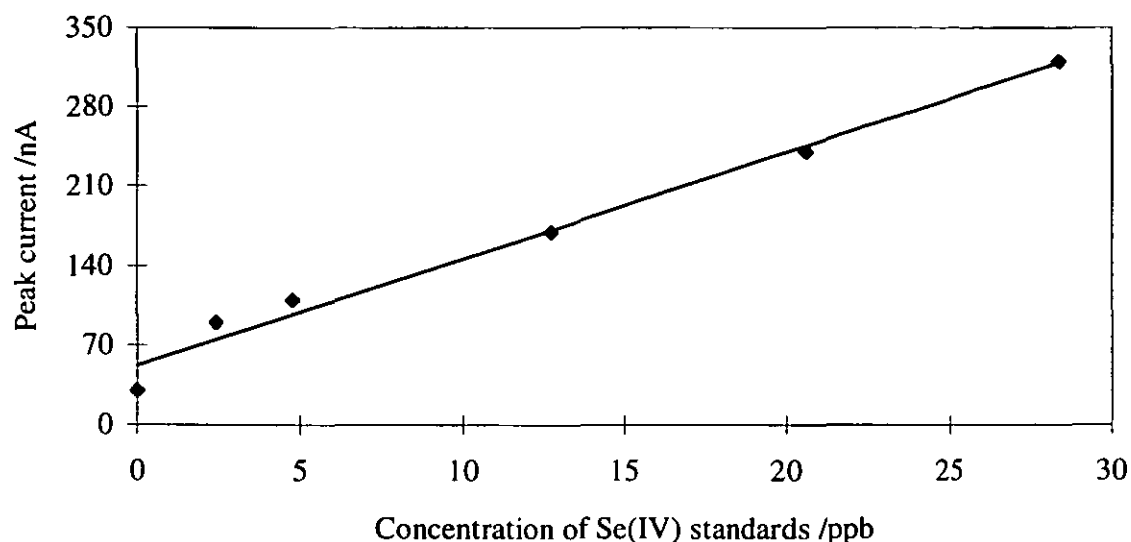


Figure 11.17 Graph of peak current against concentration of Se(IV), determined by DPCSV on MFGCE (TCM used for film formation). Slope, 9.39 nA/ppb; y-intercept, 52.21 nA, and regression coefficient, 0.984.

The determination of Se(IV) was repeated with the Hg film formed onto the glassy carbon electrode precoated with hexadecyltrimethyl ammonium bromide using mercury nitrate at -0.7 V. The results of peak currents obtained showed no linear dependence on the concentration of Se(IV). This might have been due to formation of a poor quality film at a few sites on the modified electrode, resulting in saturation of the film even with low concentration of the analyte.

The results with the modified electrodes for which deposition potential of -0.5 and -0.7 V were used for Hg film formation were no better than those obtained using the MFGCE formed from mercury nitrate at a deposition potential of -1.0 V.

A study of the influence of the pH of the KNO_3 electrolyte on the formation of Hg film on a glassy carbon electrode using DC voltammetry was carried out. The reason for conducting this study was to find the most suitable pH of the electrolyte which would favour a shift (in the negative direction) of the potential at which hydrogen was evolved.

This potential shift should be further away from the potential usually used for Hg film formation (-1.0 V). The highest peak current was obtained when a pH of 2.1 of KNO_3 (supporting electrolyte) was employed. As the pH of the electrolyte was decreased, the hydrogen overpotential also decreased, even though the size of the current peak increased. A pH of 2.1 of KNO_3 was therefore used in the subsequent experiments.

11.7 DETERMINATION OF SELENIUM (IV) BY DIFFERENTIAL PULSE CATHODIC STRIPPING VOLTAMMETRY AT MODIFIED MERCURY FILM ELECTRODE

Again the reasons for attempting to use the modified electrode was to increase the sensitivity of the DPCSV method for the determination of Se(IV) . Poly-l-lysine is positively charged at low pH. It is therefore expected to exert stronger electrostatic attraction to Se(IV) in an alkaline medium. In a neutral medium such as KNO_3 , it is still expected to interact with Se(IV) . This chemically modified electrode was employed as the working electrode in the determination of Se(IV) (no added Cu) by the DPCSV method.

In this Section, a deposition potential of -1.0 V (versus Ag/AgCl) was applied for the formation of mercury film on chemically modified glassy carbon electrode based on hexadecyltrimethyl ammonium bromide and poly-l-lysine modifiers. The mercury film was prepared from either TCM or $\text{Hg(NO}_3)_2$. The reason for reverting to this potential for the formation of modified mercury film electrodes was that no advantages were achieved by using such electrodes which had been formed at deposition potentials lower than -1.0 V. A study aimed at preparing a stable Hg film on a glassy carbon electrode modified in variety of ways with poly-l-lysine or hexadecyltrimethyl ammonium bromide was therefore carried out using a deposition potential of -1.0 V for the formation of the Hg film.

11.7.1 Using poly-l-lysine

A chemically modified mercury film electrode was prepared by adding effective concentration of 8 ppm of mercury nitrate and poly-l-lysine (molecular mass 61,800) to 25 ml of 0.1 M KNO₃ electrolyte and then applying a deposition potential of -1.0 V for a period of 10 minutes.

The results of peak currents obtained showed no linear relationship with the concentration of Se(IV) standards. In addition, the reproducibility of the results was poor. There was therefore no advantage gained by using chemically modified electrode based on poly-l-lysine modifier, even at the more negative deposition potential.

A new Hg film modified by poly-l-lysine was prepared again and then used for the determination of Se(IV) in the presence of added Cu (effective concentration of 4×10^{-5} M). The results of peak currents obtained showed no linear relationship with the concentration of Se(IV) standards. The reason for this may be due to a number of factors which include problems of forming films reproducibly, reproducibly modifying the films with poly-l-lysine, and possibly due to positively charged sites on the poly-l-lysine repelling Cu²⁺ away from the Hg film electrode.

11.7.2 Using Hexadecyltrimethyl ammonium bromide

11.7.2.1 *Formation of Hg film after coating glassy carbon electrode manually with hexadecyltrimethyl ammonium bromide and TCM solution*

A well polished glassy carbon electrode was coated manually with hexadecyltrimethyl ammonium bromide (anion exchanger) by adding 20 µl drops of 1000 ppm of this quaternary ammonium salt directly to the electrode surface using a micropipette. The electrode was allowed to dry before applying 20 µl of 0.04 M TCM. The Hg film was

then formed electrochemically by applying a deposition of -1.0 V to the modified glassy carbon electrode in a cell containing 25 ml of 0.1 M KNO_3 supporting electrolyte. Thus Hg^{2+} was reduced to Hg^0 .

Se(IV) (no Cu added) was determined by the DPCSV using this chemically modified Hg film electrode by serial addition of known volumes of 1 ppm Se(IV) standard.

Results

The results obtained are shown in the calibration graph in Figure 11.18. The calibration graph has a slope of 108.2 nA/ppb, a y-intercept of 396.6 nA and a regression coefficient of 0.988. A sensitivity of 108.2 nA/ppb and a detection limit of 1.91 ppb were obtained.

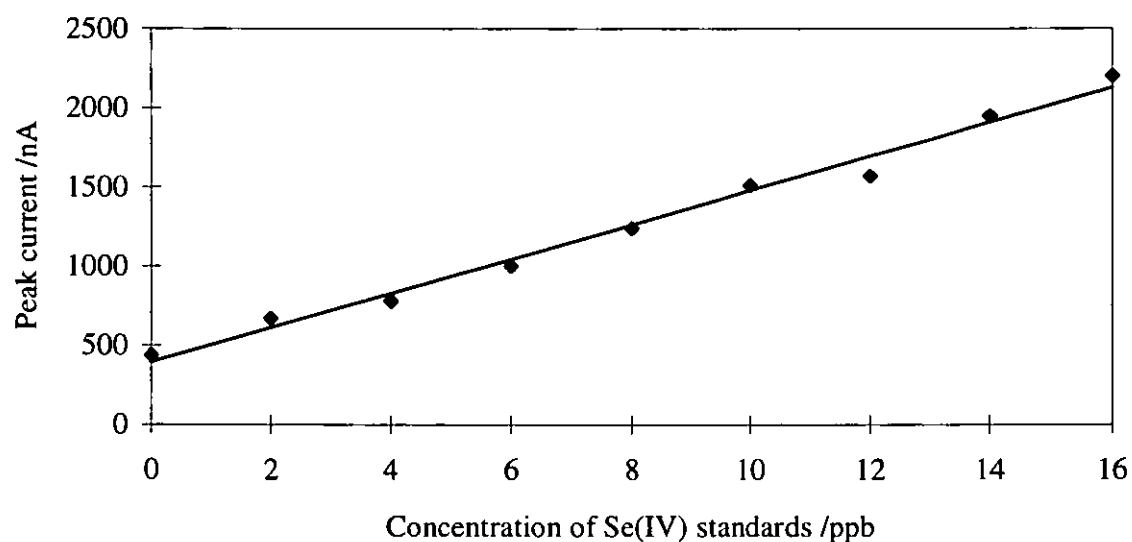


Figure 11.18 Calibration graph of peak current versus concentration of Se(IV) standards, determined by DPCSV on modified MFE (hexadecyltrimethyl ammonium bromide used as modifier, and TCM for mercury film formation)

11.7.2.2 *In situ* coating of glassy carbon electrode with hexadecyltrimethyl ammonium bromide and Hg film formation using TCM.

Hexadecyltrimethyl ammonium bromide and TCM solution in the ratio 1:1 were added to the cell. A chemically modified Hg film electrode was obtained by applying a deposition potential of -1.0 V to the glassy carbon electrode in 0.1 M KNO₃.

This electrode was then employed as a working electrode for the determination of Se(IV) in the absence of Cu.

Results

The calibration graph shown in Figure 11.19 has a slope of 53.63 nA/ppb, a y-intercept of 174.28 nA and a regression coefficient of 0.977. A sensitivity of 53.5 nA/ppb and a detection limit of 2.13 ppb of Se(IV) were achieved by this method.

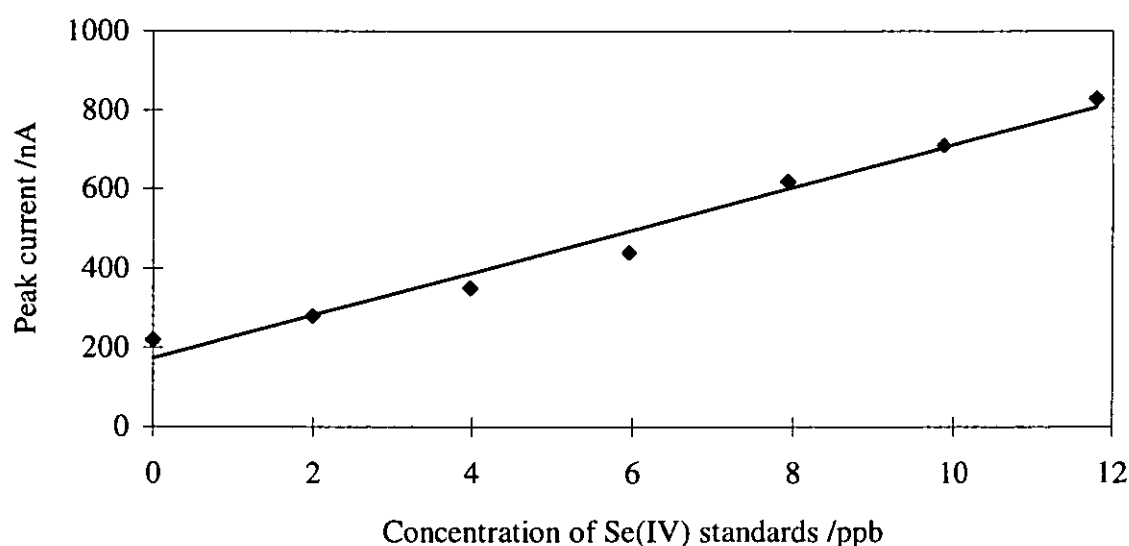


Figure 11.19 Calibration graph of peak current versus concentration of Se (IV) standards, determined by DPCSV at modified MFE (hexadecyltrimethyl ammonium bromide used as modifier and TCM for Hg film formation on glassy carbon electrode).

Again the procedure of forming the chemically modified Hg film electrode was repeated after the glassy carbon had been polished and thoroughly cleaned. This film electrode was subsequently used for the determination of Se(IV) in the presence of Cu.

Results

The calibration graph shown in Figure 11.20, has a slope of 119 nA/ppb, a y-intercept of 805 nA, and a regression coefficient of 0.962. This method offered a sensitivity of 119 nA/ppb and a detection limit of 1.8 ppb of Se(IV).

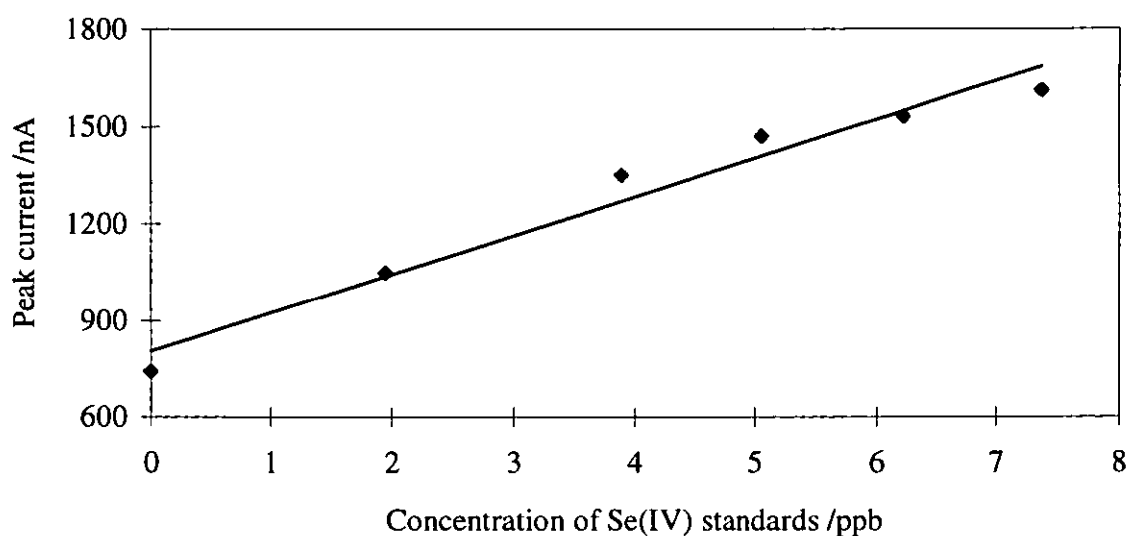


Figure 11.20 Calibration graph of peak current versus concentration of Se(IV), determined in the presence of added Cu by DPCSV at modified MFE using hexadecyltrimethyl ammonium bromide (TCM used for mercury film formation).

11.7.2.3 *Formation of mercury film using TCM after coating the glassy carbon electrode with hexadecyltrimethyl ammonium bromide*

By means of a micropipette, 20 μl of 1000 ppm hexadecyltrimethyl ammonium bromide was coated on a well polished glassy carbon electrode. After giving the electrode time to dry, it was then fixed in position in the multi mode polarograph. 400 μl of TCM was then transferred into the cell containing 25 ml of 0.1 M KNO_3 . Again the Hg film was formed by applying a deposition potential of -1.0 V to the working electrode.

This electrode was subsequently used in the DPCSV method for the determination of known volumes of 1 ppm Se(IV) added into the cell.

Results

The calibration graph in Figure 10.21, constructed using the obtained results, had a slope of 70.1 nA/ppb, a y-intercept of 285.4 nA, and a regression coefficient of 0.974. Sensitivity of 70.1 nA/ppb and detection limit of 2.1 ppb of Se(IV) were obtained.

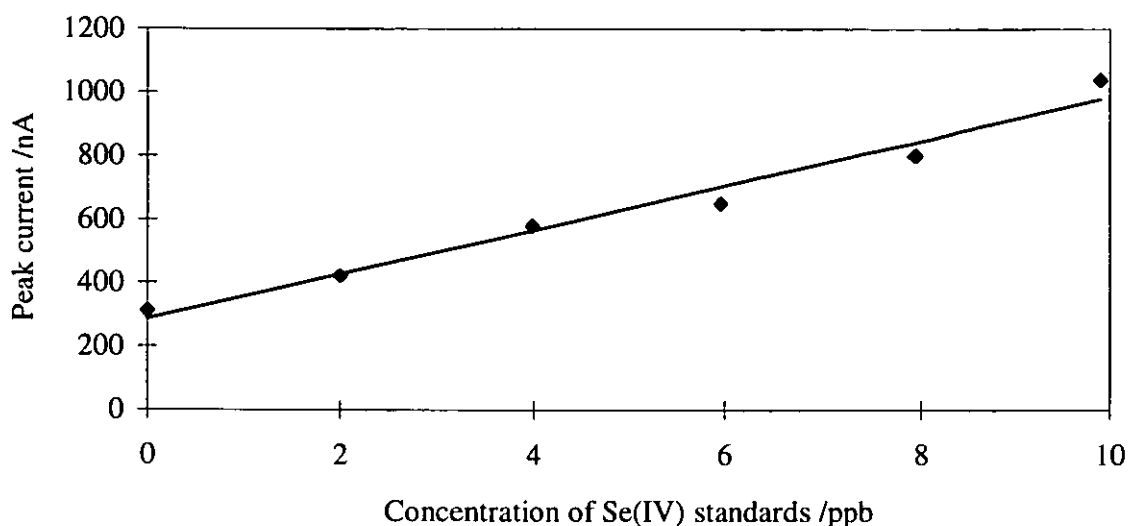


Figure 10.21 Calibration graph of peak current against concentration of Se(IV), determined by DPCSV on modified MFE (hexadecyltrimethyl ammonium bromide used as a modifier and TCM for mercury film formation)

11.7.3 Discussion

The chemically modified mercury film based on poly-l-lysine modifier was found to be unsuitable for the determination of Se(IV). This was because the results of peak current obtained showed no linear dependence on Se(IV) concentration.

The results of peak current obtained when the chemically modified mercury film electrode based on hexadecyltrimethyl ammonium bromide was employed were found to have a linear relationship with Se(IV) concentration. The highest sensitivity of 118 nA/ppm obtained with this electrode was when Se(IV) was determined in the presence of Cu. This sensitivity was one order of magnitude lower than that obtained with the unmodified Hg film electrode. There was, therefore, no advantage gained in terms of sensitivity and improvement of stability of the film by using chemically modified mercury film instead of mercury film electrode.

11.8 CONCLUSIONS

In the determination of Se(IV) by DPCSV on the HMDE in a static system, a sensitivity of 6.1 nA/ppb and a detection limit of 6.8 ppb Se(IV) (at 3σ above the blank) were achieved. However, when this was done in the presence of added Cu, a sensitivity of 10 nA/ppb and a detection limit of 5.4 ppb Se(IV) were obtained. The addition of Cu had the effect of enhancing the sensitivity by 1.64 times. It also had the effect of shifting the peak potential from -0.51 to 0.69 V (versus Ag/AgCl). This has the benefits of removing interference in the presence of complexing agents such as EDTA.⁹ Interference due to Zn(II) can be removed and that due to Cd(II) reduced considerably by using added EDTA and Cu in the determination of Se(IV).

The determination of Se(IV) by DPCSV on the HMDE in a flow system involving the conversion of Se(IV) to H_2Se by NaBH_4 and HCl, and oxidation of the vapour to Se(IV) by Ce(IV) in the DPGD-FI system resulted in a sensitivity of 1 nA/ppb and a detection limit of 11 ppm when 0.5 m long PTFE membrane was employed. A sensitivity of 3.7 nA/ppm and a detection limit of 7.7 ppm was obtained when 1 m long PTFE membrane was employed. The best separation efficiency obtained was of order of 10 %. The poor sensitivity was due to the low separation efficiency of the membrane (10 %) for H_2Se and the extensive dilution of the sample in the flow system and in the cell (74 times).

The optimum potential for the formation of mercury film on the glassy carbon electrode was found to be -1.0 V versus Ag/AgCl (3 M KCl) reference electrode. Reproducible results were obtained when this potential was applied for the mercury film formation which was subsequently used for the determination of Se(IV) by DPCSV. However, when potentials lower than -1.0 V (e.g. -0.5, -0.7 V) were employed for the mercury film formation, irreproducible results were obtained and there was no linear relationship between the peak currents and the concentration of Se(IV) standards. This may have been due to the formation of mercury patches rather than a perfect mercury film on the glassy carbon support.

The determination of Se(IV) in the presence of Cu by DPCSV at a MFGCE in a static system yielded a detection limit of 0.22 ppb and a sensitivity of 1029 nA/ ppb. This sensitivity was ten times of that obtained when the determination of Se(IV) in the presence of added Cu was carried out on HMDE.

The determination of Se(IV) in the presence of added Cu by the DPCSV at a MFGCE in a wall jet configuration system, after the generation of H_2Se in FI system followed by its separation and oxidation of Se(IV) by Ce(IV), gave voltammograms for every first injection of the S(IV) standard whenever a new mercury film was used. With subsequent injections of Se(IV) standards into DPGD-FI system, asymmetric peaks, and in some cases no peaks, were obtained. This might have been due to the mercury film on the glassy carbon electrode being destroyed (washed off). In an attempt to solve this problem, the flow rates of the reagent and carrier streams were reduced so as to have a laminar flow, but no improvement was obtained. The "wall jet electrode" did not show the characteristics of a true wall jet. There was not enough space between the surface of the electrode and the end of the tube through which the liquid stream entered the working electrode. For an ideal wall jet, this space, should be about 10 mm.

For the determination of Se(IV) in the presence of added Cu by DPCSV on modified HMDE using poly-lysine in a static system, a detection limit of 6.6 ppb Se(IV) and a sensitivity of 3.8 nA/ppb were obtained. However, when HMDE without the application of poly-lysine modifier was employed, a detection limit of 9.3 Se(IV) and a sensitivity of 5.9 nA/ppb were achieved. No significant advantage was therefore obtained by using poly-l-lysine.

The application of a chemically modified mercury film electrode made from poly-l-lysine modifier for the determination of Se(IV) by DPCSV yielded peak currents which did not have linear relationship with the concentration of Se(IV) concentration. This might have been due to the problems of forming a uniformly distributed film on the substrate.

The highest sensitivity of 119 nA/ppb was obtained when Se(IV) was determined in the presence of added Cu by DPCSV on hexadecyltrimethyl ammonium bromide based chemically modified electrode. This electrode was prepared by applying manually the TCM solution on the glassy carbon electrode coated with hexadecyltrimethyl ammonium bromide before electrochemically reducing Hg^{2+} to Hg^0 . This sensitivity was 10 times less than that achieved by the mercury film electrode.

There was no advantage in employing chemically modified mercury films based on poly-l-lysine or hexadecyltrimethyl ammonium bromide as compared to the unmodified mercury film electrode in terms of sensitivity and stability. Chemically modified electrodes were not therefore tried for the determination of Se(IV) by DPCSV in flow systems.

REFERENCES

1. Hill, S. J., Pitts, L. and Worsfold, P., *J. Anal. At. Spectrom.*, 1995, **10**, 409.
2. Quijano, M. A., Gutierrez, A. M., Conde, M. C. P. and Camara, C., *J. Anal. At. Spectrom.*, 1995, **10**, 871.
3. Olivas, R. M., Donard, O. F. X., Camara, C. and Quevauviller, P., *Anal. Chim. Acta*, 1994, **286**, 357.
4. Jarzabek, G. and Kublik, Z., *Anal. Chim. Acta*, 1982, **143**, 121.
5. Dennis, B. L., Moyers, J. L. and Wilson, G. S., *Anal. Chem.*, 1976, **48**, 1611.
6. Sarwicki, E., *Anal. Chem.*, 1957, **29**, 1376.
7. Watkinson, J. H., *Anal. Chem.*, 1960, **32**, 981.
8. Lott, P. F., Cukor, P., Moriber, G. and Solga, J., *Anal. Chem.*, 1963, **35**, 1159.
9. Baltensperger, U. and Hertz, J., *Anal. Chim. Acta.*, 1985, **172**, 49.
10. Manning, D. C., *At. Absorp. Newl.*, 1971, **10**, 123.
11. Pollock, E. N. and West, S. J., *At. Absorp. Newl.*, 1973, **12**, 6.
12. Thomson, K. C. and Thomerson, D. R., *Analyst*, 1974, **99**, 595.
13. Buckley, W. T., Budac J. J., Godfrey, D. V. and Koenig, K. M., *Anal. Chem.*, 1992, **64**, 724.
14. Olivas, R. M., Quetel, C. R. and Donard, O. F. X., *J. Anal. At. Spectrom.*, 1995, **10**, 865.
15. Vollkopf U., Gunsel, A. and Janssen, A., *At. Spectrosc.*, 1990, **11**, 13.
16. Stroh, A. and Vollkopf, U., *Anal. Proc.*, 1992, **29**, 274.
17. Pretty, J. R., Blubaugh, E. A. and Caruso, J. A., *Anal. Chem.*, 1993, **65**, 3396.
18. Andrews, R. W. and Johnson, D. C., *Anal. Chem.*, 1975, **47**, 294.
19. Alam, A. M. S., Vittori, O. and Porthault, M., *Anal. Chim. Acta.*, 1976, **87**, 437.
20. Alam, A. M. S., Vittori, O. and Porthault, M., *J. Electroanal. Chem.*, 1975, **61**, 191.
21. Christian, G. D., Knoblock, E. C. and Purdy, W. C., *Anal. Chem.*, 1967, **35**, 1128.

22. Ahmad, R., Hill, J. O. and Magee, R. J., *Analyst*, 1983, **108**, 835.
23. Aydin, H. and Tan, G. H., *Analyst*, 1991, **116**, 941.
24. Lanza, P. and Zappoli S., *Anal. Chim. Acta*, 1986, **185**, 219.
25. Van Den Berg C. M. G. and Khan S. H., *Anal. Chim. Acta*, 1990, **231**, 221.
26. Florence, T. M., *Electroanal. Chem. Interfacial Electrochem.*, 1970, **27**, 273.
27. Gunasingham, H., *Electroanal. Chem.*, 1989, **16**, 89.

Chapter 12

CHAPTER TWELVE

CONCLUSIONS AND RECOMMENDATIONS FOR FURTHER WORK.

12.1 CONCLUSIONS

A DPGD-FI interface has been employed in this work for the generation and subsequent separation of gaseous analytes from a liquid donor stream prior to their introduction into an isotope ratio mass spectrometer. Wet chemical methods were shown to be a viable alternative to the widely used combustion interface. Wet chemical methods provide a convenient means of dealing with solution samples which are common in environmental and biological research and are also less expensive to operate than the combustion methods.

An on-line degassing system, consisting of dual PTFE membranes, was shown to be an efficient device for the removal of dissolved gases in both sample and reagent streams. It was incorporated into the DPGD-FI system employed for the generation of N_2 and CO_2 for isotope ratio mass spectrometry. The degassing system was used to overcome the interference of the dissolved gases which can cause a bias in the measured isotope ratios.

The DPGD-FI system was successfully employed for producing CO_2 from organic and inorganic carbon and N_2 from nitrogen containing compounds for isotope mass ratio measurements. The atom percent (abundance), isotope ratios ($^{13}C/^{12}C$, $^{15}N/^{14}N$), and delta values ($\delta^{15}N$ and $\delta^{13}C$) determined using the DPGD-FI system interfaced to the isotope ratio mass spectrometer compared favourably with the reported values obtained using the IRMS/combustion system.

The DPGD-FI interface was also shown to be a versatile tool for generating and separating other gaseous analytes. For example, it was employed for generating SO_2 and H_2S from SO_3^{2-} , H_2S from S^{2-} ; Cl_2 from Cl^- ; Br_2 from Br^- ; CO_2 from CO_3^{2-} ; and N_2 from

nitrogen containing compounds. The versatility of DPGD-FI has also been shown in the variety of detectors with which it can be interfaced. In this work an isotope ratio mass spectrometer, a TCD and a UV/VIS spectrophotometer were used for detection. Additionally, the system has been used for generating H_2Se from Se (IV) . This was followed by its separation from the liquid donor stream into a Ce (IV) acceptor and then subsequent detection by DPCSV.

Speciation has been achieved by performing specific reactions within the DPGD-FI system, different species of sulphur (sulphide, sulphite and sulphate) and carbon (organic and inorganic) were determined with TCD and UV/VIS spectrophotometry detectors. It is also possible to perform speciation studies using an isotope ratio mass spectrometer as the detector.

11.2 RECOMMENDATIONS FOR FURTHER WORK

Although the experimental conditions for generating H_2S from S^{2-} , SO_2 from SO_3^{2-} , Br_2 from Br^- , Cl_2 from Cl^- and H_2Se from Se(IV) in the DPGD-FI system were optimised in this work, these gases/vapours were not introduced into the isotope ratio mass spectrometer for isotope mass ratio measurements. This was mainly due to a lack of time, but clearly this should be pursued and might extend the range of applications for which isotope ratio mass spectrometry can be used.

An improvement in the performance of a DPGD-FI system for the generation of gases/vapours for MS can be achieved by employing very high quality plumbing. This involves the replacement of the PTFE tubes with stainless steel tubes which prevent the atmospheric N_2 or CO_2 from entering the system and causing background contamination.

An easy route for generating H_2S from sulphate should be developed, the Johnson Nshita method, which employs a reducing mixture of hydriodic, formic, and hypophosphorous acids, could not be conveniently incorporated into the DPGD-FI system. This was due to

high viscosity of hypophosphorous acid which caused a build up of pressure within the FI manifold and hence a leakage of the liquid at the connection points. In addition, the production of H_2S takes place after the digestion of sulphate with the reducing mixture at a high temperature (115°C) for a period of 1.5 to 2 hours. Application of such a high temperature resulted in water vapour passing through the PTFE membrane along with the H_2S analyte. The passage of water into the acceptor stream (He gas) can damage the TCD filaments. The application of high temperature also caused a general problem of leakage of the liquid through the points of connection along the FI manifold. A long period of sulphate digestion with the reducing mixture increases the total analysis time and this makes the method unsuitable for routine analysis.

A MFGCE, in a wall jet configuration, has the potential of enhancing the sensitivity of DPCSV method for the determination of Se(IV) in a flow system. In this work, the wall jet electrode used worked for every first injection and not for subsequent injections of Se(IV) standard into the DPGD-FI system. The reason for this might have been due to combination of several factors which include problems of producing a reproducible Hg film on the glassy carbon electrode, destruction of the Hg film, probably due to hydrogen evolution or turbulent conditions in the flow system, and the working electrode not showing the characteristics of a true wall jet. A MFGCE in a wall jet configuration exhibiting the characteristics of a true wall jet electrode is therefore recommended.

